1999

Extratropical Storms of the Gulf of Mexico and Their Effects Along the Northern Coast of a Barrier Island: West Ship Island, Mississippi.

Phillip Lynn Chaney
Louisiana State University and Agricultural & Mechanical College

INFORMATION TO USERS

This manuscript has been reproduced from the microfilm master. UMI films the text directly from the original or copy submitted. Thus, some thesis and dissertation copies are in typewriter face, while others may be from any type of computer printer.

The quality of this reproduction is dependent upon the quality of the copy submitted. Broken or indistinct print, colored or poor quality illustrations and photographs, print bleedthrough, substandard margins, and improper alignment can adversely affect reproduction.

In the unlikely event that the author did not send UMI a complete manuscript and there are missing pages, these will be noted. Also, if unauthorized copyright material had to be removed, a note will indicate the deletion.

Oversize materials (e.g., maps, drawings, charts) are reproduced by sectioning the original, beginning at the upper left-hand corner and continuing from left to right in equal sections with small overlaps. Each original is also photographed in one exposure and is included in reduced form at the back of the book.

Photographs included in the original manuscript have been reproduced xerographically in this copy. Higher quality 6" x 9" black and white photographic prints are available for any photographs or illustrations appearing in this copy for an additional charge. Contact UMI directly to order.

UMI

A Bell & Howell Information Company
300 North Zeeb Road, Ann Arbor MI 48106-1346 USA
313/761-4700 800/521-0600

EXTRATROPICAL STORMS OF THE GULF OF MEXICO AND THEIR EFFECTS ALONG THE NORTHERN COAST OF A BARRIER ISLAND: WEST SHIP ISLAND, MISSISSIPPI

A Dissertation

Submitted to the Graduate Faculty of the
Louisiana State University and
Agricultural and Mechanical College
in partial fulfillment of the
requirements for the degree of
Doctor of Philosophy

in

The Department of Geography and Anthropology

by
Phillip L. Chaney
B.S., University of Arkansas, 1980
M.A., University of Arkansas, 1990
May, 1999

ACKNOWLEDGEMENTS

This research was made possible by support from the Department of Geography and Anthropology at Louisiana State University through the award of a graduate assistantship, and two grants from the Robert C. West Field Research Fund. Additional support was provided by the National Park Service, the Geological Society of America, and SIGMA XI: The Scientific Research Society.

The following personnel from the Gulf Islands National Seashore provided substantial support to this project: Jerry Eubanks, Riley Hoggard, Gary Hopkins, Mike Hobbs, Jeff Woods, Bernie Doyle, and Keith "Spider" Husley. Captain Louis Skrmetta of Ship Island Excursions in Gulfport, Mississippi, along with his excellent staff and crew, provided transport to and from West Ship Island.

The members of the dissertation committee contributed to this research in the classroom, and in editorial comments: Dr. Keith G. Henderson (chair), Dr. Carville Earle, and Dr. Anthony J. Lewis of the Department of Geography and Anthropology, and Dr. Gregory W. Stone and Dr. Harry H. Roberts of the Coastal Studies Institute. Dr. S.A. Hsu and Dr. Ping Wang of the Coastal Studies Institute also made significant contributions. Field assistance and transportation was also provided by the following personnel from the CSI Shop: Rodney Fredericks, Joel Chaky, Bill Gibson, and Floyd DeMers. Dr. JingPing Xu also contributed in the lab and in the field.

Dr. Carville Earle made an exceptional contribution to this research, and my education at LSU, by supporting me when I was recovering from knee surgery, and by introducing me to many different aspects of geographical thought and inquiry.

The following students gladly donated their time to participate in field work: Chuck Armbruster, Chris Ayles, Paul Hudson, Michael Hawkins, David Pepper, Mike Steinberg, and Matthew Taylor. The following students and friends provided moral support: Xionping Zhang (XP), John Ellis, Luigi Cipriani, Tina Swaye, Elizabeth Vaughan, Katie Algeo, Lisa Adams, Jodi and Etienne Brandehoff-Pracht, Mary "Murgy" Pyles and Rick Ellis, George Imrie, Glenda Cade, and Sam Bishop. Elizabeth "Betty" Vaughan provided additional assistance in completing this project.

Chuck Armbruster and Michael Hawkins made extraordinary contributions and will always be considered best friends. Chuck helped tremendously over the years in discussions on practically every coastal subject in the book. Michael Hawkins was a tremendous help in the field (at Ship Island and elsewhere) and probably taught me more about geography, among other things, than anyone. Thanks also to my colleagues in The Draft Horse Club: Paul Hudson, Mike Steinberg, and Steve Raney.

The following members of the faculty at the University of Arkansas made significant contributions to my education which made this research possible: David Stahle, Malcolm Cleaveland, John Hehr, Tom Graff, John Dixon, Earle Neel, Dick Smith, and Orland Maxfield of the Department of Geography; David Knowles of the Department of Engineering; Harold MacDonald of the Department of Geology; and Jack Perkins of the Department of Agriculture.

Finally, I would like to acknowledge the extraordinary contributions of the person who is by far my greatest fan and sponsor: Thanks Mom!

TABLE OF CONTENTS

LIST OF TABLES

LIST OF FIGURES

ABSTRACT

The north-facing, estuarine shores of barrier islands along the northern Gulf of Mexico are experiencing severe shoreline erosion. This erosion process is related to storm events that occur when cold fronts pass along the coast. These cold fronts are associated with the migration of extratropical (mid-latitude) cyclones and anticyclones across the region in winter.

Wind data collected by a NOAA weather buoy over the period 1981-1997 were used, in conjunction with daily weather maps, to evaluate winter storm activity. Seven synoptic weather patterns that produced extratropical storm events along the northern Gulf Coast were identified. Statistics were computed for the mean and maximum speeds of the "northerly" winds produced by the 506 storms identified in the study. Similar statistics were computed for the northwesterly and northeasterly winds. The data indicate that northeasterly winds prevail over northwesterly winds by a margin of approximately 2:1 between September and May, which may be used to infer that the predominant direction of sediment transport is westward. This finding was attributed to the clockwise wind rotation pattern of anticyclones that dominate wind flow patterns in the region after cold fronts pass along the coast.

Oceanographic data collected during 3 storm events showed that low tide levels reduced water depth across the shallow, nearshore platform which resulted in waves expending their energy on the platform before reaching the foreshore. High tide levels allowed waves to traverse the nearshore platform and expend their energy on the foreshore. Thus, sediment transport occurs along the platform during low-tide periods and along the foreshore during high tide periods. Variations in tides,

therefore, may influence the predominant direction of sediment transport along the foreshore and the nearshore platform during storms in which the wind shifts from northwest to northeast, which occurred in approximately 70% of the storms.

Tropical Storm Josephine (October, 1996) disrupted the beach response study; however, a noteworthy response was observed. The storm increased the width of the beach by transporting sediment from the backshore to the foreshore. Extratropical storm impacts re-stored the beach to its original morphology by the end of the winter storm season.

CHAPTER 1

INTRODUCTION

The coastal perimeter of the Gulf of Mexico is lined with barrier islands that buffer estuaries and mainland shores from the high-energy impacts of waves produced by storms on the open sea. The estuaries are generally perceived as environments where low-energy wave conditions prevail, especially when compared with the central region of the Gulf of Mexico. However, physical evidence and historical maps indicate that the north-facing, estuarine shores of barrier islands along the northern Gulf Coast have experienced severe cases of chronic erosion.

Chronic erosion of the northern shores of barrier islands in Mississippi (Henry 1977a; Chaney and Stone 1996) and northwest Florida (Armbruster *et al.* 1995; Armbruster 1997) has been attributed to northerly winds associated with winter storm events, however, many questions remain unanswered. In Louisiana, the problem appears to be complicated by relative sea-level rise where rates in excess of 10 mm yr^{-1} have been recorded in recent history (Penland and Ramsey 1990). The objectives of this research are to evaluate the variability in wind conditions (wind speed, direction, and duration) that occur during these winter storm events, and to evaluate the impacts of these storms along the northern coast of a barrier island. West Ship Island, Mississippi, was chosen for this study because it is one of the more prominent sites of coastal erosion in the region (Figure 1.1), and because relative sea-level rise is not considered to be a significant factor at the site (Chaney and Stone 1996).

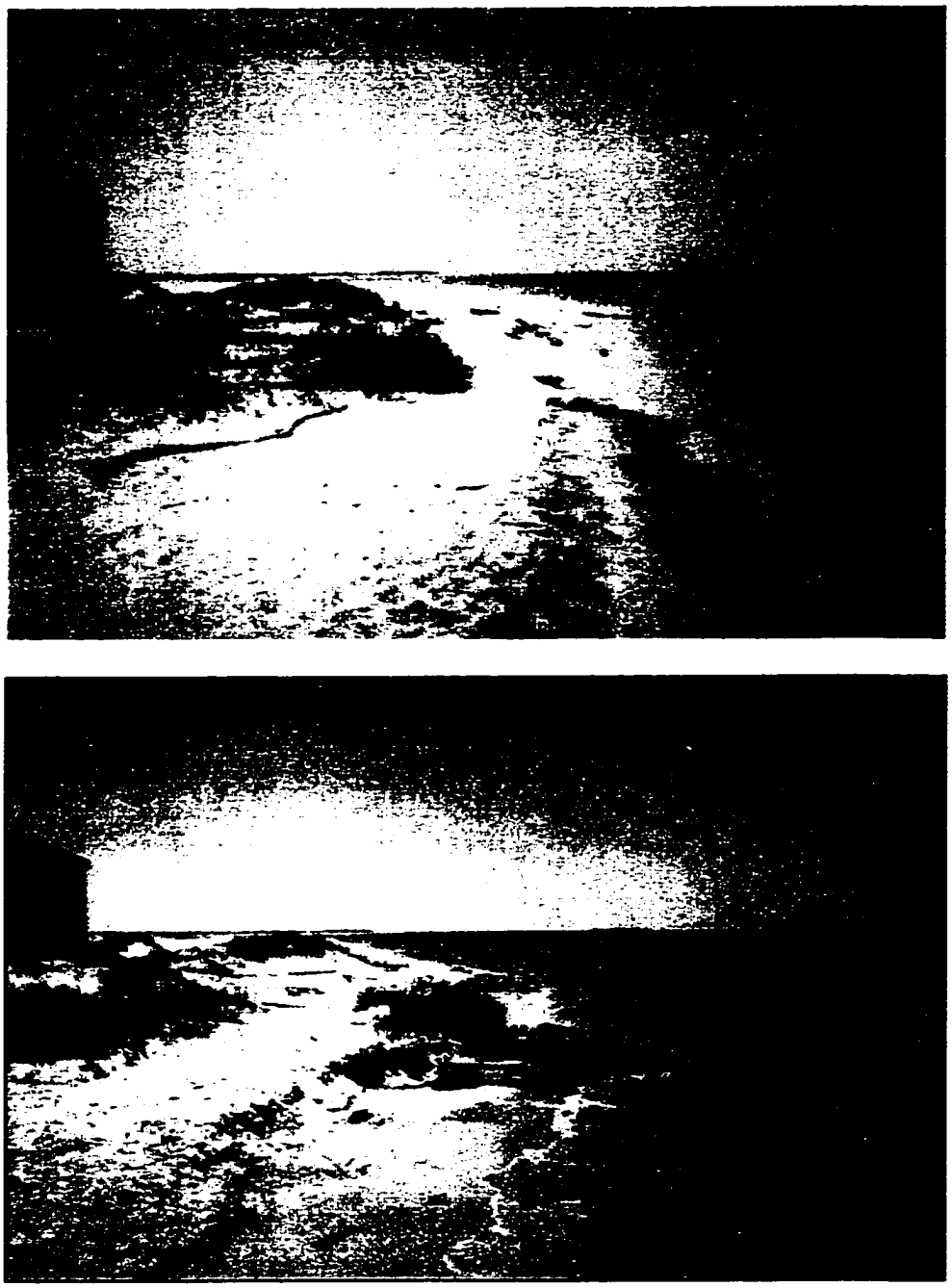

Figure 1.1. Evidence of wave erosion associated with "northerly" winds produced by winter storms in the northern Gulf of Mexico. The upper photo shows the condition of the northern coast of West Ship Island, Mississippi, at the beginning of the winter storm season in September, 1993. The lower photo shows the condition of the coast near the end of the winter storm season in March, 1994. Note the exposure of rocks along the shoreline that were at one time part of a breakwater system constructed by local citizens to protect the foundation of Fort Massachusetts (at left of photo).

As noted, physical evidence observed along the northern shores of barrier islands of the northern Gulf of Mexico indicates that these islands have experienced chronic erosion. A common sight along the northern shores of these islands is the exposed remnants of an ancient marsh (Figure 1.2). The marsh material was originally located in a low-lying area in the interior of the island. The exposure of this material along the foreshore indicates that the shoreline has retreated landward a significant distance over an extended period. A more common site along the northern shores of these islands is the exposed roots of living trees and shrubs. The trees and shrubs originally developed landward of the foredunes; however, their roots were subsequently exposed along the foreshore as the shoreline retreated landward (Figure 1.3). These types of physical evidence of chronic coastal erosion have been observed at multiple sites along the northern Gulf of Mexico including West Ship Island, Mississippi, Santa Rosa Island, Florida, and near Fort Morgan, Alabama.

Historical maps also indicate that the northern shores of barrier islands of the northern Gulf of Mexico have experienced severe cases of chronic erosion. The northern coast of West Ship Island, Mississippi retreated landward 0.5 m yr^{-1} over the period 1847-1986 (McBride *et al.* 1995), and the northern coast of Santa Rosa Island, Florida retreated landward 0.6 m yr^{-1} over the period 1856-1976 (USACE 1979). It is important to note that the rate of relative sea-level rise averaged 1.5 mm yr^{-1} over the period 1939-1983 at a National Ocean Survey (NOS) tide gauge located near West Ship Island, Mississippi, and the rate of relative sea-level rise averaged 2.3 mm yr^{-1} over the period 1923-1980 at a NOS tide gauge located near Santa Rosa Island, Florida (Penland *et al.* 1989). The tide data collected at these two sites

Figure 1.2. Ancient marsh material (peat) exposed along the shoreline by wave erosion of the northern coast of West Ship Island, Mississippi. Photo taken by the author in June, 1997.

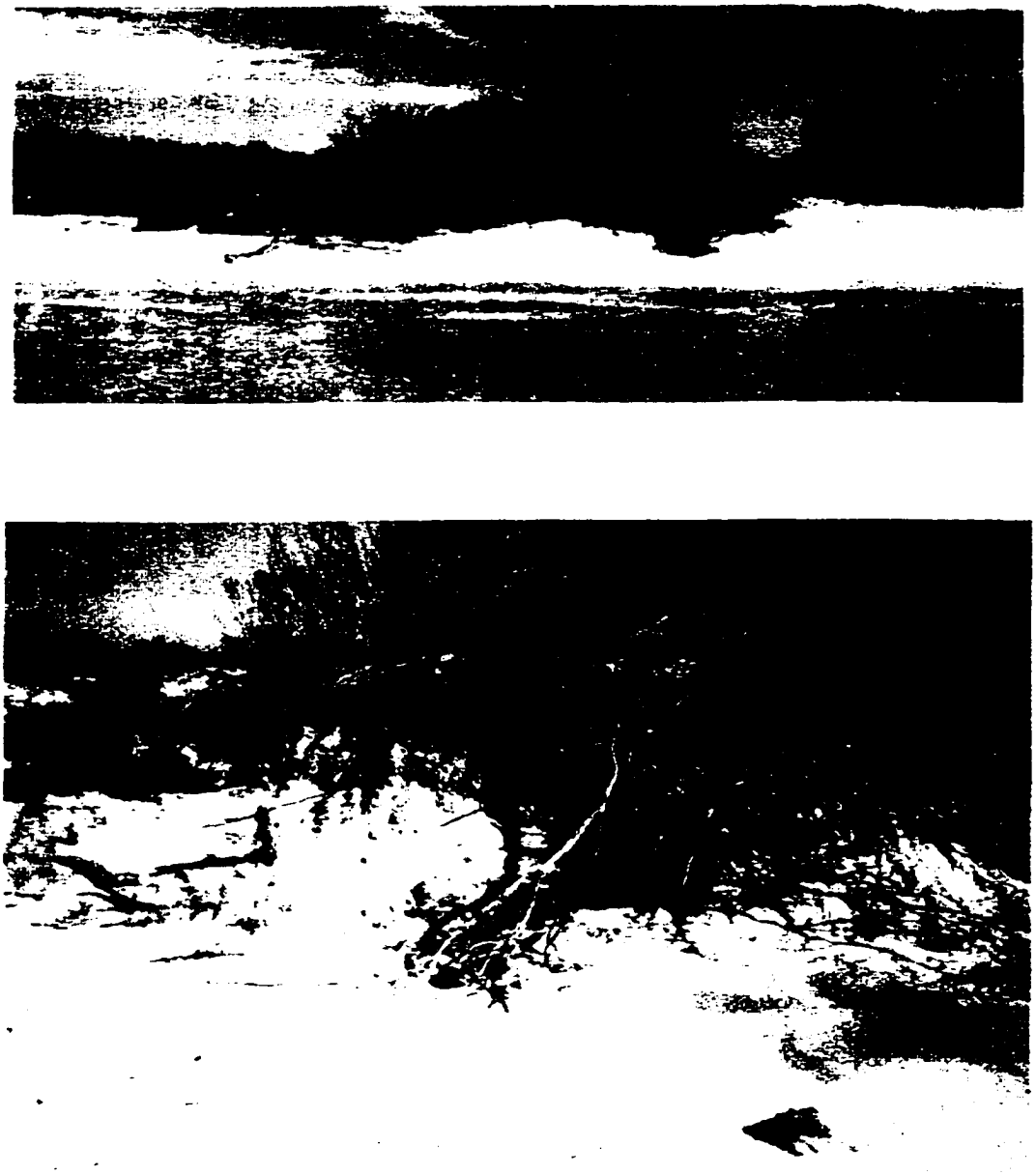

Figure 1.3. Roots of trees and shrubs exposed along the foreshore by wave erosion of the northern coast of West Ship Island, Mississippi. Both photos were taken along the eastern end of the island by the author. The upper photo was taken in August, 1996; the lower photo was taken in August, 1993.

suggest that the local rates of relative sea-level rise were too low to have had significant influences on the rates of shoreline retreat observed along the islands.

In south-central Louisiana, historical maps indicate that the northern shores of Raccoon Island, Trinity Island, Whiskey Island, and East Island of the Isles Dernieres barrier island complex retreated an average of approximately 2.1 m yr^{-1} over the period 1906-1988 (Williams *et al.* 1992). However, high rates of relative sea-level rise have been observed in the region (Penland and Ramsey 1990). The Isles Dernieres are located approximately halfway between Eugene Island and Grand Isle, which are located approximately 100 miles apart. The rate of relative sea-level rise averaged 11.9 mm yr^{-1} over the period 1934-1974 at a NOS tide gauge located at Eugene Island, Louisiana, and the rate of relative sea level rise averaged 10.4 mm yr^{-1} over the period 1934-1974 at a NOS tide gauge located at Grand Isle, Louisiana (Penland and Ramsey 1990). The rates of relative sea-level rise observed near the Isles Dernieres (10.4 mm yr^{-1} and 11.9 mm yr^{-1}) were approximately five times higher than the rates observed near West Ship Island, Mississippi (1.5 mm yr^{-1}), and Santa Rosa Island, Florida (2.4 mm yr^{-1}). The rate of shoreline retreat observed along the Isles Dernieres (2.1 m yr^{-1}) was approximately four times higher than the rates observed at West Ship Island (0.5 m yr^{-1}) and Santa Rosa Island (0.6 m yr^{-1}). The tide data collected at Eugene Island and Grand Isle suggest that the higher rate of relative sea-level rise along the south-central Louisiana coast may have had a significant influence on the rate of shoreline retreat observed along the Isle Dernieres barrier islands.

As noted earlier, the erosion problem observed along the northern shores of barrier islands in Mississippi and northwest Florida has largely been attributed to winter storm activity. At the conclusion of a beach nourishment monitoring program along the northern coast of West Ship Island, Mississippi, which was conducted as a response to severe erosion at the site, Henry (1977a) observed that "strong northers during the winter months" were the primary forcing agent in erosion observed during the study period. The term "norther" that Henry (1977a) used in the report refers to northerly winds associated with cold air masses migrating southward in winter (Moore 1988). The southward migrations of these cold air masses are influenced by mid-latitude cyclones (Moore 1988).

Mid-latitude cyclones are low-pressure weather systems with counter-clockwise wind rotation patterns. The rotation pattern of a mid-latitude cyclone acts as a heat-transfer mechanism which transports cold air into southerly latitudes and warm air into northerly latitudes. A distinguishing feature of a mature mid-latitude cyclone is the development of a "frontal system," with the fronts representing the leading edges of a cold air mass migrating southward and a warm air mass migrating northward (Lutgens and Tarbuck 1992) (Figure 1.4). The cyclonic rotation of these weather systems produces a distinctive reversal in wind directions along the northern Gulf Coast. As the cyclone migrates eastward across the central U.S., southerly, "pre-frontal" winds from the Gulf of Mexico flow northward towards the center of the low-pressure system. The leading edge of the southward migrating cold air mass, the "cold front," subsequently crosses the coast and northerly, "post-frontal" winds

prevail. These "northerly, post-frontal" winds are what Henry (1977a) was referring to in the comment on "strong northers during the winter months."

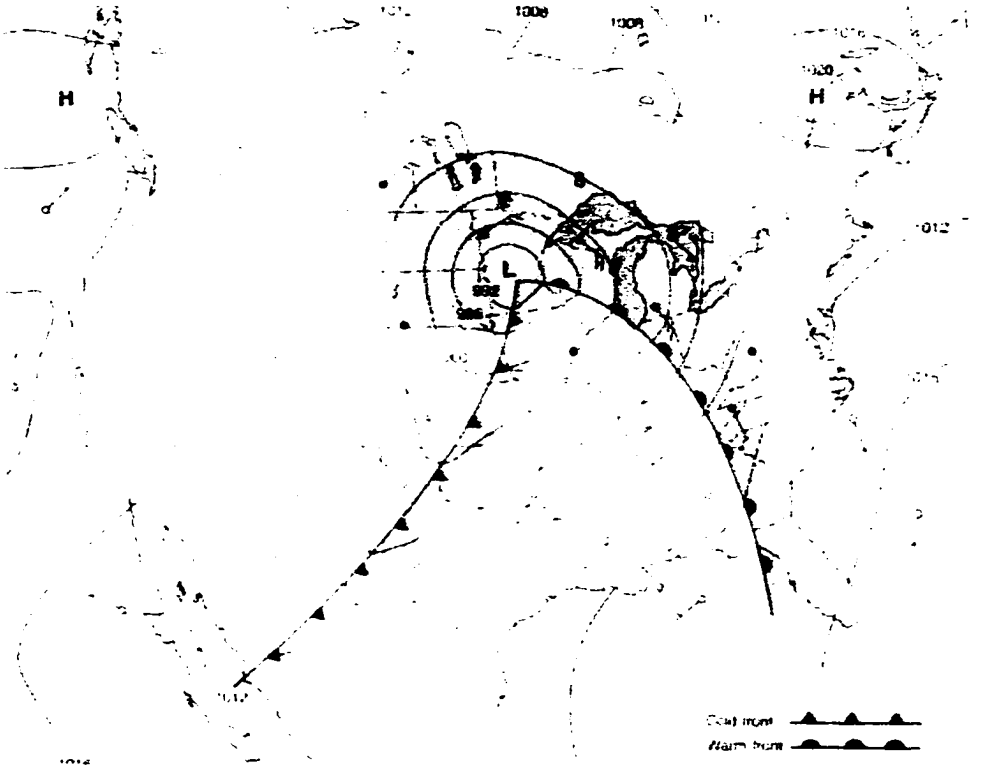

Figure 1.4. Diagram of a mid-latitude cyclone. The illustration shows the low-pressure center, frontal structure, and cyclonic (counter-clockwise) wind flow patterns associated with a typical mid-latitude cyclone. This figure was originally published by Lutgens and Tarbuck (1992).

Many characteristics of storms associated with mid-latitude cyclone activity along the northern Gulf of Mexico have been observed and noted in previous studies (Davis 1972; Fox and Davis 1976; Henry 1977a; Kemp and Wells 1987; Roberts *et al.* 1987, 1989; Reed 1989; Dingler and Reiss, 1990; Dingler *et al.* 1992, 1993; Hsu 1993; Leonard *et al.* 1995; Armbruster *et al.* 1995; Armbruster 1997; Chaney and Stone 1996). This body of literature contains invaluable data on storm dynamics and their impacts in a diverse range of coastal environments, but is limited in comprehensive studies.

In contrast, storm conditions and impacts associated with mid-latitude cyclone activity along the U.S. Atlantic Coast are better understood and documented because coastal storms in this area have received greater attention from the scientific community (Mather *et al.* 1964, 1967, Davis *et al.* 1972; Hayden and Dolan 1977; Nordstrom 1980; Dolan *et al.* 1988; Nordstrom and Jackson 1992; Jackson 1995; Dolan and Davis 1992a, 1992b; Davis *et al.* 1993; Davis and Dolan 1993; Jones and Davis 1995). Among the contributions of these studies are the identification of a complex assortment of weather patterns associated with storm activity along the Atlantic Coast (8 distinct storm types) (Davis *et al.* 1993; Davis and Dolan 1993), the development of a sophisticated, five-class, storm-magnitude scale for evaluating the impacts of individual storm events (Dolan and Davis 1992a), and the determination of the average frequency of storms in each of the five storm-magnitude classes for evaluating the annual variability in storm activity (Dolan and Davis 1992a).

Although Roberts *et al.* (1987) and Hsu (1993) have conducted research on storm types and storm magnitudes for the Gulf of Mexico, the two major storm types

identified by Roberts *et al.* (1987) were identified as the end members of a "spectrum of cold front types," and Hsu's (1993) research focused on Gulf cyclones which were not identified as a major storm type by Roberts *et al.* (1987).

A noteworthy finding of the research conducted along the U.S. Atlantic Coast is that coastal storms were also produced by "anticyclones" that originated in mid-latitude regions (Dolan *et al.* 1988; Davis *et al.* 1993; Davis and Dolan 1993). Anticyclones are the exact opposite of cyclones in that they are high-pressure weather systems with clockwise wind rotation patterns. Although Roberts *et al.* (1987) did not specifically identify anticyclones as one of the two major storm types for the Gulf of Mexico, one of the supporting diagrams of the two major storm types resembles an anticyclone. Furthermore, a subsequent field study of a cold front passage at Trinity Island, Louisiana, noted that the prevailing wind direction shifted from onshore to offshore when the "high-pressure" weather system (*i.e.* anticyclone) moved out of the area (Dingler *et al.* 1993). Coastal storms along the Gulf Coast and the Atlantic Coast are evidently associated with both mid-latitude "cyclones" and "anticyclones."

Another point worth noting is that the terms "extratropical storm" and "extratropical cyclone" are consistently used in the Atlantic Coast literature to distinguish between coastal storms associated with tropical weather system (*i.e.* hurricanes), and coastal storms associated with extratropical (mid-latitude) weather systems (Mather *et al.* 1967, Hayden and Dolan 1977; Dolan *et al.* 1988; Dolan and Davis 1992; Davis *et al.* 1993; Davis and Dolan 1993; Jones and Davis 1995). Since coastal storms along the Gulf Coast and the Atlantic Coast are evidently associated

with both "cyclones" and "anticyclones," the term "extratropical storm," appears to be the most "inclusive" term for describing these coastal storm events. And since the term "extratropical storm" is well established in the literature on coastal storms along the Atlantic Coast, this term will be used in subsequent discussions in this paper when referring to coastal storms associated with mid-latitude cyclone and anticyclone activity along the northern Gulf of Mexico.

The remainder of this chapter includes two sections on the findings of previous research on extratropical storm dynamics and impacts along the U.S. Atlantic Coast and the Gulf Coast, and a section on the objectives and methods of this dissertation research. The research design includes a comprehensive study of extratropical storm activity at West Ship Island, Mississippi (based on a multi-year record of weather conditions in the area), and a one-year field study of storm impacts along the northern coast of the island. This dissertation research was designed to build upon the present body of scientific literature on extratropical storm activity in the northern Gulf of Mexico which is evidently at an early stage of development.

EXTRATROPICAL STORMS

One of the most active areas of mid-latitude cyclone formation is along the lee (eastern) side of the Rocky Mountains (Reitan 1974; Zishka and Smith 1980; Roebber 1984). These cyclones follow the path of the polar jet stream which flows along the boundary of the circumpolar vortex. The annual cycle of differential heating associated with the Earth's orbit causes the circumpolar vortex in the northern hemisphere to expand in autumn and recede in spring. This annual cycle steers mid-latitude cyclones into more southerly latitudes in winter (Hayden and

Dolan 1977) which increases the frequency of cold front passages, and thus extratropical storm activity, along the northern Gulf Coast in winter (Figure 1.5). Approximately 45 cold fronts pass along the northern Gulf Coast each year (DiMego *et al.* 1976; Henry 1977b).

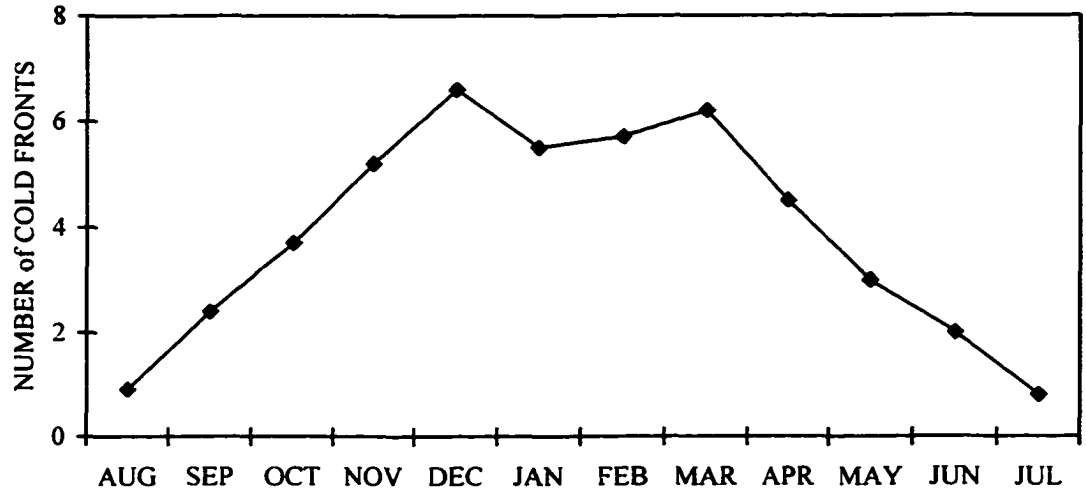

Figure 1.5 Average monthly frequency of cold front passages along the northern Gulf Coast over the period 1967-1977. This figure is based on data published by Henry (1977b).

The path of the polar jet stream around the globe resembles a series of standing waves with poleward ridges and equatorward troughs known as Rossby waves (Lydolph 1985; Lutgens and Tarbuck 1992). The amplitude of Rossby waves across the U.S. is influenced by the Pacific / North American (PNA) teleconnection (Wallace and Gutzler 1981; Leathers *et al.* 1991). The PNA teleconnection is composed of three upper-level atmospheric pressure centers: a low-pressure center over the Aleutian Islands, a high-pressure center over western Canada, and a low-pressure center over the eastern U.S. If the intensities of these pressure centers are

weak (negative PNA Index), then the polar jet stream follows a zonal (flat) path across the U.S. that steers cyclones along a more northerly track (Figure 1.6). If the intensities of these pressure centers are strong (positive PNA Index), then the polar jet stream follows a meridional (amplified) path across the U.S. that steers cyclones into more southerly latitudes. Since a relationship has been identified between the PNA Index and rainfall patterns over the southeastern U.S. (Henderson and Robinson 1994), the PNA Index may also prove to be an indicator of extratropical storm activity along the Gulf Coast.

Roberts *et al.* (1987, 1989) identified two distinct types of "cold fronts" which produced storms along the northern Gulf of Mexico (Figure 1.7). These two weather patterns were identified as the eastward migrating cyclone and the arctic surge, however, it was noted that these two types of "cold fronts" were the end-members of a spectrum of "cold front types." The diagram of the eastward migrating cyclone provided by Roberts *et al.* (1987) resembles the diagram of a classic mid-latitude cyclone shown in Figure 1.4, especially with the cold front passing along the northern Gulf Coast. The diagram of the arctic surge provided by Roberts *et al.* (1987) shows the cold front along the northern Gulf Coast as the leading edge of an anticyclone which appears to have migrated southward from Canada. The arctic surge was associated with "southward surges of arctic air" (Roberts *et al.* 1987) which evidently refers to the southward migration of a "continental arctic" air mass (Lutgens and Tarbuck 1992). Continental arctic air masses are high-pressure weather systems (*i.e.* anticyclones) that reside over northern Canada (Lutgens and Tarbuck 1992).

(A)

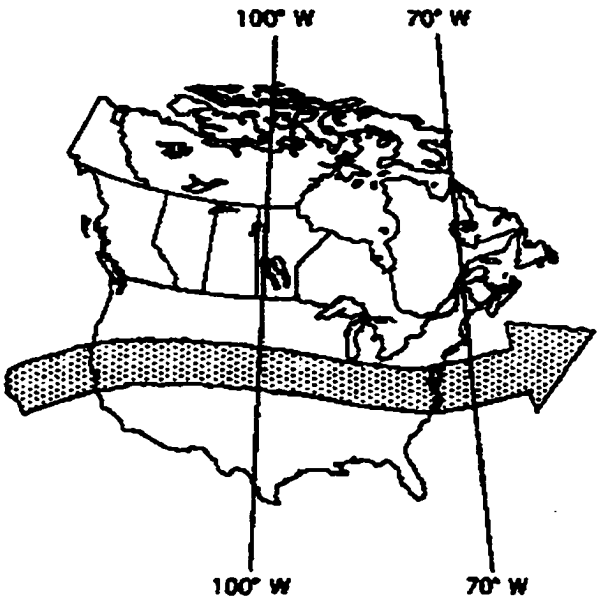

(B)

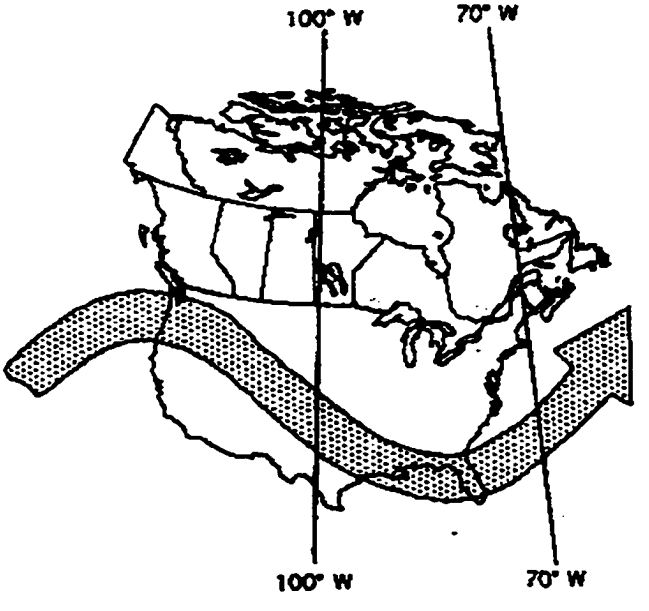

Figure 1.6. Zonal (a) and Meridional (b) flow patterns of the polar jet stream across the central U.S. This figure was originally published by Jones and Davis (1995).

Figure 1.7. Cold front types identified by Roberts *et al.* (1987). The upper diagram shows the eastward migrating cyclone and the lower diagram shows the arctic surge.

The diagram of the arctic surge identified by Roberts *et al.* (1987) also resembles the diagram of the Continental High "synoptic weather type" identified by Muller and Wax (1977), and the diagram of the eastward migrating cyclone identified by Roberts *et al.* (1987) resembles the diagram of the Pacific High identified by Muller and Wax (1977) (Figure 1.8). Muller and Wax (1977) also identified a synoptic weather type known as Frontal Overrunning that occurs after a cold front passes over the coast. The average annual frequency of Frontal Overrunning is approximately 66.4 days per year, with the highest average frequency in January (11.5 days) (LOSC 1997). It is important to note that the frequencies of these "synoptic weather types" are recorded by the "number of days" the weather type is observed, not by the "number of events."

Another type of mid-latitude cyclone associated with storm activity in the Gulf of Mexico is the Gulf cyclone. Approximately 10 Gulf cyclones develop over the eastern Texas / western Gulf of Mexico region each year (Saucier 1949; Hsu 1993). Gulf cyclones may develop over land or water (Saucier 1949), and may intensify as they migrate eastward over the Gulf of Mexico (Johnson *et al.* 1984; Lewis and Hsu 1992). Research on coastal storm activity along the U.S. Atlantic Coast suggests that Gulf cyclone storm tracks often pass across the central region of the Gulf of Mexico, make landfall along the Florida panhandle, then migrate northeastward along the Atlantic Coast (Davis and Dolan 1993; Davis *et al.* 1993).

Although a frontal system may develop as the cyclone matures over the Gulf of Mexico (Atlas *et al.* 1983; Lewis and Hsu 1992), it appears that the cold fronts rarely impact the north-central Gulf Coast because of the southerly storm track. The

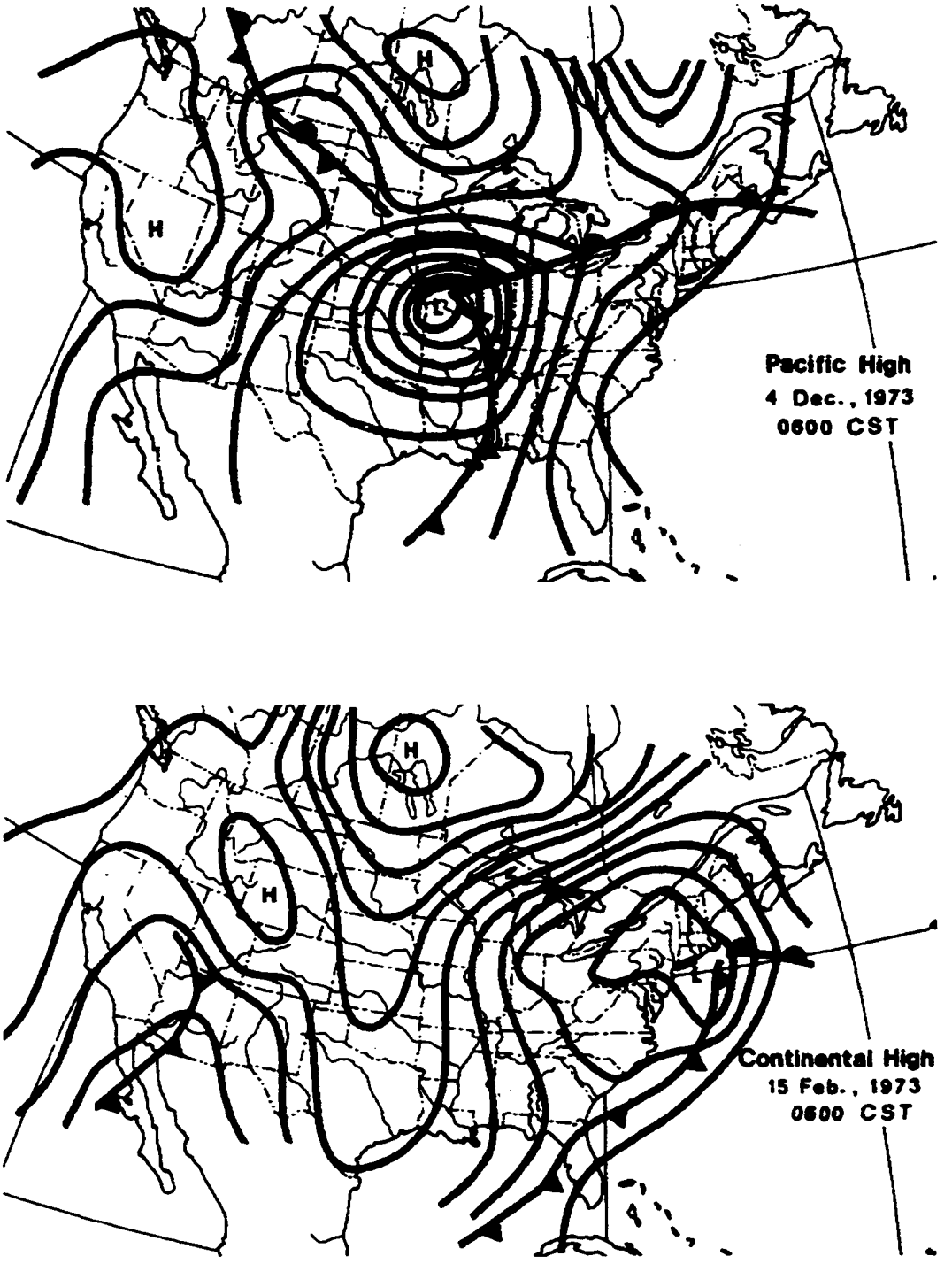

Figure 1.8. Synoptic weather types identified by Muller and Wax (1977). The upper diagram shows the Pacific High weather type associated with the eastward migration of a high-pressure air mass behind a cold front. The lower diagram shows the Continental High weather type associated with the southward migration of a high-pressure air mass behind a cold front.

low-pressure weather system, however, sets up a pressure gradient in the region that produces intense, northerly winds along the northern Gulf Coast. Therefore, these weather systems still represent a threat to the northern shores of barrier islands along the northern Gulf of Mexico. Furthermore, if the storm track turned northward, the impact along the barrier islands would most likely resemble the impact of a minor hurricane. Hsu (1993) proposed an intensity scale for Gulf cyclones based on the minimum central pressure of the cyclone which relates to wind speed (Table 1.1). The "Hsu scale" suggests that the physical impact of a Class 5 Gulf cyclone would approach the impact of Class 1 hurricane (Table 1.2).

Table 1.1 Hsu Scale of storm intensity for Gulf cyclones. The scale was based on the minimum central pressure of extratropical cyclones in the Gulf of Mexico from 1972-1982 (Hsu 1993).

Gulf Cyclone Storm Class	Sustained Wind Speed (m/s)	Sustained Wind Speed (mph)	Central Pressure (mb)
1	8-10	18-24	1014-1013
2	11-14	25-33	1012-1007
3	15-17	34-39	1006-1001
4	18-21	40-48	1000-991
	22-25	49-56	990-981

Table 1.2. Saffir-Simpson Scale of storm intensity for hurricanes. The scale is based on the sustained wind speed of tropical cyclones (Simspon 1974).

Hurricane Storm Class	Sustained Wind Speed (m/s)	Sustained Wind Speed (mph)	Central Pressure (mb)
1	33-42	74-95	> 979
2	43-49	96-110	965-979
3	50-58	111-130	945-964
4	59-69	131-155	920-944
5	> 69	> 155	< 920

Atmospheric instability associated with a cold front passage has been cited as a significant factor in Gulf cyclone development (Saucier 1949; DiMego *et al.* 1976; Johnson *et al.* 1984). A classic example is the "Storm of the Century" of March, 1993 (Walker 1993; Schuman *et al.* 1995). The storm initially developed along a cold front stalled over the Gulf of Mexico. The cyclone then migrated eastward across the Gulf and produced a 4 m storm surge when it made landfall along the Florida panhandle (Schuman *et al.* 1995). The central pressure of the cyclone was approximately 977 mb when it made landfall (Schuman *et al.* 1995). This equates to a wind speed of approximately 26 m sec^{-1} (Hsu 1993) which indicates that the storm was greater than a Class 5 cyclone on the "Hsu Scale." The storm subsequently migrated northeastward along the Atlantic Coast and grew to the size of a full-scale, mid-latitude cyclone when it reached the northeastern U.S. The tremendous amount of damage caused by the storm led to its famous name (Schuman *et al.* 1995).

Coastal storms associated with mid-latitude cyclone activity along the Atlantic Coast are commonly known as "northeasters" because northeasterly winds often prevail during the storm (Davis and Dolan 1993). Mather *et al.* (1964) reviewed northeaster activity along the Atlantic Coast for the period 1921-1962 and identified eight types of weather patterns which produced coastal storms. Tropical cyclones were identified as one storm type, localized storms associated with squall lines that precede cold fronts were identified as a second storm type, and various forms of mid-latitude cyclone activity were associated with the remaining six storm types. These six storm types included cyclones that developed eastward of the Atlantic Coast near Cuba or the Bahamas, cyclones that developed along stationary

fronts over the southeastern U.S. (or just off the Atlantic Coast), cyclones that developed along stationary fronts over the Gulf of Mexico (Gulf cyclones), cyclones that developed along the mid-Atlantic Coast near Cape Hatteras, North Carolina, cyclones that developed in the interior of the U.S. and migrated eastward across the Atlantic Coast, and cyclones that developed in the interior of the U.S. and migrated northeastward along the Atlantic Coast (but remained over land). Mather *et al.* (1967) subsequently published an evaluation of the spatial extent of the impacts of these storms along the Atlantic Coast over the period 1935-1964.

Hayden and Dolan (1977) evaluated extratropical storm activity along the Atlantic Coast for the period 1952-1974 and noted a distinct relationship between the average latitudinal position of the polar jet stream each month of the year and the monthly frequency of storms at Cape Hatteras, North Carolina. An updated review of variability in the position of the polar jet stream and extratropical storm activity along the Atlantic Coast was most recently published by Jones and Davis (1995). Dolan *et al.* (1988) used estimates of deep-water wave heights during storms at Cape Hatteras, North Carolina, to evaluate seasonal variability in extratropical storm intensity and duration for the period 1942-1984. Dolan and Davis (1992a, 1992b) subsequently proposed a storm intensity scale based on those estimates (Table 1.3).

Davis *et al.* (1993), and Davis and Dolan (1993) identified eight synoptic weather patterns associated with extratropical storm activity along the Atlantic Coast, seven of which corresponded with those previously identified by Mather *et al.* (1964). These seven storm types were identified as the Bahamas Low, Florida Low, Gulf Low, Coastal Plain Cyclogenesis, Hatteras Low, Continental Low, and the

Coastal Front. The additional storm type identified by Davis *et al.* (1993) and Davis and Dolan (1993) was the Anticyclone. Davis *et al.* (1993) noted that anticyclones originate over the Great Basin and northern Plains of the U.S., and over central Canada, and then migrate eastward across the U.S. to the Atlantic Coast to produce northeaster storms. It should be noted that Dolan *et al.* (1988) had previously associated anticyclones with extratropical storm activity along the Atlantic Coast. Extratropical storms have therefore been associated with both mid-latitude "cyclone" and "anticyclone" activity along both the Atlantic Coast (Dolan *et al.* 1988; Davis *et al.* 1993; and Davis and Dolan 1993), and the Gulf Coast (Roberts *et al.* 1987; Dingler *et al.* 1993). The storm types identified by Davis *et al.* (1993) and Davis and Dolan (1993) are shown in Figure 1.9.

Table 1.3. Dolan-Davis Scale of storm intensity for northeasters at Cape Hatteras, North Carolina. The scale was based on data collected for 1942-1984. Storm duration (T) was identified as the total number of hours that significant wave heights (H_s) exceeded 1.6 m. Storm power was based on the following equation [(Maximum $H_s)^2$ * T]. (Dolan and Davis 1992a).

Northeaster Storm Class	Avg. Annual Frequency (# of storms)	Avg. Significant Wave Height (m)	Average Storm Duration (hours)	Average Storm Power (m^2 hr)
1	16.0	2.0	8	32
2	8.1	2.5	18	107
3	7.1	3.3	34	353
4	0.8	5.0	63	1455
5	0.1	7.0	96	4548

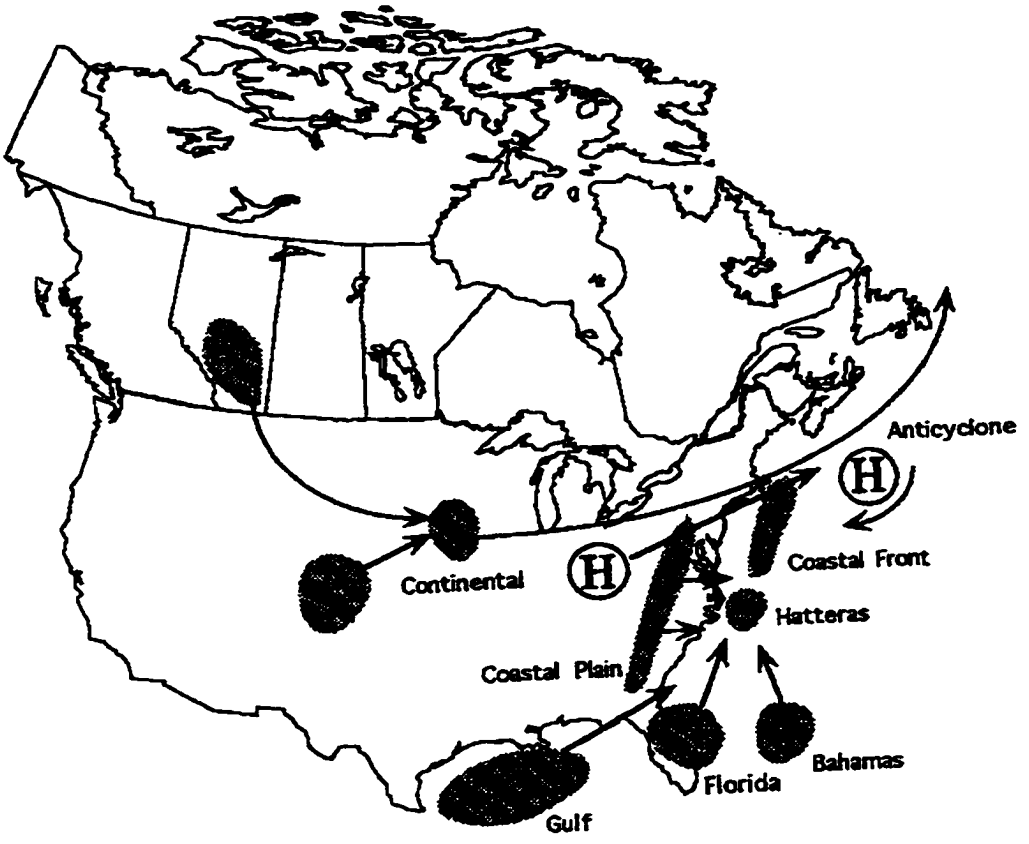

Figure 1.9. Formation regions and storm tracks of the eight northeaster storm types identified by Davis *et al.* (1993) and Davis and Dolan (1993). The shaded areas show the areas of formation and the arrows show the storm tracks. This diagram was originally published by Jones and Davis (1995).

A number of the more recent studies on northeaster activity along the Atlantic Coast emphasized the need to distinguish between storms associated with extratropical weather systems and tropical weather systems because they differed considerably in size, frequency, and intensity (Dolan and Davis 1992; Davis *et al.* 1993; Davis and Dolan 1993; and Jones and Davis 1995). These studies noted that although tropical cyclones (*i.e.* hurricanes) are associated with extremely intense storm events (as evidenced by the Saffir-Simpson hurricane intensity scale shown in Table 1.2), extratropical weather systems actually produce geographically larger and more frequent storm events. They also noted that extratropical storms were shown by Mather *et al.* (1964) to be responsible for a greater amount of damage along Atlantic Coast barrier islands.

The same points regarding the impacts of northeasters and hurricanes along the Atlantic Coast were made in an earlier paper by Wolman and Miller (1960) which considered "the relative importance in geomorphic processes of extreme or catastrophic events and more frequent events of smaller magnitude." Roberts *et al.* (1987) made a similar observation on the difference between the impacts of cold fronts and hurricanes along the northern Gulf of Mexico and noted that cold fronts "appear to drive greater cumulative physical change."

Coastal storm research in the U.S. has traditionally focused on tropical cyclone (*i.e.* hurricane) activity (Sheets 1990), and the impacts of Hurricane Andrew in 1992 (Stone and Finkl 1995) and Hurricane Opal in 1995 (Stone *et al.* 1996) provided more recent opportunities for research on these storms in the Gulf of Mexico. The frequency of tropical cyclone activity in the Gulf, however, is relatively

low at approximately 3 storms per year. More specifically, approximately 1.1 "hurricanes" and 1.6 "tropical storms" per year made landfall in the Gulf of Mexico over the period 1941-1990 (NOAA 1993). It should be noted that tropical cyclones with sustained wind speeds equal to or greater than 18 m sec^{-1} (38 mph), but less than 33 m sec^{-1} (74 mph), are technically classified as "tropical storms," and tropical cyclones with sustained wind speeds of 33 m sec^{-1} (74 mph) or greater are technically classified as "hurricanes" (NOAA 1977, 1993).

In recent years, extratropical storms have received greater attention from researchers working along both the Atlantic Coast and the Gulf Coast. The scientific interest in extratropical storm activity along the northern Gulf of Mexico appears justly warranted, especially when considering the chronic shoreline erosion problem observed along the northern shores of barrier islands in the region, the limited availability of scientific literature on extratropical storm activity in the region, the significant difference in the frequency of cold fronts and tropical cyclones that impact the Gulf Coast each year, and the observations of Roberts *et al.* (1987) on the predominant influence of cold fronts along the northern Gulf Coast.

FIELD STUDIES OF EXTRATROPICAL STORM IMPACTS

Field research on extratropical storm impacts has been conducted in a diverse range of environmental settings along the Gulf Coast, the Atlantic Coast, and the shores of Lake Michigan. In the Gulf of Mexico, studies have been conducted along the coastal plain shores of Tabasco, Mexico (Psuty 1965, 1967); the Gulf coast of Mustang Island, Texas (Davis 1972; Fox and Davis 1976); the muddy, chenier plain coasts of southwestern Louisiana (Kemp and Wells 1987; Roberts *et al.* 1987, 1989),

the Gulf coast of Trinity Island, Louisiana (Dingler and Reiss 1990; Dingler *et al.* 1992, 1993); along the north-facing, bayside shores of Santa Rosa Island, Florida (Armbruster *et al.* 1995; Armbuster 1997) and West Ship Island, Mississippi (Chaney and Stone 1996); and in the coastal marsh settings of Terrebonne Bay, Louisiana (Reed 1989) and Crystal River, Florida (Leonard *et al.* 1995).

Field studies on cold fronts have also been conducted along both eastern and western shores of Lake Michigan (Fox and Davis 1970, 1976). The impacts of northeasters have been studied along both ocean and bayside coasts of Sandy Hook Spit, New Jersey (Nordstrom 1980), and along the estuarine shores of Raritan Bay and Delaware Bay, New Jersey (Nordstrom 1980; Nordstrom and Jackson 1992; and Jackson 1995).

These studies identified a number of ways in which extratropical storms influenced coastal environments and proposed several conceptual models on storm dynamics and beach responses. The following review discusses the more significant contributions of these studies. The morphological zones of the beach referred to in this discussion are illustrated in Figure 1.10.

A field study of beach ridge development along the coastal plain shores of Tabasco, Mexico (Psuty 1965, 1967) was one of the earliest studies to suggest that extratropical storms play a significant role in the evolution of coastal environments of the Gulf of Mexico. Cold fronts penetrating deep into the Gulf produce strong northerly winds along the Tabasco coast which are locally known as "*Nortes.*" *Norte* winds were observed increasing wave heights and water levels which repeatedly overwashed the beach. These overwash events redistributed sediment supplied by a

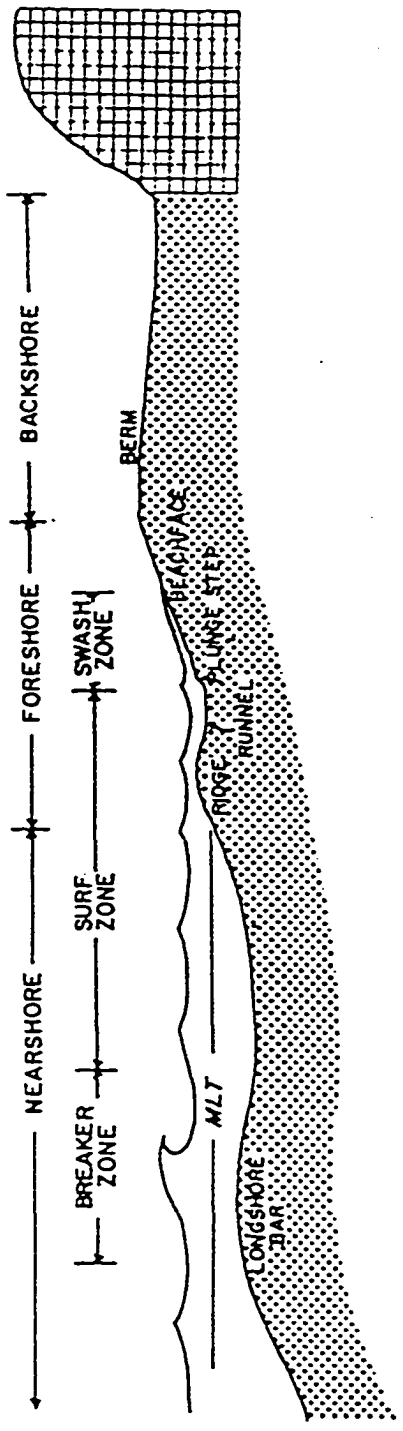

Figure 1.10. Morphological zones of the beach (Schwartz 1982).

local source, the Grijalva River, which contributed to the development of the beach-ridge plain along the coast. Taylor and Stone (1996) have since disputed Psuty's (1965, 1967) interpretation of the role of storms in beach ridge development.

Fox and Davis (1976) proposed a conceptual model of storm dynamics for a cold front passage along the Texas coast based on the experienced gained in three 30-day field studies conducted along the shores of Lake Michigan and two 30-day field studies conducted along the Gulf coast of Mustang Island, Texas (Fox and Davis 1970, 1976). The model for the Texas coast (Figure 1.11) shows that barometric pressure decreases as the front passes over the coast, and then barometric pressure and wind speed subsequently increase. Also, a reversal in wind direction as the front passes over the coast results in a reversal in alongshore current direction. More specifically, Fox and Davis (1976) suggested that wind direction shifts from southwest to northeast when a cold front passes along the Texas coast. After the front passes over the coast, wind speeds peak at 15 m sec^{-1}, wave heights peak at 1.2 m, and alongshore surface currents peak at 60 cm sec^{-1}. Also, wind speeds average 8-10 m sec^{-1} over the duration of a storm.

Roberts *et al.* (1987, 1989) proposed a three-phase conceptual model of storm dynamics for a cold front passage along the Louisiana coast (Figure 1.12 and 1.13). The three phases of the model are the pre-frontal, the frontal passage, and the post-frontal. The pre-frontal phase consists of southerly winds which direct waves onshore and setup water levels along the coast. The frontal passage phase consists of a decrease in barometric pressure and increase in wind speed. The post-frontal phase consists of a distinct shift from southerly to northerly winds which consequently re-

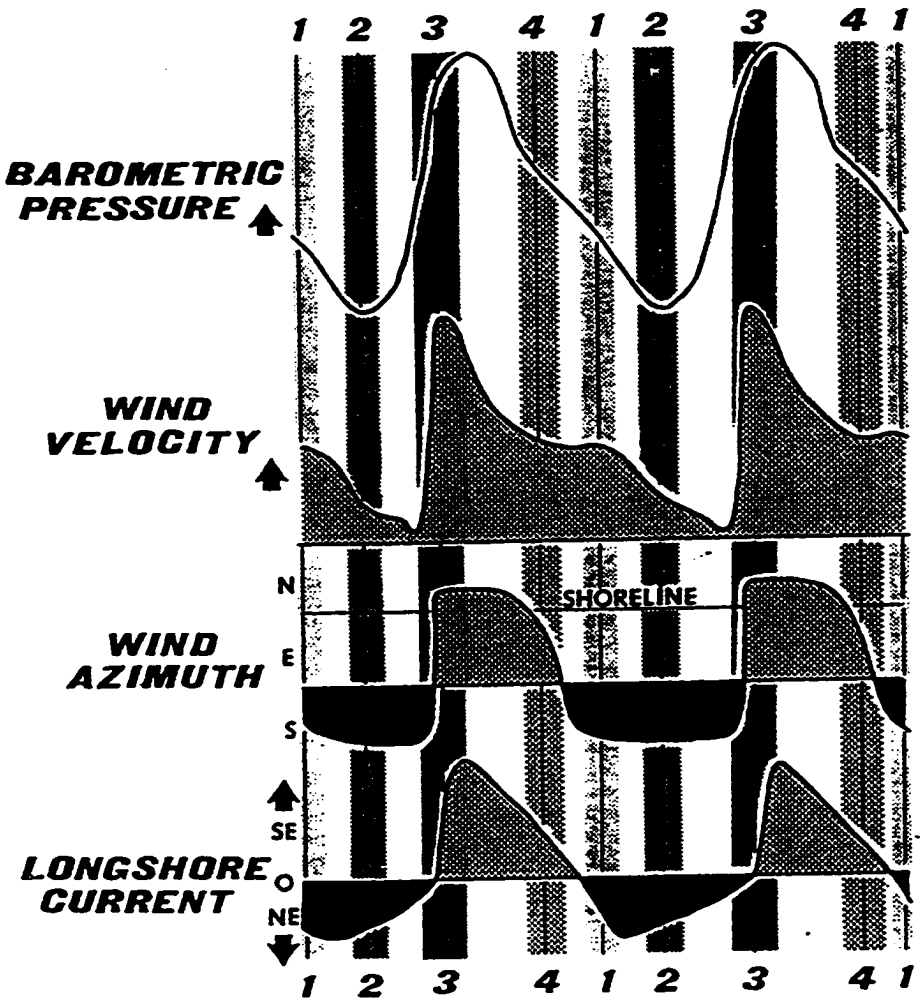

Figure 1.11. Conceptual model of storm dynamics for a cold front passage along the Gulf coast of Mustang Island, Texas. The numbers along the bottom of the diagram correspond to different phases of the storm with #3 representing the frontal passage (Fox and Davis 1976).

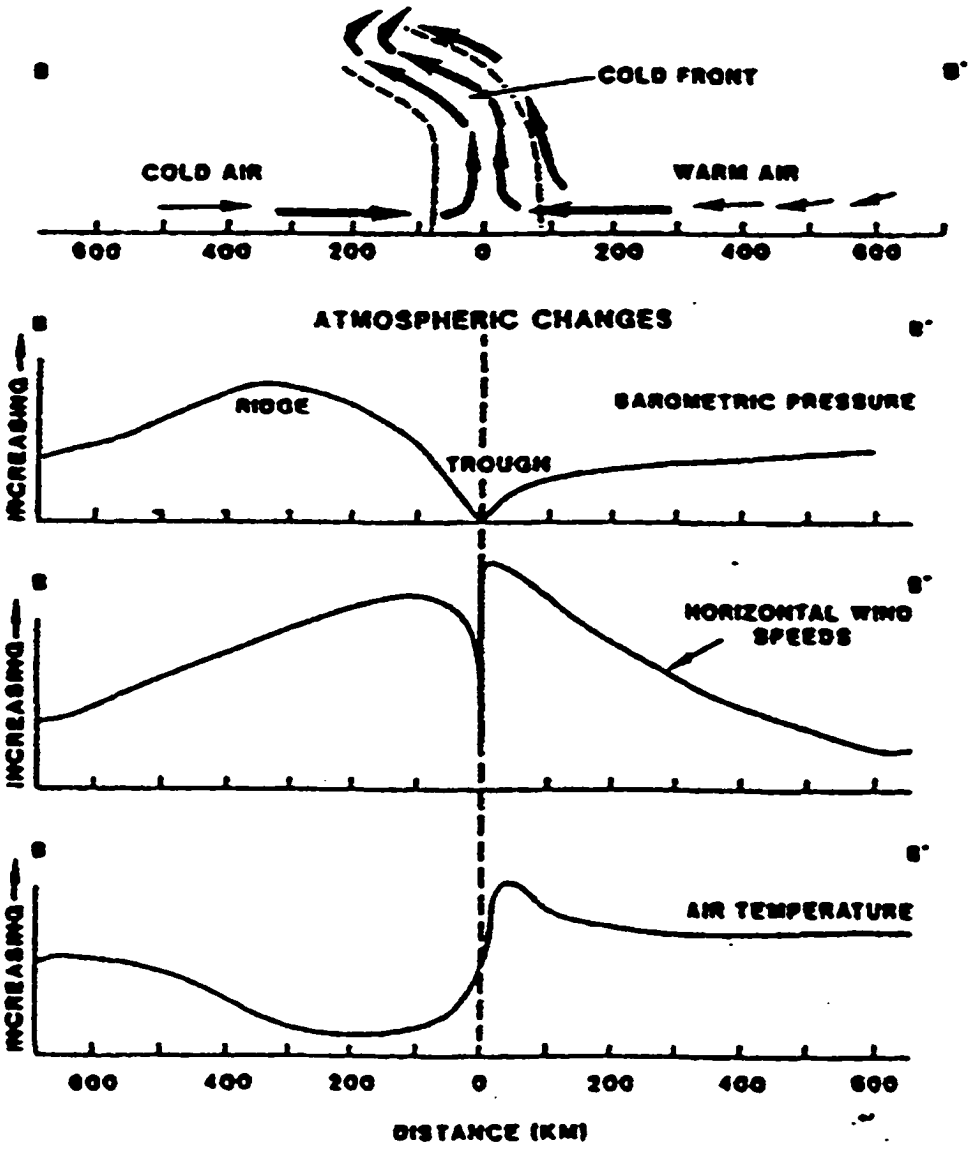

Figure 1.12. Conceptual model of atmospheric conditions along a cross-sectional profile of a cold front (Roberts *et al.* 1987).

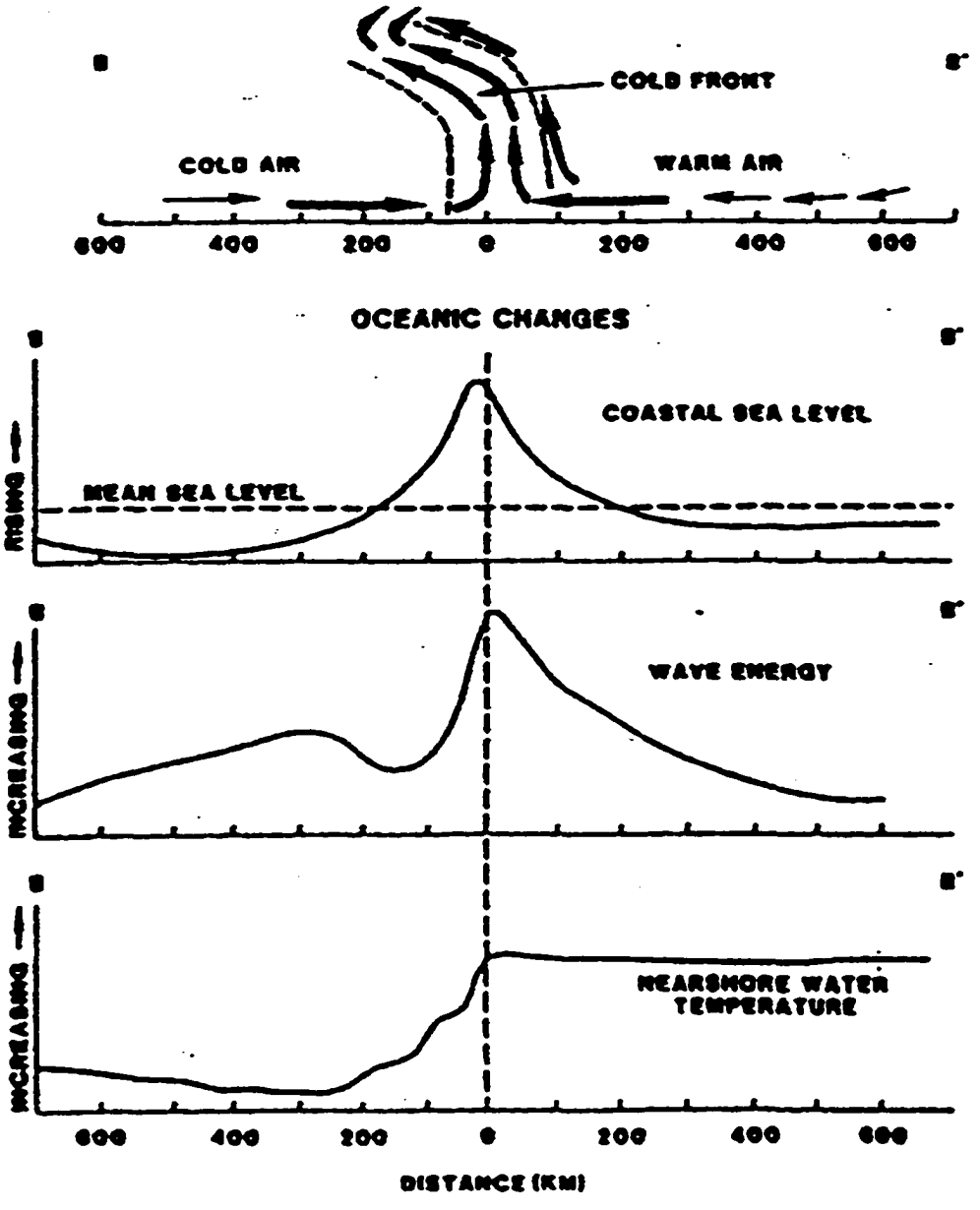

Figure 1.13. Conceptual model of oceanographic conditions along a cross-sectional profile of a cold front (Roberts *et al.* 1987).

direct waves offshore and setdown water levels along the coast. The post-frontal phase also includes an increase in barometric pressure and a decrease in temperature. Fronts oriented at oblique angles (NE-SW) to the Louisiana coast were associated with southeasterly, pre-frontal winds, and fronts oriented parallel to the coast (E-W) were associated with southwesterly, pre-frontal winds.

As noted earlier, Roberts *et al.* (1987, 1989) identified two distinct types of cold fronts: the eastward migrating cyclone and the arctic surge. The eastward migrating cyclone was identified as having "stronger" pre-frontal winds, but "weaker" post-frontal winds, than the arctic surge type. The eastward migrating cyclone was also associated with fronts oriented at oblique angles to the coast, and the arctic surge was associated with fronts oriented parallel to the coast.

Roberts *et al.* (1987) observed that although hurricanes produced more "violent" storms, cold fronts appeared to have a "greater cumulative effect" along Louisiana coasts because of their "uniform direction of approach, repeated pattern of wind changes, large spatial scales, and much higher frequency of occurrence." Roberts *et al.* (1987) discussed a number of ways in which pre- and post-frontal storm conditions may impact Louisiana's coastal environments which include the sediment-rich coast of the Atchafalaya Delta, the transitional coast of the chenier plain in southwestern Louisiana, and the sediment-poor coasts of Louisiana's barrier islands. The most relevant aspect of this discussion to the focus of this dissertation research was the observation that northerly, post-frontal winds produced "short-fetch" waves in the back-barrier lagoons which impact the northern shores of the barrier islands.

As suggested by Roberts *et al.* (1987), subsequent research indicated that cold fronts had a significant influence on sediment transport processes along the muddy, chenier plain coasts of southwestern Louisiana (Roberts *et al.* 1989). Field observations indicated that southeasterly, pre-frontal winds and waves directed sediment-laden waters of the Atchafalaya River "mud-stream" westward along the coast and overwashed the beach. Northerly, post-frontal winds subsequently setdown water levels and desiccated the muddy washover deposits. The end result was progradation of the shoreline through armoring of the beach with muddy, cohesive sediments (Roberts *et al.* 1989).

Dingler *et al.* (1992) monitored the post-frontal phase of an arctic surge during an 8-day field study along the Gulf coast of Trinity Island, Louisiana. The front stalled along the coast and produced strong northerly winds in excess of 6 m sec^{-1} for approximately 4 days. The maximum wind speed during this period was approximately 11 m sec^{-1}. The northerly, post-frontal winds transported backshore sands to the upper beach face while waves transported lower beach face sediment offshore. Erosion along the backshore of the 400 m wide monitoring site was 1.26 m^3 m^{-1}. During the remaining 4 days of the study, weak southerly winds (6 m sec^{-1} or less) transported upper beach face sands to the backshore. Deposition along the backshore was 0.45 m^3 m^{-1}. The end result was minimal erosion of the backshore by aeolian transport and moderate erosion of the beach face by storm waves.

Dingler *et al.* (1993) presented evidence for a cyclical pattern of beach profile responses to storm impacts based on a 5-year study along the Gulf coast of Trinity Island, Louisiana. Survey data showed that between August, 1986, and mid-

September, 1988, shoreline retreat at the site averaged approximately 17.5 m yr^{-1}. In late-September, 1988, storm waves from Hurricane Gilbert overwashed the site and eroded 9 m of shoreline. The position of the shoreline remained relatively unchanged during the post-hurricane period from late-September, 1988, to November, 1989. Between November, 1989, and April, 1991, shoreline retreat returned to its pre-hurricane Gilbert rate. Although the initial impact of the hurricane eroded the shoreline, the end result was a temporary reduction in the rate of shoreline retreat.

In the first phase of the cycle, hurricane-induced storm waves overwash the beach and flatten the profile (Figure 1.14). In the second phase, southerly, pre-frontal storm waves repeatedly overwash the beach and deposit sediment along the crest of the berm and the backshore. In the third phase, the profile reaches a critical state where the elevation of the berm crest and the slope of the beach face inhibit further overwash. At this critical point, the beach face begins to erode and returns to its pre-hurricane rate of shoreline retreat. Finally, a subsequent hurricane impact overwashes the beach and the cycle repeats (Dingler *et al.* 1993).

Nordstrom and Jackson (1992) proposed a conceptual model of profile responses to storm impacts for estuarine beaches. The model was based on a long-term study of northeaster impacts along the Atlantic coast. The field research was conducted on Raritan Bay and Delaware Bay, New Jersey, over the period 1972-1990. Both estuaries are micro-tidal environments with spring tidal ranges of approximately 2.0 m. The model includes two alternative responses of the profile to storm impacts based on wave height (Figure 1.15). In the first response, the slope of the beach flattens as sediment is eroded from the upper beach face and deposited

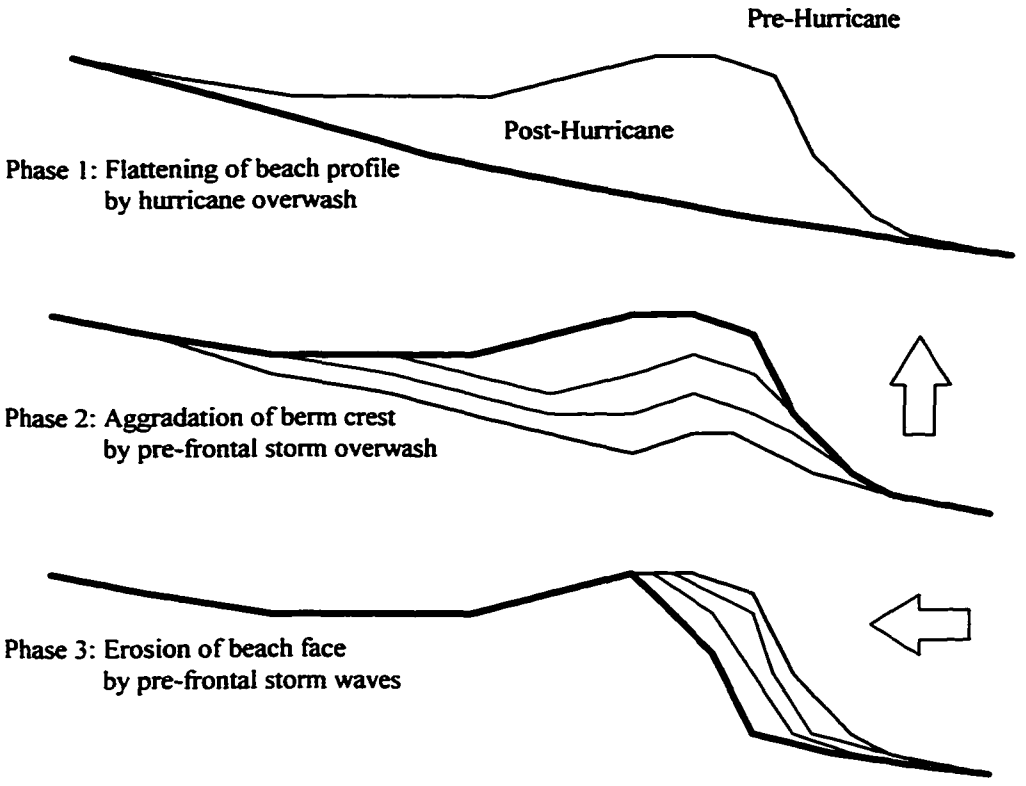

Figure 1.14. Conceptual model of beach profile responses to hurricane overwash and cold front impacts along the Gulf coast of Trinity Island, Louisiana. In phase 1, hurricane-induced storm waves overwash the beach and flatten the slope of the profile. In phase 2, pre-frontal passage storm waves deposit sediment along the crest of the berm. In phase 3, pre-frontal passage storm waves erode the beach face once the elevation of the berm and the slope of the beach reach a critical level. The diagram is based on the observations of Dingler *et al.* (1993).

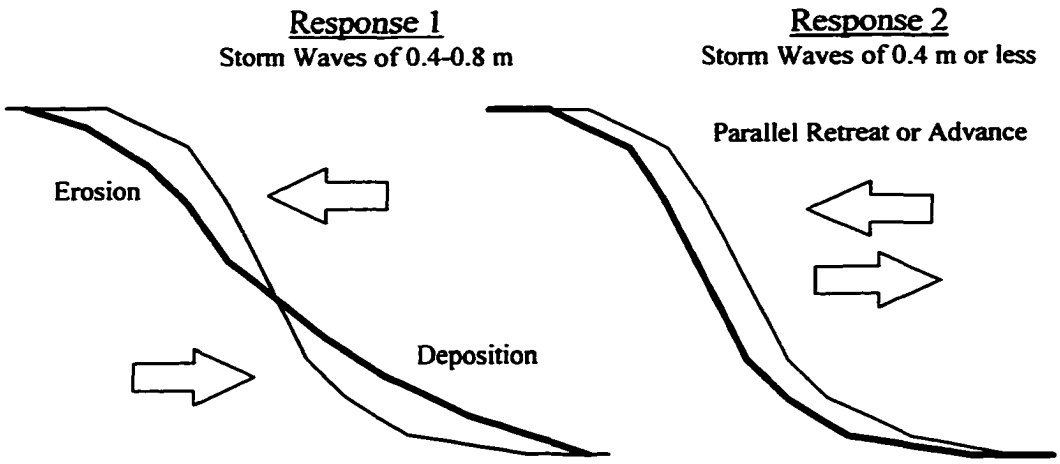

Figure 1.15. Conceptual models of beach profile responses to northeaster storm impacts along an estuarine coast. Response 1 shows upper foreshore erosion and lower foreshore deposition. This response occurs at all locations along the beach. Response 2 shows parallel retreat or advance of the entire beach face. The response at any given point is related to its relative location within an isolated cell, and the direction of sediment transport. This diagram is based on models published in Nordstrom (1992) and Nordstrom and Jackson (1992).

along the lower beach face and step. The volume of sediment exchanged between upper and lower sections of the foreshore determines the magnitude of change in the slope of the beach. This response was associated with storm wave heights of 0.4-0.8 m.

In the second response, the slope of the beach remains constant as the entire beach face undergoes either parallel retreat or advance. This response occurs within isolated cells between headlands or man-made structures. The response at any given location is related to the direction of sediment transport within the cell, and the relative location of the profile along the cell. Therefore, profiles located near endpoints of cells show greater magnitudes of change than profiles located near midpoints (Nordstorm 1992). This response was associated with storm wave heights of 0.4 m or less.

In each response, sediment exchange was restricted to the beach: no post-storm recovery phase was detected. Sediment eroded from the beach was thought to be distributed as a thin veneer across the low-tide terrace. Because each site has semi-diurnal tides, the high level of activity across the low-tide terrace was thought to inhibit nearshore bar formation which contributed to the absence of a post-storm recovery phase (Nordstorm 1992).

Armbruster *et al.* (1995) conducted a 28-day field study of cold front impacts along the north-facing, bayside coast of Santa Rosa Island, Florida. The impacts of an arctic surge and three migrating cyclones were observed during the study. The post-frontal phase of the arctic surge was associated with a significant decrease in water levels in Pensacola Bay, Florida, and the pre-frontal phases of the migrating cyclones

were associated with significant increases in water levels in the bay. Data presented for the post-frontal phase of the third migrating cyclone observed during the study indicated that winds were from the northwest, wind speeds exceeded 6 m sec^{-1} for 10 hours (max. = 9.3 m sec^{-1}) and significant wave heights exceeded 14 cm for 6 hours (max. = 18 cm). Eastward, alongshore currents exceeded 5 cm sec^{-1} throughout the 14 hour monitoring period (max. = 11 cm sec^{-1}), and onshore currents remained under 4 cm sec^{-1} throughout the 14 hour monitoring period.

Survey data collected by Armbruster *et al.* (1995) indicated that the foreshore of the beach increased 0.25 m in width (at 0 elevation NGVD), but decreased 0.69 m^3 in volume, from the impact of the first storm (the arctic surge). The foreshore increased in width and volume (+0.26 m and + 0.75 m^3 , respectively) from the impacts of the second and third storms, combined. The foreshore subsequently decreased 1.75 m in width and 1.98 m^3 in volume from the impact of the final storm. The final results indicated that the foreshore decreased 1.65 m in width and decreased 1.76 m^3 in volume from the impact of the four storms.

Armbruster (1997) presented additional results from the field study conducted along the northern coast of Santa Rosa Island, Florida (Armbruster *et al.* 1995). Two sites had been monitored during a 21-week study period that extended from December, 1994, to May, 1995. Site 1 extended 120 m along the coast and consisted of 5 profile lines spaced at 30 m intervals. Site 2 extended approximately 300 m along the coast and was composed of 4 profile lines spaced at approximately 100 m intervals. Site 1 was located westward of Site 2. Site 1 decreased in volume approximately 1.65 m^3 m^{-1} by the end of the study period. The western 200 m of Site

2 decreased in volume approximately 0.3 m^3 m^{-1} during the study period, but the eastern 100 m increased in volume approximately 1.5 m^3 m^{-1}. The shoreline retreated landward an average distance of 0.76 m^3 at the two sites, but distances varied considerably and ranged from +3.0 m to -3.5 m.

Armbruster (1997) suggested that changes in water level were a significant component of storm dynamics because they influenced the height at which storm waves impacted the foreshore. Armbruster (1997) also noted that the depth of water across the nearshore platform was a significant factor in storm dynamics. The coincidence of a storm and a low tidal period would result in a significant dissipation of wave energy along the platform, thus reducing the impact of storm waves on the foreshore. A significant amount of variability in foreshore responses to storms was also observed laterally along the beach. Different sectors of the beach appeared to serve as sources of sediment to other sectors of the beach, with the backshore / foredune area serving as the primary source of sediment along the beach, and the nearshore platform serving as the ultimate sink. The foreshore consequently experiences short-term, localized increases in width and volume, but ultimately suffers chronic erosion as sediment is removed from the foreshore (alongshore) sediment transport system and deposited on the nearshore platform.

Chaney and Stone (1996) reported the results of a beach monitoring study that was conducted by the National Park Service along the north-facing, soundside coast of West Ship Island, Mississippi. The data were collected along a section of the coast adjacent to Fort Massachusetts. The fort was constructed in the 1860s and is registered as a historic national monument. The National Park Service had nourished

the beach on several occasions to protect the fort from shoreline erosion. Survey data collected along a section of the coast nourished 10 years earlier indicated that a typical profile experienced approximately 3.8 m of shoreline retreat and 4.0 m^3 of volume loss per year. More importantly, the winter surveys showed the highest annual rates of erosion (-6.5 m and -5.0 m^3), and the summer surveys showed little or no deposition.

Lastly, Reed (1989) investigated the impacts of cold fronts in a coastal marsh environment in Terrebonne Bay, Louisiana. This research indicated that southerly, pre-frontal winds re-suspended bottom sediments and increased water levels. Northerly, post-frontal winds subsequently decreased water levels which stranded sediment on the surface of the marsh. Since these environments are subject to high rates of subsidence, cold front-induced sedimentation was thought to play a significant role in the evolution of the marsh. A similar pattern of sediment redistribution within a coastal marsh was observed in later research at Crystal River, Florida (Leonard *et al.* 1995).

In summary, these studies have shown that extratropical storms play a significant role in the evolution of a diverse spectrum of coastal environments, their contributions may be either constructive or destructive, and their influence extends over a broad latitudinal range.

RESEARCH OBJECTIVES

As noted in the introductory section, northerly winds associated with winter storm events have been identified as the primary forcing agent in severe cases of chronic erosion observed along the northern coasts of barrier islands of the northern

Gulf of Mexico (Henry 1977a; Armbruster *et al.* 1995; Armbruster 1997; and Chaney and Stone 1996). These winter storm events were shown to be associated with mid-latitude cyclones and anticyclones (Roberts *et al.* 1987, 1989; Dingler *et al.* 1993). A considerable amount of research has been conducted on coastal storms associated with mid-latitude cyclones and anticyclone activity along the U.S. Atlantic Coast where these events are technically known as extratropical storms, and commonly referred to as northeasters (Dolan and Davis 1992; Davis and Dolan 1993). Scientific studies along the Atlantic Coast have identified eight distinct weather patterns associated with extratropical storm activity (Davis *et al.* 1993; Davis and Dolan 1993), developed a five-class storm magnitude scale for evaluating the impacts of individual storm events (Dolan and Davis 1992), and determined the average frequency of storms in each of the five storm-magnitude classes for evaluating the annual variability in storm activity (Dolan and Davis 1992).

Roberts *et al.* (1987) identified two distinct types of cold fronts for the northern Gulf of Mexico. However, the full range of storm wind conditions (wind speed, direction, and duration) associated with the pre- and post-frontal phases of the two storm types have not been quantified in a comprehensive analysis. Hsu (1993) developed a storm-magnitude scale for Gulf cyclones which relates to wind speeds, but two other significant characteristics of storms produced by Gulf cyclones have not been quantified yet: wind direction and storm duration.

It is clearly evident that further research needs to be conducted on extratropical storms in the northern Gulf of Mexico to attain the level of understanding of extratropical storm activity that presently exists along the U.S.

Atlantic Coast. The primary issue that needs to be addressed at this stage of the research is the range of storm wind conditions that occur along the northern Gulf Coast. The purpose of determining the range of storm wind conditions that occur in the region is to establish a baseline for evaluating the range of storm impacts that occur in the region. The primary objective of this dissertation research, therefore, is to conduct a historical study of extratropical storm activity at the study site, West Ship Island, Mississippi.

In keeping with the focus of this dissertation research on the chronic erosion problem observed along the northern shores of barrier islands, the research will be restricted to the northerly winds produced by storms. A long-term collection of wind data recorded by a National Oceanographic and Atmospheric Administration (NOAA) weather buoy will be used, in conjunction with daily weather maps produced by NOAA, to determine the basic characteristics of the northerly winds produced by storms (mean wind speed, maximum wind speed, storm duration). The storm characteristics data will be used to evaluate the variability in wind conditions that occur during an individual storm event, and the variability in storm activity (frequency and wind conditions) that may occur during each month of the storm season (September to May).

The storm characteristics data will also be used to construct a five-class, storm-magnitude scale. The purpose of developing a storm-magnitude scale is to lay the groundwork for developing a verifiable correlation between storm wind conditions and storm impacts. Quantifying this relationship would be of tremendous value to both the coastal management community and the scientific community.

Lastly, the storm characteristics data will be used to evaluate the predominant direction of winds during storms. The purpose of this exercise is to lay the groundwork for developing a reliable estimate of the predominant direction of alongshore sediment transport (eastward vs westward) along the northern shores of barrier islands as a result of storm activity.

In addition to the historical study of storm activity, the research design includes a field study of storm dynamics that will document the influence of storm winds on nearshore wave height, water level, and current conditions. The present body of literature on extratropical storm dynamics along the northern shores of barrier islands in the region is limited to a 14-hour study conducted along the north-facing, bayside coast of Santa Rosa Island, Florida (Armbruster *et al.* 1995; Armbruster 1997). Although Roberts *et al.* (1987), Armbruster *et al.* (1995), and Armbruster (1997) observed and discussed a number of ways that storms influence water levels, wave heights, and sediment transport processes along the northern coast of a barrier island, it is clearly evident that additional field data are needed to quantify the effects of storms on nearshore conditions in these environments.

The critical issues that the field study of storm dynamics will focus on are the effects of storm winds on wave heights (for comparison of storm vs non-storm conditions), the effects of changing water levels on wave heights (for evaluating the influence of tides), and the predominant direction of alongshore and cross-shore currents during storms (for evaluating sediment transport pathways).

Finally, the research design includes a field study of storm impacts that will document the effects of storms along the northern coast of West Ship Island over an

entire storm season. Although previous studies along the northern shores of barrier islands of the northern Gulf Coast documented rates of shoreline retreat and volume loss (Armbruster *et al.* 1995; Armbruster 1996; Chaney and Stone 1996), and identified both alongshore and offshore trends in sediment transport (Armbruster *et al.* 1995; Armbruster 1997), these studies were restricted to relatively short sections of the coast (100 m to 600 m). It is clearly evident that additional field data are needed to evaluate the effects of storms over greater spatial and temporal scales (*i.e.* changes along the entire length of the island over an entire storm season).

The issues that this field study will focus on include the effects of storms on the total changes in beach width and volume for the entire northern coast of the island, lateral changes in beach width and volume along the coast (*i.e.* alongshore and cross-shore sediment transport trends), and variations in the cross-sectional morphology of the beach (*i.e.* evolution of the profile) over the entire storm season. Beach profiles will be surveyed at approximately 600 m intervals along the entire length of the island, and at 50 m intervals along a 250 m section of the beach adjacent to Fort Massachusetts. West Ship Island was chosen for this study because it has a long history of erosion along its northern shore which has been documented in a previous study (Chaney and Stone 1996). Furthermore, this site provides an opportunity to extend the record of monitoring at a single location which is a critical limitation of the present body of literature on this topic.

The greatest "potential" contribution of this research is in laying the foundation for using storm wind data as a "proxy" measure of a storm's impact along the northern coasts of barrier islands of the northern Gulf of Mexico. Historical storm

wind data could be used to evaluate the variability of storm impacts in previous years. Storm wind data could also be used to remotely evaluate recent storm impacts which is a difficult task because of the logistical problems associated with conducting field research in these remote environments. More importantly, seasonal and annual weather predictions could be used to evaluate the potential impacts of forthcoming storm seasons. This information would be of tremendous value to both coastal managers and members of the scientific community concerned with the evolution of coastal environments of the northern Gulf of Mexico.

This dissertation research is designed to address the present needs of this field of study by evaluating the "northerly" winds associated with extratropical storm activity along the northern Gulf Coast, the effects of those winds on nearshore wave and current conditions along the northern coast of a barrier island, and the impacts of those waves and currents on the beach. The findings of this research will contribute toward a greater understanding of the role of extratropical storms in the evolution of coastal environments of the northern Gulf of Mexico, and similar mid-latitude settings around the globe.

CHAPTER 2

THE PHYSICAL SETTING

The field study for this research was conducted at West Ship Island, Mississippi. The physical setting is a typical barrier-lagoon environment along the northern Gulf of Mexico (Figure 2.1). The island is separated from the mainland by a shallow lagoon known as Mississippi Sound. The seaward extent of the lagoon is marked by an elongated Holocene sand platform (Ludwick 1964) that supports the chain of barrier islands along the Mississippi-Alabama coast (Otvos 1979). The shores of the mainland coast and the barrier islands are composed of medium to coarse sands; the central region of the lagoon is covered with fine silts and clays (Upshaw *et al.* 1966).

MISSISSIPPI SOUND

Mississippi Sound is approximately 20 km wide near West Ship Island. The bed gradually slopes seaward to depths of 8-10 m below Mean Lower Low Water along the coast of West Ship Island. The sound is a relatively low-energy, estuarine environment with significant wave heights averaging 30 cm (Jensen 1983). Diurnal tides average 47 cm at the National Ocean Service tide gauge at Biloxi Bay, Mississippi (NOAA 1990); tropic and equatorial tides average 69 cm and 10 cm, respectively (Veal 1996). Relative sea-level rise at the Biloxi Bay tide gauge averaged 1.5 mm yr^{-1} over the period 1939-1983 (Penland *et al.* 1989).

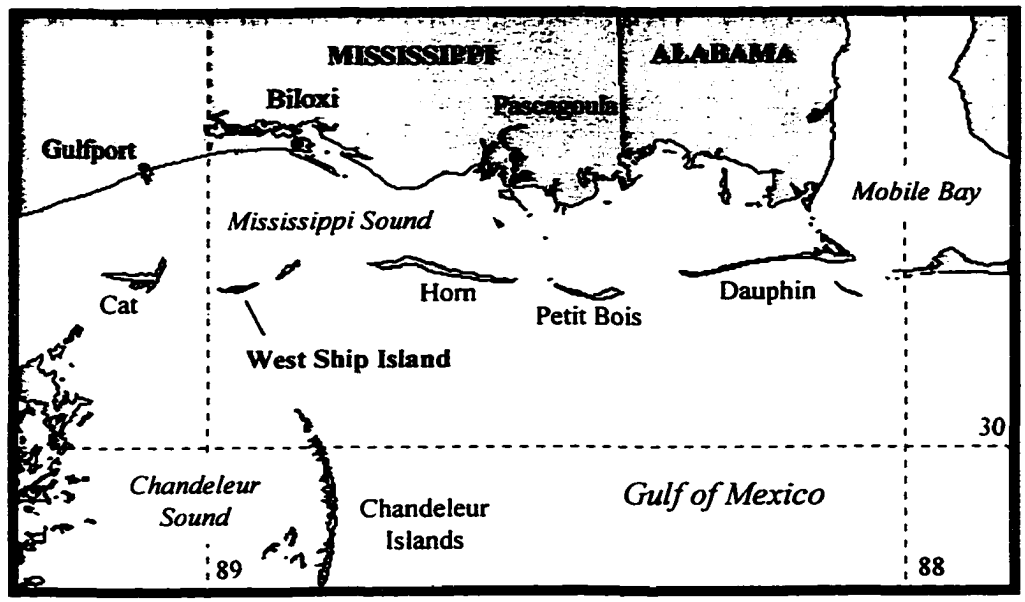

Figure 2.1. Location of West Ship Island and Mississippi Sound along the northern coast of the Gulf of Mexico.

BARRIER ISLAND FORMATION AND STRATIGRAPHY

Previous research suggests that the barrier islands along the Mississippi-Alabama coast were formed by upward aggradation of submerged shoals during the late-Holocene (Otvos 1970, 1979). Otvos (1981) suggests that the primary source of sediment to the barrier islands was the Alabama coast, and that Mobile Bay ebb-tidal currents transported sediment from the Alabama coast seaward where westerly, alongshore drift prevailed (Otvos 1970, 1979). Sediment trapping along a Pleistocene ridge eventually formed Dauphin Island. This led to the development of a sand platform along the seaward extent of Mississippi Sound. Finally, localized shoaling or aggradation initiated barrier island formation (Otvos 1985).

The stratigraphy of West Ship Island was interpreted as three distinct facies overlaying a Pleistocene clay bed (Otvos 1981). The lower facies is a 3-12 m thick layer of silty-muddy Holocene sea bed deposits. The intermediate facies is a 7-12 m thick layer of sand and mud, with mud content increasing with depth. The upper facies is composed entirely of sand. The intermediate sand-mud platform provides a wide, shallow shelf along the soundside of the island and a narrower, steeper shelf along the Gulf side. Depths at the edge of the shelf drop rapidly from 1 m to 8-10 m along the soundside and from 2 m to 5-6 m along the Gulf side (Figure 2.2).

HISTORICAL MIGRATION PATTERNS

Historical shoreline maps of West Ship Island indicate that the soundside coast retreated 0.5 m yr^{-1} while the Gulf coast advanced seaward 0.7 m yr^{-1} over the period 1847-1986 (McBride *et al.* 1995). The historical shoreline maps also indicate that the Mississippi Sound barrier islands are migrating westward. Data for the 1847-

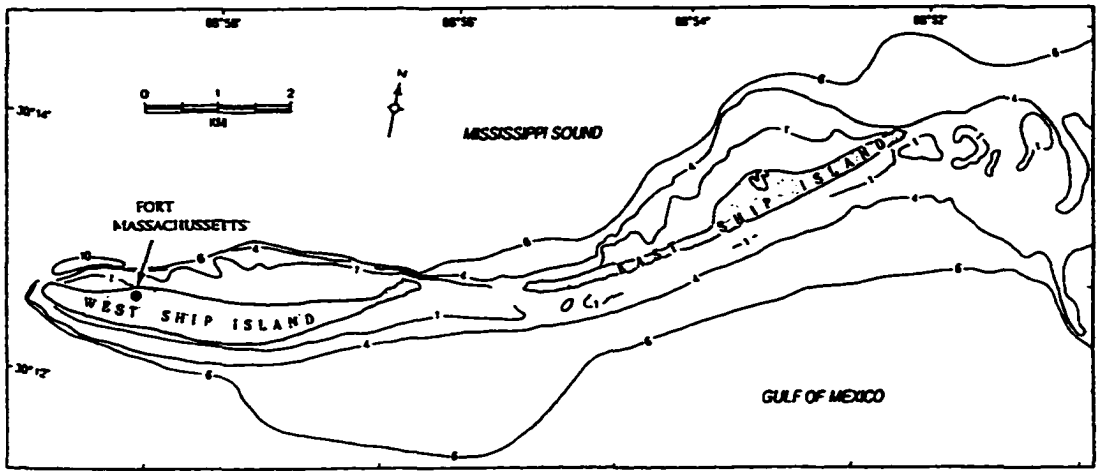

Figure 2.2. Nearshore bathymetry of the Ship Island complex. (Isobaths in meters below Mean Lower Low Water). Source: U.S. Coast and Geodetic Survey (1992).

1986 period show the following distances of westward migration of the western tips: Dauphin (7.6 km), Petit Bois (4.3 km), Horn (4.7 km), and Ship (1.3 km) (Byrnes *et al.* 1991). West Ship Island's annual rate of westward migration was 9.6 m yr^{-1}. However, the island was stable from 1966-1976, then migrated eastward at a rate of 4.7 m yr^{-1}. The termination of westward migration was attributed to dredging of the navigation channel along the west tip of the island (Byrnes *et al.* 1991). The navigation channel was recently relocated one mile farther west; however, the abandoned channel was not backfilled. This may have a significant impact on the evolution of the island.

A recent study of sediment transport along the Gulf coast of the Mississippi-Alabama barrier islands indicated that the predominant direction of transport was westward (Cipriani 1998). Sediment transport rates computed for East Ship Island increased from 2,000 m^3 yr^{-1} at the eastern tip to 13,000 m^3 yr^{-1} at the western tip, and sediment transport rates for West Ship Island increased from 24,000 m^3 yr^{-1} at the eastern tip to 37,000 m^3 yr^{-1} at the western tip (Cipriani 1998). The modern-day (westward) sediment transport trends identified by Cipriani (1998) support the historical (westward) migration patterns of the barrier islands identified by Byrnes *et al.* (1991).

WEST SHIP ISLAND

West Ship Island was detached from East Ship Island by storm waves accompanying Hurricane Camille in 1969 (Byrnes *et al.* 1991; Bowden 1994). Presently, the island is 5.2 km long and 0.6 km wide. The soundside coast has a relatively narrow beach (5-10 m) with foredunes of 2-3 m above the high tide line

along most of the island. Ancient marsh deposits exposed along the lower foreshore are a common site. The beach along the eastern end has completely eroded and become impassable, even at low tide, with *in situ* tree roots exposed along a 400 m section of the coast.

The beach along the Gulf coast side of West Ship Island is composed of three different environments that decrease in width from west to east. The western section has a wide, sandy beach (50 m) with foredunes of 3-4 m above the high tide line. The central section is a transitional zone with lower foredunes and a narrower beach (10-20 m). The eastern section has the narrowest beach (5-10 m) and practically no foredunes. The eastern tip of the island is a low-lying, recurved spit that extends into Camille Cut. Large sections of the spit are frequently overwashed by storm waves. The western tip of the island is also frequently overwashed by storm waves.

Boone (1973) and Otvos (1982) determined that the beaches were composed of well-sorted, quartz sands. Median grain sizes of upper foreshore beach sands were found to range from 0.26-0.33 mm along the Gulf coast and 0.33-0.56 mm along the soundside coast (Otvos 1982). The difference in grain size was attributed to the difference in wave energy in the Gulf and in Mississippi Sound (Otvos 1982). Along the Gulf coast, finer grain sizes were attributed to a constant supply of finer sediments from alongshore and offshore sources, and the ability of higher waves to transport coarser grains alongshore. Along the soundside coast, coarser grain sizes were attributed to lower wave heights that were unable to transport larger grains alongshore, or to transport finer grains to the beach from offshore (Otvos 1982). Cipriani (1998) recently found that mean grain sizes of mid-tide beach sands along

the Gulf coast ranged from 1.650-2.079 phi (0.24-0.34 mm) and were very-well sorted (sorting values ranged from 0.26 to 0.32). These results support the earlier findings of Boone (1973) and Otvos (1982).

As noted earlier, West Ship Island was chosen for this study because it is one of the more prominent sites of soundside erosion in the region. Fort Massachusetts, a historic national monument, was constructed on the island in the 1860s approximately 100 m from the soundside coast (USACE 1864). By the 1920s, erosion threatened the fort's structural integrity (Henry 1977a). Local citizens constructed a make-shift breakwater to protect the fort, but this effort had little impact (Figure 2.3). West Ship Island came under the protection of the National Park Service (NPS) when the Gulf Islands National Seashore was established in 1971. The beach adjacent to Fort Massachusetts was nourished in 1974 to protect the structure. However, several beach nourishment projects have been conducted over the years to replace lost fill material (Table 2.1; Figure 2.4 and 2.5).

Table 2.1. Volume of material placed along the beach adjacent to Fort Massachusetts during each nourishment project conducted along the northern coast of West Ship Island (Hopkins 1996).

Year	Volume (yds^3)	Volume (m^3)
1974	500,000	382,300
1980	100,000	76,460
1984	210,000	160,566
1991	58,000	44,346
1996	50,000	38,230

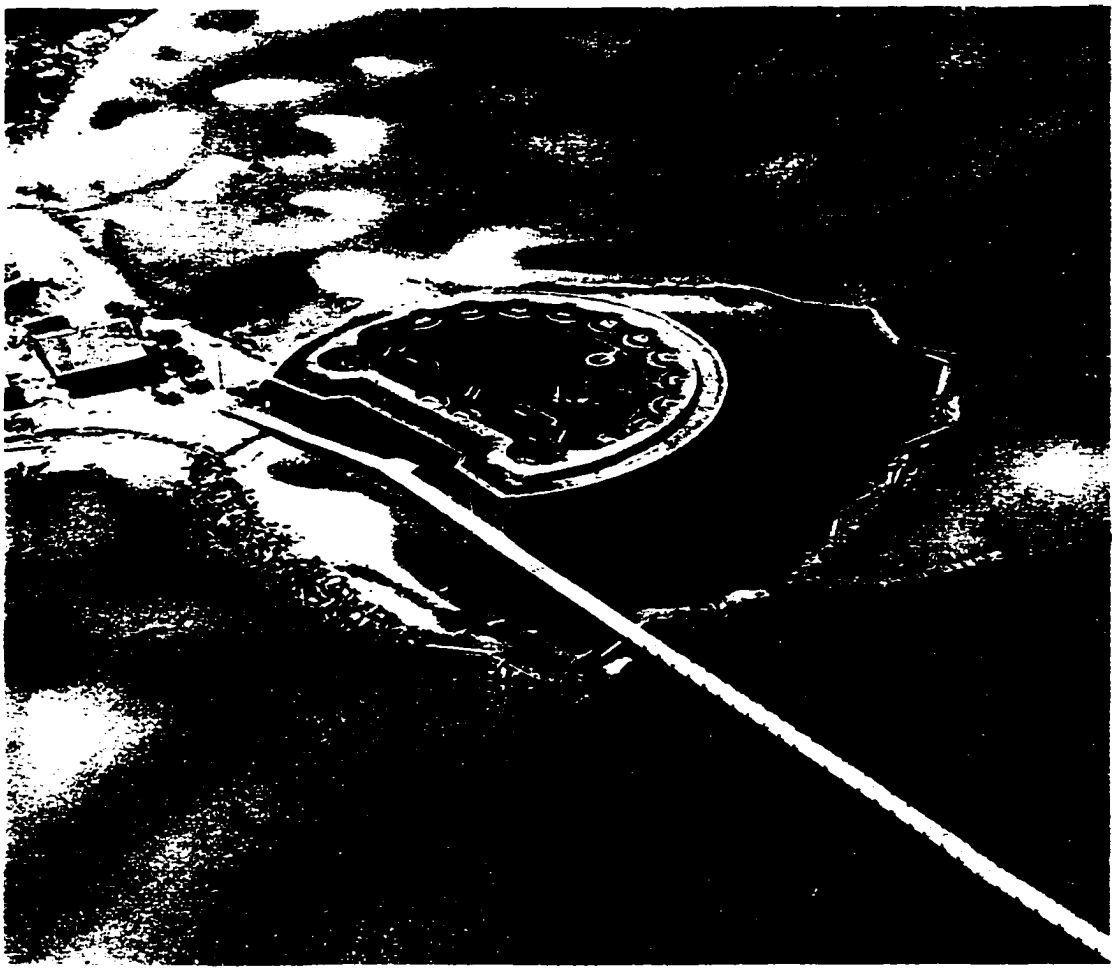

Figure 2.3. Aerial photo (facing southwest) showing the extent of shoreline erosion at Fort Massachusetts in 1967. Note the make-shift breakwater constructed by local citizens and the standing water at the base of the fort. (Gulf Islands National Seashore Historical Archives).

Figure 2.4. Aerial photo (facing east) showing the beach nourishment site adjacent to Fort Massachusetts in 1985. Note the position of the pre-nourishment (1974) shoreline (see Figure 2.3). Photo taken by W.T. Triplett.

Figure 2.5. Aerial photo (facing east) showing the beach nourishment site adjacent to Fort Massachusetts in February, 1997. Note the condition of the beach since nourishment was conducted in May, 1996. Photo taken by G.W. Stone.

In April, 1989, the National Park Service began a beach monitoring program along a 600 m section of the soundside coast adjacent to Fort Massachusetts. Along the western (200 m) section of the nourishment site, which is directly adjacent to the fort, shoreline retreat and beach erosion averaged 5.9 m yr^{-1} and 11.4 m^3 m^{-1} yr^{-1} between April, 1989, and July, 1991. In September, 1991, additional nourishment was placed along the western section of the beach. During the post-nourishment period (October, 1991, to July, 1993), shoreline retreat and beach erosion along the western section averaged 24.7 m yr^{-1} and 29.1 m^3 m^{-1} yr^{-1}. In May, 1996, the western section of the beach was nourished again. Along the eastern (400 m) section of the monitoring area, shoreline retreat and beach erosion remained relatively consistent at 3.8 m yr^{-1} and 4.0 m^3 m^{-1} yr^{-1} over the duration of the monitoring period (April, 1989, to July, 1993) (Chaney and Stone 1996). It is important to note that nourished beaches are expected to lose significant quantities of sediment immediately after the nourishment is conducted. This response occurs as the profile re-equilibrates (Dean and Yoo 1993). The eroded sediment is generally deposited along the lower foreshore or on nearshore bars (Houston 1991).

The NPS beach profile surveys were conducted at 2 to 5 month intervals that corresponded favorably with winter seasons prior to the 1991 nourishment. These data show that the highest rates of shoreline retreat and beach erosion occurred along both eastern (6.5 m yr^{-1} and 5.0 m^3 m^{-1} yr^{-1}) and western (9.6 m yr^{-1} and 14.7 m^3 m^{-1} yr^{-1}) sections of the monitoring area over winter periods. These results suggest that winter cold front activity was responsible for the greatest amount of erosion observed

at the nourishment site. Unfortunately, the timing of the beach surveys conducted after the 1991 nourishment do not correspond favorably with the seasons of the year, so data for that period cannot be used to evaluate seasonal trends (Chaney and Stone 1996).

CHAPTER 3

EXTRATROPICAL STORMS OF THE GULF OF MEXICO: TYPE, FREQUENCY, AND MAGNITUDE

The term "extratropical storm" used in this chapter refers to all coastal storms associated with either mid-latitude "cyclone" or "anticyclone" activity along the northern Gulf Coast. As noted earlier, this term is well established in the literature on coastal storms along the U.S. Atlantic Coast. The objective of this study is to address the present limitations of the scientific literature on extratropical storms of the northern Gulf of Mexico as they pertain to the erosion problem observed along the northern shores of barrier islands (as discussed in Chapter 1). The following paragraph provides a brief review of the existing storm literature.

Roberts *et al.* (1987) identified two distinct types of cold fronts that produced storms along the northern Gulf Coast; however, these two were identified as the end members of a "spectrum of cold front types." The "spectrum of cold front types" identified by Roberts *et al.* (1987) has not yet been investigated. Roberts *et al.* (1987) also proposed a conceptual model of storm dynamics for cold front passages that included two distinctly different phases: a pre-frontal phase that produced southerly winds along the coast, and a post-frontal phase that produced northerly winds along the coast. At present, the existing data on wind conditions during cold front passages along the northern Gulf Coast were collected during two 30-day field studies at Mustang Island, Texas (Fox and Davis 1976), an 8-day field study at Trinity Island, Louisiana (Dingler *et al.* 1992), and a 14-hour study at Santa Rosa Island, Florida (Armbruster *et al.* 1995). The full range of storm wind

conditions (wind speed, direction, and duration) associated with the two storm types identified by Roberts *et al.* (1987) has not yet been quantified. Hsu (1993) developed a storm-magnitude scale for Gulf cyclones; however, Gulf cyclones were not identified as a major storm type by Roberts *et al.* (1987), and wind direction and storm duration for Gulf cyclones has not been evaluated.

The objective of this study was to address these limitations as they relate to the northerly winds produced by extratropical storms. The study was based on a review of daily weather maps published by the National Oceanic and Atmospheric Administration (NOAA), and atmospheric data collected by a NOAA weather buoy located near West Ship Island, Mississippi. The daily weather maps were used to identify weather patterns associated with extratropical storms and to track their migration along the Gulf Coast. The atmospheric data were used to evaluate the basic characteristics of northerly winds (wind speed, direction, and duration) produced by the storms. The study period extended from January, 1981 (the month the weather buoy was deployed) through May, 1997 (the end of the 1996-1997 storm season). The study was restricted to active storm season months from September to May.

The buoy was maintained by a branch of NOAA known as the National Data Buoy Center (NDBC). The buoy was identified as NDBC Station 42007 and was located approximately 13 km southeast of West Ship Island (Figure 3.1). The buoy recorded air temperature, barometric pressure, wind speed, and wind direction data at 1 hour intervals. At the beginning of each hour, the buoy sampled wind conditions for 8 minutes and then recorded the average wind speed and direction.

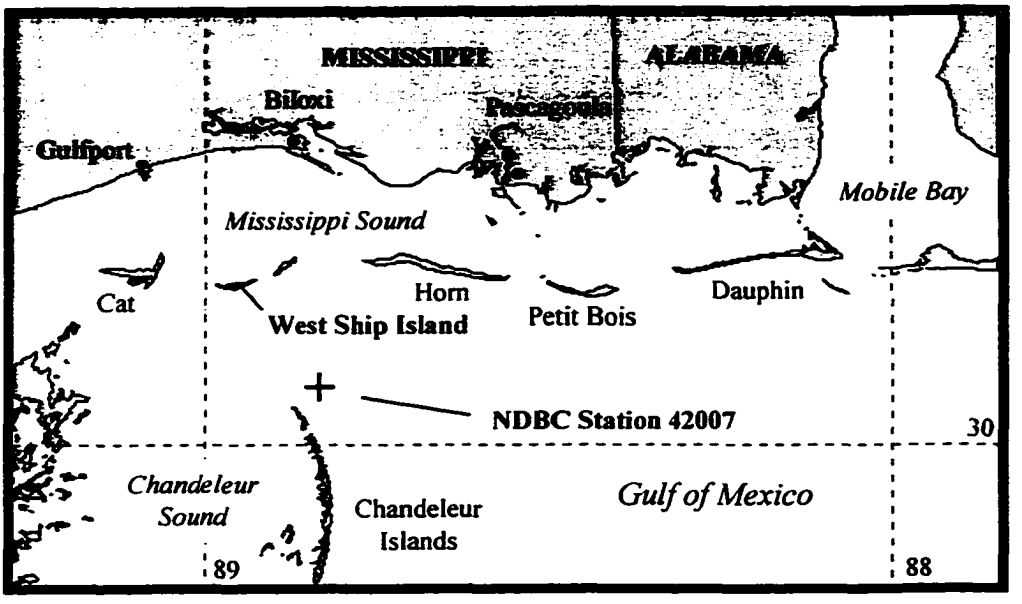

Figure 3.1. Location of NDBC Station 42007 in the northern Gulf of Mexico. The buoy was located at 30.1^0 N Latitude and 88.8^0 W Longitude.

The anemometer on the buoy was mounted 10 m above sea level. The buoy was deployed in January, 1981, and the data collected since that time were archived as "Standard Meteorological Data" at the NDBC Internet site where they were made available to the public (NDBC 1981-1997).

Since NDBC Station 42007 is located farther offshore than West Ship Island, there are several potential problems that should be recognized in using the buoy data to evaluate storm conditions at the island. Northerly winds travel over a greater distance of open sea (longer fetch / reduced friction) before reaching the buoy, so northerly wind speeds at the buoy may be higher than northerly wind speeds at the island. Wind directions and the timing of wind shifts may also vary at the two locations. Furthermore, cold fronts may stall after passing over West Ship Island, but before passing over the buoy.

Wind speed and direction data were collected along the northern coast of West Ship Island during an 18-day field study to evaluate the difference in wind conditions at the two sites. The wind data were collected at an elevation of approximately 7.5 m above mean sea level which was approximately 2.5 m lower than the anemometer on the buoy. Plots of the data are shown in Chapter 4. The average speed of northerly winds recorded at NDBC Station 42007 (8.65 m sec^{-1}) was approximately 1 m sec^{-1} higher than the average speed of northerly winds recorded at West Ship Island (7.68 m sec^{-1}). However, the maximum northerly wind speed recorded at NDBC Station 42007 (13.8 m sec^{-1}) was approximately 1.4 m sec^{-1} lower than the maximum northerly wind speed recorded at West Ship Island (15.2 m sec^{-1}). Higher average wind speeds were expected at NDBC Station 42007 because of the differences in fetch and elevation. It should be noted that differences in instrument calibration may have increased or decreased the discrepancy in recorded wind speeds.

Wind directions recorded at West Ship Island were consistently shifted approximately 30 degrees westward of wind directions recorded at NDBC Station 42007. The wind vane deployed at West Ship Island was calibrated with a hand-held compass which could easily account for the discrepancy in wind directions. Although the actual wind speed and direction values differed, identical changes in both wind speed and wind direction were recorded at approximately the same time at each site. These findings suggest that the wind data recorded at NDBC Station 42007 represent a reasonable sample of wind conditions at West Ship Island.

Roberts *et al.* (1987) observation on "the spectrum of cold front types" that occurred along the northern Gulf Coast was considered when reviewing the daily weather maps (NOAA 1981-1997). A wide variety of synoptic weather patterns were in fact observed to produce extratropical storm events along the Gulf Coast. These weather patterns were sorted into seven distinct classes identified in this study as "extratropical storm types." The seven storm types include: 1) Primary Front, 2) Secondary Front, 3) Secondary Gulf Front, 4) Secondary Gulf Low, 5) Gulf Front, 6) Gulf Low, and 7) Primary Low. Detailed illustrations of the synoptic weather patterns associated with the seven storm types are shown in Figures 3.2 - 3.5. The following paragraphs describe the weather patterns associated with each storm type and relate them to storm types identified in earlier studies.

The cold front associated with a typical mid-latitude cyclone (Figure 1.4) was identified in this study as the "primary front," and the storm event that occurred when the front crossed the coast was identified as the Primary Front storm type. On occasions when the primary front stalled over the southeastern U.S., without actually crossing the coast, a "secondary" low-pressure center often developed along the front over the south-central U.S. When the secondary low-pressure center developed into a full-scale cyclone, with a fully-developed cold front, it migrated northeastward and the "secondary" cold front passed along the coast. The storm system associated with this weather pattern was identified as a Secondary Front.

On occasions when the primary front stalled over the Gulf of Mexico, after it crossed the coast, a secondary low-pressure center (Gulf cyclone) often developed along the front over the eastern Texas / western Gulf of Mexico region. If the

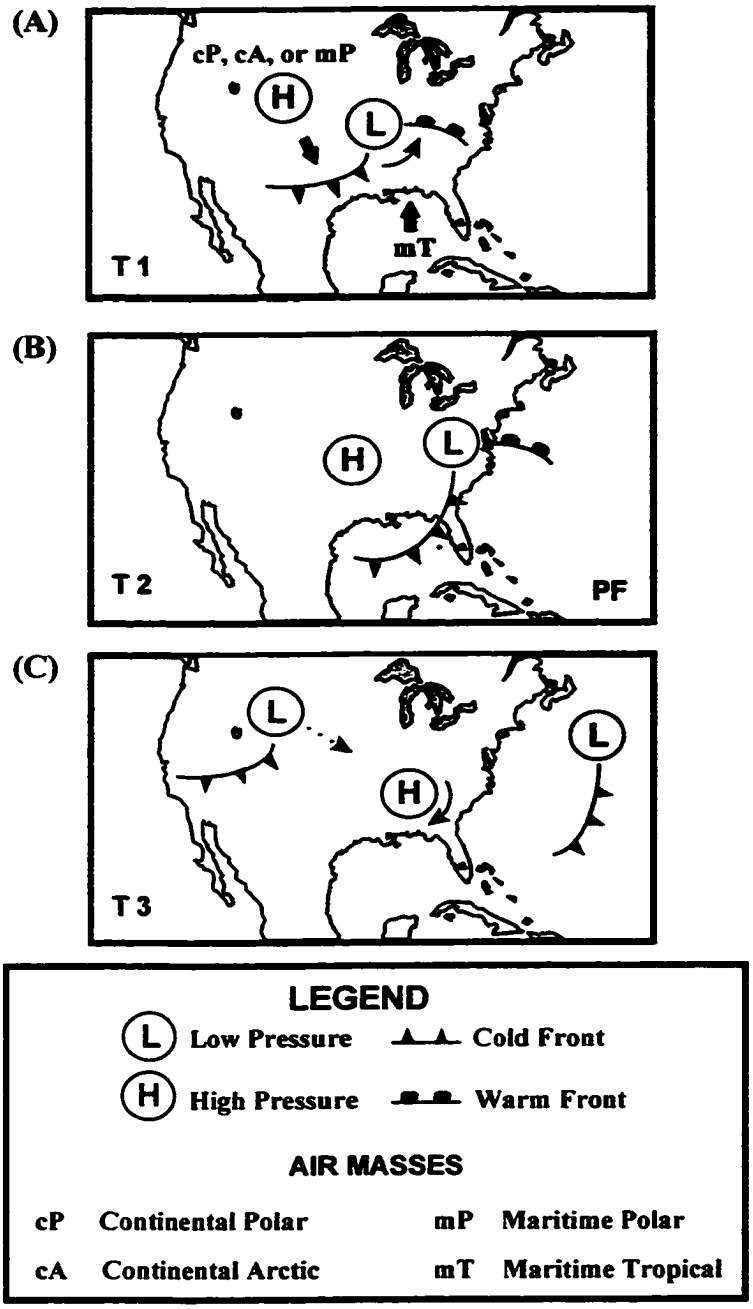

Figure 3.2 Synoptic weather patterns associated with a Primary Front (PF). The upper plot (A) shows the cyclonic (counter-clockwise) rotation pattern of winds around the low-pressure system, and the position of the fronts that represent the leading edges of the high-pressure, cold air mass (cP, cA, or mP) migrating southward and the warm air mass (mT) migrating northward. The center plot (B) shows the cold front passing along the Gulf coast. The lower plot (C) shows the anticyclonic (clockwise) rotation pattern of winds around the high-pressure system that dominates the Gulf coast until a subsequent frontal system moves into the region.

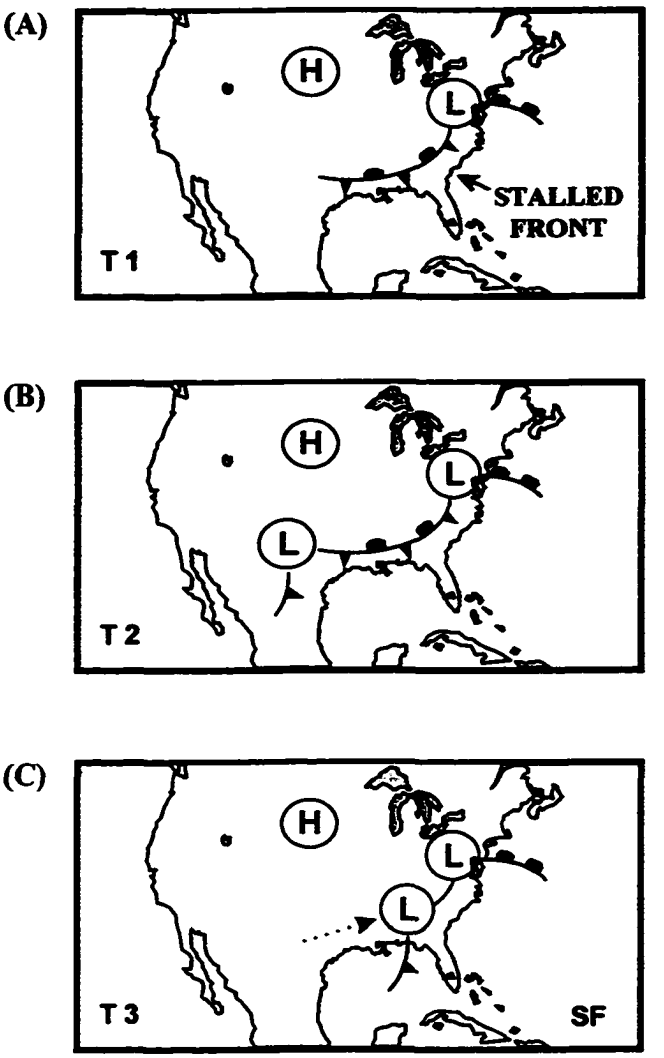

Figure 3.3. Synoptic weather patterns associated with a Secondary Front (SF). The upper plot (A) shows a primary front stalled over land north of the Gulf coast. The center plot (B) shows a secondary low-pressure center develop along the front over the south-central U.S. The lower plot (C) shows the secondary low migrating northeastward and the accompanying cold front passing along the Gulf Coast. The map symbols are identified on the legend in Figure 3.2.

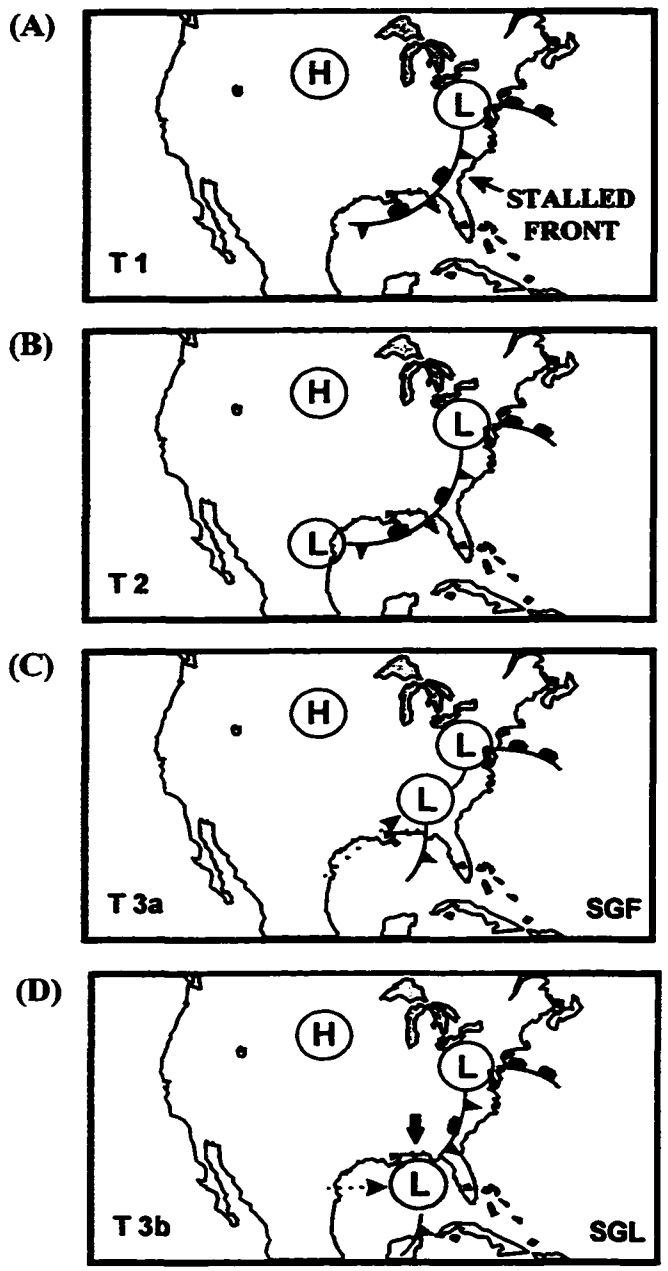

Figure 3.4. Synoptic weather patterns associated with a Secondary Gulf Front (SGF) and a Secondary Gulf Low (SGL). The upper plot (A) shows a primary front stalled over the Gulf of Mexico. The second plot (B) shows a secondary low-pressure center develop along the front over the eastern Texas / western Gulf of Mexico region. The third plot (C) shows the secondary low migrating northeastward and the accompanying cold front passing along the Gulf coast. The fourth plot (D) shows an alternative storm track where the secondary low migrates eastward across the Gulf of Mexico and produces northerly winds along the Gulf coast. The map symbols are identified on the legend in Figure 3.2.

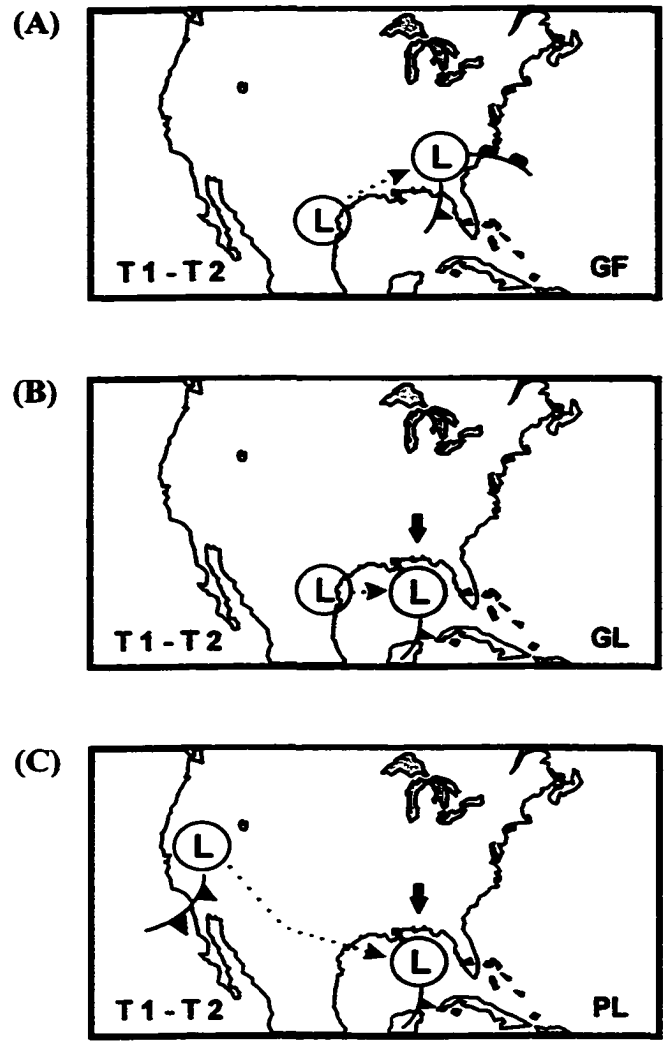

Figure 3.5. Synoptic weather patterns associated with a Gulf Front (GF), a Gulf Low (GL), and a Primary Low (PL). The upper plot (A) shows a low-pressure center develop over the eastern Texas / western Gulf of Mexico region, then shows the low-pressure center migrating northeastward and the accompanying cold front passing along the Gulf coast. The center plot (B) shows an alternative storm track where the low-pressure center migrates eastward across the Gulf of Mexico and produces northerly winds along the Gulf coast. The lower plot (C) shows a low-pressure center associated with a primary front following a southerly storm track across the Gulf of Mexico that produces northerly winds along the Gulf coast. The map symbols are identified on the legend in Figure 3.2.

secondary low-pressure center migrated northeastward, then the secondary cold front passed along the coast and produced a second storm at West Ship Island. This type of storm system was identified as a Secondary Gulf Front. If the secondary low-pressure center migrated eastward across the Gulf of Mexico, then the cold front passed south of the study site. However, the low-pressure center setup a pressure gradient in the region that still produced northerly winds along the northern Gulf Coast. This type of storm system was identified as a Secondary Gulf Low.

A low-pressure center (Gulf cyclone) occasionally developed along the eastern Texas / western Gulf of Mexico region without a pre-existing front in the region. If the low-pressure center migrated northeastward, then the front passed along the coast and the storm system was identified as a Gulf Front. If the low-pressure center migrated eastward across the Gulf of Mexico, then the storm system was identified as a Gulf Low. Lastly, a low-pressure center associated with a primary front occasionally followed a southerly storm track that passed over the southwestern U.S. and the central Gulf of Mexico. This type of storm system was identified as a Primary Low.

The Primary Front storm type identified in this study most closely corresponds to the eastward migrating cyclone identified by Roberts *et al.* (1987). In reviewing the daily weather maps, however, it was noted that these storm systems appear to be composed of two "linked" pressure systems in that the low-pressure system (cyclone) and the high-pressure, cold air mass (anticyclone) appear to migrate together as a single weather system. Since the counter-clockwise wind

rotation patterns of mid-latitude cyclones promote the southward migration of cold air masses (high-pressure, anticyclones), it seems natural that these two pressure systems would appear to migrate as a single "linked" weather system.

If the low-pressure center of a mid-latitude cyclone followed a southerly storm track and passed near the Gulf Coast, then the low-pressure center would dominate the region and produce strong "southerly, pre-frontal" winds along the coast. This storm system would consequently be classified as an eastward migrating cyclone by Roberts *et al.* (1987) description. If the low-pressure center of a mid-latitude cyclone followed a northerly storm track, then the trailing anticyclone would dominate the region when it passed along the Gulf Coast. This scenario would produce strong "northerly, post-frontal" winds along the coast and consequently be classified as an arctic surge by Roberts *et al.* (1987) description. Since the latitudinal position of the low-pressure system appears to have the greatest influence on "pre- and post-frontal" wind conditions associated with eastward migrating cyclones and arctic surges, no attempt was made to distinguish between these two "cold front types" for the purposes of this study.

The intermediate classes of the "spectrum of cold front types" identified Roberts *et al.* (1987) would most likely include the Secondary Front, the Secondary Gulf Front, and the Gulf Front storm types identified in this study. The Gulf Low, Secondary Gulf Low and the Gulf Front storm types identified in this study correspond to the storm systems that Hsu (1993) evaluated in developing the storm intensity scale for Gulf cyclones. If one of these storms were to migrate eastward across Florida and impact the Atlantic Coast, it would correspond to the Gulf Low

storm type identified by Davis *et al.* (1993) and Davis and Dolan (1993). According to the descriptions of storm types identified by Davis *et al.* (1993) and Davis and Dolan (1993), Primary Fronts would be classified as Continental Lows or Anticyclones when they impact the Atlantic Coast (based on the latitudinal position of the low-pressure system), and Secondary Fronts would be classified as Coastal Plain Cyclogenesis storms when they impact the Atlantic Coast. There does not appear to be any previous acknowledgment of the Primary Low storm type identified in this study and, as the following analysis will indicate, it was not found to be a significant storm type for the Gulf Coast in this study either.

After an extratropical storm event was identified on the daily weather maps, the wind data collected by NDBC Station 42007 were used to determine the duration of the storm. In reviewing the buoy data, it was noted that northerly wind speeds often increased significantly before a cold front passed along the coast. These northerly winds were associated with the squall line that often precedes the front. These conditions normally lasted for only a brief period. However, they occasionally persisted for an extended period, and on many occasions the front retreated northward without crossing the coast. Therefore, the temperature and pressure data collected by the buoy were used, in conjunction with the daily weather maps, to determine the time that a cold front passed over the study site.

The daily weather maps were also used, in conjunction with the buoy data, to determine when the high-pressure air mass (anticyclone) behind the cold front ceased to influence wind conditions along the coast. The duration of a storm event was therefore defined as the period from the time the front passed until the high-

pressure air mass moved out of the region. For the Gulf Low, Secondary Gulf Low, and Primary Low storm types, the duration of a storm event was defined as the time period that the low-pressure center passing eastward across the Gulf produced northerly winds at the study site.

The analysis of wind conditions during a storm was restricted to northerly winds only. In compiling the data, it was noted that there were two distinct stages of a storm event when wind speeds often decreased significantly for a brief period. The first stage was immediately after the front passed overhead. The second stage was during the middle of a storm event when the center of the high-pressure system passed overhead. In order to present a reasonable estimate of the duration of a storm event, only wind speeds equal to, or greater than, 5.5 m sec^{-1} were included in the analysis. This value was used as the minimum limit for evaluating a storm because the summary statistics posted on the NDBC Internet site indicated that the average annual wind speed at NDBC Station 42007 over the period 1981-1993 was 10.75 knots (5.5 m sec^{-1}). The duration of a storm was therefore defined as the number of hours that a storm produced northerly winds equal to, or greater than, 5.5 m sec^{-1}. The mean and maximum wind speed were determined from the data that met these requirements. The statistics computed for all northerly winds were also computed for northwesterly and northeasterly winds for the purpose of evaluating alongshore sediment transport trends as discussed in Chapter 1.

A simple measure of storm magnitude which considered variability in both wind speed and storm duration was also computed for each storm event. The storm

magnitude value was based on the standard formula for kinetic energy shown in Equation 1:

$$k_e = \frac{1}{2} pv^2 \qquad \text{(Equation 1)}$$

where k_e = kinetic energy, p = density, and v = velocity (Huschke 1959). Since the density of dry air at 1000 mb (approx. sea level pressure) varies only slightly between 0° C (1.28 kg/m^3) and 30° C (1.15 kg/m^3) (Hsu 1988), density was considered constant for this application. Therefore, the kinetic energy of a storm over the duration of the event was considered to be equal to one-half the sum of the squares of the wind velocities as shown in Equation 2:

$$\frac{1}{2} [\Sigma (v^2)] \qquad \text{(Equation 2)}$$

where v = all northerly winds equal to, or greater than, 5.5 m sec^{-1}. However, only the sum of the squares of the wind velocities [$\Sigma (v^2)$] was computed for each storm because no further application of this value was intended. The product of this calculation was identified as the V square value.

The atmospheric data collected by the buoy were evaluated on a monthly basis. Months in which the buoy was either non-operational or temporarily out-of-service were excluded from the study. Exceptions, however, were made for months in which the gap in data did not coincide with a storm period identified on the daily weather maps. The study period, as defined earlier, included 149 months. However, only 98 months of data were determined to be acceptable for analysis (Table 3.1). After the analysis of each storm identified in the study was completed, the data were used to evaluate the following aspects of storm activity: 1) variability in northerly winds of all storms, 2) variability in northerly winds of each storm type,

3) variability in northerly winds of each storm-magnitude class, 4) variability in northwesterly and northeasterly winds of all storms, 5) seasonal variability in northwesterly and northeasterly winds of all storms, and 6) variability in storm activity during the 1996-1997 storm season (for evaluating the significance of the results of the storm impact study presented in Chapter 5).

Table 3.1. Months of the study period (1981-1997) included in the storm analysis. The buoy was deployed in January, 1981. The months included in the study are identified by an "x". (Total number of months in study = 98).

YEAR	SEP	OCT	NOV	DEC	JAN	FEB	MAR	APR	MAY
80-81					-	-	x	-	-
81-82	-	-	x	-	-	-	x	x	x
82-83	x	x	x	x	x	x	-	-	-
83-84	-	-	-	-	-	-	-	x	x
84-85	x	x	x	x	x	-	x	x	-
85-86	x	-	-	-	-	-	-	x	x
86-87	x	x	-	-	-	-	-	-	-
87-88	x	x	x	-	-	-	x	x	x
88-89	x	x	x	x	x	x	x	-	x
89-90	x	x	x	x	x	x	x	x	x
90-91	x	x	x	x	x	-	-	x	x
91-92	-	-	-	-	-	-	-	-	-
92-93	x	x	x	x	x	x	x	x	x
93-94	x	-	x	-	x	x	x	x	x
94-95	x	x	x	x	x	x	x	x	x
95-96	x	x	x	x	x	x	x	x	x
96-97	x	x	x	x	x	x	x	x	x
# Months	13	11	12	9	10	8	11	12	12

As noted earlier, the analyses were restricted to a monthly basis, rather than an annual basis, because of the gaps in the data recorded at NDBC Station 42007 (Table 3.1). The annual frequency and storm characteristic data presented in the following sections are therefore based on composites of the mean values determined for each month of the storm season (September to May).

ALL STORMS

A total of 506 extratropical storm events were identified in the 98 months included in the study (Table 3.2). These data were used to determine the average frequency and standard deviation in storms for each month of the storm season. The northerly wind data for each storm event were used to determine the average characteristics of a storm event for the entire study period, and for each month of the storm season (September to May).

The results of the analyses indicate that the average annual frequency of storms at the study site was approximately 47.5. The average distribution of storms during the season resembled a bell curve with the highest frequency in January. (Table 3.3, Figure 3.6). These results compare favorably with the findings of previous studies which indicated that the average annual frequency of cold fronts along the Gulf coast was approximately 45 (DiMego *et al* . 1976; Henry 1977b), and the highest average frequency was in December (6.6) (Henry 1977b) (Figure 1.4).

Based on the definition of a storm event used in this study, the average duration of a storm was determined to be 37.8 hours (std. dev. = 27.7 hours). The average mean wind speed was 8.3 m sec^{-1} (std. dev. = 1.8 m sec^{-1}), and the average maximum wind speed was 11.6 m sec^{-1} (std. dev. = 2.9 m sec^{-1}) (Figures 3.7-3.9). These results compare favorably with the findings of Fox and Davis (1976) at Mustang Island, Texas. Their research indicated that mean wind speed varied from 8-10 m sec^{-1}, and maximum wind speed peaked at approximately 15 m sec^{-1}. Their conclusions, however, were based on the results of two 30-day field studies. The

duration of storms was not reported by Fox and Davis (1976), so this research appears to be the first evaluation of storm duration along the Gulf Coast. It should be noted that 10 storm events identified in this dissertation research did not produce "northerly" winds of 5.5 m sec^{-1} or greater. Several of these events produced extremely low wind speeds (weak frontal passages); the remainder of these events produced strong southerly winds, but no northerly winds.

Table 3.2. Total number of extratropical storm events observed at NDBC Station 42007 during each month included in the study. (Total number of storms = 506; total number of months = 98).

YEAR	SEP	OCT	NOV	DEC	JAN	FEB	MAR	APR	MAY
80-81					-	-	6	-	-
81-82	-	-	7	-	-	-	3	6	1
82-83	4	3	5	6	8	7	-	-	-
83-84	-	-	-	-	-	-	-	4	4
84-85	4	0	6	5	7	-	7	2	-
85-86	4	-	-	-	-	-	-	3	2
86-87	2	4	-	-	-	-	-	-	-
87-88	2	7	4	-	-	-	6	5	5
88-89	2	7	7	7	9	5	6	-	4
89-90	4	6	5	6	8	6	5	6	5
90-91	2	7	6	6	9	-	-	3	2
91-92	-	-	-	-	-	-	-	-	-
92-93	3	6	6	9	10	7	6	6	4
93-94	6	-	4	-	6	5	7	5	4
94-95	4	5	6	5	7	8	3	3	2
95-96	5	5	7	5	7	5	4	6	2
96-97	4	3	5	7	6	4	8	8	6
Total	46	53	68	56	77	47	61	57	41

Table 3.3. Frequency statistics for extratropical storms at NDBC Station 42007.

STATS	SEP	OCT	NOV	DEC	JAN	FEB	MAR	APR	MAY
Min	2	0	4	5	6	4	3	2	1
Max	6	7	7	9	10	8	8	8	6
Mean	3.5	4.8	5.7	6.2	7.7	5.9	5.5	4.8	3.4
Std Dev	1.2	2.1	1.0	1.2	1.3	1.3	1.6	1.7	1.5

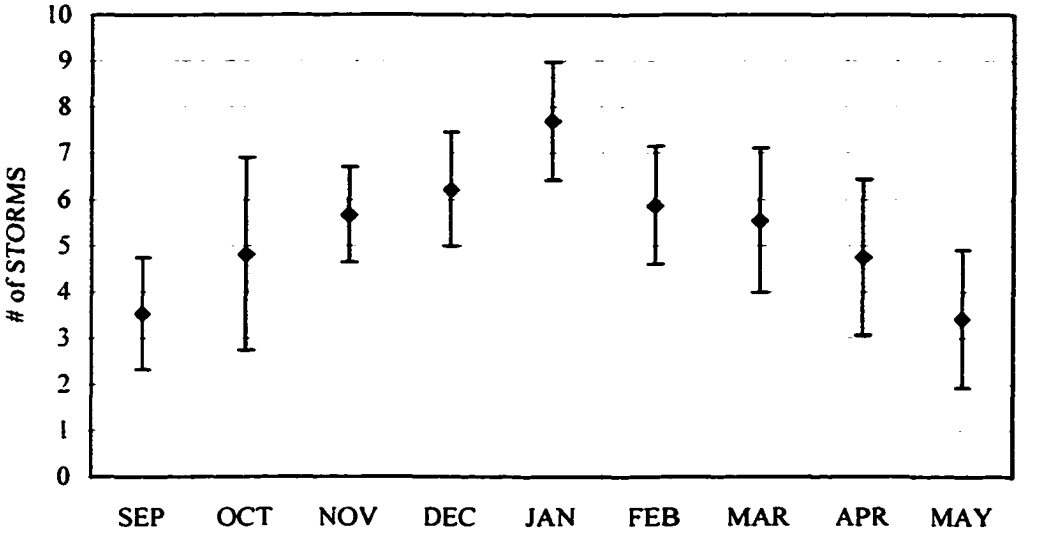

Figure 3.6. Average frequency of extratropical storms at NDBC Station 42007. The plot shows the mean and (+/-) one standard deviation error bars for each month. The average annual frequency was 47.5.

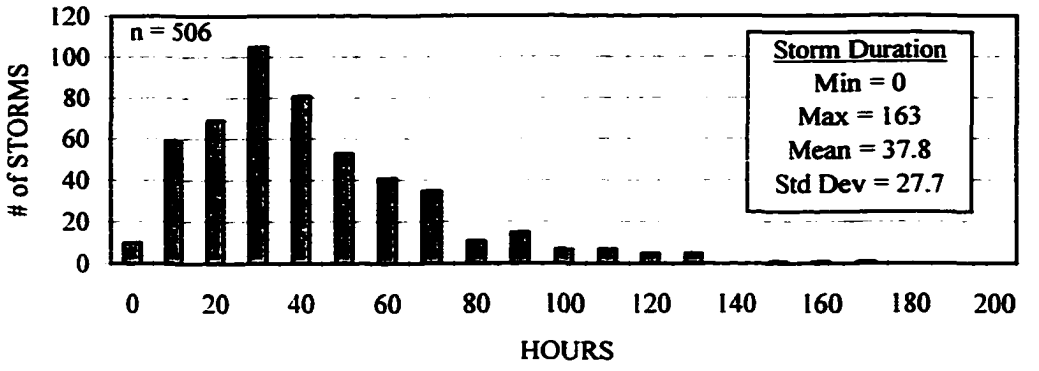

Figure 3.7. Histogram of storm duration data. Values along the X-axis represent the upper limit of the class. Ten events did not produce "northerly" winds equal to the minimum limit of 5.5 m sec^{-1}.

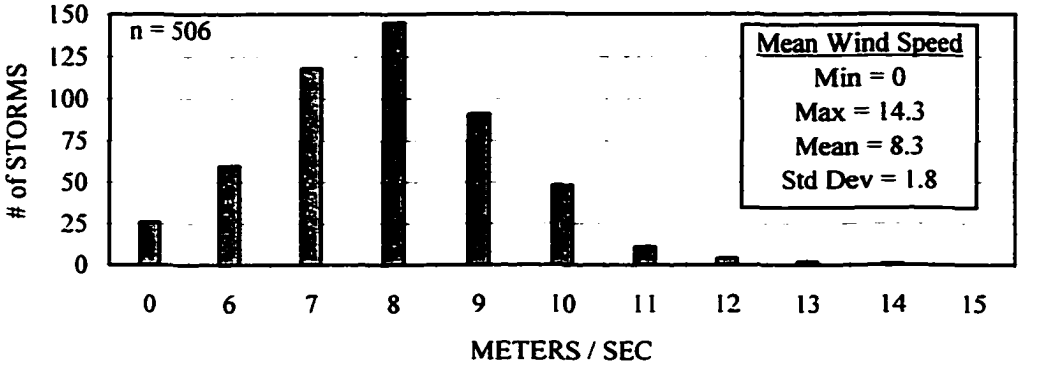

Figure 3.8. Histogram of mean wind speed data. Values along the X-axis represent the lower limit of the class. Ten events did not produce "northerly" winds equal to the minimum limit of 5.5 m sec^{-1}.

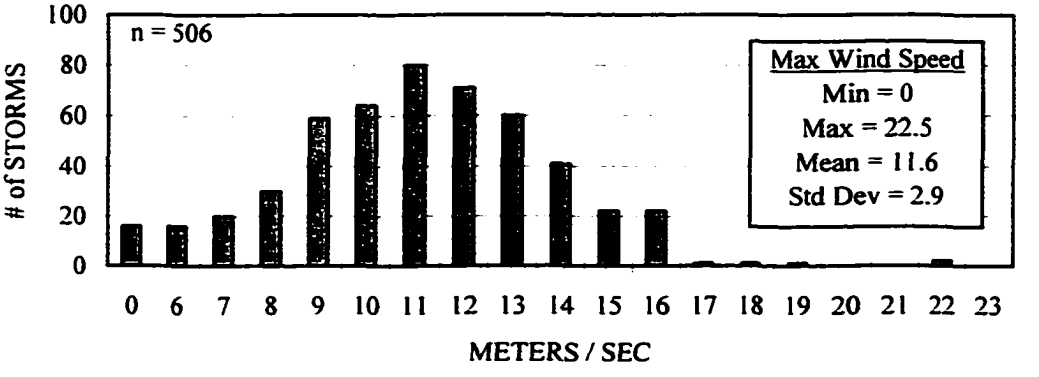

Figure 3.9. Histogram of maximum wind speed data. Values along the X-axis represent the lower limit of the class. Ten events did not produce "northerly" winds equal to the minimum limit of 5.5 m sec^{-1}.

Storm duration varied considerably at the study site whereas mean and maximum wind speeds were relatively consistent (Figure 3.10). These results may have been influenced by the location of the study site relative to the storm tracks of cyclones migrating along the Gulf Coast. Higher winds speeds, and greater variability in winds speeds, may occur at locations closer to the storm track of cyclones migrating across the central U.S., or at locations closer to the Texas coast where Gulf cyclones originate. Hsu's (1993) storm intensity scale clearly indicates that higher mean wind speeds, and greater variability in mean wind speeds, occur at the low-pressure center of Gulf cyclones. The observation made here is that low variability in wind speeds recorded at the study site may be a function of relative location (*i.e.* distance from storm tracks), rather than storm intensity. These findings suggest that the spatial variability in wind speeds should be evaluated in future research.

Storm duration was consistently higher during the autumn months and decreased considerably by the end of the storm season in spring (Table 3.4, Figure 3.11). The month with the highest average storm duration was November (46.0 hours), and the month with the lowest average storm duration was May (24.7 hours). Mean and maximum wind speeds were relatively consistent over the storm season with slightly higher wind speeds occurring in late-winter. February had the highest average mean wind speed (8.8 m sec^{-1}), and the highest average maximum wind speed (12.3 m sec^{-1}). However, wind speeds decreased considerably at the end of the storm season with May having the lowest average mean (7.4 m sec^{-1}) and maximum (9.8 m sec^{-1}) wind speeds.

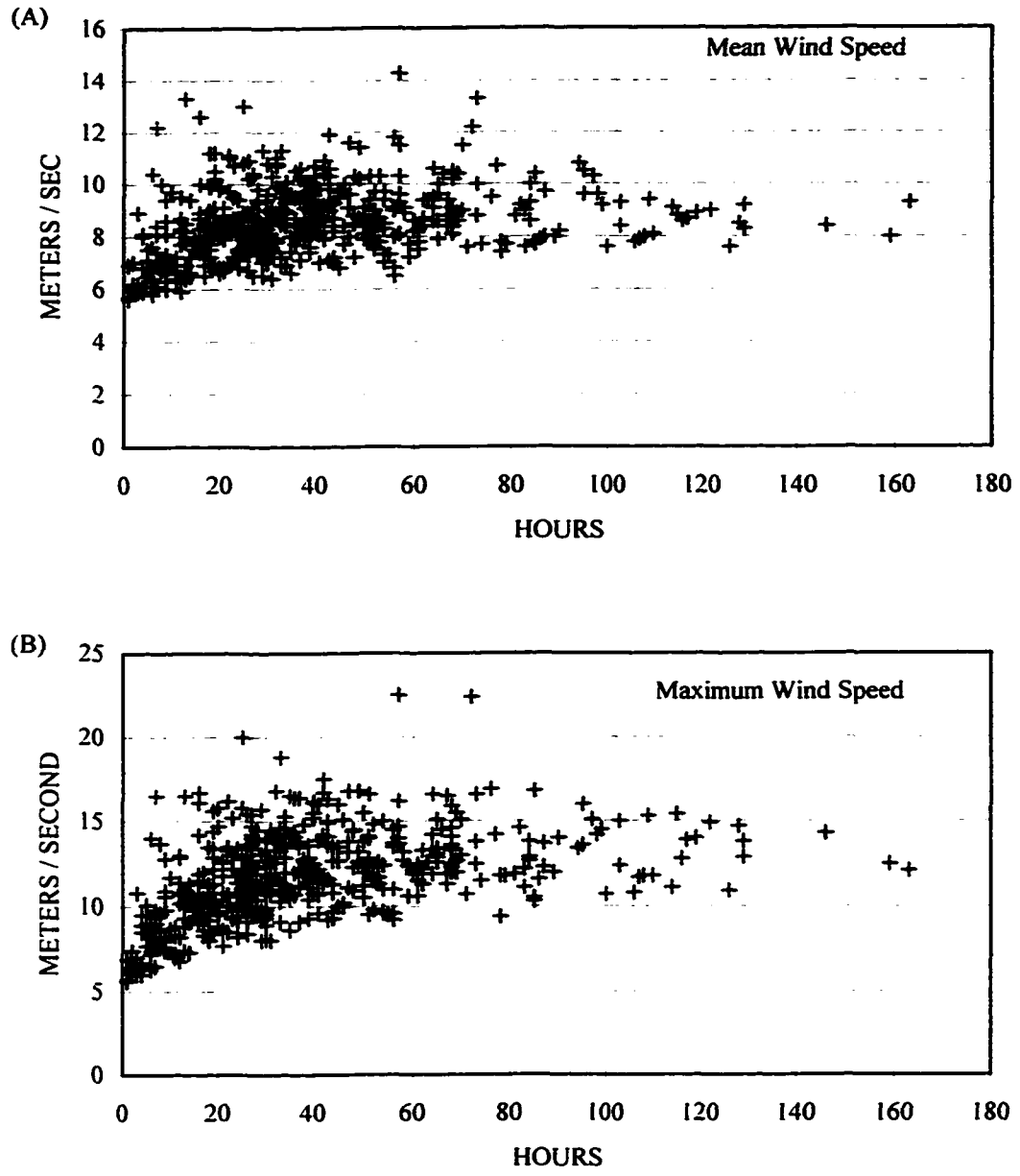

Figure 3.10. Distribution of all storms by storm duration and wind speed at NDBC Station 42007. The upper plot (A) shows the distribution by mean wind speed and the lower plot (B) shows the distribution by maximum wind speed. The 10 storm events that did not produce "northerly" winds equal to the minimum limit of 5.5 m sec^{-1} are not shown.

Table 3.4. Northerly wind statistics for storm events at NDBC Station 42007. The categories are storm duration (T), mean wind speed (Vavg), and maximum wind speed (Vmax).

MONTH	# obs	STATS	T hours	Vavg m/s	Vmax m/s
SEP	46	Mean	44.4	7.9	10.5
		Std Dev	35.6	1.3	2.1
OCT	53	Mean	45.5	8.2	11.3
		Std Dev	34.9	1.8	2.8
NOV	68	Mean	46.0	8.5	12.0
		Std Dev	32.5	1.5	2.3
DEC	56	Mean	39.3	8.4	11.6
		Std Dev	25.3	1.7	2.7
JAN	77	Mean	36.7	8.4	11.8
		Std Dev	23.4	1.9	2.9
FEB	47	Mean	41.8	8.8	12.3
		Std Dev	21.9	1.8	2.6
MAR	61	Mean	33.3	8.6	12.1
		Std Dev	26.5	2.1	3.6
APR	57	Mean	26.8	8.4	11.8
		Std Dev	15.2	2.0	3.3
MAY	41	Mean	24.7	7.4	9.8
		Std Dev	15.7	1.7	2.8

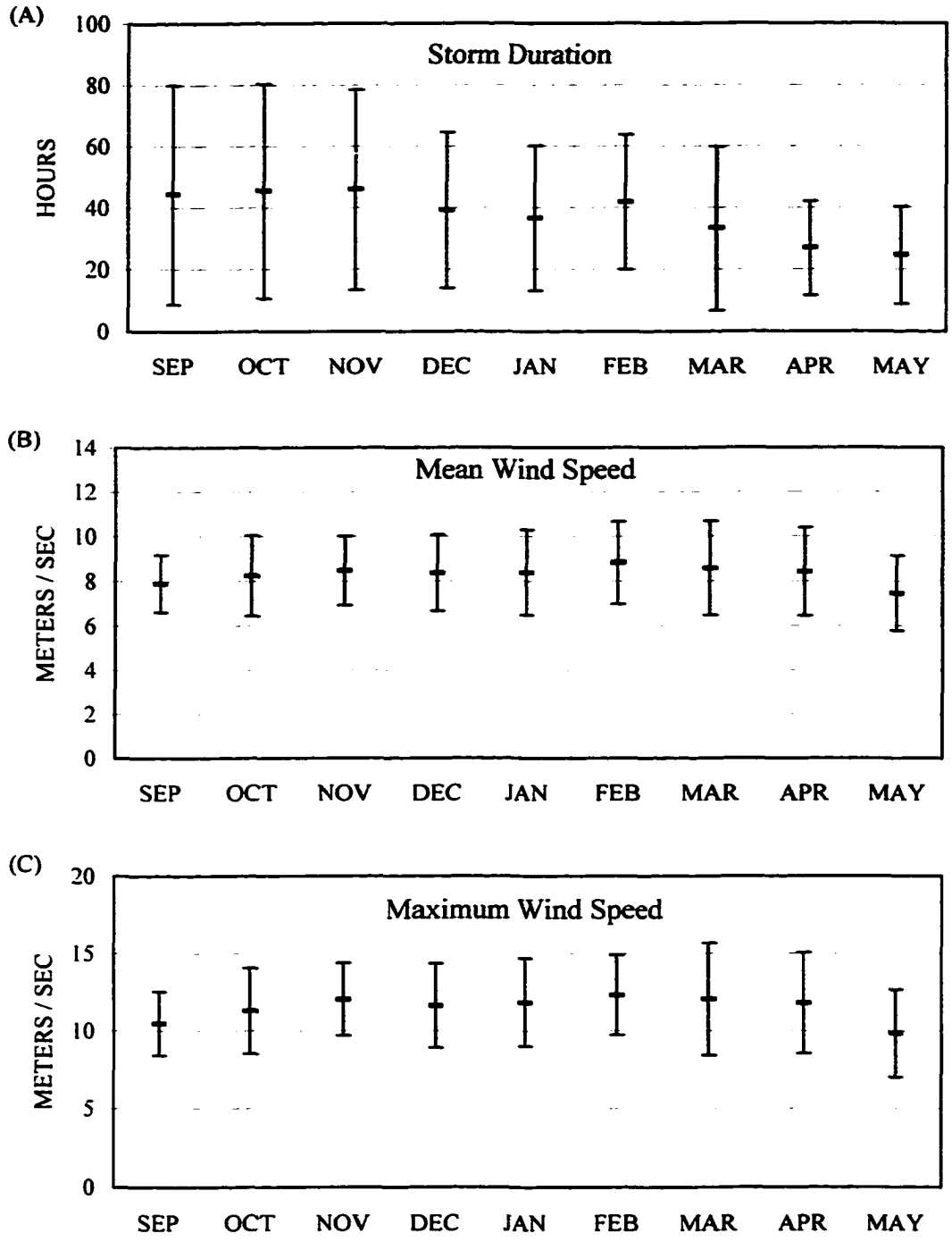

Figure 3.11. Northerly wind statistics for storm events at NDBC Station 42007. The plots show the mean and (+/-) one standard deviation error bars for storm duration (A), mean wind speed (B), and maximum wind speed (C).

STORM TYPES

The Primary Front storm type proved to be the most common of the seven storm types identified in this study (Figures 3.2-3.5). The average frequency of Primary Fronts was 35.9 storms per year which accounted for approximately 75% of all storm activity (Table 3.5). The Secondary Front was the next most common storm type. These storms had an average frequency of 6.9 storms per year which accounted for an additional 15% of storm activity. These two storm types accounted for approximately 90% of all extratropical storm activity in the region.

Table 3.5. Average monthly and annual frequency of storm types at NDBC Station 42007.

TYPE	SEP	OCT	NOV	DEC	JAN	FEB	MAR	APR	MAY	TOTAL
PF	3.1	4.0	4.3	5.2	5.4	4.3	4.2	3.1	2.3	35.9
SF	0.3	0.4	1.3	0.7	0.7	0.5	0.8	1.3	0.9	6.9
SGF	-	-	0.1	-	0.4	0.5	-	0.2	0.1	1.3
SGL	0.1	0.3	-	0.2	1.1	0.1	0.4	0.1	-	2.3
GF	-	-	-	0.1	-	-	-	-	-	0.1
GL	-	0.1	-	-	0.1	0.2	-	0.1	0.1	0.6
PL	-	-	-	-	-	0.3	0.1	-	-	0.4
Total	3.5	4.8	5.7	6.2	7.7	5.9	5.5	4.8	3.4	47.5

Primary Fronts had higher average storm values than Secondary Fronts in each of the following categories: storm duration (40.3 hours vs 32.0 hours), mean wind speed (8.3 m sec^{-1} vs 7.8 m sec^{-1}), and maximum wind speed (11.5 m sec^{-1} vs 11.0 m sec^{-1}) (Table 3.6, Figure 3.12). Both storm types showed greater variability in storm duration than in mean or maximum wind speed (Figures 3.13 and 3.14). An explanation for this pattern was discussed in the previous section.

Table 3.6. Northerly wind statistics for storm types at NDBC Station 42007. The categories include storm duration (T), mean wind speed (Vavg), and maximum wind speed (Vmax).

TYPE	# obs	STATS	T hours	Vavg m/s	Vmax m/s
PF	382	Mean	40.3	8.3	11.5
		Std Dev	28.8	1.6	2.6
SF	77	Mean	32.0	7.8	11.0
		Std Dev	25.9	2.3	3.7
SGF	13	Mean	23.0	7.9	11.2
		Std Dev	13.8	2.6	2.8
SGL	24	Mean	29.8	9.9	13.9
		Std Dev	14.0	2.0	3.5
GF	1	Mean	1.0	5.7	5.7
		Std Dev	-	-	-
GL	6	Mean	28.2	9.1	12.5
		Std Dev	10.2	1.0	2.1
PL	3	Mean	37.0	9.8	14.4
		Std Dev	9.1	2.3	4.4

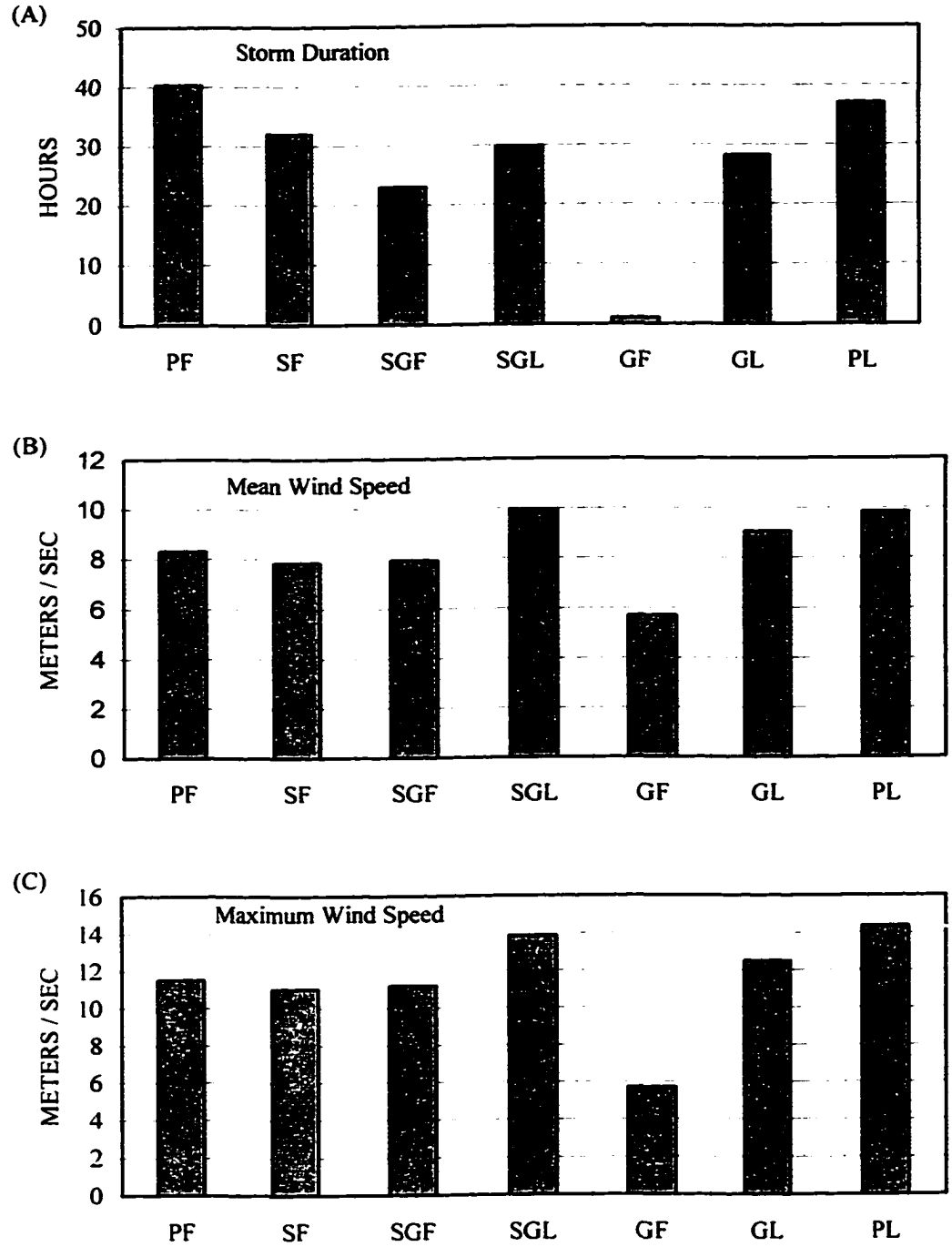

Figure 3.12. Northerly wind statistics for storm types at NDBC Station 42007. The plots show the mean values for storm duration (A), mean wind speed (B), and maximum wind speed (C).

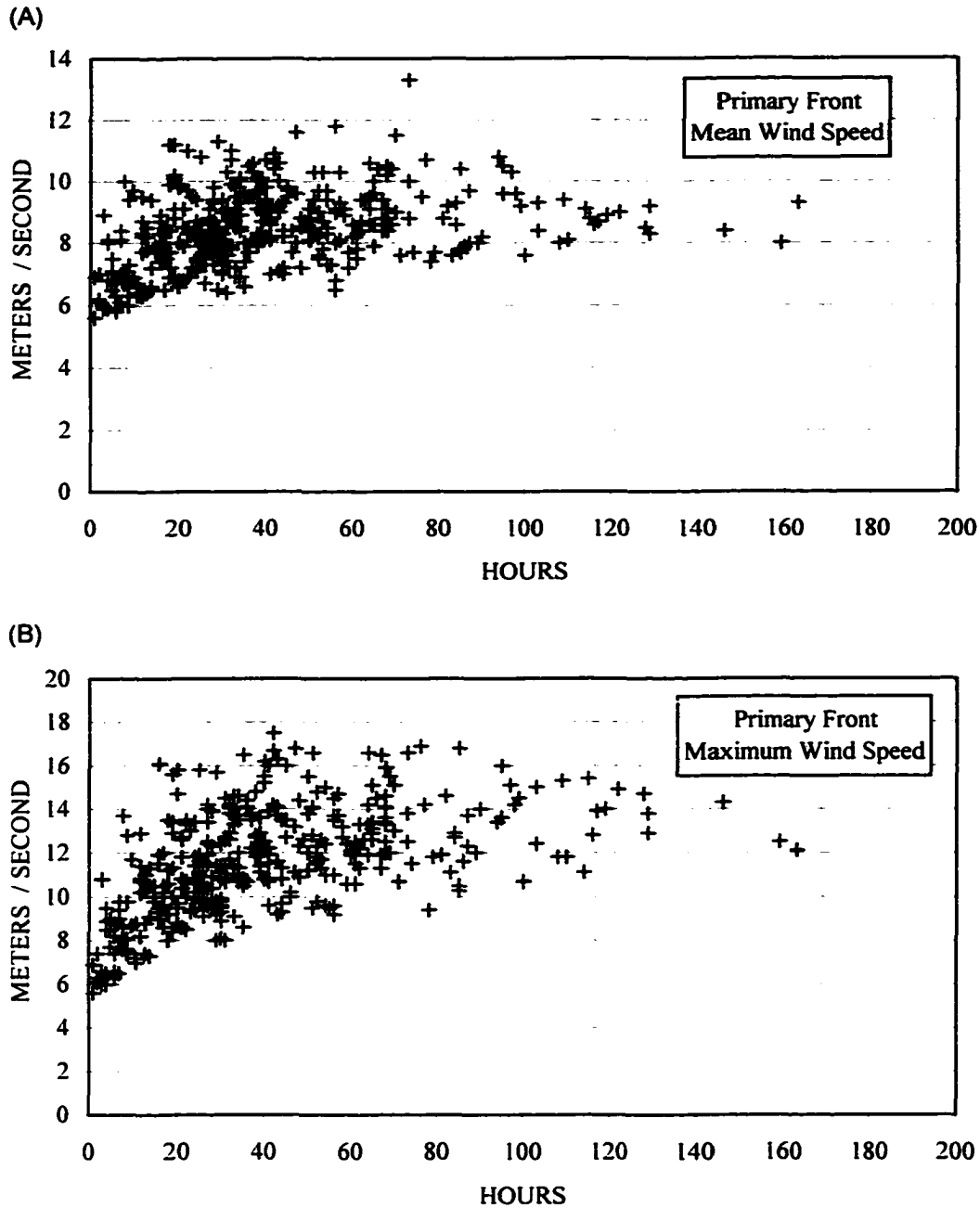

Figure 3.13. Distribution of Primary Fronts by storm duration and wind speed at NDBC Station 42007. The upper plot (A) shows the distribution by mean wind speed and the lower plot (B) shows the distribution by maximum wind speed.

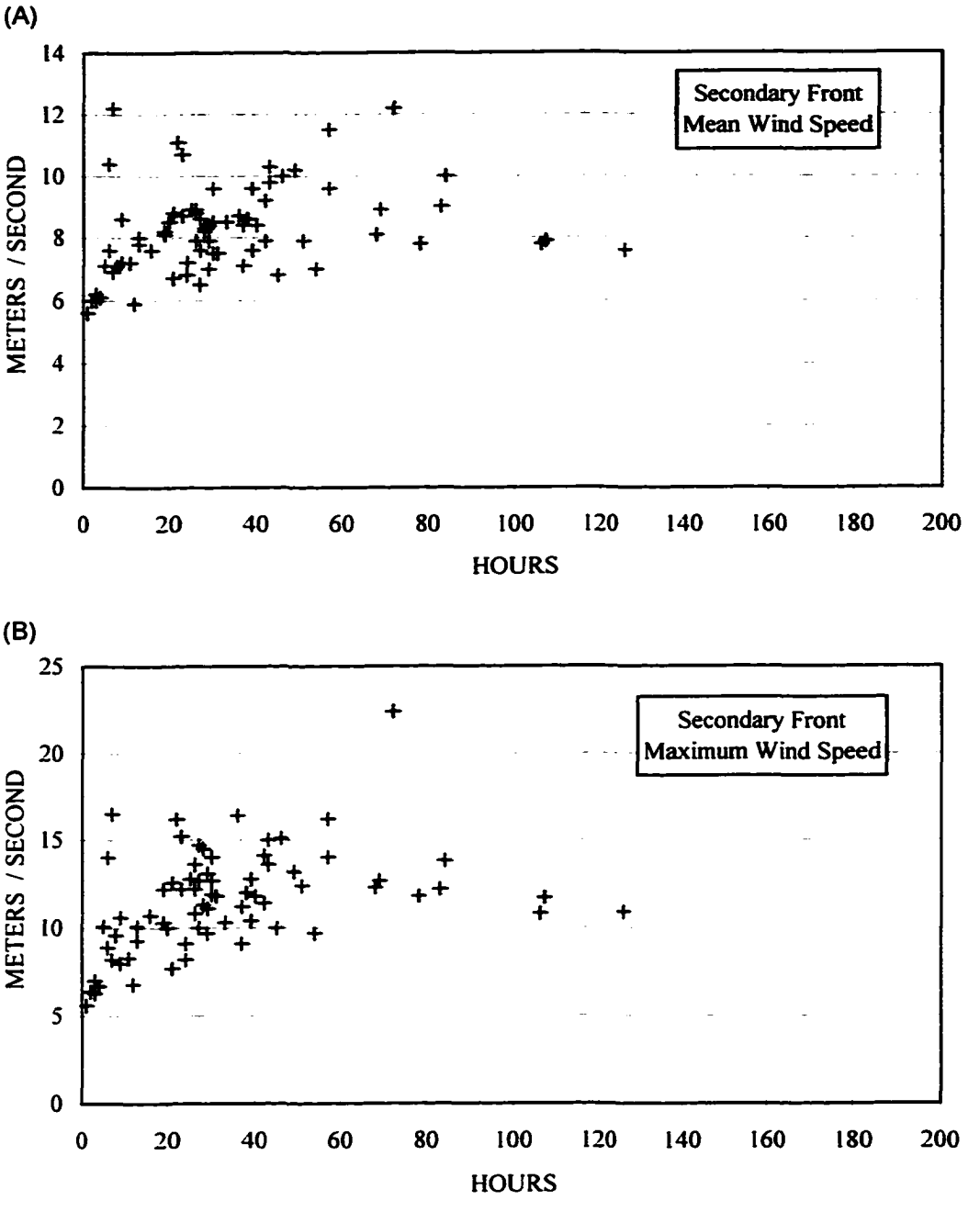

Figure 3.14. Distribution of Secondary Fronts by storm duration and wind speed at NDBC Station 42007. The upper plot (A) shows the distribution by mean wind speed and the lower plot (B) shows the distribution by maximum wind speed.

The number of observations (n) for each of the remaining five storm types was below the generally accepted quantity for a representative sample (*i.e.*, n = 30), so additional data should be evaluated before drawing conclusions. Nevertheless, three of these storm types produced the highest average mean and maximum wind speeds in the study. These were the Secondary Gulf Low, the Gulf Low, and the Primary Low (Table 3.6). The intensity of the wind speeds for these storm types was related to the fact that they had low-pressure centers that passed near NDBC Station 42007. Although these storms only accounted for 7% of storm activity at the study site, the high wind speeds suggest that these storm types would have the greatest impact on the coast. An increase in the frequency of these three storm types would evidently increase the variability in mean and maximum wind speeds observed at the study site (Figure 3.10).

Since the Primary Front proved to be the most common storm type, the average characteristics of Primary Fronts were computed for each month of the storm season (Table 3.7). The highest average duration of Primary Front storm events occurred in November (50.7 hours). The highest average mean wind speeds occurred in February (8.8 m sec^{-1}) and November (8.7 m sec^{-1}), and the highest average maximum wind speeds occurred in February (12.3 m sec^{-1}) and November (12.3 m sec^{-1}). Storm duration varied greatly in autumn and then declined throughout the storm season. Mean and maximum wind speeds remained relativly consistent throughout the storm season. These data (Figure 3.15) were extremely similar to those presented for all storm events (Figure 3.11), and clearly indicate that Primary Fronts had a significant influence on the results of that study.

Table 3.7. Northerly wind statistics for Primary Fronts at NDBC Station 42007. The categories are storm duration (T), mean wind speed (Vavg), and maximum wind speed (Vmax).

MONTH	# obs	STATS	T hours	Vavg m/s	Vmax m/s
SEP	40	Mean	48.7	7.9	10.7
		Std Dev	36.0	1.2	1.9
OCT	45	Mean	45.9	8.4	11.5
		Std Dev	32.9	1.3	2.2
NOV	51	Mean	50.7	8.7	12.3
		Std Dev	35.0	1.2	2.3
DEC	47	Mean	39.1	8.4	11.7
		Std Dev	25.6	1.7	2.7
JAN	54	Mean	36.7	8.2	11.6
		Std Dev	23.7	2.0	2.9
FEB	34	Mean	47.0	8.8	12.3
		Std Dev	20.3	1.1	2.0
MAR	46	Mean	34.4	8.2	11.5
		Std Dev	28.2	1.8	3.0
APR	37	Mean	30.0	8.6	11.8
		Std Dev	16.1	1.8	2.9
MAY	28	Mean	24.4	7.6	9.7
		Std Dev	16.0	1.2	2.2

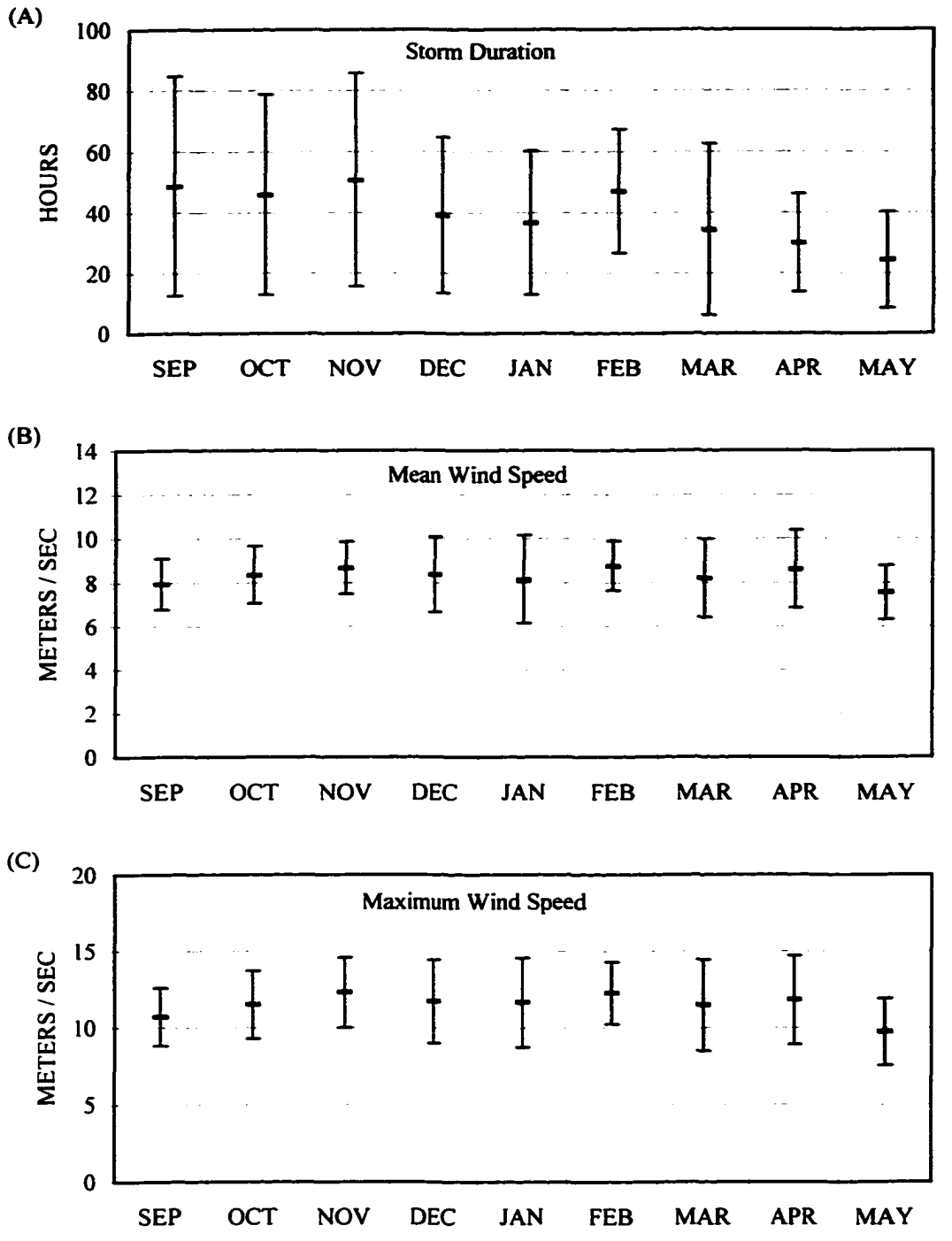

Figure 3.15. Northerly wind statistics for Primary Fronts at NDBC Station 42007. The plots show the mean and (+/-) one standard deviation error bars for storm duration (A), mean wind speed (B), and maximum wind speed (C).

STORM MAGNITUDE

The storm-magnitude data (V square values) were used to construct a 5 class storm-magnitude scale. The 10 storm events that did not produce northerly winds of 5.5 m sec^{-1} or greater were excluded from the analysis. The class boundaries were determined with an analysis of variance test known as the "Jenks" or "optimization" method (Jenks and Caspall 1971, Smith 1986, Moore *et al*. 1990). The Goodness of Variance Fit (GVF) value for the 5 class scale constructed by the Jenks method was 93.9. The class limits produced by this method were slightly adjusted for practical use. The GVF value for the "adjusted" classification was 93.8 (Table 3.8).

The storms with the highest V square values were grouped into Class 5, and the storms with the lowest V square values were grouped into Class 1. The Class 5 storms had the highest average values in each of the basic storm characteristic categories: storm duration (105.4 hours), mean wind speed (9.7 m sec^{-1}), and maximum wind speed (14.6 m sec^{-1}) (Table 3.9). The curve of the mean storm duration values and mean V square values for the 5 classes were extremely similar (Figure 3.16), so a regression analysis was used to evaluate the relationship between the V square data and the storm data. The regression analysis of the storm data (x) and the V square data (y) produced the following R square values: storm duration (0.84), mean wind speed (0.31) and maximum wind speed (0.41) (Figure 3.17). An enlarged version of the plot of the storm duration data and the V square data showing the class boundaries is provided in Figure 3.18.

Table 3.8. Storm-magnitude scale for extratropical storms. The scale was based on the V square values of the 496 storms that produced "northerly" winds of 5.5 m sec^{-1} or greater at NDBC Station 42007.

STORM CLASS	CLASS LIMITS $\Sigma (v^2)$	# STORMS
0	0	10
1	1 - 1499	137
2	1500 - 2999	145
3	3000 - 4999	124
4	5000 - 7999	62
5	8000+	28

Table 3.9. Northerly wind statistics for storms in each class at NDBC Station 42007. The categories are storm duration (T), mean wind speed (Vavg), maximum wind speed (Vmax), and V square value (Vsq).

CLASS	# obs	STATS	T hours	Vavg m/s	Vmax m/s	Vsq $\Sigma (v^2)$
1	137	Mean	12.6	7.3	9.1	720
		Std Dev	7.4	1.1	2.0	440
2	145	Mean	30.2	8.4	11.7	2157
		Std Dev	8.1	1.1	1.7	429
3	124	Mean	46.1	9.2	13.2	3889
		Std Dev	12.3	1.2	2.0	575
4	62	Mean	70.4	9.4	13.6	6279
		Std Dev	18.4	1.1	1.8	897
5	28	Mean	105.4	9.7	14.6	10132
		Std Dev	25.8	1.2	2.0	1389

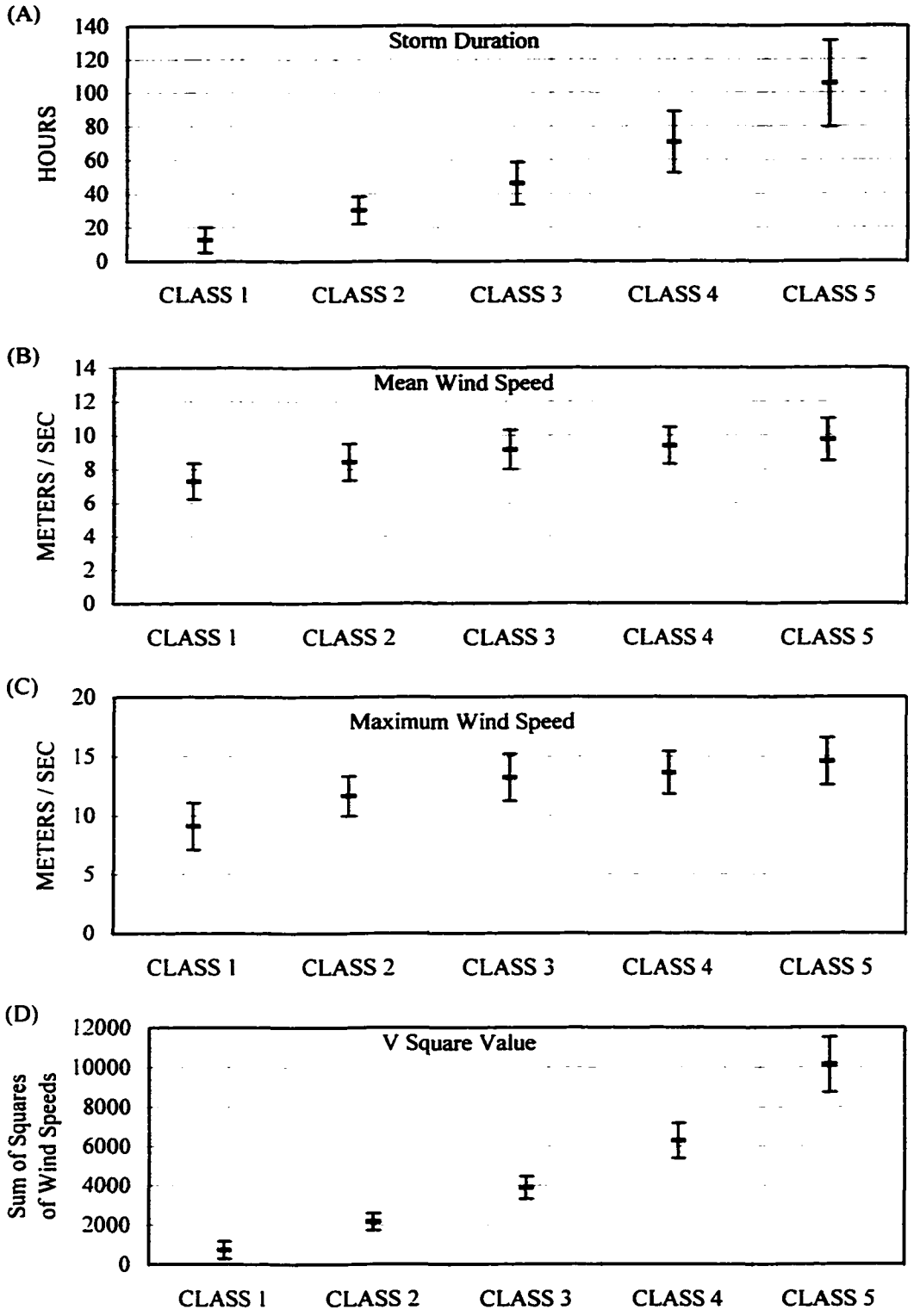

Figure 3.16. Northerly wind statistics for storms in each class at NDBC Station 42007. The plots show the mean and (+/-) one standard deviation error bars for storm duration (A), mean wind speed (B), maximum wind speed (C), and V square value (D).

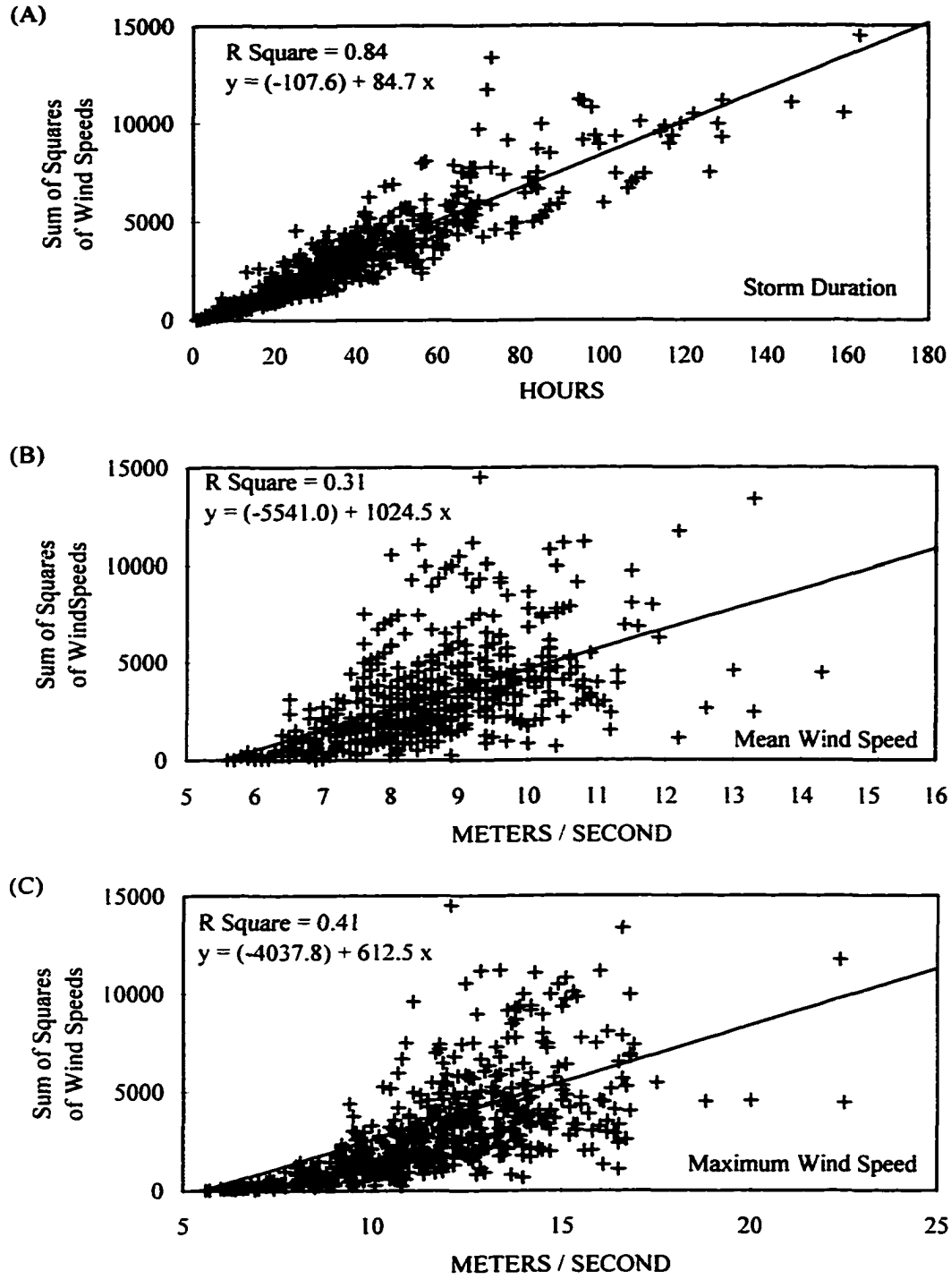

Figure 3.17. Regression analysis of the storm data (x) and the V square data (y). The scatter plots show the results of the analysis for storm duration (A), mean wind speed (B), and maximum wind speed (C). The 10 storms that did not produce "northerly" winds of 5.5 m sec^{-1} or greater (Class 0) were excluded from the analysis.

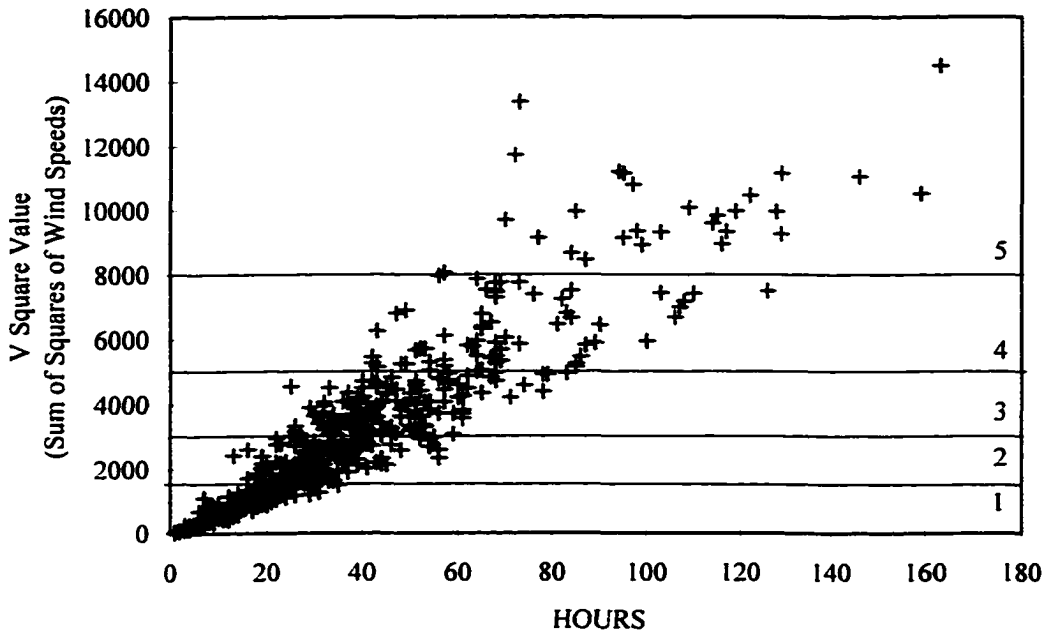

Figure 3.18. Distribution of storms by storm duration and V square value. The plot also shows limits of the storm-magnitude classes.

The method used to assign storm magnitude values in this study was intentionally biased toward higher wind speeds. Storm duration, however, still proved to be the more dominant variable in determining storm magnitude. The regression analysis indicated that storm duration had a greater influence on V square values (R square = 0.84) than did mean wind speed (R square = 0.31) or maximum wind speed (R square = 0.41) (Figure 3.17). The scatter plots of the

storm duration and wind speed data for all storm events (Figure 3.10) clearly indicated that there was greater variability in storm duration (std. dev. = 27.7 hours) than in mean wind speed (std. dev. = 1.8 m sec^{-1}) or maximum wind speed (std. dev. = 2.9 m sec^{-1}), therefore, these results were to be expected. These findings appear to substantiate the perception of extratropical storms as low-magnitude, high-frequency events.

The storm-magnitude data indicate that the distribution of storm impacts varied considerably during a storm season. The distribution of Class 1, 2, and 3 storms (the lower magnitude storms) resembled the distribution of all storms with the highest frequency in January (6.4) (Table 3.10, Figure 3.19). The distribution of Class 4 and 5 storms was skewed toward the earlier part of the storm season with the highest frequencies in October and November (1.4, each). Although storm activity was lower during the autumn months, these findings suggest that storm impacts along the coast may have been greater during this period. One possible explanation for the high frequency of Class 4 and 5 storms during the autumn months is that cold fronts may have stalled along the coast for extended periods, thereby increasing storm duration in autumn. Although no data are presented to support this theory, this pattern may be related to delayed cooling of water temperatures in the Gulf, or the position of the high-pressure system that resides over the northern Atlantic Ocean (Bermuda High) (Christopherson 1997) which may inhibit the southward migration of cold air masses at this time of year. This pattern of storm variability should be investigated in future research.

Table 3.10. Average monthly and annual frequency of storms in each class at NDBC Station 42007.

CLASS	SEP	OCT	NOV	DEC	JAN	FEB	MAR	APR	MAY	TOTAL
0	0.0	0.1	0.1	0.1	0.2	0.1	0.1	0.2	0.1	1.0
1	1.2	1.4	0.9	1.6	1.9	0.6	2.0	1.3	1.5	12.4
2	0.9	1.2	1.8	1.4	2.3	1.9	1.2	1.6	1.4	13.7
3	0.5	0.8	1.5	2.0	2.0	2.3	1.4	1.5	0.2	12.1
4	0.5	0.9	1.0	0.8	0.9	0.8	0.5	0.2	0.3	5.8
5	0.4	0.5	0.4	0.3	0.4	0.3	0.4	0.0	0.0	2.6
Total	3.5	4.8	5.7	6.2	7.7	5.9	5.5	4.8	3.4	47.5

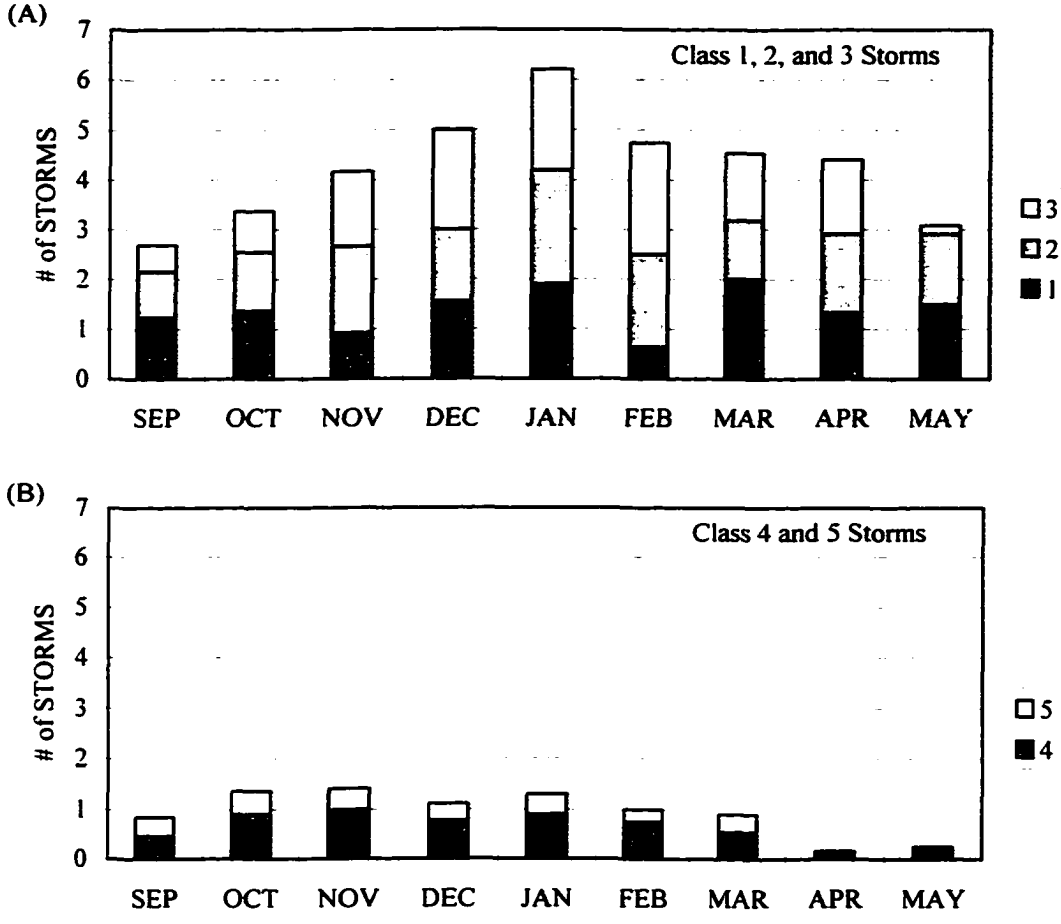

Figure 3.19. Average frequency of storms in each class at NDBC Station 42007. The upper plot (A) shows the average frequency of Class 1, 2, and 3 storms and the lower plot (B) shows the average frequency of Class 4 and 5 storms.

Each of the seven storm types identified in this study were evaluated to determine which storm types produced the highest magnitude storm events. Primary and Secondary Fronts accounted for all Class 5 storms. Primary Fronts, Secondary Fronts, and Secondary Gulf Lows accounted for all Class 4 storms (Table 3.11). These results indicate that Primary Fronts and the Secondary Fronts were the two most dominant storm types at the study site.

Table 3.11. Total number of storm types in each storm-magnitude class at NDBC Station 42007.

CLASS	PF	SF	SGF	SGL	GF	GL	PL	TOTAL
0	5	4	1	-	-	-	-	10
1	99	25	5	6	1	1	-	137
2	106	28	4	3	-	3	1	145
3	95	10	3	12	-	2	2	124
4	52	7	-	3	-	-	-	62
5	25	3	-	-	-	-	-	28
Total	382	77	13	24	1	6	3	506

STORM SUB-TYPES

The northwesterly and northeasterly winds produced by each storm event were analyzed for the purpose of evaluating the predominant direction of sediment transport along the north-facing shores of barrier islands in the region. The analysis

indicated that there were a significant number of storms that produced only northwesterly or northeasterly winds. This information was used to define three storm sub-types: sub-type A (northwesterly winds), sub-type B (northeasterly winds), and sub-type C (northwesterly and northeasterly winds).

Sub-type A storms had an average annual frequency of 4.9 storms per year, and an average storm duration of 18.9 hours. Sub-type B storms had an average annual frequency 8.6 storms per year, and average storm duration of 28.5 hours. Sub-type C storms had an average annual frequency of 33.0 storms per year, and an average storm duration of 44.6 hours. The average ratio of northeasterly winds (29.3 hours) to northwesterly winds was (15.3 hours) was approximately 2:1 (Table 3.12 and 3.13).

The average frequency (Table 3.13; Figure 3.20) and average storm duration (Table 3.14; Figure 3.21) data were used to determine the average duration of northwesterly and northeasterly winds for each month of the storm season (Table 3.15; Figure 3.21). The average annual duration of northeasterly winds was 1,212.0 hours, and the average annual duration of northwesterly winds was 597.5 hours, which was a ratio of approximately 2:1 (Table 3.15; Figure 3.22). Although wave measurements at the beach are needed to determine the actual direction of alongshore sediment transport, the inference can be made from the wind data that the predominant direction of sediment transport along the northern coast of barrier islands in the region was westward.

Table 3.12. Northwesterly and northeasterly wind statistics for storm sub-types at NDBC Station 42007. The categories include storm duration (T), mean wind speed (Vavg), and maximum wind speed (Vmax). Sub-type 0 was included in this table to account for the 10 storms that did not produce northerly winds of 5.5 m sec^{-1}.

SUB-TYPE	#obs	STATS	NW T hours	NW Vavg m/s	NW Vmax m/s	NE T hours	NE Vavg m/s	NE Vmax m/s
0	10	Mean	0	-	-	0	-	-
		Std Dev	0	-	-	0	-	-
A	50	Mean	18.9	8.6	11.3	0	-	-
		Std Dev	13.6	1.7	3.2	0	-	-
B	95	Mean	0	-	-	28.5	8.1	10.4
		Std Dev	0	-	-	26.6	1.7	2.7
C	351	Mean	15.3	8.7	11.0	29.3	8.3	11.0
		Std Dev	14.0	1.8	2.8	24.8	1.3	2.3

Table 3.13. Average monthly and annual frequency of storm sub-types at NDBC Station 42007. Sub-type 0 was included in this table to account for the 10 storms that did not produce northerly winds of 5.5 m sec^{-1}.

SUB-TYPE	SEP	OCT	NOV	DEC	JAN	FEB	MAR	APR	MAY	TOTAL
0	0.0	0.1	0.1	0.1	0.2	0.1	0.1	0.2	0.1	1.0
A	0.1	0.3	0.3	0.6	1.3	0.9	0.5	0.8	0.1	4.9
B	1.5	0.8	0.5	1.4	1.3	0.3	1.3	0.6	0.9	8.6
C	1.9	3.6	4.8	4.1	4.9	4.6	3.6	3.3	2.3	33.0
Total	3.5	4.8	5.7	6.2	7.7	5.9	5.5	4.8	3.4	47.5

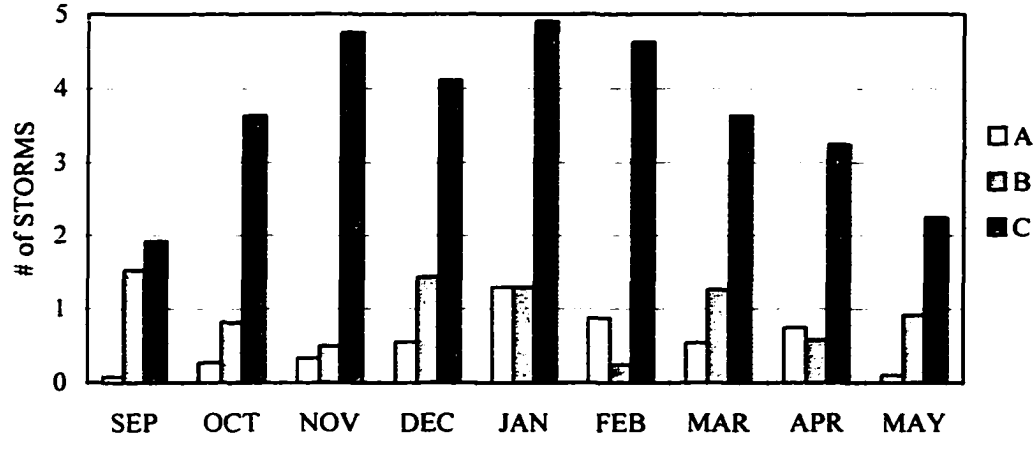

Figure 3.20. Average frequency of storm sub-types at NDBC Station 42007.

Table 3.14. Northwesterly and northeasterly wind statistics for storm sub-types (by month) at NDBC Station 42007. The categories include storm duration (T), mean wind speed (Vavg), and maximum wind speed (Vmax). Only "mean" values are shown for each category.

MONTH	SUB-T	# obs	NW T hours	NW Vavg m/s	NW Vmax m/s	NE T hours	NE Vavg m/s	NE Vmax m/s
SEP	A	1	5.0	6.5	7.7	-	-	-
	B	20	-	-	-	32.3	7.8	9.8
	C	25	7.3	7.7	9.2	48.4	8.0	10.8
OCT	A	3	11.7	6.9	8.2	-	-	-
	B	9	-	-	-	41.3	8.2	11.1
	C	40	12.4	8.5	10.5	37.8	8.5	11.4
NOV	A	4	19.5	8.6	10.9	-	-	-
	B	6	-	-	-	37.2	7.9	10.0
	C	57	14.8	8.9	11.4	34.9	8.4	11.3
DEC	A	5	17.2	8.2	10.7	-	-	-
	B	13	-	-	-	29.4	8.0	10.2
	C	37	19.3	9.1	11.6	27.5	8.5	11.3
JAN	A	13	20.8	8.5	11.1	-	-	-
	B	13	-	-	-	37.3	8.9	12.2
	C	49	15.9	8.8	11.4	26.4	8.1	10.5
FEB	A	7	18.7	9.4	12.6	-	-	-
	B	2	-	-	-	38.5	10.3	14.9
	C	37	18.3	8.7	11.1	29.2	8.3	11.0
MAR	A	6	22.3	9.0	12.4	-	-	-
	B	14	-	-	-	15.9	8.2	10.1
	C	40	19.1	9.0	11.9	22.7	8.4	11.2
APR	A	9	20.1	8.9	12.0	-	-	-
	B	7	-	-	-	15.4	8.4	10.4
	C	39	13.3	8.9	11.2	18.5	8.6	11.2
MAY	A	2	13.5	7.7	9.5	-	-	-
	B	11	-	-	-	17.4	7.2	8.4
	C	27	8.5	7.6	9.4	20.9	7.7	9.9

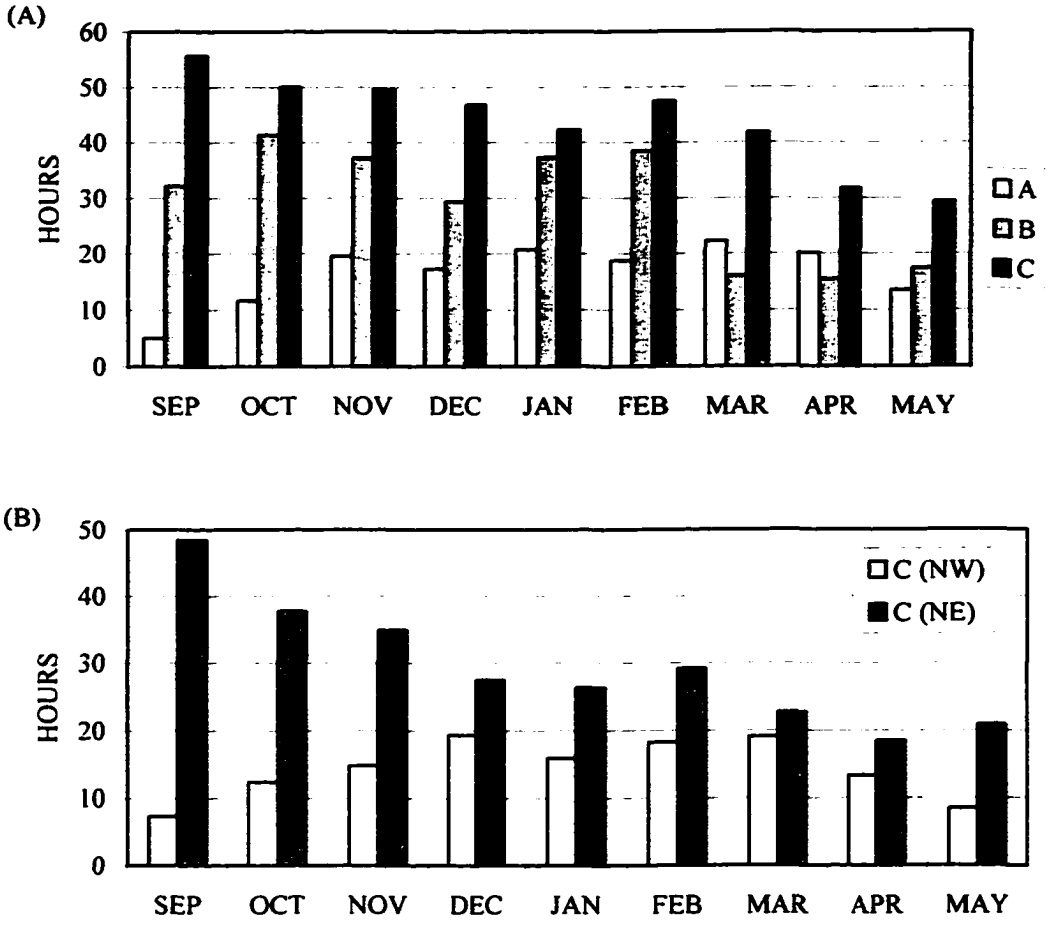

Figure 3.21. Average storm duration statistics for storm sub-types at NDBC Station 42007. The upper plot (A) shows the average duration of the storm sub-types and the lower plot (B) shows the average duration of northwesterly and northeasterly winds for sub-type C storms.

Table 3.15. Average total duration of northwesterly and northeasterly winds of all storms combined at NDBC Station 42007. These data are based on the average frequency and average duration of the storm sub-types for each month of the storm season.

QUAD	SEP hours	OCT hours	NOV hours	DEC hours	JAN hours	FEB hours	MAR hours	APR hours	MAY hours	Total hours
NW	14.4	48.2	76.9	89.5	105.0	101.0	79.9	60.3	22.3	597.5
NE	140.4	169.1	186.1	153.9	177.9	145.9	102.4	72.6	63.7	1,212.0

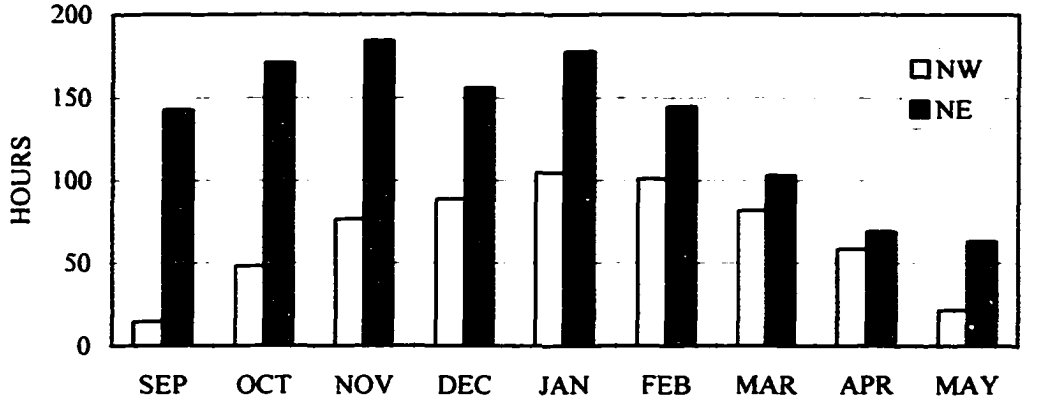

Figure 3.22. Average total duration of northwesterly and northeasterly winds of all storms combined at NDBC Station 42007.

The distribution of northeasterly winds was highly skewed toward the early part of the storm season (Figure 3.22). The distribution of northwesterly winds resembled a bell curve with the apex in January. Northeasterly winds prevailed each month, and the margin was extreme during the early part of the storm season. These results were related to the seasonal variability in the average duration of the storm sub-types. The average duration of sub-type A storms was lowest in autumn. The

average duration of sub-type B storms was highest in autumn. For sub-type C storms, the difference in the average duration of northeasterly winds and northwesterly winds was greatest in autumn (Figure 3.21).

The average difference in storm duration between northwesterly and northeasterly winds during the 3 autumn months was 356.1 hours, the average difference during the 3 winter months was 182.2 hours, and the average difference during the 3 spring months was 76.2 hours (Table 3.15). Although the average total duration of northerly winds was highest in winter (773.2 hours), the margin between northwesterly and northeasterly winds was greater in autumn (Figure 3.22) which suggests that a greater amount of "net" westward sediment transport (more westward than eastward) may occur in autumn. This observation presumes that wind direction and wave direction are directly related; however, their are a number of factors that may influence this relationship such as wind speed, tidal flow, and nearshore bathymetry / wave refraction patterns.

The distribution of storm sub-types by storm types was evaluated to determine if there was a relationship which might explain the variability in wind directions (Table 3.16). No obvious relationships were detected. Sub-type A storms were produced by 5 different storm types, sub-type B storms were produced by 4 different storm types, and sub-type C storms were produced by 6 different storm types. Also, 3 different storm types (PF, SF, and SGL) produced all 3 sub-types, 2 storm types (SGF and PL) produced only 2 sub-types, and 2 storm types (GF and GL) produced only 1 sub-type.

Table 3.16. Total number of sub-types for each storm type at NDBC Station 42007.

SUB-TYPE	PF	SF	SGF	SGL	GF	GL	PL	TOTAL
0	5	4	1	-	-	-	-	10
A	29	8	5	7	1	-	-	50
B	76	11	-	7	-	-	1	95
C	272	54	7	10	-	6	2	351
Total	382	77	13	24	1	6	3	506

SEASONAL VARIABILITY

The seasonal variation in the average duration of northwesterly and northeasterly winds identified in the previous section (Figure 3.22) was evaluated to determine if these results had been influenced by an extreme storm season. The total duration of northwesterly and northeasterly winds of all storms was determined for the autumn (September, October, and November), winter (December, January, and February) and spring (March, April, and May) months of years in which complete data sets were available. The mean and standard deviation were then determined for the total duration of the northwesterly winds, the northeasterly winds, and for all northerly winds, for each of the three seasons.

The results for autumn indicate that the variability in northeasterly winds (std. dev. = 123.0 hours) was considerably higher than the variability in northwesterly winds (std. dev. = 33.4 hours) (Table 3.17). However, northeasterly winds prevailed in all 10 years included in the analysis (Figure 3.23), and the average difference was 374.0 hours. These results indicate that northeasterly winds consistently prevailed by a significant margin.

Table 3.17. Total duration of northwesterly and northeasterly winds of all extratropical storms combined at NDBC Station 42007 during the autumn, winter, and spring season months. Seasons in which a complete data set was not available were excluded from the analysis.

YEAR	SEP-OCT-NOV			DEC-JAN-FEB			MAR-APR-MAY		
	NW hours	NE hours	Total hours	NW hours	NE hours	Total hours	NW hours	NE hours	Total hours
81-82	-	-	-	-	-	-	73	265	338
82-83	169	461	630	335	394	729	-	-	-
83-84	-	-	-	-	-	-	-	-	-
84-85	73	462	535	-	-	-	-	-	-
85-86	-	-	-	-	-	-	-	-	-
86-87	-	-	-	-	-	-	-	-	-
87-88	136	343	479	-	-	-	278	145	423
88-89	155	455	610	196	523	719	-	-	-
89-90	152	619	771	324	387	711	180	260	440
90-91	164	329	493	-	-	-	-	-	-
91-92	-	-	-	-	-	-	-	-	-
92-93	167	691	858	255	684	939	228	226	454
93-94	-	-	-	-	-	-	161	252	413
94-95	83	618	701	431	426	857	93	289	382
95-96	170	673	843	382	392	774	222	224	446
96-97	136	494	630	257	449	706	152	379	531
Mean	140.5	514.5	655.0	311.4	465.0	776.4	173.4	255.0	441.3
Std Dev	33.4	123.0	129.2	75.1	99.7	82.5	64.7	61.8	52.7

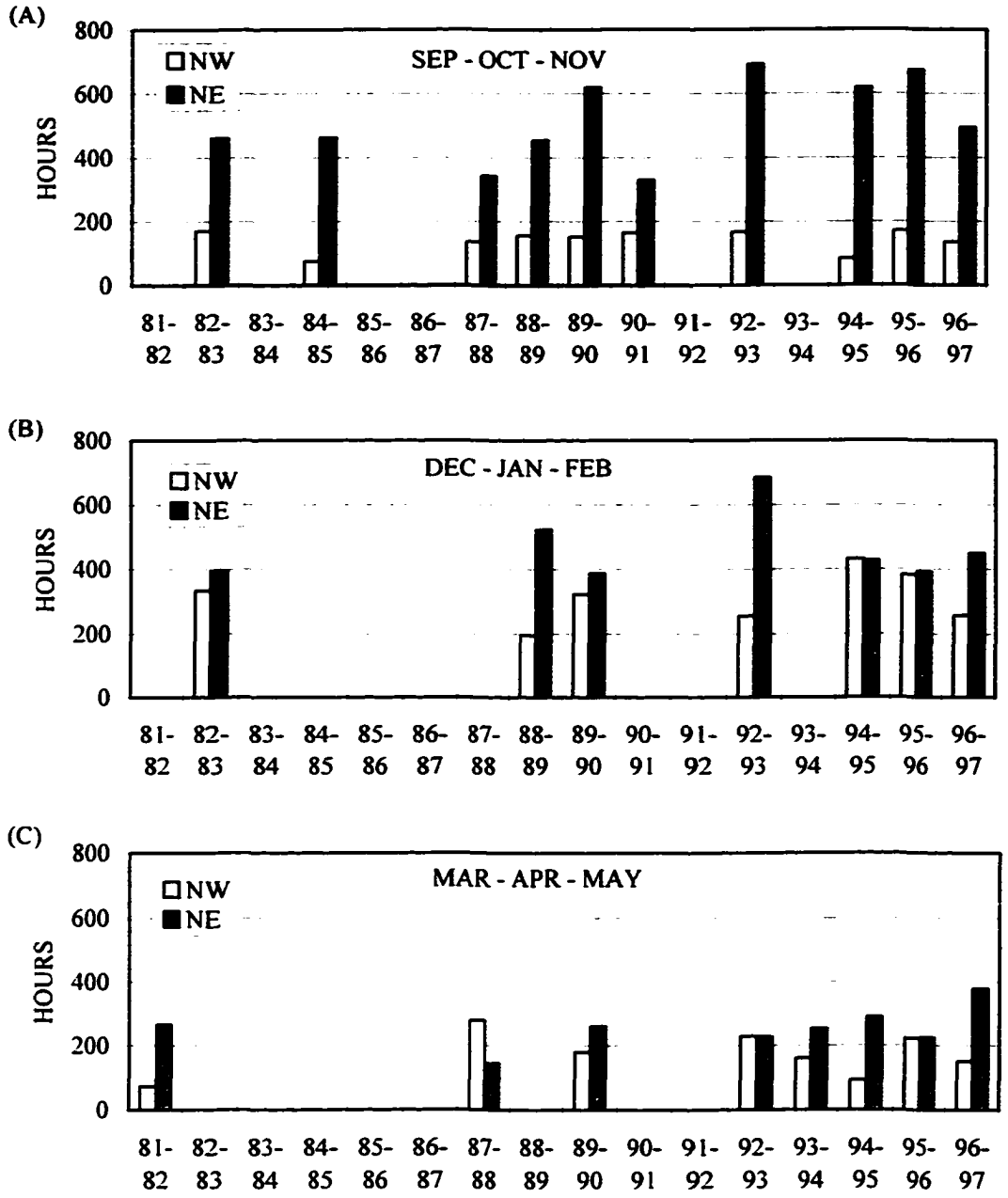

Figure 3.23. Total duration of northwesterly and northeasterly winds of all extratropical storms combined at NDBC Station 42007 during the autumn (A), winter (B), and spring (C) months for all years with complete data sets.

The results for winter indicate that the variability in northeasterly winds (std. dev. = 99.7 hours) was slightly greater than the variability in northwesterly winds (std. dev. = 75.1 hours) (Table 3.17). Northeasterly winds prevailed in 6 of the 7 years included in the analysis (Figure 3.23), and the average difference was 153.6 hours. These results indicate that northeasterly winds prevailed most years, but not all, and the average difference appears to have been influenced by one extreme year (1992-93).

The results for spring indicate that the variability in northeasterly winds (std. dev. = 61.8 hours) and northwesterly winds (std. dev. = 64.7 hours) was practically identical (Table 3.17). Northeasterly winds, however, prevailed in 6 of the 8 years included in the analysis (Figure 3.23), and the average difference was 81.6 hours. These results indicate that northeasterly winds prevailed most years, but not all, and the difference was consistently minimal.

The results also indicate that there was greater variability in the total duration of northerly winds in autumn (std. dev. =129.2 hours) than in winter (82.5 hours) (Table 3.17). There were seven years included in this analysis in which data were available for both autumn and winter seasons. The winter season prevailed in 5 of the 7 years, and the average difference was 121.4 hours (Table 3.17, Figure 3.24). These results indicate that the winter storm season prevailed most years, but not all, and the difference was consistently minimal.

There are three basic "inferences" that can be made from these results when presuming a direct relationship between wind direction and wave direction,: 1) the predominant direction of sediment transport was westward, 2) the "net volume" of

sediment transported westward was "consistently greater" in autumn than in winter (Figure 3.25), and 3) the impact of the winter storm season on the coast was "not consistently greater" than the impact of the autumn season. The trends identified in the data, however, need to be evaluated over a longer time period, and need to be supported with field data. As noted earlier, these observations presume a direct relationship between wind direction and wave direction, and do not account for the influence of wind speed, tidal flow, and nearshore bathymetry / wave refraction.

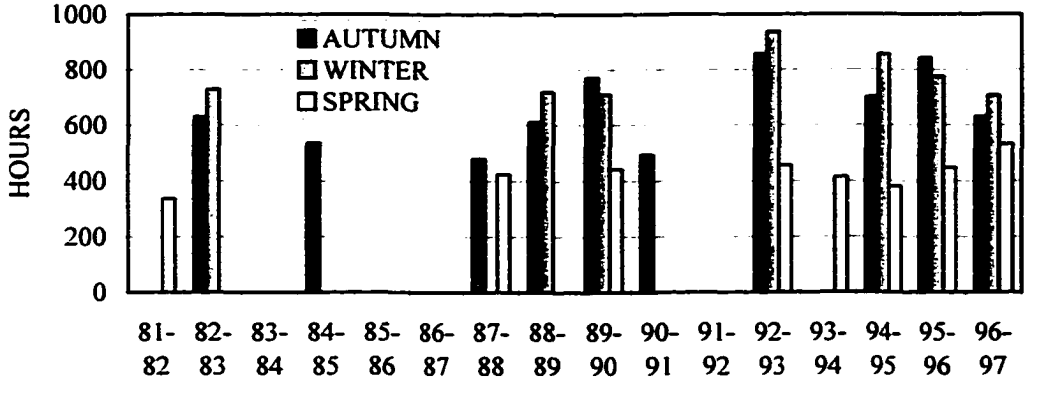

Figure 3.24. Total duration of all northerly winds of all extratropical storms combined at NDBC Station 42007 during the autumn, winter, and spring months. Only years with complete data sets are included.

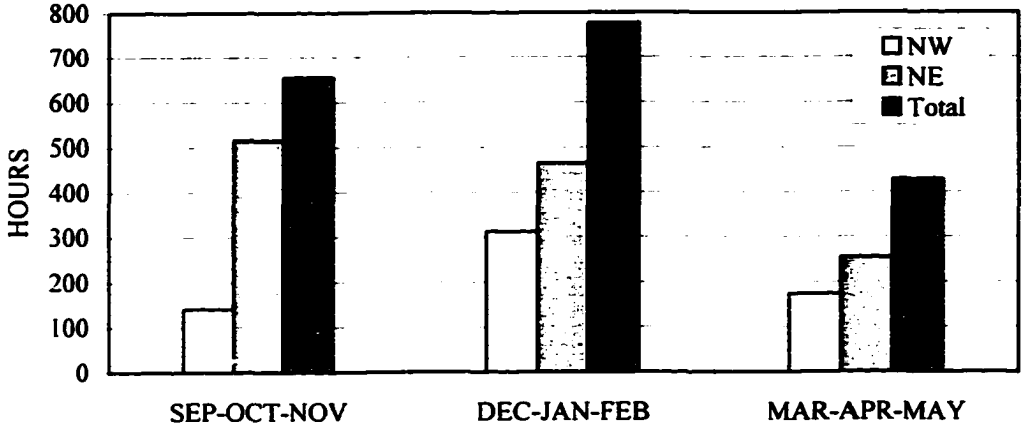

Figure 3.25. Average total duration of northwesterly, northeasterly, and all northerly winds of all extratropical storms combined at NDBC Station 42007 during the autumn, winter, and spring months.

1996-1997 STORM SEASON

This section presents the results of a "case study" of the 1996-1997 storm season (Figures 3.26-3.28). The data are reviewed here because they indicate how closely storm activity during the 1996-1997 storm season resembled a typical year which has significant implications for the field study of storm impacts presented in Chapter 5. The total number of storms observed during the 1996-1997 storm season (51) (Figure 3.26) was higher than the average annual frequency of storms expected at the study site (47.5) (Table 3.3). The frequency of storms observed in March (8), April (8), and May (6) were the highest totals observed in this study for each of these months (Table 3.3). The frequency of storms observed in January (6) and February (5), however, were the lowest totals for each of these months.

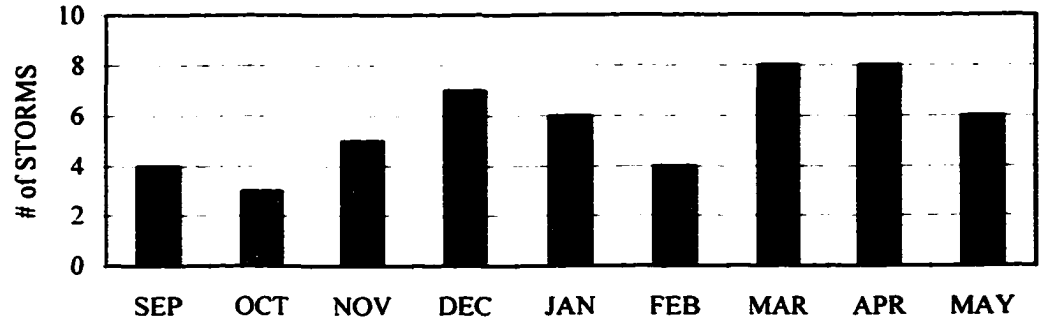

Figure 3.26. Frequency of storms at NDBC Station 42007 during the 1996-1997 storm season. The total # of storms was 51. The # of storms by storm types were: PF (40), SF (7), SGF (1), SGL (2), PL (1).

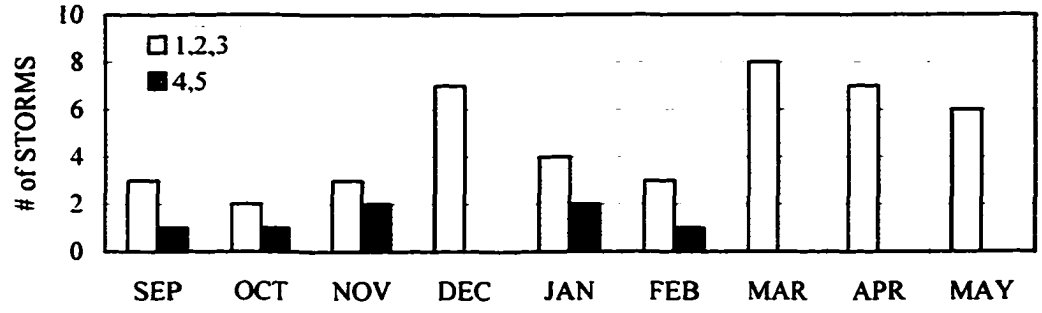

Figure 3.27. Frequency of storms by storm-magnitude class at NDBC Station 42007 during the 1996-1997 storm season. The # of storms in each class were: Class 0 (1), 1 (13), 2 (16), 3 (14), 4 (2), 5 (5).

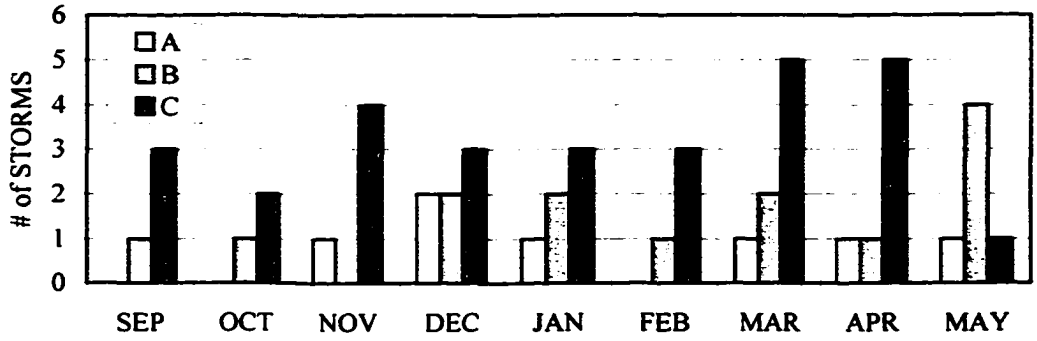

Figure 3.28. Frequency of storms by sub-type at NDBC Station 42007 during the 1996-1997 storm season. The # of storms in each sub-type were: sub-type A (7), B (14), C (29).

The frequency of Primary Front storm types (40) (Figure 3.26) observed during the 1996-1997 storm season was higher than expected (35.9) (Table 3.5), and the frequency of Secondary Front storm types (7) was identical to the expected value (6.9). The frequencies of the Secondary Gulf Front (1), Secondary Gulf Low (2), and Primary Low (1) storm types were each similar to the expected values. The frequency of "Frontal Overrunning" (Muller and Wax 1977) observed at New Orleans during the 1996-1997 storm season (55 days) was lower than expected (61.1 days), based on a 30-year record extending from 1961-1990 (LOSC 1997). Frequency of Frontal Overrunning, however, refers to the "number of days" that this synoptic weather type was observed, not the "number of events." Therefore, this discrepancy in expected versus observed "frequency of frontal activity" does not appear to be significant.

The frequencies of Class 1, 2, and 3 storms were close to the expected values; however, the distribution of Class 1, 2, and 3 storms was highly skewed toward the end of the year (Figure 3.27; Table 3.10). The frequency of Class 5 storms (5) was higher than expected (2.6), and the frequency of Class 4 storms (2) was lower than expected (5.7). However, the distribution of Class 4 and 5 storms was normally skewed toward the early and middle part of the year (Figure 3.19). This pattern suggests that although the frequency of storms in spring was higher than expected (Figure 3.26), the storms were low-magnitude events that had a lower impact on the coast than initially expected.

The frequency of sub-type A storms (7) was higher than expected (4.9), the frequency of sub-type B storms (14) was higher than expected (8.6), and the

frequency of sub-type C storms (29) was lower than expected (33.0) (Figure 3.28; Table 3.13). Northeasterly winds prevailed each month, except December, which had the highest frequency of sub-type A storms (2) (Table 3.18; Figure 3.29). The total duration of northwesterly winds (545 hours) was below average (597.5 hours), and the total duration of the northeasterly winds (1,322 hours) was above average (1,212.0 hours) (Table 3.15 and 3.18). The inference can be made from these results that the "net volume" of sediment transported westward (alongshore) may have been higher than average, that is, presuming a direct relationship between wind direction and wave direction.

The total duration of northerly winds in autumn was 630 hours, the total duration in winter was 706 hours, and the total duration in spring was 531 hours (Table 3.18). Northeasterly winds prevailed over northwesterly winds by 358 hours in autumn, 192 hours in winter, and 227 hours in spring. These results suggest that storms had a greater impact on the coast in winter, but a greater "net volume" of sediment was transported westward (alongshore) in both autumn and spring (Figure 3.29).

In summary, the distribution of storms varied considerably from the expected pattern. The frequencies and durations of the storm sub-types, however, were evidently close enough to the expected values to produce a relatively normal ratio of northwesterly and northeasterly winds. This pattern was especially true in autumn and winter when the differences between northwesterly and northeasterly winds (358 hours and 192 hours, respectively) were extremely close to the expected values for autumn (374.0 hours) and winter (153.6 hours) (Table 3.17 and 3.18). In

Table 3.18. Total duration of northwesterly and northeasterly winds of all extratropical storms combined at NDBC Station 42007 during the 1996-1997 storm season.

QUAD	SEP hours	OCT hours	NOV hours	DEC hours	JAN hours	FEB hours	MAR hours	APR hours	MAY hours	TOTAL hours
NW	18	26	92	115	81	61	56	80	16	545
NE	182	103	209	84	211	154	156	145	78	1322

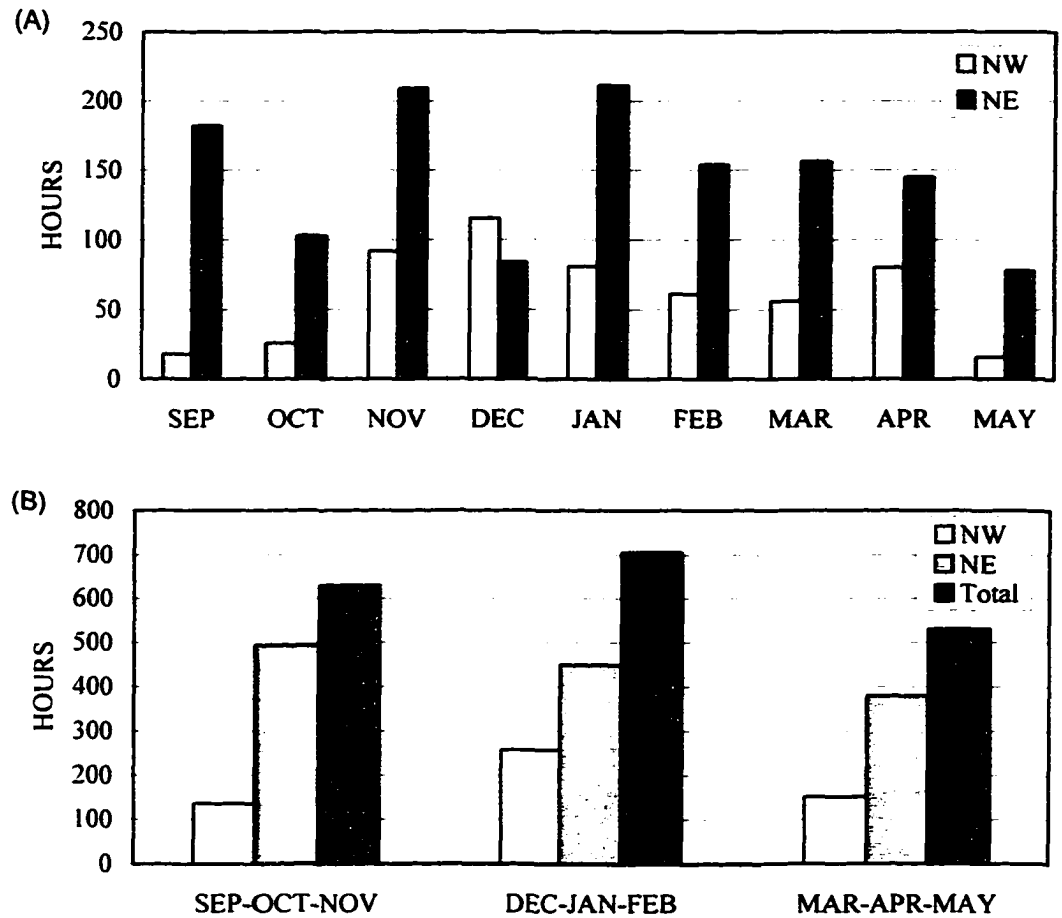

Figure 3.29. Total duration of northwesterly and northeasterly winds of all extratropical storms combined at NDBC Station 42007 during the 1996-1997 storm season. The upper plot (A) shows the total duration data for each month and the lower plot (B) shows the total duration data for each season.

spite of the unusual distribution of storms during the season, the "observed" results were relatively close to the "expected" results. That is, northeasterly winds prevailed each month, except December, and the greatest "net volume" of westward sediment transport most likely occurred in autumn.

SUMMARY

Three categories of attributes were identified in this research that define the basic characteristics of extratropical storm activity along the northern Gulf coast: 1) storm type, 2) storm-magnitude class, and 3) storm sub-type. The storm type describes the synoptic weather pattern that produced the storm event, the storm-magnitude class describes the duration of the event, and the intensity of "northerly" wind speeds during the event, and the storm sub-type describes the direction of northerly (northwest vs northeast) winds during the event.

Seven extratropical storm types were identified in this study. Earlier research by Roberts *et al.* (1987) on cold fronts and Hsu (1993) on Gulf cyclones suggested that these storm types should be incorporated into an extratropical storm classification system for the region. The two "cold front types" identified by Roberts *et al.* (1987) (the eastward migrating cyclone and the arctic surge) were consolidated into the most common storm type identified in this study, the "Primary Front." The "Secondary Front," "Secondary Gulf Front," and "Gulf Front" storm types identified in this study evidently correspond to the intermediate classes of the "spectrum of cold front types" noted by Roberts *et al* (1987). The Gulf cyclone storm system that Hsu (1993) developed a storm intensity scale for was used as the basis for two storm types identified in this study, the "Gulf Low" and the

"Secondary Gulf Low." The final storm type identified in this study, the "Primary Low," is evidently a new storm type for the region. The results indicated, however, that the frequency of the Primary Low storm type was extremely low which would account for its absence from the literature.

The average annual frequency of storms at the study site was determined to be approximately 47.5. These results compare favorably with the findings of previous studies (DiMego *et al* . 1976; Henry 1977b). The average annual frequency of Primary Fronts was 35.9 which accounted for 75% of storm activity. The average annual frequency of Secondary Fronts was 6.9 which accounted for an additional 15% of storm activity. The other five storm types accounted for the remaining 10% of storm activity at the study site.

Storm wind data for 506 events were used to evaluate the basic characteristics of an extratropical storm event at the study site. Average storm duration at the study site was 37.8 hours (std. dev. = 27.7 hours), average mean wind speed was 8.3 m sec^{-1} (std. dev. = 1.8 m sec^{-1}), and average maximum wind speed was 11.6 m sec^{-1} (std. dev. = 2.9 m sec^{-1}). The storm wind data were also used to evaluate storm wind conditions for each month of the storm season, and for each storm type. Storm duration was highest in autumn, and varied considerably throughout the year. Mean and maximum wind speeds were relatively consistent throughout the year. Primary Fronts had higher values than Secondary Fronts in each of the basic storm wind categories. Gulf Lows, Secondary Gulf Lows, and Primary Lows had the highest average mean and maximum wind speeds; however, these three storm types accounted for a mere 7% of storm activity at the study site.

The storm wind data were subsequently used to develop a storm-magnitude scale. The methodology was designed to assign higher magnitude values to storms that produced higher wind speeds; however, the higher magnitude storms proved to be the higher duration storms. This result was attributed to the earlier finding that the duration of storm events was highly variable, whereas, mean and maximum wind speeds were relatively consistent. The storm-magnitude data indicate that the highest frequency of Class 4 and 5 storms (the higher magnitude storms) was in autumn which indicates that storm duration was highest during the early part of the storm season, as noted earlier. The explanation for this pattern is unknown; however, it may be related to warm water temperatures in the Gulf, or the position of the North Atlantic high-pressure system, either of which may have some influence on the southward migration of cold air masses into the region in autumn.

Three storm sub-types were identified in this study based on the direction of the northerly winds: sub-type A (northwest winds, only), sub-type B (northeast winds, only) and sub-type C (northwest and northeast winds). Sub-type A storms had an average annual frequency 4.9 storms per year, and an average duration of 18.9 hours. Sub-type B storms had an average annual frequency of 8.6 storms per year, and an average duration of 28.5 hours. Sub-type C storms had an average annual frequency of 33.0 storms per year, and an average duration of 44.6 hours. The ratio between northeasterly (29.3 hours) and northwesterly (15.3 hours) winds for sub-type C storms was approximately 2:1, and the margin between northeasterly and northwesterly winds was greatest in autumn. The duration of sub-type B storms

was highest in autumn, and the duration of sub-type A storms was lowest in autumn.

The average frequency and duration of the storm sub-types resulted in three significant trends: 1) the average annual ratio of northeasterly winds to northwesterly winds was approximately 2:1, 2) the average duration of northeasterly winds prevailed over northwesterly winds in each month of the storm season, and 3) the average duration of northeasterly winds prevailed over northwesterly winds by an extreme margin in autumn. These results were found to be relatively consistent over the time span covered in this study. The data indicated that storm activity in winter would have the greatest impact on the coast; however, the extreme difference in the duration of northeasterly and northwesterly winds in autumn leads to the inference that a greater amount of westward (alongshore) sediment transport would occur in autumn, that is, presuming a direct relationship between wind direction and wave direction which disregards critical factors such as wind speed, tidal flow, and nearshore bathymetry / wave refraction.

This study made four significant contributions to the present body of scientific literature on extratropical storm activity in the northern Gulf of Mexico, especially as it pertains to the erosion problem observed along the northern shores of barrier islands in the region. The first contribution is the identification and classification of synoptic weather patterns that produce extratropical storm events in the region. The extratropical storm types identified in this study incorporate, and expand upon, the findings of earlier studies (Roberts *et al*. 1987; Hsu 1993) to

provide a more complete understanding of storm activity along the northern Gulf Coast.

The second contribution is the quantification of the range of "northerly" wind conditions (storm duration, mean and maximum wind speed) that occur during extratropical storm events at the study site. The present body of scientific literature on storm wind conditions for the northern Gulf of Mexico is based on the findings of two 30-day field studies at Mustang Island, Texas (Fox and Davis 1976), an 8-day field study at Trinity Island, Louisiana (Dingler *et al*. 1992), and a 14-hour study at Santa Rosa Island, Florida (Armbruster *et al*. 1995). Approximately 10 storms were monitored in these studies. The findings of this study make a significant contribution toward understanding the range of storm conditions that may occur during an individual storm event, and the range of storm conditions associated with each storm type, and each month of the storm season.

The third contribution is the development of a storm-magnitude scale for extratropical storm events at the study site (based on storm duration and wind speed). This contribution lays the groundwork for correlating storm wind conditions with storm impacts along the northern Gulf Coast. This contribution may have the greatest potential in that storm wind data could be used as a "proxy" measure of storm impacts. The ability to estimate the impact of a storm based on wind data would be of tremendous value to both coastal managers and the scientific community because it would provide a way to estimate the impacts of recent storms, and it would provide a way to estimate the impacts of forthcoming storm seasons based on seasonal and annual weather predictions.

The fourth contribution is the quantification of the predominant direction and duration of northerly (northeast vs northwest) winds during extratropical storm events at the study site. The findings of this study make a significant contribution toward understanding the "potential" effects of storms on the lateral migration of sediment along the coast, which in turn contributes toward understanding how storms ultimately influence the evolution of the beach, especially in terms of lateral changes along the coast.

The values of these many contributions were demonstrated in the "case study" of storm activity for the 1996-1997 storm season. The results of this analysis indicated that the frequency of storms was higher than normal (Primary Fronts in particular), and that the distribution of storms was highly skewed toward the later part of the storm season in spring. These late-season storms proved to be short-duration, low-magnitude storms that most likely had little impact on the coast. The long-duration, high-magnitude storms were normally skewed toward the early part of the storm season in autumn. The storm sub-type data indicated that northeasterly winds prevailed over northwesterly winds each month, except December, when the highest frequency of sub-type A storms was observed. The duration of northerly winds was greatest in winter, but the margin between northeasterly and northwesterly winds was greater in autumn and spring. These data can be used to infer that storms had a greater impact on the coast in winter, and that the greatest amounts of sediment were transported westward (alongshore) in autumn and spring (presuming a direct relationship between wind and wave direction). Although the distribution of storms varied from the expected pattern, the end results appear to

have been close to normal. That is, northeasterly winds prevailed throughout the storm season, especially in autumn, and the greatest total amount of northerly winds was observed in winter.

One final aspect of the findings of this dissertation research needs to be clarified. This point applies directly to the erosion problem observed along the northern coast of barrier islands, and it is in regard to the northeasterly winds that were found to prevail throughout the storm season. The northeasterly winds are related to the clockwise (anticyclonic) rotation of winds around the high-pressure, cold air mass that migrates along the northern Gulf Coast behind the "cold front." The point that needs to be clarified is that mid-latitude "anticyclones" produce the "northeasterly" winds that prevail along the Gulf Coast, and that these northeasterly winds were shown to be the predominant component of the "post-frontal, northerly winds" that are considered to be the primary forcing agent in coastal erosion observed along the northern coast of barrier islands. It was noted at the beginning of this chapter, while defining the Primary Front extratropical storm type, that mid-latitude cyclones and anticyclones appear to migrate together as a "linked" weather system. It is herein recommended that the linkage between these high- and low-pressure systems, and especially the role of anticyclones, be recognized in future research.

CHAPTER 4

STORM DYNAMICS

The data presented in Chapter 3 suggest that westward sediment transport prevails along the northern coast of West Ship Island; however, this observation is based solely on wind data. The objective of this chapter is to gain a more complete understanding of how storms affect sediment transport processes by evaluating the influence of storm winds on nearshore wave height, water level, and current conditions. The present body of literature on this subject for the Gulf of Mexico is limited to a 14-hour study conducted during the passage of an eastward migrating cyclone along the north-facing, bayside coast of Santa Rosa Island, Florida (Armbruster *et al.* 1995; Armbruster 1997). It is clearly evident that additional data are needed to understand the effects of these storms on nearshore conditions in the Gulf of Mexico.

The results of the 14-hour study at Santa Rosa Island (Armbruster *et al.* 1995; Armbruster 1997), indicated that winds were from the northwest, wind speeds exceeded 6 m sec^{-1} for 10 hours (max. = 9.3 m sec^{-1}), significant wave heights exceeded 14 cm for 6 hours (max. = 18 cm), eastward, alongshore currents exceeded 5 cm sec^{-1} throughout the storm (max. = 11 cm sec^{-1}), and onshore currents remained under 4 cm sec^{-1} throughout the storm. Armbruster *et al.* (1995) noted that the northwesterly winds produced an eastward current with a weak onshore component. At the end of 21 weeks of monitoring at the site, Armbruster (1997) made a noteworthy observation concerning wave heights and water levels

during storms which will be considered in this study. The depth of water across the shallow, nearshore platform at Santa Rosa Island was considered to be significant because the coincidence of a storm and a low tidal level would result in a significant dissipation of wave energy along the platform, thus reducing the impact of storm waves on the foreshore. Furthermore, high tide / high water level conditions would result in storm waves impacting the foreshore at a higher elevation, thus increasing the impact of storm waves on the foreshore, and increasing the potential for overwash events.

Four critical issues will be considered in this field study: 1) the influence of wind directions on nearshore current directions for evaluating sediment transport pathways, 2) the influence of storms on water levels, 3) the influence of water levels on wave heights for evaluating the influence of the nearshore platform, and 4) the potential for storms to impact and overwash the foreshore.

Atmospheric data collected by a National Oceanographic and Atmospheric Administration (NOAA) weather buoy were used, in conjunction with daily weather maps published by NOAA, to monitor storm activity at the study site. The buoy was maintained by a branch of NOAA known as the National Data Buoy Center (NDBC). The buoy was identified as NDBC Station 42007 and was located approximately 13 km southeast of West Ship Island in approximately 16 m water depth (Figure 4.1). The buoy recorded air temperature, barometric pressure, wind speed, and wind direction data at 1 hour intervals. At the beginning of each hour, the buoy sampled wind conditions for 8 minutes and then recorded the average wind speed and direction. The data were subsequently made available to the public

at the NDBC Internet site (NDBC 1997). The anemometer on the buoy was located 10 m above sea level.

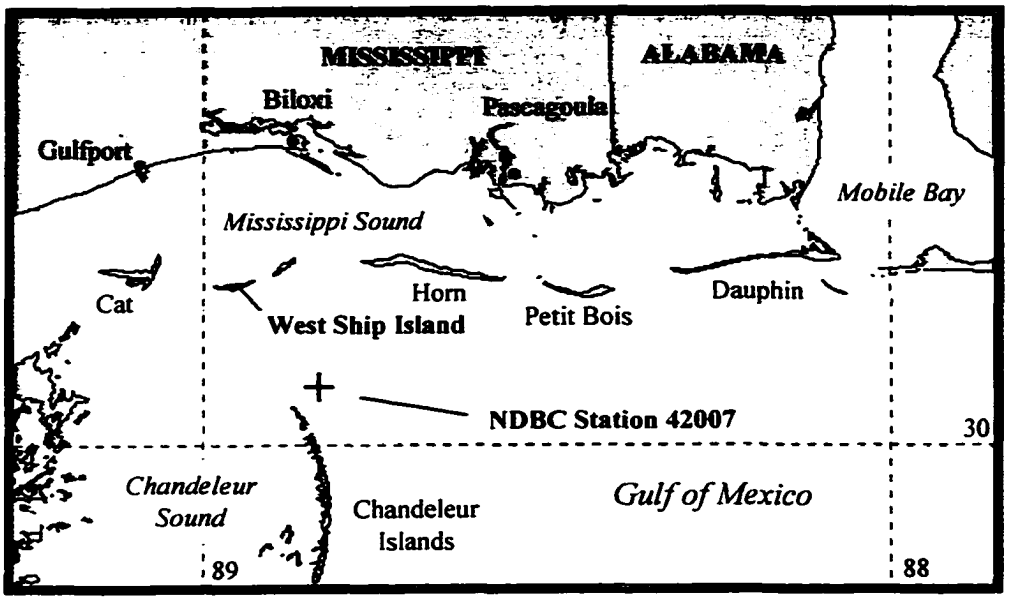

Figure 4.1. Location of NDBC Station 42007 and West Ship Island in the northern Gulf of Mexico. The buoy is located at 30.1^0 N Latitude and 88.8^0 W Longitude.

Since NDBC Station 42007 is located farther offshore than West Ship Island, there are several potential problems that should be recognized in using the buoy data to evaluate storm conditions at the island. Northerly winds travel over a greater distance of open sea (longer fetch / reduced friction) before reaching the buoy, so northerly wind speeds at the buoy may be higher than northerly wind speeds at the island. Wind directions and the timing of wind shifts may also vary at the two locations. Furthermore, cold fronts may stall after passing over West Ship Island, but before passing over the buoy.

In order to evaluate the difference in wind conditions at the two sites, a wind vane and anemometer were deployed at West Ship Island to collect wind speed and direction data during an 18-day study period. The wind vane was attached to the top of an aluminum pole that was erected on the crest of the primary dune overlooking the soundside beach (Figure 4.2). The anemometer was mounted on the pole at a height of 3.60 m above the crest of the dune. The elevation of the dune crest was determined to be 3.89 m above the National Geodetic Vertical Datum (NGVD) of 1929, which is approximate to sea level, so the elevation of the anemometer was 7.49 m NGVD. The wind vane and anemometer collected data at 1 hour intervals. At the beginning of each hour, wind conditions were sampled at 10 second intervals for 6 minutes. The average wind speed and direction were recorded at the end of the sampling period. Plots of the data are shown in Figure 4.3.

The average speed of "northerly" winds recorded at NDBC Station 42007 (8.65 m sec^{-1}) was approximately 1 m sec^{-1} higher than the average speed of "northerly" winds recorded at West Ship Island (7.68 m sec^{-1}). However, the maximum northerly wind speed recorded at NDBC Station 42007 (13.8 m sec^{-1}) was approximately 1.4 m sec^{-1} lower than the maximum northerly wind speed recorded at West Ship Island (15.2 m sec^{-1}). Higher average wind speeds were expected at NDBC Station 42007 because of the difference in fetch, and because the anemometer on the buoy was mounted approximately 2.5 m higher above sea level than the anemometer at West Ship Island. It is also important to note that differences in instrument calibration may have increased or decreased the discrepancy in wind speeds recorded at the two sites.

(A)

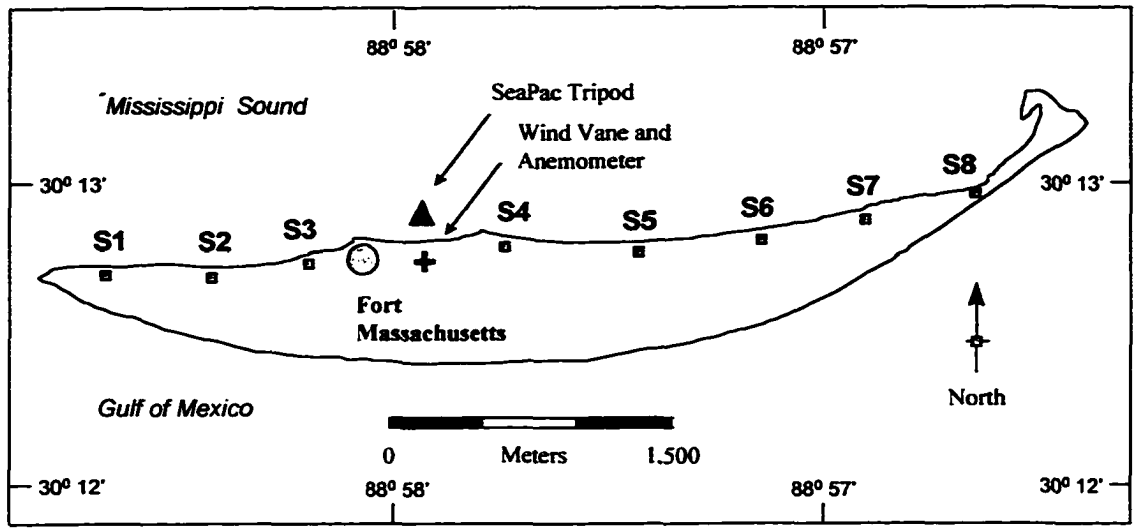

(B)

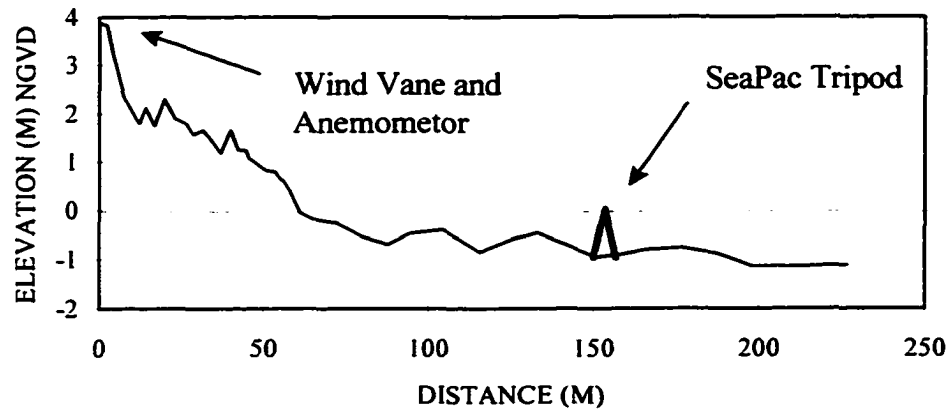

Figure 4.2. Location of the wind and wave monitoring instruments deployed along the north-facing coast of West Ship Island. The upper plot (A) shows the location of the instruments along the soundside coast. The lower plot (B) shows the location of the instruments along a cross-sectional profile of the beach.

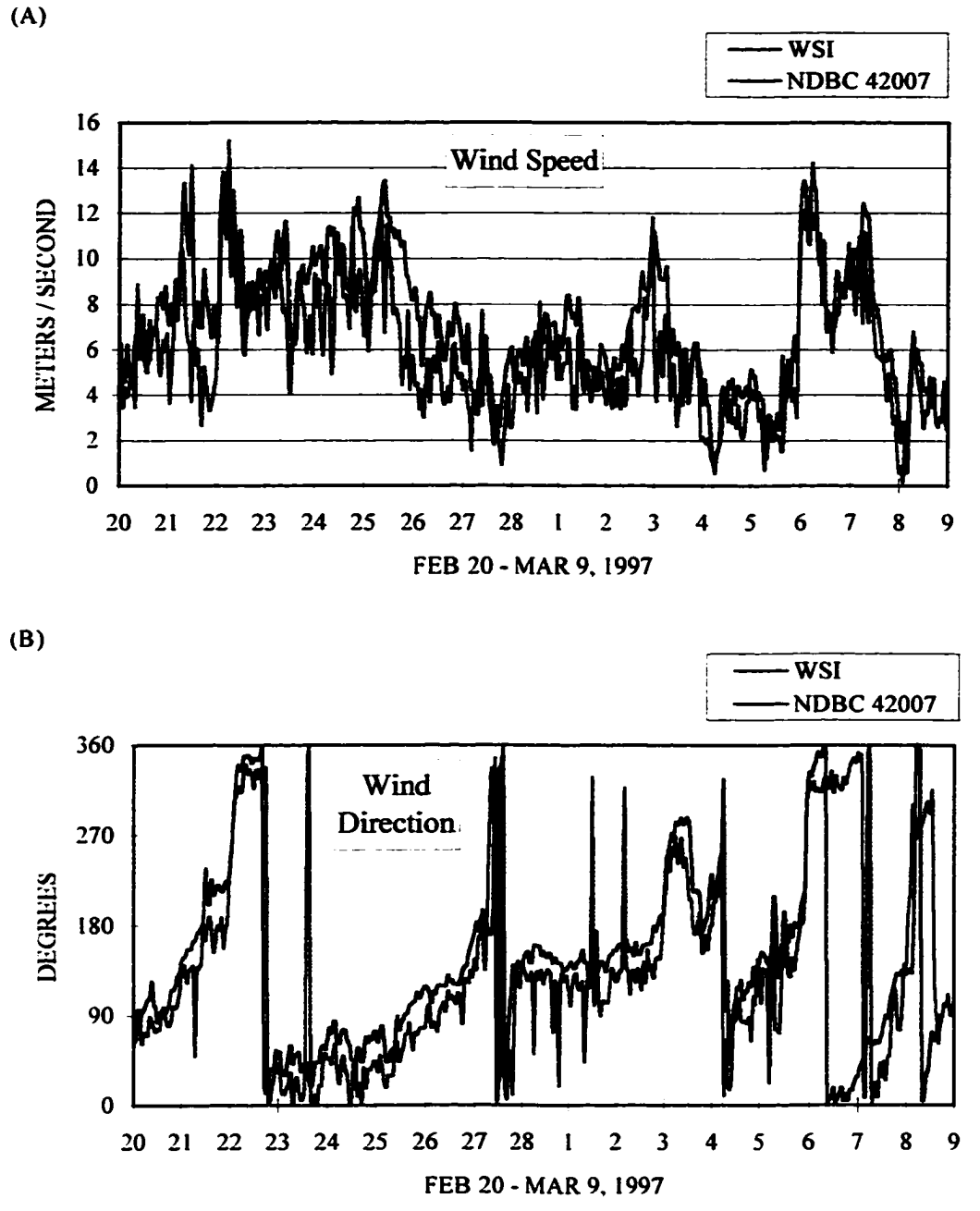

Figure 4.3. Wind speed and wind direction data collected at West Ship Island and at the NOAA weather buoy (NDBC Station 42007) from February 20, to March 9, 1997. The upper plot (A) shows a comparison of the wind speed data and the lower plot (B) shows a comparison of the wind direction data.

Wind directions recorded at West Ship Island were consistently shifted approximately 30 degrees westward of wind directions recorded at NDBC Station 42007. The wind vane deployed at West Ship Island was calibrated with a hand held compass which could easily account for the discrepancy in wind directions. Although the actual wind speed and direction values differed, identical changes in both wind speed and wind direction were recorded at approximately the same time at each site. These findings suggest that the wind data recorded at NDBC Station 42007 represent a reasonable sample of wind conditions at West Ship Island.

A SeaPac Model 2100 Wave, Tide, and Current Gauge (Woods Hole Instrument Systems 1996a) was used to collect wave height, tide, and alongshore (east-west) and cross-shore (north-south) current data. The instrument was attached to an aluminum tripod with weighted legs (Figure 4.4) and deployed approximately 100 m offshore in approximately 1 m water depth (Figure 4.2). The SeaPac instrument collected data at 1 hour intervals. At the beginning of each hour, water conditions were sampled for 512 seconds. The water pressure sensor was located 21 cm above the seabed and recorded water level data at 0.25 second intervals. These data were used to compute the significant wave height and tide level during the sampling period. The WavePro (Woods Hole Instrument Systems 1996b) software program used to compute significant wave heights was based on the Wave Data Analysis Standard established by the U.S. Army Corps of Engineers (Earle *et al.* 1995). The bi-directional current sensor was located 27 cm above the seabed and recorded alongshore and cross-shore current speed data at 1 second intervals. The data were used to determine the mean and maximum

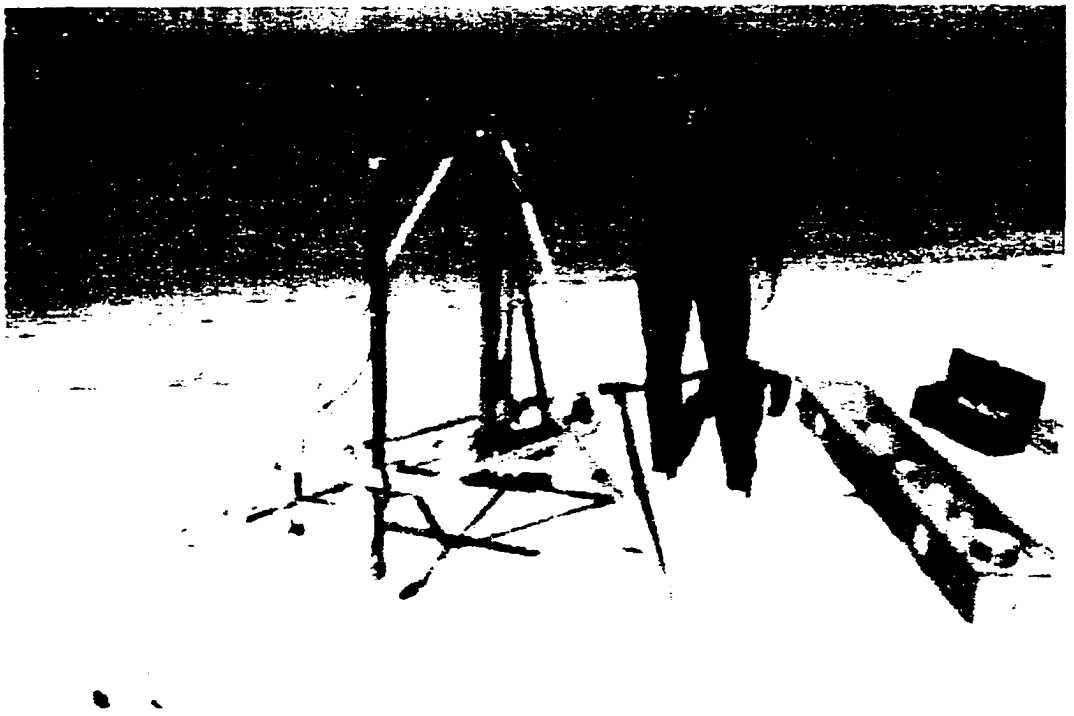

Figure 4.4. SeaPac Model 2100 Wave, Tide, and Current Gauge attached to an aluminum tripod for deployment along the northern coast of West Ship Island. Matthew Taylor is shown inspecting the instrument before deployment. Photo taken by author in February, 1997.

significant wave height during storms, the tidal range during storms, and the mean and maximum alongshore and cross-shore current speeds during storms.

The field study was conducted during a three week period between February 17, and March 9, 1997. Daily weather maps published by the National Oceanic and Atmospheric Administration (NOAA 1997) indicate that three cold fronts passed along the Gulf Coast during this period. The dates of the frontal passages were February 22, March 3, and March 6 (Figure 4.5-4.7). It is important to note that a cold front stalled along the coast on February 27, and that the squall line that preceded the front increased wind speeds and wave heights at West Ship Island for a brief period on that date. However, an official storm event was not declared until the front passed the study site on March 3.

The SeaPac instrument was deployed at 4 p.m. on February 17, 1997, and recorded data until 9 a.m. on March 8, 1997 (Central Standard Time). The data, however, are displayed in Universal Coordinated Time (UTC) units for comparison with the data collected at NDBC Station 42007. There is a 6 hour difference between these two time systems, and Universal Coordinated Time uses a 24 hour clock rather than a 12 hour clock (*e.g.*, 12:00 p.m. CST = 18:00 UTC). The data for February 17, 18, and 19 were not included in the data plots because this period coincided with the later stages of an earlier storm. The following sections present the results of the wind monitoring at NDBC Station 42007, and the results of the wave, tide, and current monitoring at West Ship Island.

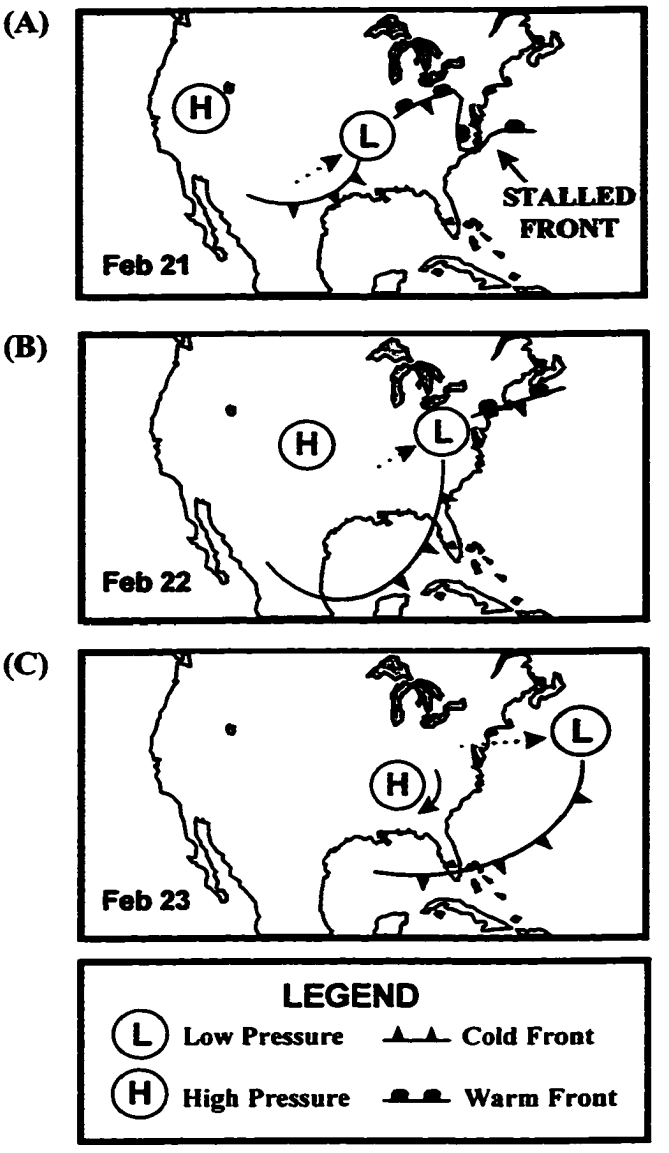

Figure 4.5. Weather patterns associated with the first cold front passage (February 22, 1997) observed during the field study at West Ship Island. The upper plot (A) shows the day before the frontal passage, the middle plot (B) shows the day of the frontal passage, and the lower plot (C) shows the day after the frontal passage. These maps are based on daily weather maps published by NOAA (1997).

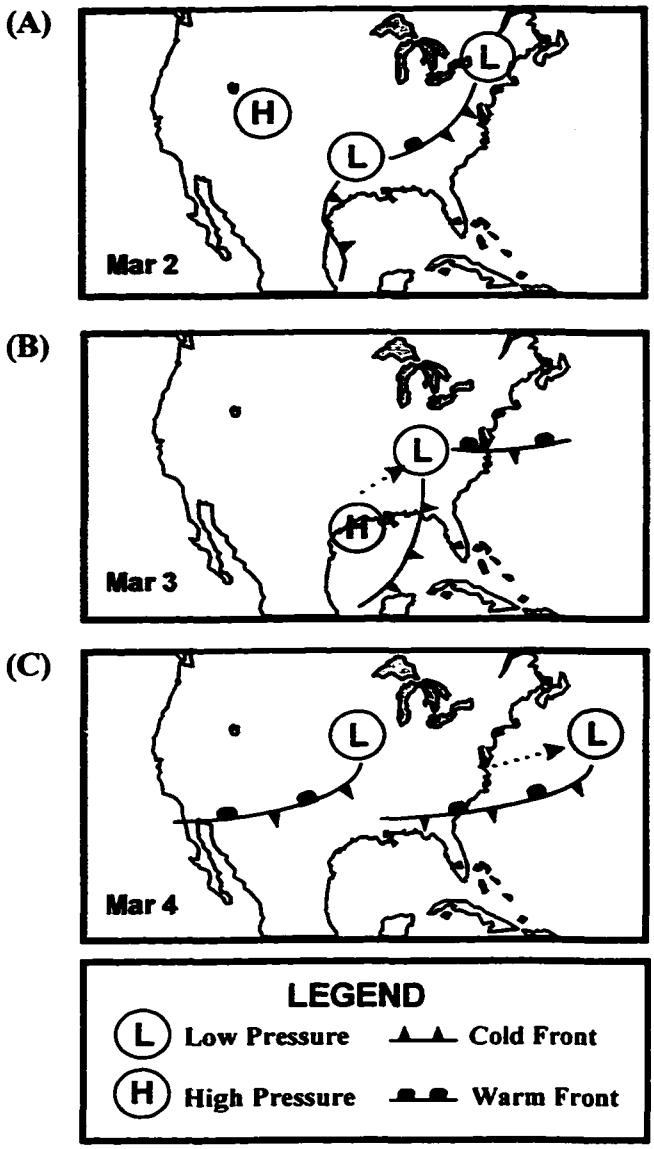

Figure 4.6. Weather patterns associated with the second cold front passage (March 3, 1997) observed during the field study at West Ship Island. The upper plot (A) shows the day before the frontal passage, the middle plot (B) shows the day of the frontal passage, and the lower plot (C) shows the day after the frontal passage. These maps are based on daily weather maps published by NOAA (1997).

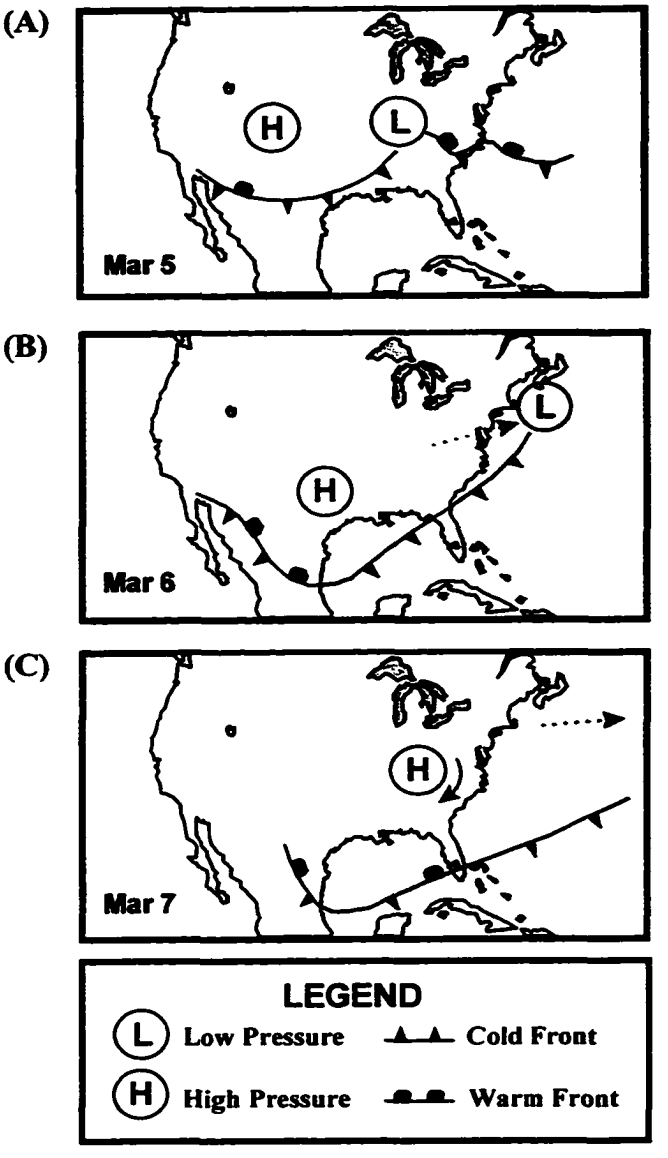

Figure 4.7. Weather patterns associated with the third cold front passage (March 6, 1997) observed during the field study at West Ship Island. The upper plot (A) shows the day before the frontal passage, the middle plot (B) shows the day of the frontal passage, and the lower plot (C) shows the day after the frontal passage. These maps are based on daily weather maps published by NOAA (1997).

WIND SPEED AND DIRECTION

The wind speed and direction data collected at NDBC Station 42007 are shown in Figure 4.8. The post-frontal phase of Storm 1 initially produced northwesterly winds with a mean azimuth of 341 degrees for 15 hours. The mean wind speed was 10.3 m sec^{-1}; the maximum speed was 13.8 m sec^{-1}. The storm subsequently produced northeasterly winds with a mean azimuth of 54 degrees for an additional 69 hours. The mean wind speed was 9.9 m sec^{-1}; the maximum speed was 13.4 m sec^{-1}. The mean wind speed for all 84 hours of northerly winds was 10.0 m sec^{-1}.

The post-frontal phase of Storm 2 produced northwesterly winds with a mean azimuth of 283 degrees for 8 hours. The mean wind speed was 7.1 m sec^{-1}; the maximum speed was 9.6 m sec^{-1}.

The post-frontal phase of Storm 3 initially produced northwesterly winds with a mean azimuth of 342 degrees for 10 hours. The mean wind speed was 11.2 m sec^{-1}; the maximum speed was 12.1 m sec^{-1}. The storm subsequently produced northeasterly winds with a mean azimuth of 34 degrees for an additional 29 hours. The mean wind speed was 9.3 m sec^{-1}; the maximum speed was 12.4 m sec^{-1}. The mean wind speed for all 39 hours of northerly winds was 9.8 m sec^{-1}.

WAVE HEIGHTS AND TIDES

The significant wave height and tide data collected at West Ship Island are shown in Figure 4.9. Storm 1 produced a maximum significant wave height of 30.4 cm; the average during the 84 hours of northerly winds was 19.8 cm. Storm 2 produced a maximum significant wave height of 18.9 cm; the average during the 10

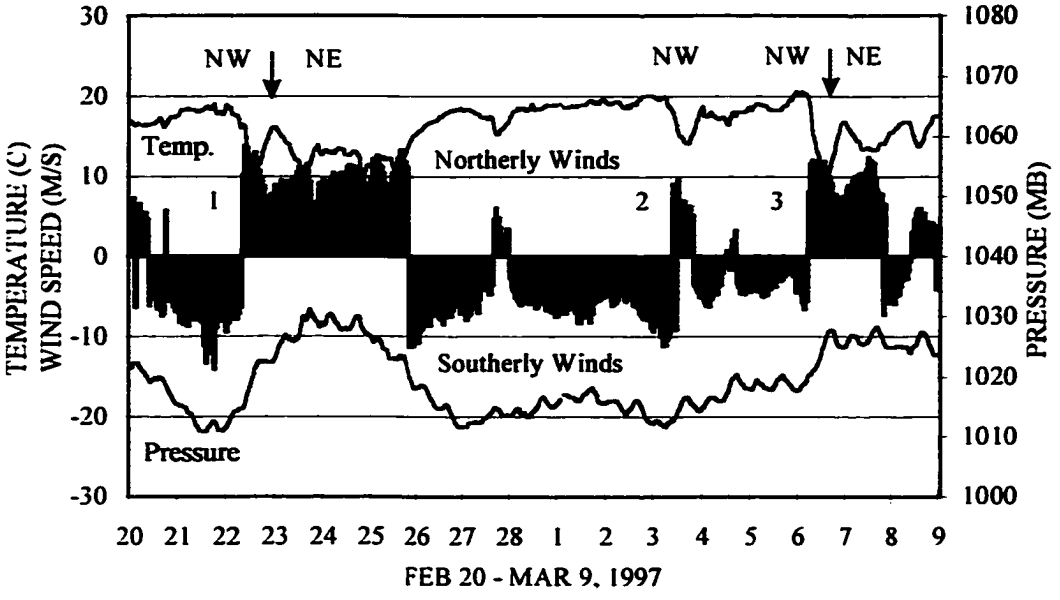

Figure 4.8. Standard meteorological data collected at NDBC Station 42007 from February 20, to March 9, 1997. The left axis shows air temperature and wind speed values. Northerly winds are plotted as positive values and southerly winds are plotted as negative values. The right axis shows barometric pressure values. Three cold fronts passed during the study period and are numbered on the plot. The arrows and labels indicate the approximate time that the wind shifted from northwest to northeast during the post-frontal phases of storms 1 and 3. As noted earlier, the event on February 27 was not considered an official storm event.

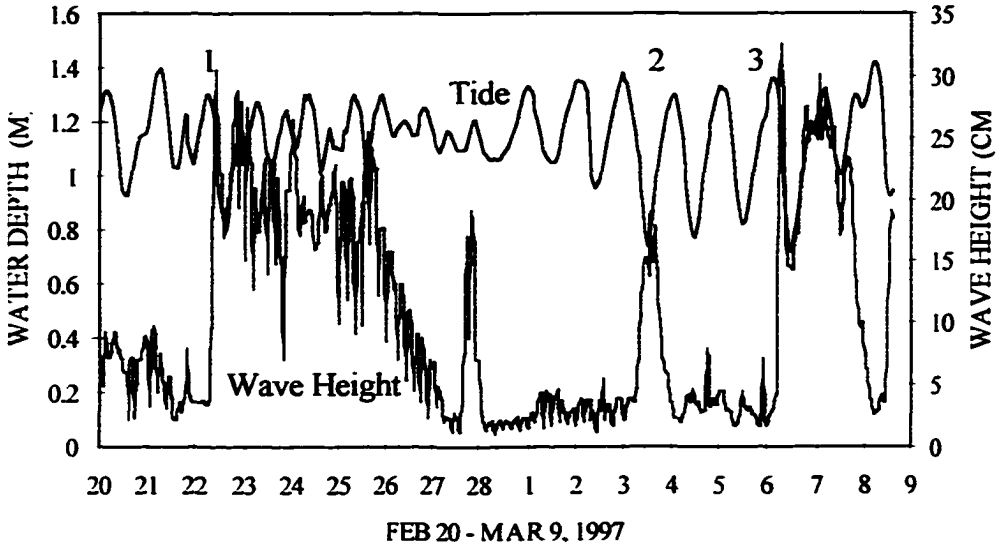

Figure 4.9. Significant wave height (H_s) and tide data collected along the northern coast of West Ship Island from February 20, to March 9, 1997. Three cold fronts passed during the study period and are noted on the plot. As noted earlier, the event on February 27 was not considered an official storm event.

hours of northerly winds was 12.4 cm. Storm 3 produced a maximum significant wave height of 32.6 cm; the average during the 39 hours of northerly winds was 22.5 cm. Wave periods varied between 2 and 3 seconds throughout the study.

The average water depth at the location of the SeaPac instrument was approximately 1.1 m. The differences between high and low tide during Storm 1 (February 22-26) were 50 cm, 22 cm, 14 cm, 30 cm, 8 cm, and 25 cm. The difference between high and low tide on the day of Storm 2 (March 3) was 64 cm. The differences between high and low tide during Storm 3 (March 6-8) were 64 cm, 32 cm, and 50 cm.

ALONGSHORE AND CROSS-SHORE CURRENTS

The alongshore and cross-shore current data collected at West Ship Island are shown in Figure 4.10. The post-frontal phase of Storm 1 initially produced northwesterly winds (341°) for 15 hours which produced an eastward current with an onshore component. The maximum eastward current speed was 4.6 cm sec^{-1}; the average speed was 2.6 cm sec^{-1}. The maximum onshore current speed was 7.1 cm sec^{-1}; the average speed was 4.3 cm sec^{-1}. The storm subsequently produced northeasterly winds (54°) for 69 hours which produced a westward current. The maximum westward speed was 11.4 cm sec^{-1}; the average speed was 6.9 cm sec^{-1}. Cross-shore currents varied during this period. The maximum onshore speed was 6.9 cm sec^{-1}, and the maximum offshore speed was 4.8 cm sec^{-1}.

The post-frontal phase of Storm 2 produced northwesterly winds (283°) for 8 hours which produced an eastward current with an offshore component. The

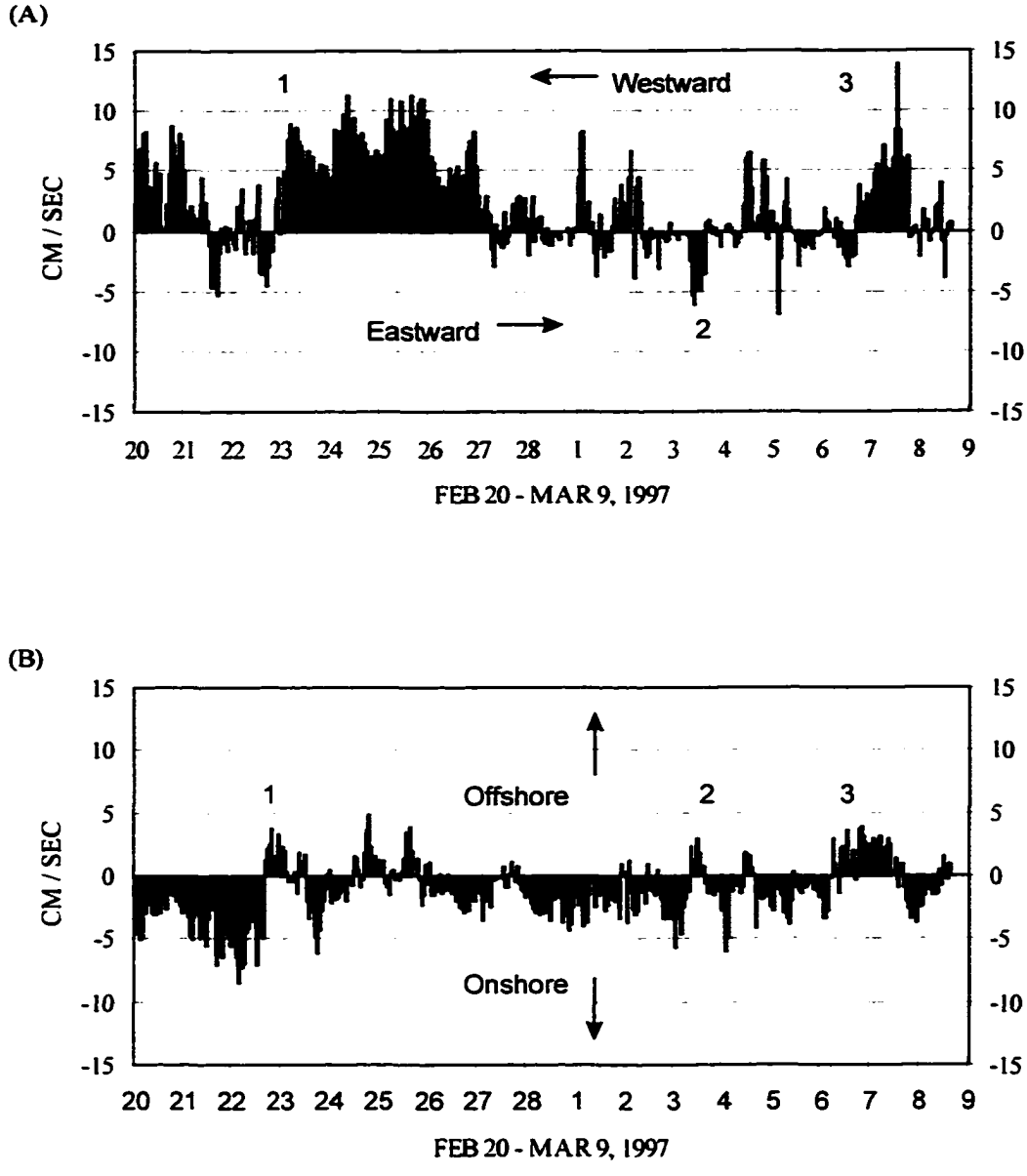

Figure 4.10. Alongshore and cross-shore current speed data collected along the northern coast of West Ship Island from February 20, to March 9, 1997. The upper plot (A) shows the alongshore current data with westward currents plotted as positive values and eastward currents plotted as negative values. The lower plot (B) shows the cross-shore current data with offshore currents plotted as positive values and onshore currents plotted as negative values. As noted earlier, the event on February 27 was not considered an official storm event.

maximum eastward speed was 6.2 cm sec^{-1}; the average speed was 4.5 cm sec^{-1}. The maximum offshore speed was 2.9 cm sec^{-1}; the average speed was 1.3 cm sec^{-1}.

The post-frontal phase of Storm 3 initially produced northwesterly winds (342°) for 10 hours which produced an eastward current with an offshore component. The maximum eastward speed was 3.0 cm sec^{-1}; the average speed was 2.1 cm sec^{-1}. The maximum offshore speed was 3.6 cm sec^{-1}; the average speed was 1.9 cm sec^{-1}. The storm subsequently produced northeasterly winds (34°) for 29 hours which produced a westward current with an offshore component. The maximum westward speed was 13.8 cm sec^{-1}; the average speed was 4.7 cm sec^{-1}. The maximum offshore speed was 3.7 cm sec^{-1}; the average speed was 1.9 cm sec^{-1}.

DISCUSSION

The first point of interest is the distinct signature in the atmospheric data recorded at NDBC Station 42007 during each of the three cold front passages (February 22, March 3, and March 6) that occurred in the study period (Figure 4.8). Each frontal passage can easily be identified by a sharp decrease in air temperature, and the transition between pre- and post-frontal phases can easily be identified by the shift from southerly to northerly winds. Furthermore, the migration of cold air masses (high-pressure, anticyclones) along the Gulf Coast can be detected by distinct increases in barometric pressure during the post-frontal phases of Storms 1 and 3.

The second point of interest is the relationship between storm wind conditions and their influence on nearshore currents. The wind speeds recorded during Storm 1 (mean = 10 m sec^{-1}; max. = 13.8 m sec^{-1}) and Storm 3 (mean = 9.8

m sec^{-1}; max. = 12.4 m sec^{-1}) compare favorably with the findings of Fox and Davis (1976) at Mustang Island, Texas (mean = 8-10 m sec^{-1}; max. = 15 m sec^{-1}) and Dingler *et al.* (1992) at Trinity Island, Louisiana (max. = 11 m sec^{-1}). Storm 2 was rather mild by comparison (mean = 7.1 m sec^{-1}; max. = 9.6 m sec^{-1}) and appears to have been similar to the storm monitored by Armbruster *et al.* (1995) (max. = 10 m sec^{-1}). Fox and Davis (1976) noted that wind direction generally shifted from southwest to northeast during a frontal passage, and the wind shift resulted in a reversal in the direction of the alongshore current. Although this research at West Ship Island was restricted to the post-frontal phase, the data show a similar shift in wind direction and reversal in alongshore current direction. Each of the three storms initially produced northwesterly winds which produced eastward currents; however, wind direction shifted to the northeast during Storm 1 and Storm 3 which resulted in a reversal in the alongshore current (Figures 3.8 and 3.10).

The eastward currents produced by Storm 1 (mean = 2.6 cm sec^{-1}; max. = 4.6 cm sec^{-1}) and Storm 3 (mean = 2.1 cm sec^{-1}; max. = 3.0 cm sec^{-1}) were considerably lower than the eastward currents produced by Storm 2 (mean = 4.5 cm sec^{-1}; max. = 6.2 cm sec^{-1}). These results were evidently related to the actual direction of northwesterly winds. The average direction of northwesterly winds during Storm 1 (341°) and Storm 3 (342 °) was almost directly onshore, whereas the average direction of northwesterly winds during Storm 2 (283°) was almost directly alongshore.

The average direction of northeasterly winds during Storm 1 (54 °) was more directly alongshore than the average direction of northeasterly winds during

Storm 3 (34°). This may explain why the average westward current speed produced by Storm 1 (6.9 cm sec^{-1}) was greater than the average westward current speed produced by Storm 3 (4.7 cm sec^{-1}). However, Storm 3 actually produced a higher maximum westward current speed (13.8 cm sec^{-1}) than Storm 1 (11.4 cm sec^{-1}).

Finally, the fact that the duration of northwesterly winds was shorter than the duration of northeasterly winds during Storm 1 (15 hours vs. 69 hours) and Storm 3 (10 hours vs. 29 hours) is significant because it resulted in the duration of eastward currents being shorter than the duration of westward currents. These results suggest that the predominant direction of alongshore sediment transport during the study period was westward. It should also be noted that offshore currents prevailed over onshore currents during Storms 2 and 3 although onshore currents clearly prevailed during the study period. More importantly, alongshore currents prevailed over cross-shore currents throughout the study period, especially during storms.

These results indicate that there are three significant points that characterize the relationship between winds and nearshore currents along the northern coast during storms: 1) a shift from northwesterly to northeasterly winds during a storm results in a reversal in the direction of alongshore currents, 2) northerly winds that flow more directly alongshore (parallel to the coast) produce higher alongshore current speeds than northerly winds that flow more directly onshore (perpendicular to the coast), and 3) the predominance of northeasterly winds over northwesterly winds during a storm results in a longer duration of westward currents than eastward currents, and thus, westward sediment transport prevails. Although this is

a limited sample, these findings could have significant implications for understanding sediment transport along the north-facing shores of barrier islands in the region.

Relating the storm wind data to the findings of the previous chapter on extratropical storm activity indicates that Storm 1 would be classified as a Class 5, sub-type C, Secondary Front, Storm 2 would be classified as a Class 1, sub-type A, Secondary Front, and Storm 3 would be classified as a Class 3, sub-type C, Primary Front. This information is significant because it can be used to determine how often storm events with characteristics similar to the ones observed in this study would be expected during an average storm season. Approximately 2.6 storms of the same magnitude as Storm 1 (Class 5), approximately 12.4 storms of the same magnitude as Storm 2 (Class 1), and approximately 13.7 storms of the same magnitude as Storm 3 (Class 3) would be expected during an average storm season (Table 3.9). These data therefore provide examples of storm conditions for approximately 28.7 storms per year which accounts for approximately 60% of the 47.5 storms per year expected at the study site. In regard to wind direction, Storms 1 and 3 were sub-type C storms (33.0 storms per year), and Storm 2 was a sub-type A storm (4.9 storms per year) (Table 3.13). These data therefore provide examples of approximately 80% of storms expected at the study site per year. Considering the relationship between wind direction and current direction observed in this chapter, these data offer strong evidence in support of the observation that westward sediment transport prevails along the northern coast of the island.

The third point of interest is the relationship between storms and tides. The tidal range on the first day of Storm 1 was 50 cm; however, the range decreased to 22 cm and 14 cm on the following days (Figure 4.9). Although the tidal cycle was approaching an equatorial phase when lower ranges are expected, it appears that the storm influenced these results. The tidal range on the first day of Storm 3 was 64 cm; however, the range decreased to 32 cm on the following day, then appeared to return to normal on the third day as it increased to 50 cm. These results suggest that Storms 1 and 3 setup water levels along the coast which reduced the variation in water level between the ebb and flood stages of the tidal cycle. The northerly storm winds evidently forced water shoreward during ebb tides which effectively reduced the variation in water level across the nearshore shelf.

The fourth point of interest is the relationship between tides and wave heights. Storm 1 began at high tide, and the maximum wave height at that time was 30.4 cm (Figure 4.9). However, wave height decreased to 17 cm at low tide, then increased to 28.7 cm as water level increased. Wind speed, however, had decreased during the second high tide period (Figure 4.8). Storm 2 occurred at low tide and produced the lowest maximum wave height of the three storms (18.9 cm); however, it was also the weakest of the three storms. Storm 3 began at high tide, and the maximum wave height on the first day was 32.6 cm. However, wave height decreased to 14.3 cm at low tide. Wave height increased to 30.2 cm at the next high tide, then decreased again to 17.1 cm at the next low tide. Finally, as water level increased again, wave height increased to a maximum of 23.4 cm before the storm

subsided. Each of the low tide / low wave height periods during Storm 3 coincided with peak periods in wind speed (Figure 4.8).

These results suggest that tides / water levels had a greater influence on wave heights during storms than did wind speeds. Storm 3 is evidently a classic example of this complex relationship. The influence of tides on wave heights was evidently related to water depth across the nearshore shelf that lies along the northern coast of the island. The average water depth across the shelf was relatively shallow at approximately 1 meter (Figure 2.2). Water depth across the shelf during low tide periods was evidently reduced to the point that larger storm waves broke farther offshore. During high tide periods, increased water depths enabled larger storm waves to traverse the nearshore shelf and impact the beach. These results support the observations by Armbruster (1997) on the relationship between water levels and wave heights during storms, and the influence of the nearshore shelf, which leads to our final point of interest.

The fifth and final point of interest is the impact of storms on the beach. The results of this study support the observation by Armbruster (1997) that the coincidence of a storm and a low tide / low water period would result in a significant dissipation of wave energy on the shallow nearshore platform, thus reducing the impact of storm waves on the foreshore. And the complimentary observation that the coincidence of a high tide / high water period would result in storm waves impacting the foreshore at a higher elevation, thus increasing the impact on the beach, and the potential for overwash events. These results have

significant implications for understanding the damage that storm waves inflict upon the foreshore under specific tidal phase / water level conditions.

Furthermore, these findings have significant implications for understanding sediment transport along the coast. As noted, the coincidence of a storm and a low-tide period would result in a significant dissipation of wave energy on the nearshore platform, thus increasing the potential for sediment transport along the shelf, and reducing the potential for sediment transport along the foreshore. High-tide periods would therefore be associated with greater sediment transport along the foreshore, and reduced sediment transport along the shelf.

This study has shown that wind direction, storm duration, tides / water level, and wave height are critical components of storm dynamics along the northern coast of West Ship Island. Variations in these factors result in storms having different impacts on the foreshore, and result in sediment transport occurring along different sections of the profile. The results have significant implications for storms in which wind directions shift from northwest to northeast. Variations in tides / water levels during a storm would have a significant influence on the predominant direction of sediment transport along the foreshore, and along the nearshore shelf.

For example, strong, northwesterly winds may be observed at the beginning of a storm at low tide (Stage 1). Wind direction subsequently shifts to the northeast, wind speeds decrease, and water level rises (Stage 2). Although wind speeds were higher in Stage 1, the low tide would reduce wave heights, reduce the impact of storm waves on the foreshore, and increase sediment transport on the shelf. Although wind speeds were lower in Stage 2, the high tide would enhance wave

heights, enhance storm wave impacts on the foreshore, and increase sediment transport along the foreshore. The end result would be greater eastward sediment transport along the shelf in Stage 1, and greater westward sediment transport along the foreshore in Stage 2. Variations in tides / water depths across the nearshore platform would therefore counter the influence of wind speeds, and alter the balance in sediment transport along the shelf and the foreshore. A conceptual model of this scenario is presented in Figure 4.11. A classic example of the complex relationship between wind speed, wave height, and water level was observed during Storm 3 on March 6-8, 1997, when wave heights decreased significantly during two low-tide periods even though each of these periods coincided with peak periods in wind speed (Figure 4.8).

It should be noted that evidence of sediment transport on the shelf was detected when recovering the SeaPac instrument at the end of the study period. Weighted metal plates (40 cm diameter) (Figure 4.4) had been attached to the legs of the aluminum tripod that supported the SeaPac instrument to stabilize the deployment. Approximately 2-3 cm of sediment had accumulated on top of the metal plates by the end of the deployment period, consequently, the plates had to be physically "dug out" of the sand. This incident provides empirical evidence that sediment transport occurs on the shelf in water depths of up to 1 m.

In the previous chapter, the observation was made that the average predominance of northeasterly winds during a storm season would result in a greater "net volume" of sediment being transported westward along the northern coasts of barrier islands during an average storm season. It was noted that this

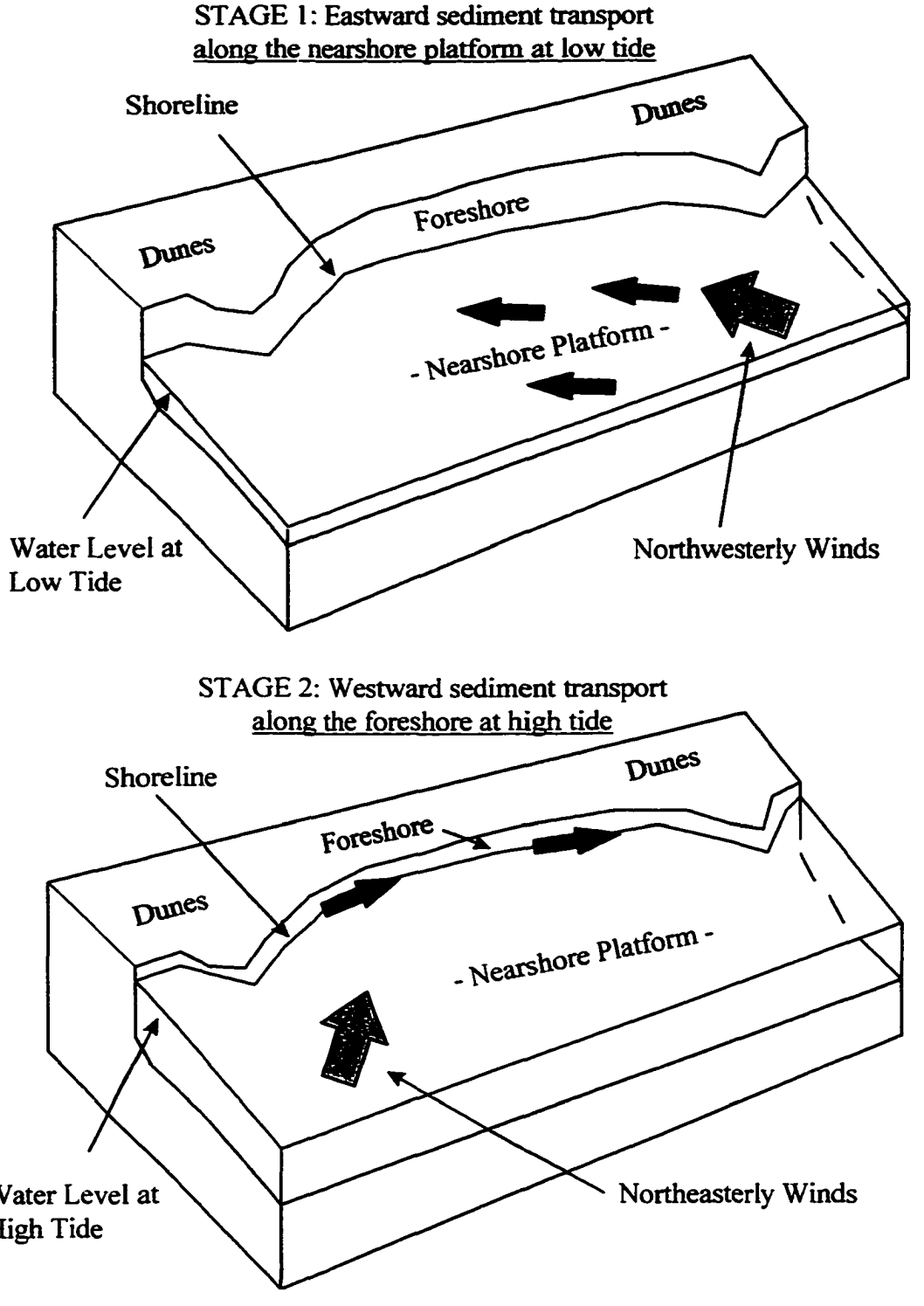

Figure 4.11. Conceptual model of the relationship between tides and the location of sediment transport along the profile. Although wind speeds may be higher during stage 1, a greater volume of sediment may be transported along the foreshore at high tide during stage 2. Thus, westward transport prevails along the foreshore.

observation was based on a direct relationship between wind direction and wave direction, and that it did not consider the influence of wind speeds or the tidal cycle. The data presented in this chapter indicate that there was a relatively direct relationship between wind direction and wave direction which supports the observation that westward sediment transport along the coast would prevail. However, the influence of tides / water levels on wave heights detected in this study suggests that sediment transport varies between the shelf and the foreshore. Therefore, the ratio of northwesterly winds to northeasterly winds does not appear to be an accurate indicator of the ratio of sediment (m^3) transported eastward and westward along the "foreshore."

This brief study identified four significant relationships that appear to be critical in understanding storm dynamics in these environments: 1) the influence of northerly wind directions on nearshore currents (current reversal, duration, and velocity), 2) the influence of storm winds on ebb tide levels (water level setup), 3) the greater influence of tides / water depths over wind speeds in controlling wave heights, and 4) the influence of tides / water depths on sediment transport across the shelf, and on sediment transport and storm wave impacts / overwash on the foreshore.

Although the conclusions presented here are based on a limited sample, the findings of this study are significant because they support the observations by Armbruster (1997) on the relationship between water levels and wave heights, and because they contribute toward a greater understanding of the range of nearshore conditions that occur in these environments (*i.e.*, variations in wind direction, wave

heights, current velocities, tides / water levels, and storm duration) which ultimately influence the evolution of the beach. The relationships identified in this study, therefore, make a significant contribution to the present body of literature on the effects of extratropical storms on nearshore wave, tide, and current conditions along the northern coasts of barrier islands of the northern Gulf of Mexico, especially when considering the limited availability of scientific literature on this topic.

CHAPTER 5

STORM IMPACTS

The data presented in Chapter 3 suggest that westward sediment transport prevails along the northern coast of West Ship Island because northeasterly winds prevail over northwesterly winds by a ratio of approximately 2:1 during an average storm season. The data presented in Chapter 4, however, suggest that the ratio of northeasterly winds to northwesterly winds would not be a reliable indicator of the ratio of sediment transport along the "foreshore." The objective of this chapter, therefore, is to evaluate the actual effects of extratropical storm activity during the 1996-1997 storm season on the beach along northern coast of West Ship Island.

The present body of literature on this subject for the Gulf of Mexico is limited to a 4-year study along a 600 m wide beach nourishment site at West Ship Island (Chaney and Stone 1996), and a 21-week study at two sites (120 m and 300 m wide) along the northern coast of Santa Rosa Island, Florida (Armbruster *et al.* 1995; Armbruster 1997). It is clearly evident that additional data are needed over greater spatial and temporal scales to fully understand the effects of extratropical storms on the evolution of these coastal environments.

Armbruster (1997) noted that foreshore responses to storms varied laterally along the beach, and attributed this to variability in storm conditions (water depth, wave heights, and wave directions). It was suggested that the backshore / foredune area served as the primary source of sediment to the foreshore, and that different sections of the foreshore subsequently served as sources of sediment to other sectors of the beach. The nearshore platform served as the terminal sink.

Consequently, various sectors of the foreshore experienced short-term, localized increases in width and volume, but the entire foreshore area ultimately suffered erosion as sediment was removed from the foreshore sediment transport system and deposited on the nearshore platform.

In regard to storm conditions, Armbruster (1997) suggested that variations in tides / water depth influenced the elevation at which storm waves impacted the foreshore. The data presented in Chapter 4 support this observation because they indicate that variations in tides / water depth could enhance or reduce the impacts of storm waves on the foreshore, and could determine whether a greater amount of sediment transport occurred along the nearshore platform or along the foreshore. These findings suggest that tides could alter the predominant direction of sediment transport along the nearshore platform and along the foreshore during storms in which wind direction shifts from northwest to northeast. Determining the predominant direction of sediment transport along the foreshore is therefore more complicated than simply determining the predominant direction of storm winds, as initially suggested in Chapter 3, which brings us to the purpose of this chapter. For future reference, the analysis of the 1996-1997 storm season indicated that the ratio of northeasterly winds (1,322 hours) to northwesterly winds (545 hours) was slightly above the average ratio of 2:1 (Table 3.18).

Three critical aspects of beach change over a storm season will be evaluated in this study: 1) total changes in beach width and volume along the entire northern coast of the island for evaluating annual rates of change, 2) lateral changes in beach width and volume along the coast for evaluating the influence of northwesterly and

northeasterly winds on sediment transport, and 3) cross-sectional changes in the morphology of the beach (*i.e.* evolution of the profile) for evaluating both alongshore and cross-shore trends in sediment transport.

The field study at West Ship Island consisted of monitoring two sets of beach profiles over a one-year study period that extended from May, 1996, to June, 1997. The two sets of profiles were established at different scales of resolution (Figure 5.1). The first set included eight profile lines established along the crest of the foredune system at approximately 600 m intervals which provided coverage along the entire length of the island. Surveys were conducted in June, October, and December, 1996, and in February, March, April, and June, 1997. The second set of profiles included six lines established at 50 m intervals along the beach nourishment site adjacent to Fort Massachusetts. Surveys were conducted in April and May, 1996, and in May, 1997.

In May, 1996, the National Park Service nourished the beach adjacent to Fort Massachusetts with approximately 50,000 m^3 of material dredged from the navigation channel located along the west tip of the island. A survey baseline was established parallel to the shoreline before the beach was nourished. Five profile lines were established at 50 m intervals along the baseline. Shoreline erosion near the fort prevented the baseline from extending eastward across the entire nourishment site, so a pre-existing profile line at the eastern end of the nourishment site was included in the study. This profile line had previously been established by the National Park Service at a U.S. Army Corps of Engineers benchmark located at the northeast corner of the fort. The five profile lines along the baseline had a

(A)

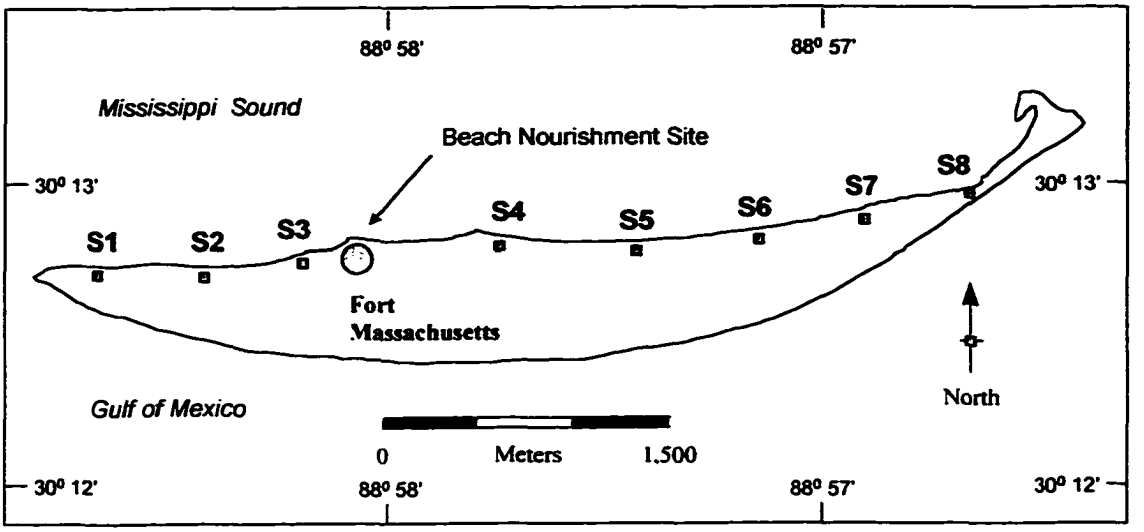

(B)

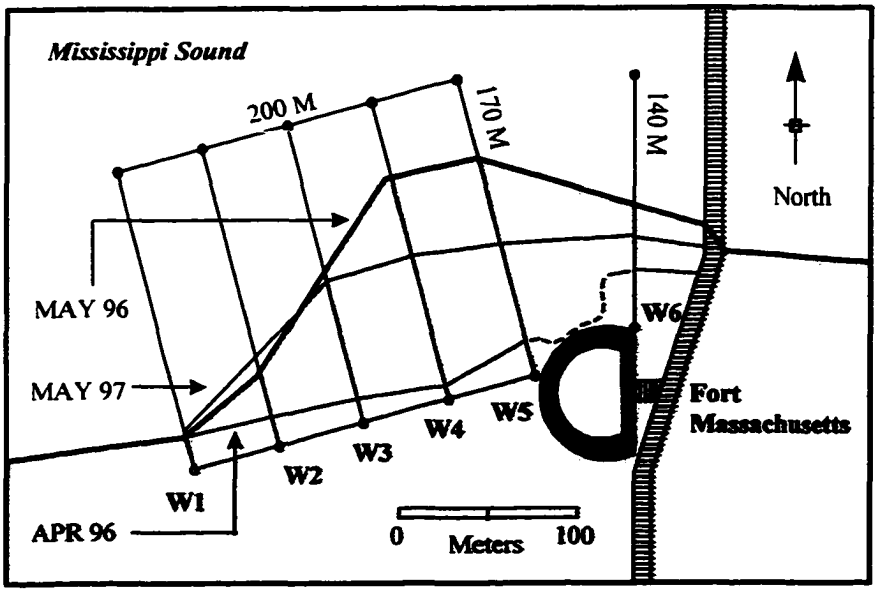

Figure 5.1. Location of the beach profile lines at West Ship Island. The upper plot (A) shows the location of the profiles along the soundside coast, and the location of the beach nourishment site adjacent to Fort Massachusetts. The lower plot (B) shows the location of the profiles at the beach nourishment site, and the position of the shoreline before and after the beach was nourished, and then one year later.

magnetic bearing of N 15^0 W. The pre-existing profile line at the benchmark had a magnetic bearing of N 00^0 W (magnetic north). This set of profiles provided coverage of the site before and after the beach was nourished (in May, 1996), and was subsequently used to document the effects of storms on the beach nourishment material after it had been in place for one year (May, 1997).

A Topcon GTS-203 Total Station with an electronic data collector was used to survey the profiles. The instrument records horizontal and vertical angles at increments of 10 arc-seconds (precision: +/- 5 arc-seconds), and records distances at increments of 0.001 m (precision: +/- (5mm + 5 ppm) (Topcon 1996). A U.S. Army Corps of Engineers benchmark located at the northeast corner of Fort Massachusetts was used to relate all elevations to the National Geodetic Vertical Datum (NGVD) of 1929. The elevation of the benchmark was +0.845 m NGVD.

Each profile was surveyed from the crest of the foredune, where present, to a set distance offshore. Elevations were recorded at significant breaks in slope along the beach, and at regular intervals along the nearshore platform. Elevations were recorded at regular intervals along the seabed because water depth and clarity made it difficult to determine breaks in slope. The length of the profile lines included in the first set of profiles (entire coast) was set at 100 m; however, one profile line (S1) was limited to 70 m because water depth restricted data collection. The length of the profile lines included in the second set of profiles (beach nourishment site) was set at 170 m; however, one profile line (W6) was limited to 140 m because water depth restricted data collection.

The survey data were used to compute beach width and volume data for each profile. The width of the beach was defined as the distance along the profile from the baseline to 0 elevation NGVD (approximate mean sea level). The survey along each profile was considered to be the centerline measurement of a 1-meter wide transect for computing volume. The volume of a profile was defined as the volume of sediment contained within the space that extended from the surface of the beach / seabed to a depth of -2 m NGVD. Depth was set at -2 m NGVD because the maximum depth of the seabed within the monitoring area was approximately -1.3 m NGVD.

In early October, 1996, Tropical Storm Josephine developed near Veracruz, Mexico, migrated northeastward across the Gulf, and made landfall along the Florida coast (Figure 5.2). The track of the storm system passed eastward of West Ship Island, but waves generated by the storm impacted the island on October 7 and 8, 1996. A NOAA weather buoy located approximately 60 km southeast of West Ship Island (NDBC Station 42040) recorded a maximum wind speed of 19.8 m sec^{-1}, and a maximum significant wave height of 6.2 m when the storm passed (Figure 5.3). This event had a significant impact on the northern coast of West Ship Island. It is critical to recognize at this point that the impact of Tropical Storm Josephine significantly altered the morphology of the soundside beach, and that the changes detected in the survey data during the "post-Tropical Storm Josephine" period do not necessarily reflect the changes that occur during an "average" storm season.

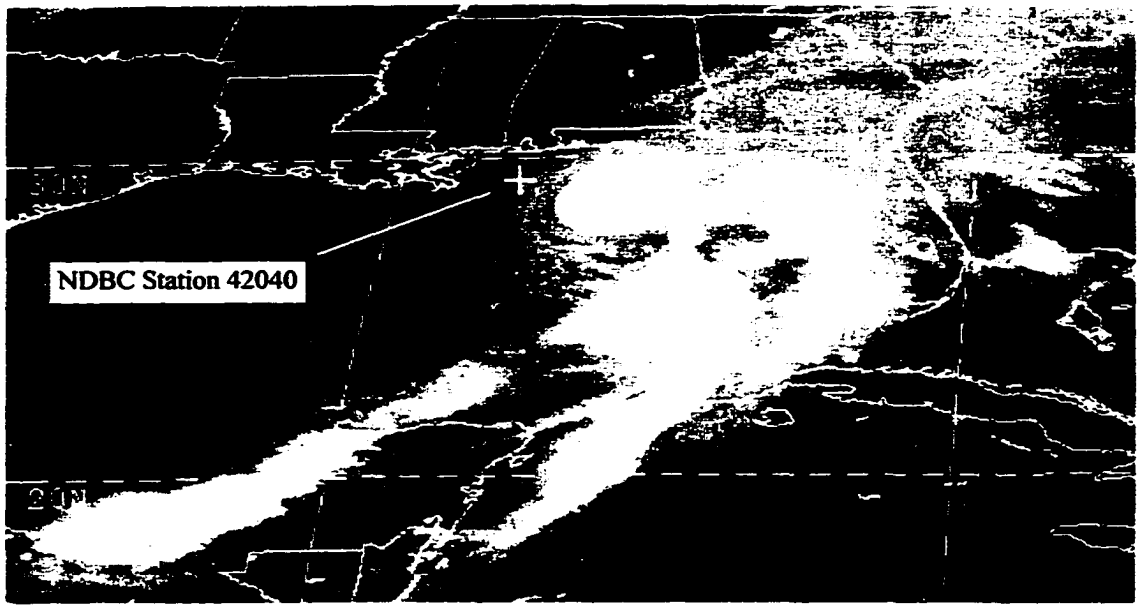

Figure 5.2. Satellite Image of Tropical Storm Josephine on October 7, 1996. The image is a Thermal I.R. image captured by the GOES-8 satellite and post-processed by the LSU Earth Scan Lab.

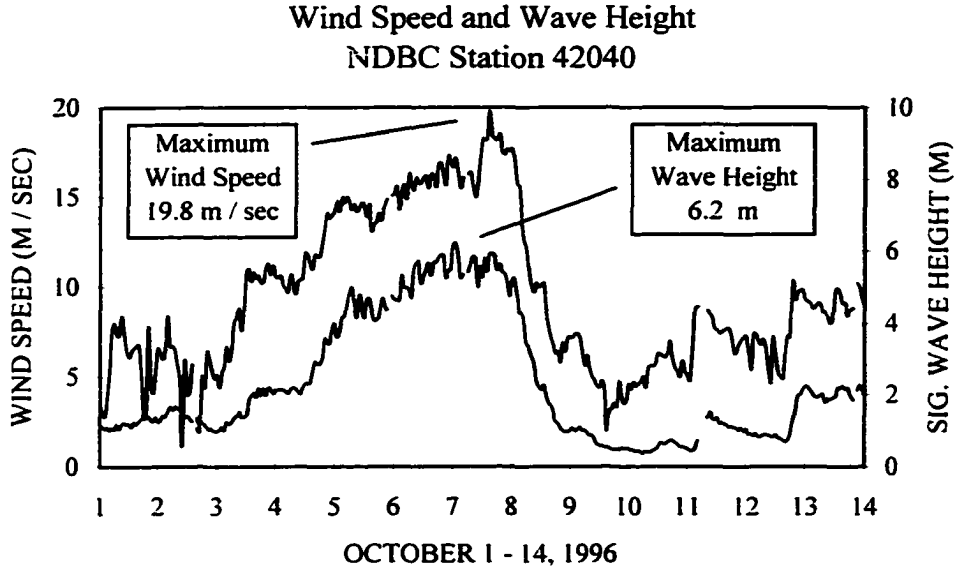

Figure 5.3. Wind speed and wave height data recorded at NDBC Station 42040 during the passage of Tropical Storm Josephine in October, 1996. NDBC Station 42040 is located approximately 45 km south of Mobil Bay, Alabama.

THE NORTHERN COAST

The initial survey of the profiles that were established at approximately 600 m intervals along the northern coast of West Ship Island was conducted in June, 1996 (Figure 5.1). The second survey was conducted on October 9, 1996, the day after Tropical Storm Josephine (TSJ) made landfall. Subsequent surveys were conducted in December, February, March, and April, and a final survey was conducted at the end of one year in June, 1997. The beach width data are presented in Table 5.1 and Figure 5.4. The volume data are presented in Table 5.2 and Figure 5.5. Summary tables of the change in beach width and volume for the "TSJ" period (June, 1996 to October, 1996), and the "post-TSJ" period (October, 1996 to June, 1997) are presented in Tables 5.3 and 5.4. Plots of the beach profile survey data are presented in Appendix 1.

It should be noted that Tropical Storm Josephine destroyed the profile markers at S4, and overwashed the beach at S8. Surveys were discontinued at S8 after subsequent overwash events dramatically changed the morphology of the profile. The data collected at profiles S4 and S8, therefore, were not included in the final results. It should also be noted that the survey markers at S1 were temporarily lost, so no data were recorded on the February, March, and April survey dates.

The results of the post-Tropical Storm Josephine survey in October, 1996, indicate that beach width increased along every profile, and the greatest increase occurred at S3 (+6.65 m) (Table 5.3). The results also show that changes in volume varied (Table 5.4). These results indicate that the average width of the beach

Table 5.1. Beach width data for the profiles along the northern coast. The table shows the beach width data for each survey date, and the annual change in beach width between June, 1996, and June, 1997. Profiles S4 and S8 were not included in the average beach width. The survey marker as S1 was temporarily lost so no data were recorded for the February, March, and April survey dates.

Survey Date	S1 (m)	S2 (m)	S3 (m)	S4 (m)	S5 (m)	S6 (m)	S7 (m)	S8 (m)	Average (m)
18-Jun-96	26.23	26.58	29.78	22.36	17.11	19.32	21.84	43.33	23.48
9-Oct-96	30.67	31.38	36.43	-	19.79	21.30	23.78	54.49	27.23
10-Dec-96	25.40	-	-	-	-	-	-	227.46	-
17-Feb-97	-	27.77	36.52	-	17.90	19.11	18.16	220.31	-
12-Mar-97	-	27.44	33.69	-	18.54	19.08	16.16	-	-
8-Apr-97	-	26.90	33.72	-	18.40	19.16	16.91	-	-
24-Jun-97	31.39	25.32	35.40	-	16.15	17.99	13.78	-	23.34
Annual Change	+5.16	-1.26	+5.62	-	-0.96	-1.33	-8.06	-	-0.14

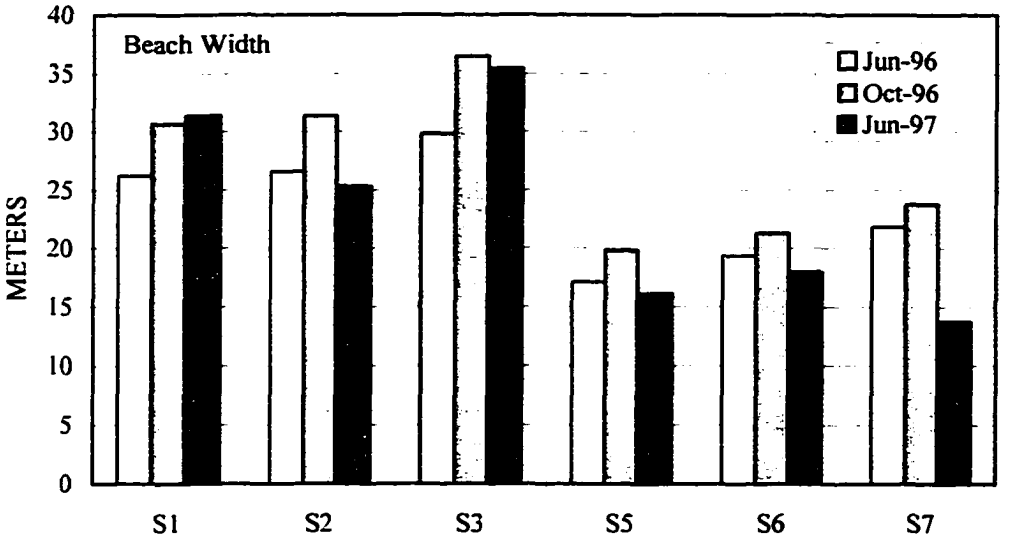

Figure 5.4. Beach width data for the profiles along the northern coast on the dates of the initial survey, the post-TSJ survey, and the final survey.

Table 5.2. Volume data for the profiles along the soundside coast. The table shows the volume data for each survey date, and the annual change in volume between June, 1996, and June, 1997. Profiles S4 and S8 were not included in the average volume. The survey marker as S1 was temporarily lost so no data were recorded for the February, March, and April survey dates.

Survey Date	S1 (m^3)	S2 (m^3)	S3 (m^3)	S4 (m^3)	S5 (m^3)	S6 (m^3)	S7 (m^3)	S8 (m^3)	Average (m^3)
18-Jun-96	163.80	175.12	204.04	170.18	172.68	190.48	192.51	217.28	183.11
9-Oct-96	154.58	178.81	206.17	-	172.57	187.93	184.89	238.59	180.83
10-Dec-96	147.96	-	-	-	-	-	-	292.44	-
17-Feb-97	-	177.31	212.71	-	170.54	188.93	185.93	291.15	-
12-Mar-97	-	177.81	209.98	-	171.50	188.28	189.64	-	-
8-Apr-97	-	178.95	209.35	-	171.01	188.07	186.97	-	-
24-Jun-97	162.21	181.69	213.17	-	169.69	187.53	183.34	-	182.94
Annual Change	-1.59	+6.57	+9.13	-	-2.99	-2.95	-9.17	-	-0.17

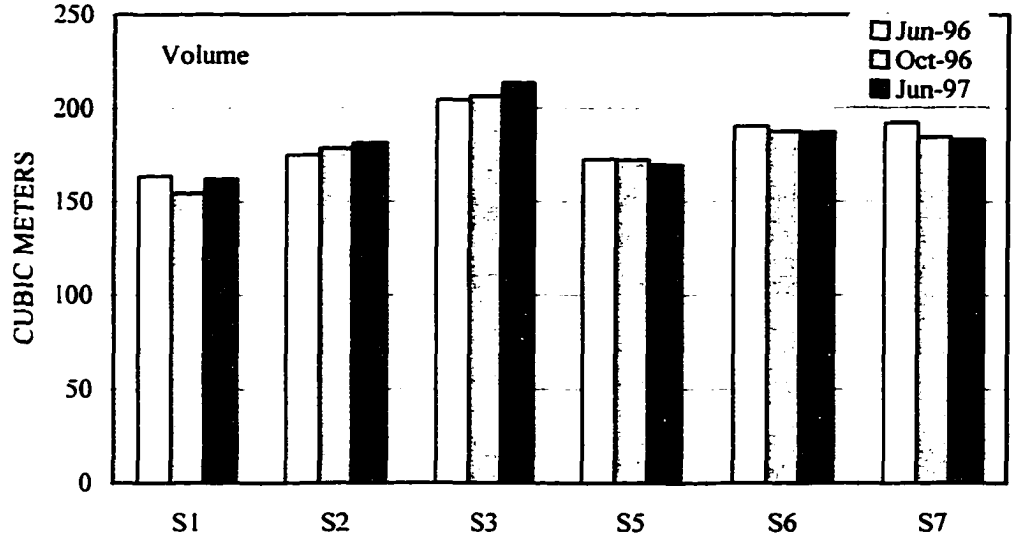

Figure 5.5. Volume data for the profiles along the northern coast on the dates of the initial survey, the post-TSJ survey, and the final survey.

Table 5.3. Total change in beach width for the profiles along the northern coast. The table shows the change in beach width associated with the impact of Tropical Storm Josephine (June, 1996, to October, 1996), and the change in beach width observed during the post-TSJ period (October, 1996, to June, 1997).

Survey Period	S1 (m)	S2 (m)	S3 (m)	S5 (m)	S6 (m)	S7 (m)	Average (m)
TSJ	+4.44	+4.80	+6.65	+2.68	+1.98	+1.94	+3.75
post-TSJ	+0.72	-6.06	-1.03	-3.64	-3.31	-10.00	-3.89
Annual Change	+5.16	-1.26	+5.62	-0.96	-1.33	-8.06	-0.14

Table 5.4. Total change in volume for the profiles along the northern coast. The table shows the change in volume associated with the impact of Tropical Storm Josephine (June, 1996, to October, 1996), and the change in volume observed during the post-TSJ period (October, 1996, to June, 1997).

Survey Period	S1 (m^3)	S2 (m^3)	S3 (m^3)	S5 (m^3)	S6 (m^3)	S7 (m^3)	Average (m^3)
TSJ	-9.22	+3.69	+2.13	-0.11	-2.55	-7.62	-2.28
post-TSJ	+7.63	+2.88	+7.00	-2.88	-0.40	-1.55	+2.11
Annual Change	-1.59	+6.57	+9.13	-2.99	-2.95	-9.17	-0.17

increased 3.75 m and the average volume of the profiles decreased 2.28 m^3 from the impact of Tropical Storm Josephine.

The results of the final survey in June, 1997, indicate that beach width decreased along every profile, except at S1 (+0.72 m), during the post-TSJ period (October, 1996 to June, 1997) (Table 5.3). The greatest decrease occurred at S7 (-10.00). The results also show that changes in volume varied (Table 5.4). Volume increased at profiles S1 (+7.63 m^3), S2 (+2.88 m^3), S3 (+7.00 m^3), and decreased at profiles S5 (-2.88 m^3), S6 (-0.40 m^3) and S7 (-1.55 m^3). These results indicate that the average width of the beach decreased 3.89 m and the average volume of the profiles increased 2.11 m^3 during the remainder of the winter storm season. In summary, the final results of the study indicate that the average width of the beach decreased 0.14 m and the average volume of the profiles decreased 0.17 m^3 over the course of the one-year monitoring period.

The data clearly show that Tropical Storm Josephine had a significant impact on the northern coast of West Ship Island. The storm surge elevated the water level in Mississippi Sound which resulted in wave erosion of the foredunes and backshore along the entire length of the soundside coast. The greatest loss occurred at S1 where a large section of the foredune was destroyed (Figure 5.6). The sediment eroded from the foredunes and backshore was evidently deposited along the lower foreshore as water level receded. This effectively increased the width of the beach and flattened the slope of the profile. The survey data (Table 5.3) and profile plots (Appendix 1) indicate that each profile experienced similar changes in beach width and morphology from this process. The second greatest loss

Figure 5.6. Erosion of the foredune and backshore at profile S1 that resulted from the impact of Tropical Storm Josephine on October 7-8, 1996. Mike Steinberg is shown measuring the height of the foredune. Photo taken by author on October 9, 1996.

of volume occurred at S7 where a nearshore bar was removed from the profile (Appendix 1). The greatest amount of the bar material was most likely eroded from the profile during the storm, and whatever remained was most likely transported offshore when the water level in Mississippi Sound receded.

Profiles S2 and S3 experienced similar changes to those observed at the other profiles (*i.e.* backshore erosion and foreshore deposition); however, profiles S2 (+3.69 m^3) and S3 (+2.13 m^3) increased in volume and the others decreased. Profiles S2 (+4.80 m) and S3 (+6.65 m) also experienced the greatest increases in beach width (Table 5.3). Additional material was evidently transported to S2 and S3 and deposited along the lower foreshore. The storm waves approached the island from the east, so sediment would have been transported westward alongshore during the storm. Profile S2 was located along the western flank of a crescent-shaped section of the shoreline. Sediment transported westward alongshore would accumulate at this type of location. Profile S3 was located along the western end of the nourishment site adjacent to Fort Massachusetts. Nourishment material was evidently transported westward alongshore during the storm and deposited along this section of the beach. Approximately 1 m^3 of material was also overwashed onto the backshore at S3.

The remainder of the study period consisted entirely of extratropical storm impacts which was the primary focus of this study. The first point of interest is the total change in beach width and volume that occurred along the coast during this portion of the winter storm season (October, 1996 to June, 1997). As noted earlier, the average width of the beach decreased 3.89 m and the average volume of the

profiles increased 2.11 m^3 during the post-TSJ period (Table 5.3 and 5.4). Erosion and deposition was observed at each profile during this period which suggests that storm conditions varied considerably (Table 5.2). Armbruster (1997) also attributed this type of response to variability in storm conditions. The analysis of storm dynamics presented in Chapter 4 indicated that variations in tides could significantly influence the impacts of individual storms, and the analysis of the 1996-1997 storm season presented in Chapter 3 indicated that storm conditions did in fact vary during the year. Nevertheless, it is important to recognize that the morphology of the beach had been disturbed by the impact of Tropical Storm Josephine, and that the changes observed during this period may not reflect the changes that occur during an "average" storm season. This observation especially applies to the annual rate of change data.

The second point of interest concerns lateral changes in beach width and volume for evaluating the influence of northwesterly and northeasterly winds on sediment transport along the northern coast. Beach width decreased at each profile, except S1, by the end of the winter storm season (Table 5.3). Volume decreased at S5, S6, and S7 (-4.83 m^3), and increased at S1, S2, and S3 (+ 17.51 m^3) (Table 5.4). These results suggest that sediment was eroded from the eastern end of the island and deposited along the western end. Profile S1 was located at the far western tip and appeared to be the end recipient of this process as it experienced the greatest increase in volume (+7.63 m^3), and was the only profile to increase in beach width (+0.72 m). As noted earlier, the analysis of the 1996-1997 storm season presented

in Chapter 3 indicated that westward sediment transport would prevail along the northern coast.

Profile S7 was located near the eastern end of the island and experienced the greatest decrease in beach width during the winter storm season (-10.00 m) (Table 5.3) (Figure 5.7). Sediment eroded from the beach was evidently deposited along a nearshore bar which would account for the minimal decrease in volume (-1.55 m^3) (Table 5.4) (Appendix 1). The high rate of shoreline retreat suggests that sediment transport along the foreshore was essentially non-existent. The profile was located approximately 15-20 m west of a 400 m section of the coast that has experienced severe erosion in the past. The beach has completely disappeared and all that remains are the exposed roots of small trees and shrubs. This area lies near the eastern tip of the island which has re-curved northward into Mississippi Sound. The re-curved tip of the island formed a small bay that was sheltered from wave activity and presently serves as a bird sanctuary. The eroded section of the coast in question now lies in the "wave shadow" of the re-curved tip of the island. The tip of the island now blocks easterly waves from reaching this section of the coast, therefore, westward sediment transport along the beach has essentially ceased. Sediment overwashed from the Gulf coast and deposited at S8 by Tropical Storm Josephine, and subsequent storms, may have enhanced the wave shadow effect at S7.

It is should be noted that a bar was also detected at S7 in June, 1996. The formation of the bar at this location suggests that there is a pattern of erosion at this site in which sediment migrates from the beach to the bar, rather than being transported alongshore. The beach material is most likely transported to the bar by

Figure 5.7. Erosion of the foreshore at profile S7 over the 1996-1997 storm season. Note the position of the white pipe near the high water line in the center of the photo. Also note the position of the foredune to the right of the 4-wheeler on the right side of the photo. The pipe was originally placed along the backshore section of the beach near the base of the foredune to mark the location of the profile line in June, 1996. This photo, which was taken by the author in June, 1997, clearly indicates that the site has experienced significant landward migration of the foreshore and the foredune. The absence of a beach farther along the coast (upper left of photo) suggests that severe erosion of the foreshore along this section of the island is common.

backwash currents during storms. The March 1997 survey detected deposition along the seaward face of the bar, but little change along the beach, which indicates that the bar also received material from transport along the platform.

Profiles S5 and S6 were located along the central section of a long, straight, stretch of the coast. Although S5 and S6 both experienced decreases in beach width (-3.64 m, and -3.31 m, respectively) and volume (-2.88 m^3 and -0.40 m^3, respectively) during the winter storm season (Table 5.3 and 5.4), the losses were minimal. Considering the relative location of these sites, (*i.e.* near the midpoint of an alongshore transport cell), the minor changes were to be expected (Nordstrom 1992).

Both S5 and S6 experienced similar changes along the foreshore as sediment was evidently eroded from the lower foreshore and re-deposited along the backshore. The resulting decrease in volume at S6 was insignificant. The decrease at S5 is noteworthy because it appears that the sediment loss occurred along the nearshore platform (Appendix 1). The field study of storm dynamics presented in Chapter 4 indicated that low tide / low water level periods would likely increase sediment transport on the nearshore platform. Sediment transport was in fact observed on the nearshore platform in the form of 2-3 cm of deposition on the base of the instrument deployment tripod. The data presented in Chapter 3 indicate that northeasterly winds prevailed during the 1996-1997 storm season which suggests that the lost sediment was most likely transported westward. However, the complex relationship between tides and wind directions identified in Chapter 4 suggests that the predominant direction of transport along the nearshore platform, and along the

foreshore, may vary for individual storm events (Figure 4.11). It is important to note that sediment located along the central section of the nearshore platform at S6 appeared to migrate farther offshore (Appendix 1), which suggests an alternative fate for the sediment eroded from the profile at S5.

Profile S3 was located along the western end of the nourishment site adjacent to Fort Massachusetts. A significant amount of sediment was deposited along the backshore during the winter storm season, and the lower foreshore experienced slight erosion (Appendix 1). Although the profile decreased in beach width (-1.03 m), the increase in volume (+7.00 m^3) suggests that this section of the coast received material from the nourishment site (Table 5.3 and 5.4). The analysis of the 1996-1997 storm season presented in Chapter 3 indicated that westward sediment transport would prevail along the northern coast. Nourishment material was evidently transported westward alongshore and overwashed onto the beach at S3 during the winter storm season.

Profile S2 was located along the western flank of a crescent-shaped section of the shoreline. A significant amount of sediment was deposited along the backshore during the winter storm season, and the lower foreshore experienced erosion. Although beach width decreased (-6.06 m), the increase in volume (+2.88 m^3) suggests that additional material was supplied to this section of the coast and overwashed onto the beach. Nordstrom's (1992) model for estuarine beaches suggests that profiles located near endpoints of transport cells experience greater increases in volume along the foreshore than profiles located near midpoints. The increase in volume at S2, therefore, appears to be related to two factors: 1) relative

location within an alongshore transport cell, and 2) predominant direction of alongshore transport within the cell. If the predominant direction of sediment transport along the coast was eastward, profile S2 would be expected to decrease in volume, not increase. The analysis of the 1996-1997 storm season presented in Chapter 3 indicates that the ratio of northeasterly winds to northwesterly winds was approximately 2:1, which suggests that westward sediment transport would prevail along the northern coast of the island. The increase in volume at S2 suggests that westward sediment transport did in fact prevail during the winter storm season.

The increase in volume at S2 during the winter storm season was slightly less than the increase observed from the impact of Tropical Storm Josephine (+2.88 m^3, and +3.69 m^3, respectively). However, the increase in volume at S3 (+7.00 m^3) during this period was considerably greater than the increase observed from the impact of Tropical Storm Josephine (+2.13 m^3). Although this was a limited sample, these data suggest that the prevailing northeasterly winds produced by extratropical storms during the 1996-1997 storm season played a role in transporting sediment westward along the coast that was at least equal to, if not greater than, the impact of Tropical Storm Josephine.

Profile S1 experienced the greatest increase in volume (+7.63 m^3), and was the only site to increase in beach width (+0.72 m), during the winter storm season (Table 5.3 and 5.4). The December 1996 survey indicated that nearly all of the sediment deposited along the foreshore and nearshore platform by Tropical Storm Josephine had been eroded from the profile (-6.62 m^3) (Table 5.2) (Appendix 1). However, the June 1997 survey indicated that a considerable quantity of sediment

had subsequently been deposited along the backshore and along the entire length of the foreshore (+14.25 m^3) (Table 5.2). The profile marker on the beach was temporarily lost (buried) during this period, so the complete pattern of change cannot be determined.

Profile S1 is located at the far western tip of the island. This site appears to have the exact opposite response to that observed at the eastern end of the island at profile S7. The beach at S1 is exposed to storm waves that approach from all northerly directions, and the beach appears to have been impacted by storms of greater intensity than the rest of the soundside coast. Washover deposits and beach scarps high above the shoreline were a common site. Three factors appear to have influenced the changes at this site. (1) Storm waves in Mississippi Sound may have overwashed the beach on a regular basis. The nearshore platform at this site is the narrowest (approximately 100 m) and steepest section along the entire northern coast, and consequently offers the least resistance to storm waves approaching from a northerly direction. (2) Storm waves along the Gulf coast may have been refracted around the tip of the island and overwashed the beach. The western tip of the island is a low-lying, sparsely-vegetated area that is frequently overwashed by storm waves. The erosion of a large section of the foredune at this site by Tropical Storm Josephine also indicates that storm waves from the Gulf may have been refracted around the tip and overwashed the beach. This process has been documented for estuarine beaches at Cape Cod (Ekwurzel 1990) and Delaware Bay (Jackson and Nordstrom 1992; Jackson 1995), and may account for the significant increase in volume and the overwashed condition of the beach at S1. (3) Westward

sediment transport may have contributed to the increase in volume detected along the foreshore. Evidence of westward transport was detected at profiles S2 and S3. As noted earlier, the analysis of the 1996-1997 storm season indicated that westward sediment transport would prevail along the northern coast of the island.

Although changes in beach width and volume varied during the winter storm season (Table 5.2), the trends observed at profiles S2, S3, and S7 clearly indicate that westward sediment transport was a significant factor along the northern coast of West Ship Island. It should also be noted that evidence of offshore transport was observed along the nearshore platform at profiles S6 (and possibly at S5), and that offshore transport of sediment from the beach to a nearshore bar was observed at S7. The bar at S7 also appeared to receive sediment by alongshore transport on the nearshore platform.

The third point of interest to be considered in this study is cross-sectional changes in the morphology of the beach for evaluating both alongshore and cross-shore trends in sediment transport. Evidence of westward, alongshore transport was identified at S1, S2, S3, and S7 (the response at S7 was evidently related to a decline in westward sediment transport along the foreshore), evidence of offshore transport was identified at S6 and S7, and evidence of onshore transport in the form of overwash was detected at every profile except S7 (Appendix 1). The direction of sediment transport observed along the nearshore platform at S5 is unclear although it appears to have been offshore.

A closer inspection of the profile data (Appendix 1) indicates that extratropical storm impacts essentially transformed the morphology of the beach

back to its original condition during the winter storm season (October, 1996 to June, 1997). The profile data indicate that a considerable amount of the sediment deposited along the lower foreshore by Tropical Storm Josephine was eroded from this section of the profile. Every profile, except S1, decreased in beach width during this period. And sediment was re-deposited along the upper foreshore and backshore at each profile, except S7 (Table 5.3). This evolutionary process consisted of three distinct phases: 1) sediment was eroded from the lower foreshore and re-deposited along the backshore, 2) a distinct ridge formed along the upper foreshore, and 3) the ridge was overwashed and sediment was re-deposited along the backshore. This process can easily be identified at profiles S2, S5, and S6, and the later phases can be identified at S3. These four profiles resembled their "pre-TSJ" morphology by the end of the study period. A conceptual model of this process is presented in Figure 5.8.

As noted, this evolutionary process was driven by extratropical storm impacts. Sediment was transported from the lower foreshore to the upper foreshore during the winter months of November to February. The ridge along the upper foreshore developed during the spring months of March and April. And at some point in May or June, the optimal storm conditions (coincidence of high tides, winds, and waves) were met for a maximum overwash event to occur. The ridge was overwashed, and sediment was transported to the backshore. The beach returned to its original morphology at this point of the cycle.

Tropical Storm Josephine had a significant impact on the northern coast of West Ship Island which altered the morphology of the beach. Therefore, the

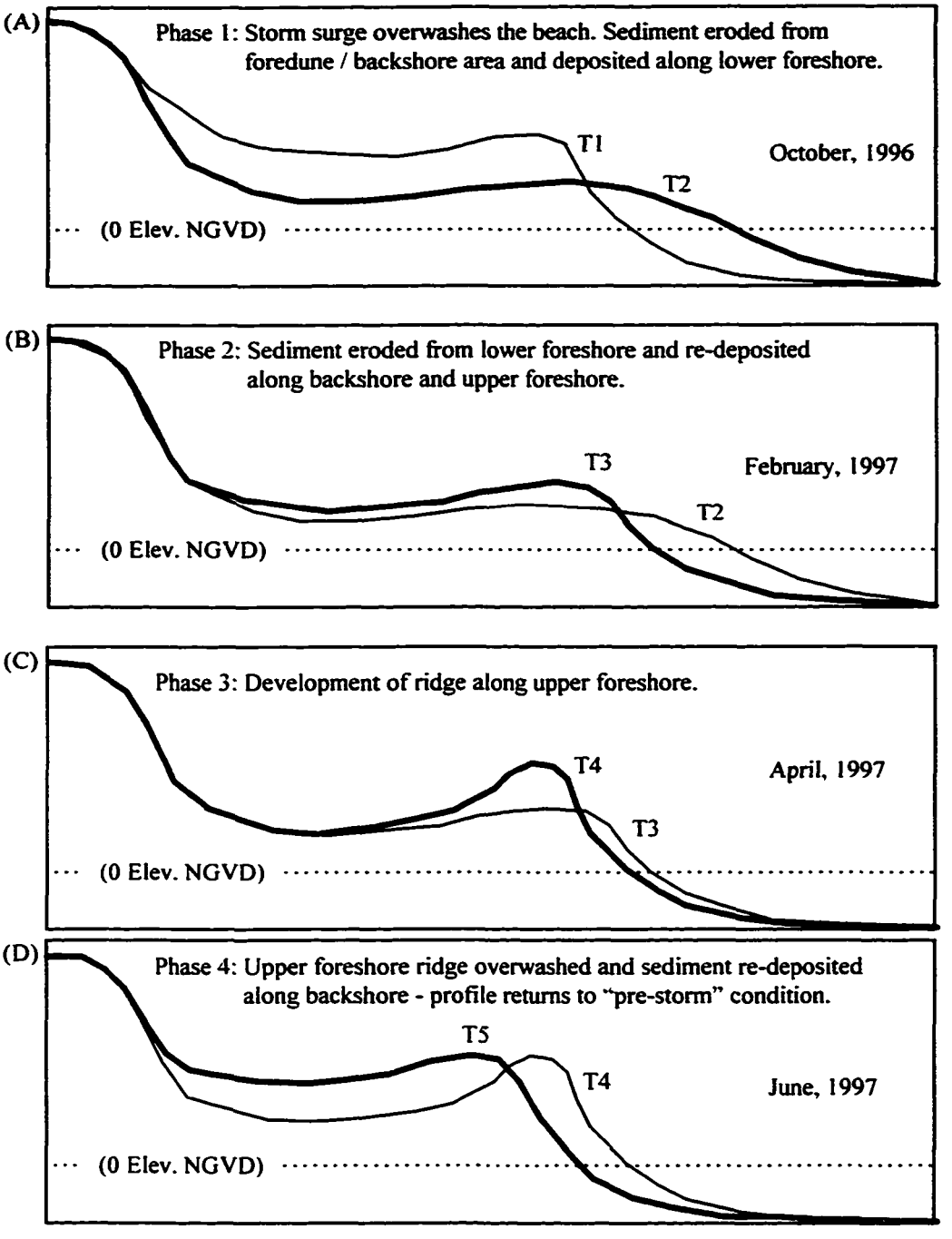

Figure 5.8. Conceptual model of beach profile responses to Tropical Storm Josephine and subsequent extratropical storm impacts. The upper plot (A) shows the impact of the initial storm surge. The lower plots (B, C, and D) show the evolution of the profile as it returns to its "pre-storm" morphology.

changes in beach width and volume observed during the winter storm season may not reflect the changes that occur during an "average" storm season. This observation especially applies to the annual rate of change data, so no conclusions were made in regard to the annual rates of change in beach width and volume that may be expected to occur along the northern coast during an "average" storm season from extratropical storm impacts. Nevertheless, four conclusions can be made from the results of this study: 1) alongshore sediment transport occurred along both the foreshore and along the nearshore platform, 2) the predominant direction of alongshore sediment transport along the northern coast was westward, and 3) both offshore and onshore forms of cross-shore sediment transport occurred along the northern coast, and 4) each of these modes of sediment transport were associated with extratropical storm impacts.

The analysis of storm dynamics presented in Chapter 3 indicated that variations in tides / water depths could result in sediment transport occurring along both the foreshore and along the nearshore platform. Evidence of alongshore transport was observed along the foreshore at profiles S1, S2, and S3, and along the nearshore platform at S7 (in the form of deposition on the nearshore bar). The analysis of the 1996-1997 storm season presented in Chapter 3 indicated that westward sediment transport would prevail along the northern coast. The increases in volume observed at S2 and S3 clearly indicate that the predominant direction of sediment transport was westward. Westward transport along the western tip of the island evidently contributed to the increase in volume observed along the foreshore at S1. And a decline in westward transport along the eastern end of the island led to

the high rate of shoreline retreat observed at S7, and to the severe erosion of the foreshore along that section of the coast. Both onshore and off-shore currents were detected in the storm dynamics data presented in Chapter 4, but more importantly, the data indicate that variations in tides / water level could enhance storm waves impacting the beach which could result in overwash. Evidence of onshore transport was observed at every profile, except S7, in the form of overwash deposition along the backshore. Evidence of offshore transport was observed along the nearshore platform at S6 (and possibly at S5), and along the foreshore at S7, where sediment was evidently transported from the beach to the nearshore bar by backwash currents during storms.

Extratropical storm impacts were evidently associated with each of the changes observed along the coast during the winter storm season. The changes observed along the foreshore in turn contributed in some part to the evolution of the foreshore observed during the study. Therefore, the results of this study also contribute toward a greater understanding of the changes that occur along the northern coast after the impact of a tropical storm. A final review shows that Tropical Storm Josephine removed sediment from the foredunes and backshore, and deposited that sediment along the lower foreshore. The result was an increase in average beach width (+3.75 m), and a decrease in average volume (-2.28 m^3). During the winter storm season, extratropical storms transported sediment from the lower foreshore back to the beach. Average beach width decreased (-3.89 m), and average volume increased (+2.11 m^3). At the end of the study period, the net changes in beach width (-0.14 m) and volume (-0.17 m^3) were insignificant. It

should be noted that these changes were influenced by the contribution of sediment from the nourishment site at Fort Massachusetts, and possibly from overwash or sediment transport around the western tip of the island.

THE NOURISHMENT SITE AT FORT MASSACHUSETTS

The initial survey of the profiles that were established at 50 m intervals along the coast at the beach nourishment site adjacent to Fort Massachusetts was conducted in April, 1996 (Figure 5.1). The beach was subsequently nourished with 50,000 m^3 of material dredged from the navigation channel located along the west tip of the island. The second (post-nourishment) survey was conducted in May, 1996. The final survey was conducted one year later in May, 1997. The beach width data are presented in Table 5.5 and Figure 5.9. The volume data are presented in Table 5.6 and Figure 5.10. Plots of the beach profile survey data are presented in Appendix 2.

The May 1996 survey data indicate that the beach nourishment material increased the average width of the beach 59.3 m and the average volume of the profiles 106.22 m^3. The June 1997 survey data indicate that the average width of the beach decreased 17.1 m and the average volume of the profiles decreased 16.85 m^3. These data indicate that beach width decreased 28.8% and volume decreased 15.9% after the nourishment material had been in place for one year.

The beach adjacent to Fort Massachusetts was previously nourished at some point between July, 1991, and October, 1991. Between October, 1991, and July, 1993, beach width decreased at a rate of 24.7 m yr^{-1} (Chaney and Stone 1996). Unfortunately, the distance surveyed along each profile on each date was

Table 5.5. Beach width data for the profiles at the nourishment site adjacent to Fort Massachusetts. The table also shows the average beach width for each survey date, and the annual change in beach width between May, 1996, and May, 1997.

Survey Date	W1 (m)	W2 (m)	W3 (m)	W4 (m)	W5 (m)	W6 (m)	Average (m)
22-Apr-96	18.9	16.6	13.6	7.8	20.1	32.2	18.2
16-May-96	17.6	41.2	88.8	126.8	123.6	67.0	77.5
29-May-97	22.5	51.3	81.3	81.8	75.2	50.8	60.4
Annual Change	+4.9	+10.1	-7.5	-45.0	-48.4	-16.2	-17.1

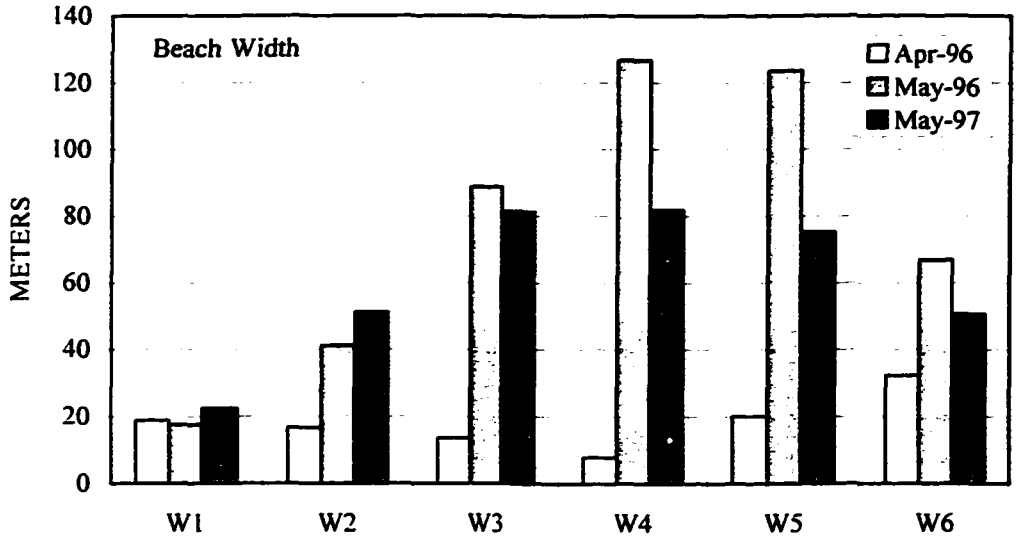

Figure 5.9. Beach width data for the profiles at the nourishment site adjacent to Fort Massachusetts.

Table 5.6. Volume data for the profiles at the nourishment site adjacent to Fort Massachusetts. The table also shows the average volume for each survey date, and the annual change in volume between May, 1996, and May, 1997.

Survey Date	W1 (m^3)	W2 (m^3)	W3 (m^3)	W4 (m^3)	W5 (m^3)	W6 (m^3)	Average (m^3)
22-Apr-96	262.47	265.01	256.71	245.93	263.11	250.24	257.25
16-May-96	262.60	300.55	387.60	448.16	479.88	302.00	363.47
29-May-97	275.85	332.00	376.66	385.44	408.28	301.49	346.62
Annual Change	+13.25	+31.45	-10.94	-62.72	-71.60	-0.51	-16.85

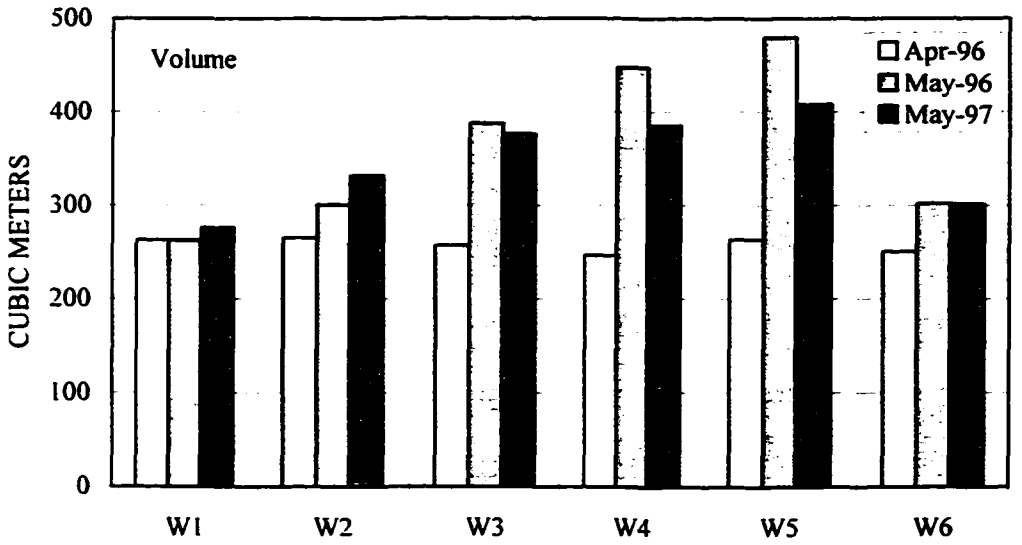

Figure 5.10. Volume data for the profiles at the nourishment site adjacent to Fort Massachusetts.

consistently shortened as the shoreline retreated landward, therefore, the volume data for that period are not suitable for comparison.

Although the rate of shoreline retreat observed after the 1996 nourishment was lower than the rate of shoreline retreat observed after the 1991 nourishment, these rates are still significantly higher than those observed along the rest of the northern coast (Table 5.3). A closer inspection of the May 1997 survey data indicates that the central section of the monitoring area experienced severe erosion, and that the western section experienced a slight increase in beach width and volume (Table 5.5 and 5.6). The changes at the nourishment site were related to four factors: 1) "expected" losses to the nearshore platform (offshore transport) after nourishment, 2) site conditions, 3) westward sediment transport (by storms), and 4) aeolian transport to the dunes along the backshore (by storms).

Although the rates of erosion observed after the 1991 and the 1996 nourishments appear to be extreme, Houston (1991) notes that high rates of erosion are expected after a nourishment project is conducted because the profile has to "re-equilibrate" to local wave and tide conditions. The re-equilibration process results in a significant loss of sediment to the nearshore zone where as much as 60% of the original nourishment material may be deposited; however, a significant amount of this material is expected to remain within the nearshore section of the nourishment area for several years (Houston 1991). Houston (1991) also notes that some of this material often returns to the beach after storms. Nourishment projects along bayside coasts appear to be rare, so it is uncertain as to how much volume

loss to expect during the "re-equilibration" process in an estuarine environment, or how long the process lasts. However, studies on beach responses to storm impacts along estuarine coasts indicate that these low-energy, micro-tidal environments may lack sufficient wave energy to re-transport sediment back to the beach (Nordstrom and Jackson 1992; Nordstrom 1992).

The conditions at the nourishment site appear to have contributed to the pattern of erosion observed laterally along the monitoring area. The seaward limit of the monitoring area was established at the point at which water depth restricted further data collection. Inspection of the monitoring area shown in Figure 5.1 indicates that water depth limited the length of profile W6 to 140 m and profile W5 to 170 m. This pattern indicates that that the central section of the nourished beach at profiles W4 and W5 extended out into the deepest section of the nearshore zone. The June 1997 survey data indicate that the greatest losses occurred along the central section of the monitoring area at profiles W4 (-45.0 m, -62.72 m^3) and W5 (-48.4 m, -71.60 m^3) (Table 5.5 and 5.6). The losses at these two profiles account for 80% of the decrease in beach width and 92% of the loss in volume. The relative location of this section of the nourished beach evidently resulted in severe erosion at W4 and W5 as the newly placed nourishment material began to fill the nearshore zone in the profile "re-equilibration" process. Evidence of offshore transport of the nourishment material at profiles W4 and W5 can be detected on the plots of the survey data (Appendix 2). Evidence of offshore transport can also be detected at W3. It is unfortunate that water depth restricted data collection along this section of the nearshore platform because it would have been very useful to track the

movement of the material into greater water depths. This information would have been useful in documenting the re-equilibration process, and in determining the fate of the material that was lost from the nearshore area.

Westward sediment transport also appears to account for some of the material lost from the central section of the monitoring area. Profiles W3, W4, and W5 decreased in volume (-145.26 m^3) and profiles W1 and W2 increased in volume (+44.70 m^3) (Table 5.6). The plot of the survey data at W2 indicates that sediment was deposited along the backshore, foreshore, and the nearshore platform (Appendix 2). The May 1997 survey data confirm that the profile increased in beach width (+10.1 m) and volume (+31.45 m^3). The plot of the survey data at W1 shows similar changes, but the increases in beach width (+4.9 m) and volume (+13.25 m^3) were lower. This pattern suggests that some of the sediment from the central section of the monitoring area was transported westward along the nearshore platform, and that some of the material was transported westward along the foreshore and overwashed on to the backshore at W1 and W2. The storm dynamics data presented in Chapter 4 indicate that extratropical storms produced northeasterly winds which in turn produced westward currents, thus westward sediment transport along the northern coast was possible. The pattern of deposition observed at profiles W1 and W2 represents empirical confirmation of westward sediment transport along the northern coast of West Ship Island.

The plot of the survey data at W6 indicates that the profile experienced substantial erosion along the foreshore, and deposition along the backshore, and along the nearshore platform (Appendix 2). The May 1997 survey data indicate that

the profile experienced a significant decrease in beach width (-16.2 m), but only a minor decrease in volume (-0.51 m^3). The profile evidently experienced a similar change to that observed at W4 and W5 in that nourishment material eroded from the foreshore was deposited along the nearshore platform as part of the "re-equilibration" process.

The nearshore zone at W6 may also have received sediment from the central section of the monitoring area by alongshore transport, as did profiles W1 and W2. This scenario, however, suggests that sediment was transported eastward. The storm dynamics data presented in Chapter 4 indicate that extratropical storms also produced northwesterly winds which in turn produced eastward currents, thus eastward sediment transport along the northern coast was possible. Another possible explanation is that sediment was transported westward alongshore to the profile site. The profile was in fact located westward of the actual limit of the nourishment area, so nourishment material could easily have been transported westward and deposited at W6. It is unfortunate that the nourishment site did not extend farther eastward because it would have provided an ideal opportunity to document the predominant direction of sediment transport along the foreshore at the nourishment site. This would be a significant contribution because the 1996-1997 storm season data presented in Chapter 3 suggest that westward sediment transport would prevail along the northern coast, but the storm dynamics data presented in Chapter 4 suggest that variations in tides during a storm could influence the predominant direction of sediment transport along the foreshore, and along the nearshore platform.

The plots of the survey data at profiles W3, W4, and W5 show substantial losses along the surface of the beach, and sediment accumulation on the foredune at W5 (Appendix 2). These changes were the result of wind transport. Northerly winds scour the surface of the beach at the nourishment site and transport the sediment to the dunes along the backshore. The dunes at this location are some of the highest dunes on the island (elevations of 5-6 m NGVD). This sediment transport process was evidently driven by extratropical storms during the winter months. Evidence of this process was previously documented at Trinity Island, Louisiana, where northerly winds associated with a cold front passage were observed eroding the surface of the beach (Dingler *et al.* 1992).

The development of the dune system along the backshore at the nourishment site evidently began when the first nourishment project was conducted in 1974. The 1967 aerial photo in Figure 2.3 shows that the area where these dunes are presently located was underwater at the time. The 1985 aerial photo in Figure 2.4 shows the approximate position of the shoreline before the beach was nourished in 1974, and the immature state of the dunes along the backshore area of the nourished beach at that point in time.

Four conclusions can be made from the results of this study: 1) sediment transport occurred by the actions of both winds and waves, 2) sediment was transported alongshore, offshore, and onshore, 3) westward, alongshore sediment transport was documented at the site, 4) extratropical storms played a significant role in both alongshore transport by waves, and onshore transport by wind. The May, 1997 survey data indicate that 145.77 m^3 of nourishment material was lost

from profiles W3, W4, W5, and W6. This material was transported away from the site by the actions of both waves and winds associated with extratropical storms. Westward sediment transport was confirmed by the pattern of deposition observed at profiles W1 and W2, which accounted for 44.70 m^3 (30.7%) of the lost material. Some of the lost material may have been transported eastward alongshore and deposited at profile W6. The survey design, however, was unable to determine the direction of sediment transport to W6. A significant amount of erosion by wind transport was observed along the surface of the beach nourishment site at profiles W3, W4, and W5. This process was evidently driven by extratropical storm activity in winter months. Wind erosion apparently accounted for some, but not all, of the remaining 101.07 m^3 (69.3%) of material lost from the monitoring area. The remainder of this material was most likely transported offshore into deeper water beyond the limits of the surveys.

It should be noted that an on-site inspection of the nourishment site was conducted on October 9, 1996, the day after Tropical Storm Josephine made landfall. No significant changes in beach width or volume were detected at that time. The response of the nourishment site appeared to be quite similar to that observed along the remainder of the coast where the average change in beach width was + 3.75 m and the average change in volume was -2.28 m^3 (Table 5.3 and 5.4). The rates of erosion observed in this study compared favorably with the results of the earlier study (Chaney and Stone 1996). This indicates that Tropical Storm Josephine did not have a significant impact on the nourishment site. At the present rates of erosion, the life expectancy of the beach nourishment is approximately 4-5

years. The National Park Service has nourished the site 4 times since 1974 which is an average interval of 5.5 years.

CHAPTER 6

SUMMARY AND CONCLUSIONS

The purpose of this research was to investigate the chronic coastal erosion problem observed along the northern shores of barrier islands of the northern Gulf of Mexico. The problem has been shown to be related to extratropical storm impacts in winter. Extratropical storms in the northern Gulf of Mexico have received little attention from the scientific community because research in this region has traditionally focused on the impacts of tropical storm systems (*i.e.* hurricanes). The primary focus of this research was on extratropical storm activity. More specifically, the research focused on identifying weather patterns associated with extratropical storms, the frequency of extratropical storms, the duration of the "northerly" winds produced by extratropical storms, and the speed and direction of the "northerly" winds produced by extratropical storms. The secondary focus of this research was on the effects of extratropical storms on nearshore wave, current, and water level conditions, and their impacts on the beach.

Extratropical storm activity along the northern Gulf Coast proved to be extremely complex. The results of the historical study of storm activity (Chapter 3) indicate that extratropical storms along the northern Gulf Coast were produced by seven distinctly different weather patterns. This study incorporated the cold front types identified by Roberts *et al.* (1987) with the Gulf cyclones studied by Hsu (1993) into a comprehensive set of extratropical storm types which makes a significant contribution to our understanding of extratropical storm activity along the northern Gulf Coast. Furthermore, the extratropical storm types for the Gulf of

Mexico identified in this study were shown to be related to extratropical storm types recognized in studies along the U.S. Atlantic Coast which contributes to a greater understanding of extratropical storm activity throughout the eastern U.S. coastal region.

The Primary Front extratropical storm type proved to be the most common and accounted for approximately 75% of storm activity. The distribution of storms during the storm season (September-May) resembled a bell curve with the highest frequency in January. The duration of storms varied considerably (avg. = 37.8 hours; std. dev. = 27.7 hours). Mean wind speeds (avg. = 8.3 m sec^{-1}; std. dev. = 1.8 m sec^{-1}) and maximum wind speeds (avg. = 11.6 m sec^{-1}; std. dev. = 2.9 m sec^{-1}) were relatively consistent. The average duration of storms was highest in the autumn months, thus the highest magnitude storm events (Class 4 and 5) were most frequent in the autumn months. These results contribute to the findings of earlier studies by Fox and Davis (1976), Dingler *et al.* (1992), Armbruster *et al.* (1995), and Armbruster (1997), and extend our knowledge of "northerly" winds produced by extratropical storms in the Gulf of Mexico.

Approximately 70% of the 506 storms evaluated in this study produced both northwesterly and northeasterly winds, and northeasterly winds prevailed by a ratio of approximately 2:1 during these storms. Approximately 10% of storms produced strictly northwesterly winds, and approximately 20% produced strictly northeasterly winds. The average frequency of storms in these three categories led to the average duration of northeasterly winds prevailing over northwesterly winds by a ratio of approximately 2:1 during a storm season. These results may be used to infer that the

predominant direction of sediment transport along the northern coasts of barrier islands of the northern Gulf of Mexico is westward. Northeasterly winds consistently prevailed over northwesterly winds by the greatest margin in autumn, which suggests that westward sediment transport consistently prevails over eastward sediment transport by the greatest margin in autumn. The inference can therefore be made that the greatest "net volume" of westward sediment transport occurs in autumn. These finding were attributed to the influence of anticyclones (high-pressure weather systems with clockwise wind rotation patterns) on wind conditions along the coast following the passage of the leading cold front. This observation contributes to our understanding of wind flow patterns during storms and dictates that future studies consider anticyclones in evaluating storm dynamics and impacts along the northern Gulf Coast.

The results of the field study of storm dynamics (Chapter 4) indicate that there is a relatively direct relationship between wind direction and current direction which supports the observation that westward sediment transport prevails. The results also indicate that there is a complex relationship between tides / water depths and wave heights. Low tides reduce water depth across the shallow, nearshore platform which evidently results in storm waves breaking farther offshore, and thereby expending much of their energy on the platform before impacting the foreshore. High tides increase water depth across the nearshore platform which evidently enables larger storm waves to traverse the platform and expend their energy on the foreshore. Thus, sediment transport occurs along the nearshore platform during low tide periods and along the foreshore during high tide

periods. This relationship has significant implications for storms in which wind direction shifts from northwest to northeast because a variation in tides could alter the balance (predominant direction) of sediment transport along the foreshore and along the nearshore platform. The findings of this study confirm the observations of Armbruster *et al.* (1995) and Armbruster (1997) on the complex relationship between tides and wave heights that determines the location of sediment transport along the profile, and extend our knowledge of this subject by noting that variations in tides can influence the effects of wind shifts during storms and thereby influence the predominant direction of sediment transport along the foreshore and the nearshore platform.

The results of the field study of storm impacts (Chapter 5) indicate that extratropical storms influenced changes along the northern coast of West Ship Island in two ways: 1) alongshore and cross-shore sediment transport by wave action, and 2) onshore sediment transport by wind action. Evidence of deposition by westward, alongshore sediment transport was observed at three of the six beach profile sites along the northern coast that were monitored over the entire study period, and erosion due to a decline in westward transport was observed at one of the remaining three profile sites. Significant evidence of westward sediment transport was documented at the beach nourishment site adjacent to Fort Massachusetts. These results indicate that the predominant direction of alongshore sediment transport was westward, and thereby confirm the previous inference that the prevailing northeasterly winds during storms would result in a predominantly westward direction of sediment transport along the northern coast of the island.

Evidence of offshore transport was observed along the foreshore at one profile site and along the nearshore platform at a nearby site. A significant amount of offshore transport evidently occurred at the beach nourishment site adjacent to Fort Massachusetts; however, the survey design was unable to determine the fate of the lost sediment. The predominant direction of cross-shore sediment transport along the remainder of the coast was onshore. This finding was related to the disturbed condition of the coast following the impact of Tropical Storm Josephine in October, 1996. The storm eroded sediment from the backshore and foredunes and deposited that sediment along the lower foreshore, thus increasing the width of the beach and reducing the slope of the profile. Extratropical storm impacts removed the sediment from the lower foreshore and re-deposited that sediment along the backshore. All but one profile experienced deposition along the backshore by onshore transport (overwash) during the winter storm season. The actions of extratropical storms effectively transformed the morphology of the beach back to its original condition by the end of the study period.

A significant amount of onshore transport by wind erosion was also observed at the beach nourishment site. Northerly winds during storms scoured the surface of the beach nourishment site and transported that sediment to the foredunes along the backshore. This process evidently began in 1974 when the initial beach nourishment project was conducted. The area where the dunes are presently located was underwater in 1974. The dunes have since grown to be some of the largest on the island. This observation on wind erosion is supported by the earlier findings of Dingler *et al.* (1993) at Trinity Island, Louisiana, that indicated that northerly winds

produced by extratropical storms eroded the surface of the beach and thereby contributed to changes in barrier island morphology.

Evidence from the historical analysis of extratropical storm activity, and from the field study of storm dynamics and impacts at West Ship Island, Mississippi, leads to the following conclusions:

1. There are seven distinctly different types of weather patterns that produce extratropical storm events along the northern Gulf Coast.
2. The most common extratropical storm type along the northern Gulf Coast is the Primary Front.
3. The duration of the "northerly" winds during storms varies considerably; however, the mean and maximum speeds of the "northerly" winds are relatively consistent.
4. Approximately 70% of storms produce both northwesterly and northeasterly winds, approximately 10% produce strictly northwesterly winds, and approximately 20% produce strictly northeasterly winds.
5. The average annual ratio of northeasterly to northwesterly winds produced by extratropical storms is approximately 2:1.
6. The anticyclone that follows the passage of the cold front is responsible for the prevailing northeasterly winds during the storm season.
7. The predominant direction of alongshore sediment transport along the northern coast of West Ship Island is westward.
8. Variations in tides during storms can determine whether sediment transport occurs along the foreshore or along the nearshore platform.

9. Variations in tides during storms in which wind direction shifts from northwest to northeast can influence the predominant direction of sediment transport along the foreshore and along the nearshore platform.
10. Northerly winds produced by extratropical storms in winter erode the surface of the beach nourishment site adjacent to Fort Massachusetts and transport that sediment to the dunes along the backshore.

It is perceived that the findings of this research will assist coastal managers and the scientific community in developing a greater understanding of extratropical storm activity and impacts along the northern Gulf Coast. Two areas in particular that this research contributes to is a greater understanding of the variability in storm activity that may occur in a forthcoming storm season, and the different roles that extratropical storms and tropical storms play in the evolution of coastal environments of the northern Gulf of Mexico.

Further research is needed on the annual variability in storm conditions that occur at a single location, and on the spatial variability in storm conditions that occur along the northern Gulf Coast. Further research is also needed on trends in alongshore sediment transport along the foreshore within isolated cells, especially in regard to the influence of variations in tides and wind directions. Additional research is also needed on cross-shore trends in sediment transport, both along the foreshore and along the nearshore platform. Researchers should especially focus on quantifying the relationship between storm magnitude and storm impact for understanding the implications of long-range predictions on weather conditions during forthcoming winter storm seasons.

REFERENCES

Armbruster, C.K., Stone, G.W. and Xu, J.P. 1995. Episodic atmospheric forcing and bayside shoreline erosion: Santa Rosa Island, Florida. *Transactions-Gulf Coast Association of Geological Societies* 45:31-38.

Armbruster, C.K. 1997. Morphologic responses of a low-energy, micro-tidal beach to winter cold front passages: North Shore Santa Rosa Island, Florida. Unpublished MS. thesis. 166 p.

Atlas, D., Chou, S.H. and Byerly, W.P. 1983. The influence of coastal shape on winter mesoscale air-sea interactions. *Monthly Weather Review* 114:1390-1405.

Boone, P.A. 1973. Depositional systems of the Alabama, Mississippi, and Western Florida coastal zone. *Transactions-Gulf Coast Association of Geological Societies* 23:266-277.

Bowden, J.E. 1994. Gulf Islands. Pensacola, Florida: Pace Printing Company. 143 p.

Byrnes, M.R., McBride, R.A., Penland, S., Hiland, M.W. and Westphal, K.A. 1991. Historical changes in shoreline position along the Mississippi Sound barrier islands. *GCSSEPM Foundation Twelfth Annual Research Conference*, pp. 43-55.

Chaney, P.L. and Stone, G.W. 1996. Soundside erosion of a nourished beach and implications for winter cold front forcing: West Ship Island, Mississippi. *Shore and Beach* 64(1):27-33.

Cipriani, L.E. 1998. Net longshore sediment transport and textural changes in beach sediments along the Southwest Alabama and Mississippi Barrier Islands. Unpublished MS. thesis. 131 p.

Davis, Jr., R.A. 1972. Beach changes, on the central Texas coast associated with Hurricane Fern, September, 1971. *Contributions in Marine Science* 16:89-98.

Davis, R.E., and Dolan, R. 1993. Nor'easters. *American Scientist* 81:428-439.

Davis, R.E., Dolan, R. and Demme, G. 1993. Synoptic climatology of Atlantic Coast north-easters. *International Journal of Climatology* 13:171-189.

Dean, R.G. and Yoo, C. 1993. Predictability of beach nourishment performance. In *Beach Nourishment Management and Engineering*, ed. D.K. Stauble and N.C. Kraus. American Society of Civil Engineers. pp. 86-102.

DiMego, G.J., Bosart, L.F. and Endersen, G.W. 1976. An examination of the frequency and mean conditions surrounding frontal incursions into the Gulf of Mexico and Caribbean Sea. *Monthly Weather Review* 104:709-718.

Dingler, J.R. and Reiss, T.E. 1990. Cold-front driven storm erosion and overwash in the central part of the Isles Dernieres, a Louisiana barrier-island arc. *Marine Geology* 91:195-206.

Dingler, J.R., Hsu, S.A. and Reiss, T.E. 1992. Theoretical and measured aeolian sand transport on a barrier island, Louisiana, USA. *Sedimentology* 39:1031-1043.

Dingler, J.R., Reiss, T.E. and Plant, N.G. 1993. Erosional patterns of the Isles Dernieres, Louisiana, in relation to meteorological influences. *Journal of Coastal Research* 9(1):112-125.

Dolan, R., Lins, H. and Hayden, B. 1988. Mid-Atlantic coastal storms. *Journal of Coastal Research* 4(3):417-433.

Dolan, R. and Davis, R.E. 1992a. An intensity scale for Atlantic Coast northeast storms. *Journal of Coastal Research* 8(4):840-853.

Dolan, R. and Davis, R.E. 1992b. Rating Northeasters. *Mariners Weather Log* 36:4-11.

Earle, M.D., McGehee, D., and Tubman, M. 1995. Field wave gaging program, wave data analysis standard. U.S. Army Corps of Engineers, Instruction Report CERC-95-1.

Ekwurzel, B. 1990. A complex bayside beach: Herring Cove Beach, Cape Cod, Massachusetts, USA. *Journal of Coastal Research* 6(4):879-891.

Fox, W.T. and Davis, Jr., R.A. 1970. Profile of a storm - wind, waves and erosion on the southeastern shore of Lake Michigan. *Proceedings - 13th Conference on Great Lakes Research.* International Association of Great Lakes Researchers. pp. 233-241.

Fox, W.T. and Davis, Jr., R.A. 1976. Weather patterns and coastal processes. In *Beach and Nearshore Sedimentation*, ed. R.A. Davis, Jr. and R.L. Eddington. SEPM Special Publication 24:1-23.

Hayden, B.P. and Dolan, P. 1977. Seasonal changes in the planetary wind system and their relationship to the most severe coastal storms. *Geoscience and Man* 18:113-119.

Henderson, K.G. and Robinson, P.J. 1994. Relationship between the Pacific/North American teleconnection patterns and precipitation events in the south-eastern USA. *International Journal of Climatology* 14:307-323.

Henry, V.J. 1977a. *Final report for West Ship Island/Ft. Massachusetts beach nourishment and shore protection study, Gulf Islands National Seashore.* University of Georgia Marine Institute, Savannah, Georgia. 39 p.

Henry, W.K. 1977b. Some aspects of the fate of cold fronts in the Gulf of Mexico. *Monthly Weather Review* 107:1078-1082.

Hopkins, G. 1996. Personal communication with the Natural Resource Manager for the Gulf Islands National Seashore, National Park Service, Ocean Springs, MS.

Houston, J.R. 1991. Beachfill performance. *Shore and Beach*, July: 15-24.

Hsu, S.A. 1988. *Coastal Meteorology*. San Diego: Academic Press. 260 p.

Hsu, S.A. 1993. The Gulf of Mexico - A breeding ground for winter storms. *Mariners Weather Log* 37(2):4-7.

Huschke, R. E. 1959. *Glossary of Meteorology*. American Meteorological Society. Boston, MA. 638 p.

Jackson, N.L. and Nordstrom, K.F. 1992. Site specific controls on wind and wave processes and beach mobility in New Jersey, USA. *Journal of Coastal Research* 8(1):88-98.

Jackson, N.L. 1995. Wind and waves: influence of local and non-local waves on mesoscale beach behavior in estuarine environments. *Annals of the Association of American Geographers* 85(1):21-37.

Jensen, R.E. 1983. Mississippi Sound wave-hindcast study. *Technical Report HL-83-8*. U.S. Army Engineer Waterways Experiment Station, Vicksburg, MS. 56 p.

Jenks, G.F. and Caspall, F.D. 1971. Error on choropleth maps: definition, measurement, reduction. *Annals of the Association of American Geographers* 61:217-244.

Johnson, G.A., Meindl, E.A., Mortimer, E.B. and Lynch, J.S. 1984. Features associated with repeated strong cyclogenesis in the western Gulf of Mexico during the winter of 1982-83. *Postprints - Third Conference on Meteorology of the Coastal Zone*. American Meteorological Society, Boston, MA. pp. 110-117.

Jones, G.V. and Davis, R.E. 1995. Climatology of nor'easters and the 30 kPa jet. *Journal of Coastal Research* 11(4):1210-1220.

Kemp, G.P. and Wells, J.T. 1987. Observations of shallow-water waves over a fluid mud bottom: implications to sediment transport. *Coastal Sediments '87.* American Society of Civil Engineers. pp. 363-378.

Leathers, D.J., Yarnal, B.M. and Palecki, M.A. 1991. The Pacific/North American teleconnection pattern and United States climate. Part I: regional temperature and precipitation association. *Journal of Climate* 4:517-528.

Leonard, L.A., Hine, A.C., Luther, M.E., Stumpf, R.P. and Wright, E.E. 1995. Sediment transport processes in a west-central Florida open marine marsh tidal creek; the role of tides and extratropical storms. *Estuarine, Coastal and Shelf Science* 41:225-248.

Lewis, J.K. and Hsu, S.A. 1992. Mesoscale air-sea interactions related to tropical and extratropical storms in the Gulf of Mexico. *Journal of Geophysical Research* 97(C2):2215-2228.

Louisiana Office of State Climatology 1997. *Monthly climate reports*. Louisiana State University, Baton Rouge.

Lutgens, F.K. and Tarbuck, E.J. 1992. *The atmosphere*. Englewood Cliffs, NJ: Prentice Hall. 430 p.

Ludwick, J.C. 1964. Sediments in northeastern Gulf of Mexico. In *Papers in Marine Geology*, ed. R.L. Miller, New York: MacMillan Publishing. pp. 204-238.

Lydolph, P.E. 1985. *The climate of the Earth*. Roman and Littlefield Publishers. 386 p.

Mather, J.R., Adams, III, H.A. and Yoshioka, G.A. 1964. Coastal storms of the eastern United States. *Journal of Applied Meteorology* 3:693-706.

Mather, J.R., Field, R.T., and Yoshioka, G.A. 1967. Storm damage hazard along the east coast of the United States. *Journal of Applied Meteorology* 6:20-30.

McBride, R.A., Byrnes, M.R. and Hiland, M.W. 1995. Geomorphic response-type model for barrier coastlines: a regional perspective. *Marine Geology* 126:143-159.

Moore, W.G. 1988. *Dictionary of Geography*. London: Penguin Books. 247 p.

Moore, J.B., Groop, R.E. and Jenks, G.F. 1990. CLASSY version 4.1. Department of Geography, Michigan State University, East Lansing, MI.

Muller, R.A. and Wax, C.W. 1977. A comparative synoptic climatic baseline for coastal Louisiana. *Geoscience and Man* 18: 121-129.

National Data Buoy Center 1981-1997. *Standard Meteorological Data -- NDBC Station 42007*. National Data Buoy Center, Stennis Space Center, MS.

National Data Buoy Center 1996. *Standard Meteorological Data -- NDBC Station 42040*. National Data Buoy Center, Stennis Space Center, MS.

National Data Buoy Center 1997. *Standard Meteorological Data -- NDBC Station 42007*. National Data Buoy Center, Stennis Space Center, MS.

National Oceanic and Atmospheric Administration 1990. *Published Bench Mark Sheet With Tidal Datums: Cadet Point, Biloxi Bay, Biloxi, Mississippi, Station 874 3735*. NOAA/National Ocean Service, Ocean and Lakes Division. 5 p.

National Oceanic and Atmospheric Administration 1977. *National hurricane operations plan*, FCM 77-2. U.S. Department of Commerce, NOAA, and Federal Coordinator for Meteorological Services and Supporting Research. 104 p.

National Oceanic and Atmospheric Administration 1993. *Tropical cyclones of the north Atlantic Ocean, 1871-1992, Historical Climatology Series 6-2*. NOAA/NWS/National Environmental Satellite, Data, and Information Service, Asheville, NC.

National Oceanic and Atmospheric Administration 1981-1997. *Daily weather maps*. U.S. Department of Commerce, NOAA. Washington, D.C.

National Oceanic and Atmospheric Administration 1997. *Daily weather maps*. U.S. Department of Commerce, NOAA. Washington, D.C.

Nordstrom, K.F. 1980. Cyclic and seasonal beach response: a comparison of oceanside and bayside beaches. *Physical Geography* 1(2):177-196.

Nordstrom, K.F. 1992. *Estuarine Beaches*. New York: Elsevier Science Publishing. 225 p.

Nordstrom, K.F. and Jackson, N.L. 1992. Two-dimensional changes on sandy beaches in meso-tidal estuaries. *Z. Geomorphologie N.F.* 36(4):465-478.

Otvos, E.G. 1970. Development and migration of barrier islands, northern Gulf of Mexico. *Geological Society of America Bulletin* 81:241-246.

Otvos, E.G. 1979. Barrier island evolution and history of migration, north central Gulf coast. In *Barrier Islands from the Gulf of St. Lawrence to the Gulf of Mexico*, ed. S.P. Leatherman. New York: Academic Press. pp. 291-319.

Otvos, E.G. 1981. Barrier island formation through nearshore aggradation - stratigraphic and field evidence. *Marine Geology* 43:195-243.

Otvos, E.G. 1982. Inverse beach sand texture - coastal energy relationship along the Mississippi coast barrier islands. *Journal of the Mississippi Academy of Sciences* 19:96-101.

Otvos, E.G. 1985. Barrier platforms: northern Gulf of Mexico. *Marine Geology* 63: 285-305.

Penland, S., Ramsey, K.E., McBride, R.A., Moslow, T.F. and Westphal, K.A. 1989. *Relative sea-level rise and subsidence in Louisiana and the Gulf of Mexico: 1908-1988*, Coastal Geotechnical Report No. 3. Louisiana Geological Survey, Baton Rouge. 65 p.

Penland, S. and Ramsey, K. E. 1990. Relative sea-level rise in Louisiana and the Gulf of Mexico: 1908-1988. *Journal of Coastal Research* 6(2):323-342.

Psuty, N. 1965. Beach-ridge development in Tabasco, Mexico. *Annals of the Association of American Geographers* 55:112-124.

Psuty, N. 1967. *The geomorphology of beach ridges in Tabasco, Mexico*, Coastal Studies Series 18. Louisiana State University, Baton Rouge. 51 p.

Reitan, C.H. 1974. Frequencies of cyclones and cyclogenesis for North America, 1951-1970. *Monthly Weather Review* 102:861-868.

Reed, D.J. 1989. Patterns of sediment deposition in subsiding coastal salt marshes, Terrebonne Bay, Louisiana: The role of winter storms. *Estuaries* 12(4):222-227.

Roberts, H.H., Huh, O.K., Hsu, S.A., Rouse, Jr., L.J. and Rickman, D. 1987. Impact of cold-front passages on geomorphic evolution and sediment dynamics of the complex Louisiana coast. *Coastal Sediments '87*. American Society of Civil Engineers, New Orleans, LA. pp. 1950-1963.

Roberts, H.H., Huh, O.K., Hsu, S.A., Rouse, Jr., L.J. and Rickman, D. 1989. Winter storm impacts on the chenier plain coast of southwestern Louisiana. *Transactions - Gulf Coast Association of Geological Societies* 39:515-522.

Roebber, P.J. 1984. Statistical analysis and updated climatology of explosive cyclones. *Monthly Weather Review* 112:1577-1589.

Saucier, W.J. 1949. Texas-west gulf cyclones. *Monthly Weather Review* 77:219-231.

Schuman, S.A., Moser, J., Johnson, G.A., Walker, N.D. and Hsu, S.A. 1995. An overview of a strong winter cyclone low in the Gulf of Mexico 12-13 March 1993. *National Weather Digest* 21(1):11-25.

Schwartz, M.L. 1982. *The encyclopedia of beaches and coastal environments*, ed. M.L. Schwartz. Stroudsburg, PA: Hutchinson Ross Publishing Company. 940 p.

Sheets, R.C., 1990. The national hurricane center – past, present, and future. *Weather and Forecasting* 5(2):185-233.

Simpson, R. H. 1974. The hurricane disaster potential scale. *Weatherwise* 27:169-186.

Smith, R.M. 1986. Comparing traditional methods for selecting class intervals on choropleth maps. *The Professional Geographer* 38:62-67.

Stone, G.W., Stapor, F.W., May, J.P. and Morgan, J.P. 1992. Multiple sediment sources and a cellular, non-integrated, longshore drift system: Northwest Florida and southeast Alabama coast, USA. *Marine Geology* 105:141-154.

Stone, G.W. and Finkl, C. W. 1995. Impacts of Hurricane Andrew on the coastal zones of Florida and Louisiana: 22-26 August 1992. *Journal of Coastal Research, Special Issue 21.* ed., Stone, G.W. and Finkl, C. W.

Stone, G.W., Grymes III, J.M., Armbruster, C.K., Xu, J.P. and Huh O.K. 1996. Researchers study impact of Hurricane Opal on Florida coast. *EOS* 77(19):181, 184.

Taylor, M. and Stone, G.W. 1996. *Beach Ridges: A review.* Journal of Coastal Research 12 (3): 612-621.

Topcon 1996. Operators Manual for the Topcon GTS-203 Total Station. Paramus, NJ: TOPCON America Corporation.

U.S. Army Corps of Engineers 1868. *Sketch of the Fort on Ship Island.* Surveyed and Drawn Under the Direction of Bvt.Colonel F.E. Prime. National Archives, File No. Dr. 84, Sht.42.

U.S. Army Corps of Engineers 1979. *Detailed project report on beach erosion control at Santa Rosa Island, Florida.* Mobile District Section 103a, Reconnaissance Report. 116 p.

U.S. Coast and Geodetic Survey 1992. *Dog Keys Pass to Waveland, Nautical Chart 11372, Intracoastal Waterway*. U.S. Department of Commerce, NOAA, NOS, Coast and Geodetic Survey. Washington, D. C.

Upshaw, C.F., Creath, W.B. and Brooks, F.L. 1966. *Sediments and microfauna off the coasts of Mississippi and adjacent states*. Mississippi Geological Survey Bulletin 106. 127 p.

Veal, C.D. 1996. *1996 Biloxi Bay Tides*. Publication 850. Mississippi-Alabama Sea Grant Consortium Report MASGP-95-010.

Wallace, J.M. and Gutzler, D.S. 1981. Teleconnections in the geopotential height field during the northern hemisphere winter. *Monthly Weather Review* 109:784-812.

Walker, N.D. 1993. A preliminary look at cyclogenesis in the Gulf of Mexico during the March 1993 Blizzard. *Mariners Weather Log* 37(2):8-9.

Williams, S.J., Penland, S. and Sallenger, Jr., A.H. 1992. *Atlas of shoreline changes in Louisiana from 1853 to 1989*. USGS Misc. Investigation Series I-2150-A. Reston, VA. 103 p.

Wolman, M.G. and Miller, J.P. 1960. Magnitude and frequency of forces in geomorphic processes. *Journal of Geology* 68: 54-74.

Woods Hole Instrument Systems 1996a. Operators Manual for the SeaPac Model 2100 Wave, Tide, and Current Gauge. Woods Hole, MA: Woods Hole Instrument Systems.

Woods Hole Instrument Systems 1996b. Software Manual for the WavePro Software. Woods Hole, MA: Woods Hole Instrument Systems.

Zishka, K.M. and Smith, P.J. 1980. The climatology of cyclones and anticyclones over North America and surrounding ocean environs for January and July, 1950-77. *Monthly Weather Review* 108(4):387-401.

APPENDIX 1

Profiles of the beach and nearshore platform along the northern coast of West Ship Island, Mississippi (Figure 5.1). A plot of the pre- and post-Tropical Storm Josephine surveys, and the final survey, is provided for each profile site. A separate plot of all surveys conducted during the study period is also provided for each site.

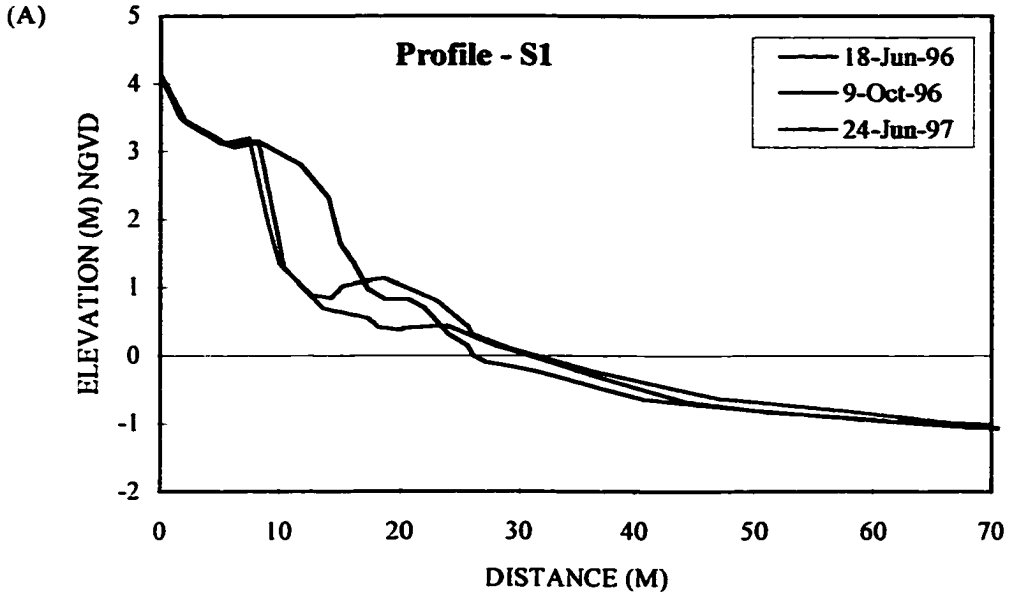

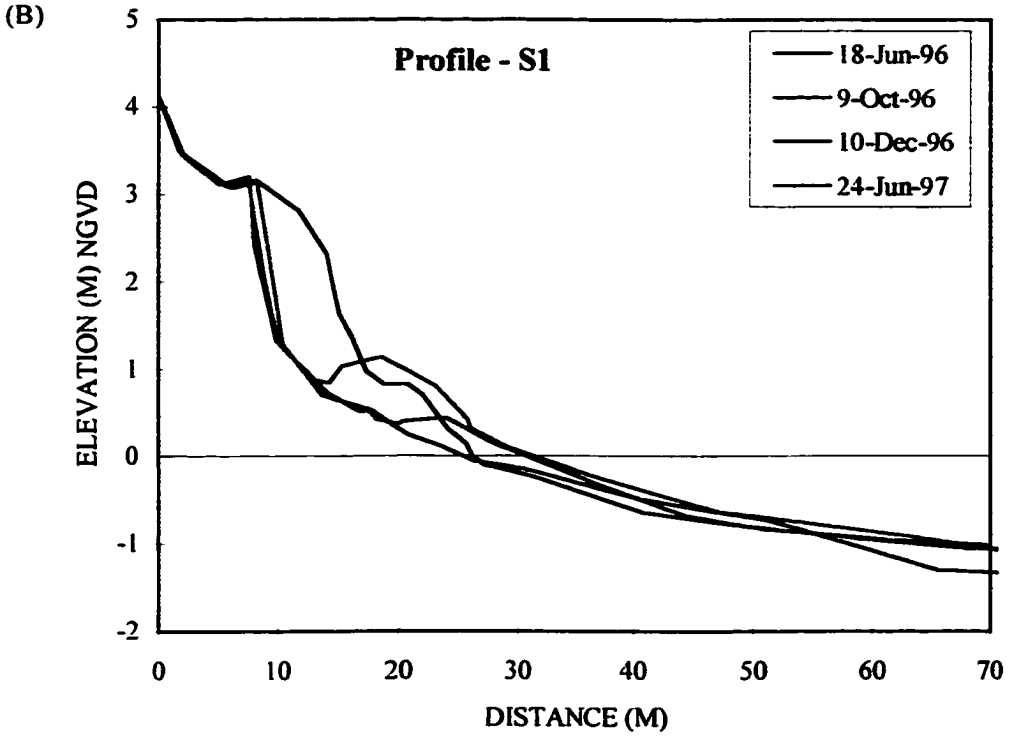

The upper plot (A) shows the pre- and post-Tropical Storm Josephine surveys, and the final survey. The lower plot (B) shows all surveys.

(A)

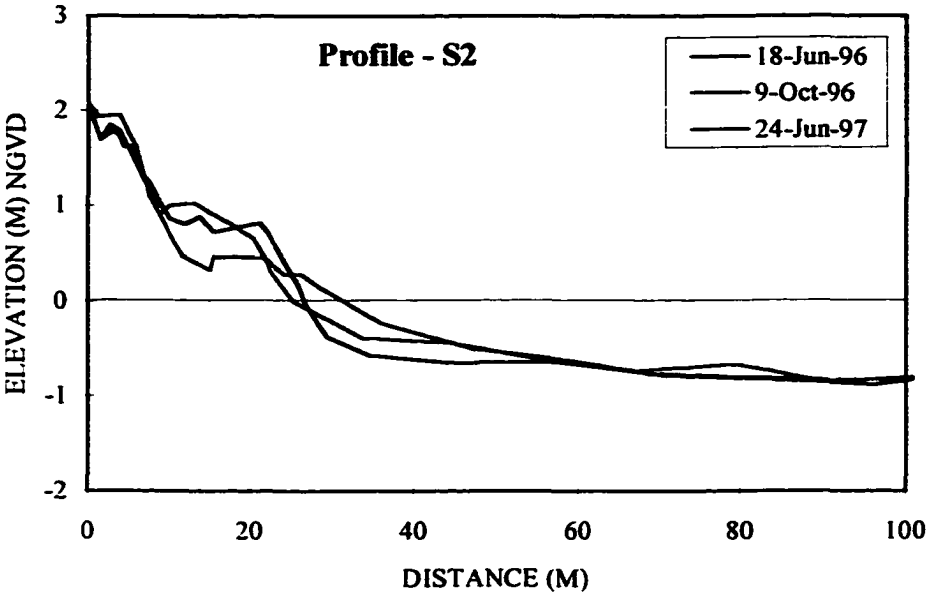

(B)

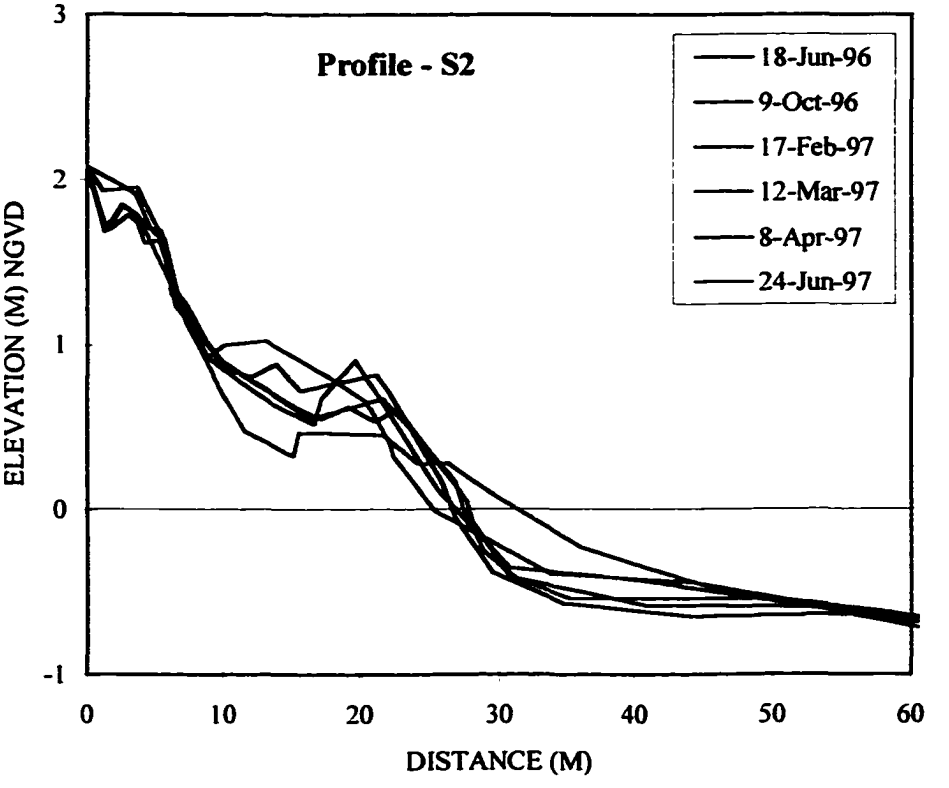

The upper plot (A) shows the pre- and post-Tropical Storm Josephine surveys, and the final survey. The lower plot (B) shows an enlarged view of the beach and includes all surveys.

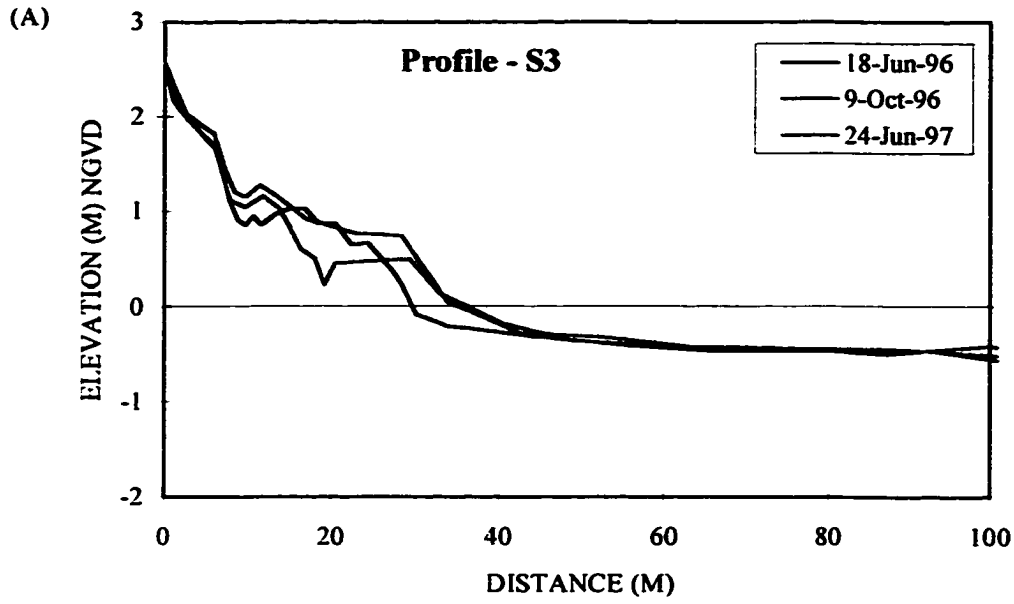

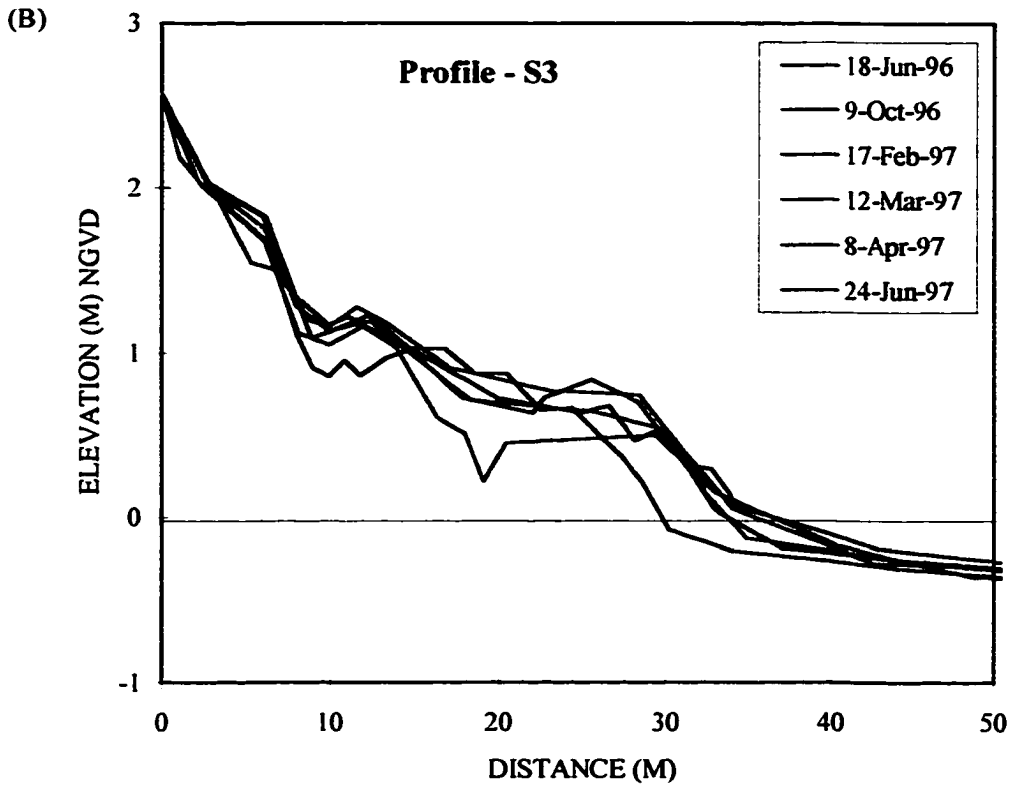

The upper plot (A) shows the pre- and post-Tropical Storm Josephine surveys, and the final survey. The lower plot (B) shows an enlarged view of the beach and includes all surveys.

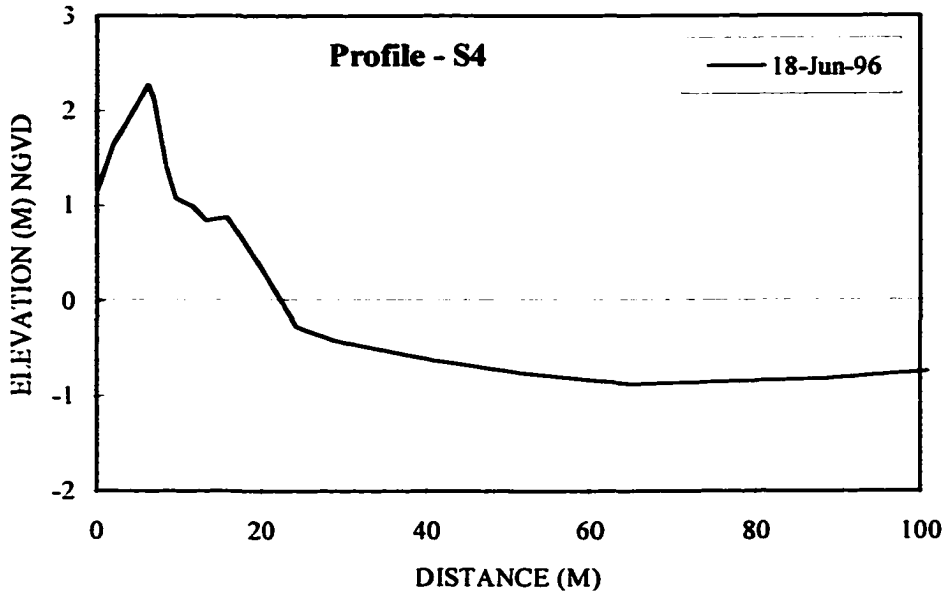

Tropical Storm Josephine destroyed the profile markers along the beach at this site so monitoring was discontinued.

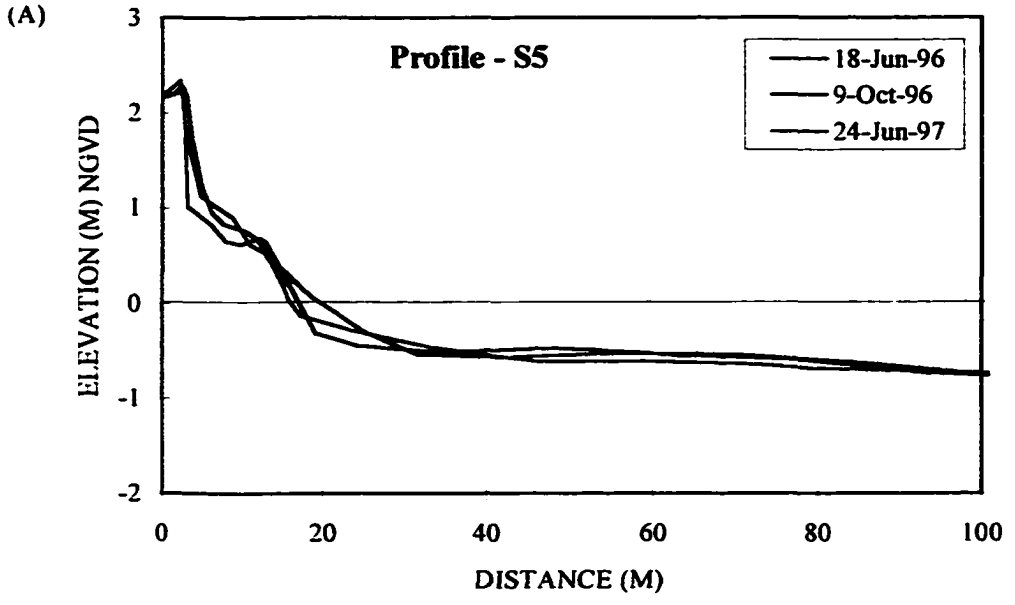

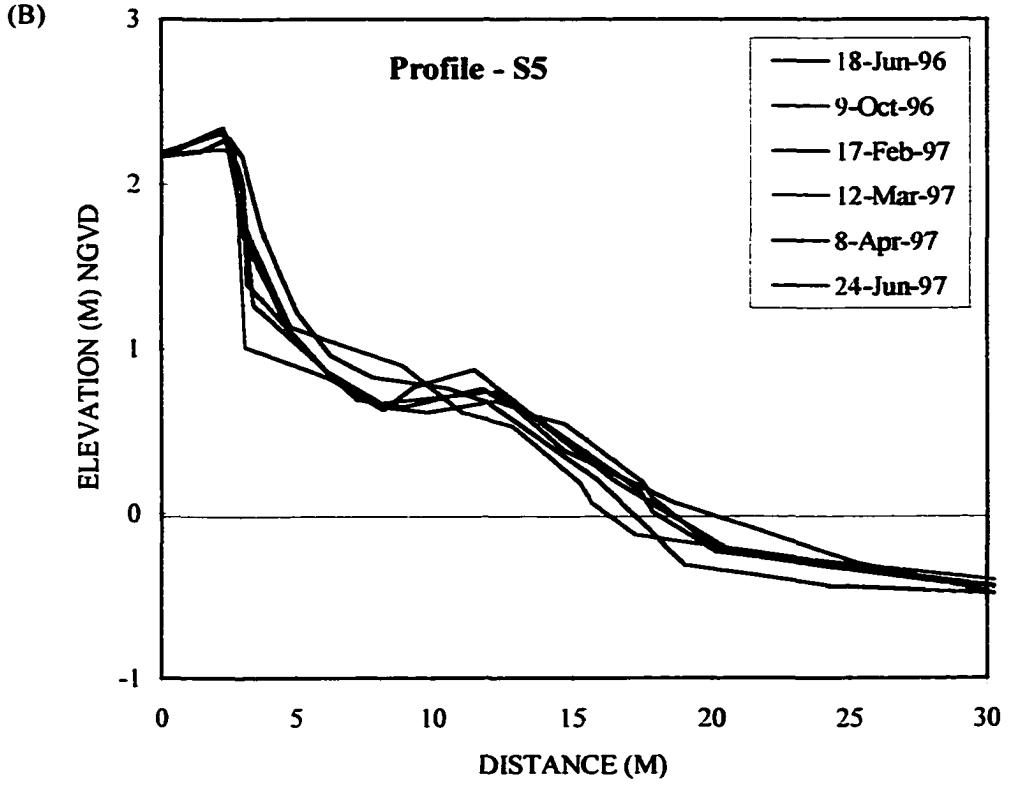

The upper plot (A) shows the pre- and post-Tropical Storm Josephine surveys, and the final survey. The lower plot (B) shows an enlarged view of the beach and includes all surveys.

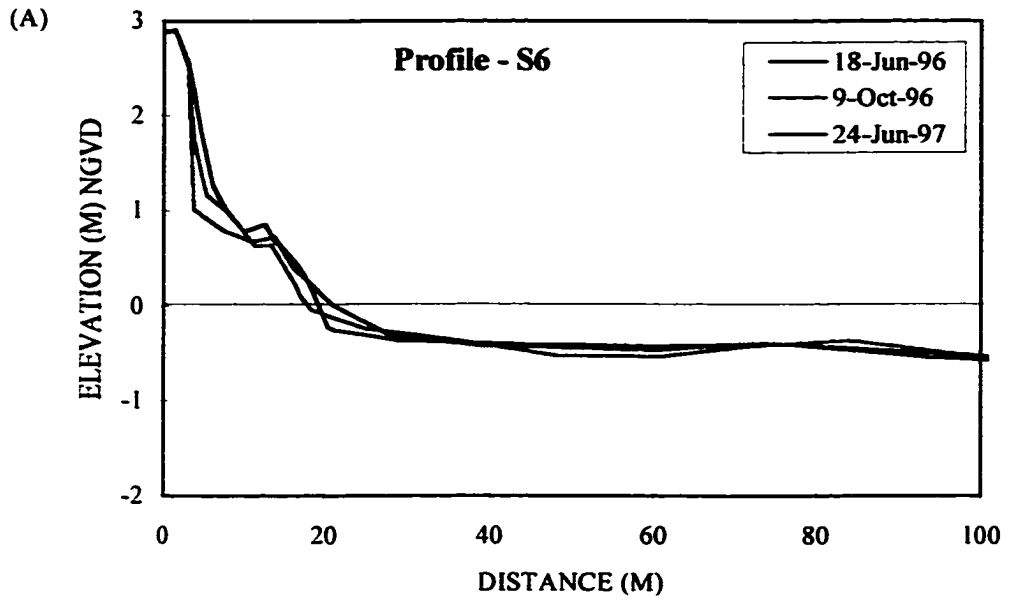

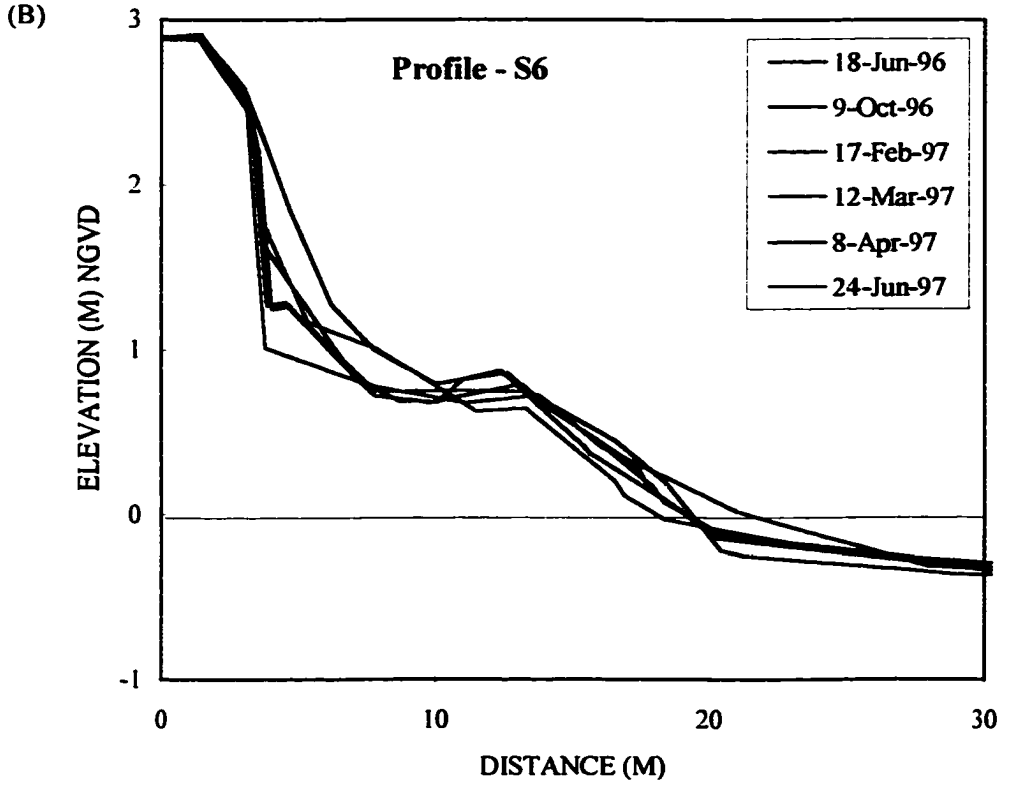

The upper plot (A) shows the pre- and post-Tropical Storm Josephine surveys, and the final survey. The lower plot (B) shows an enlarged view of the beach and includes all surveys.

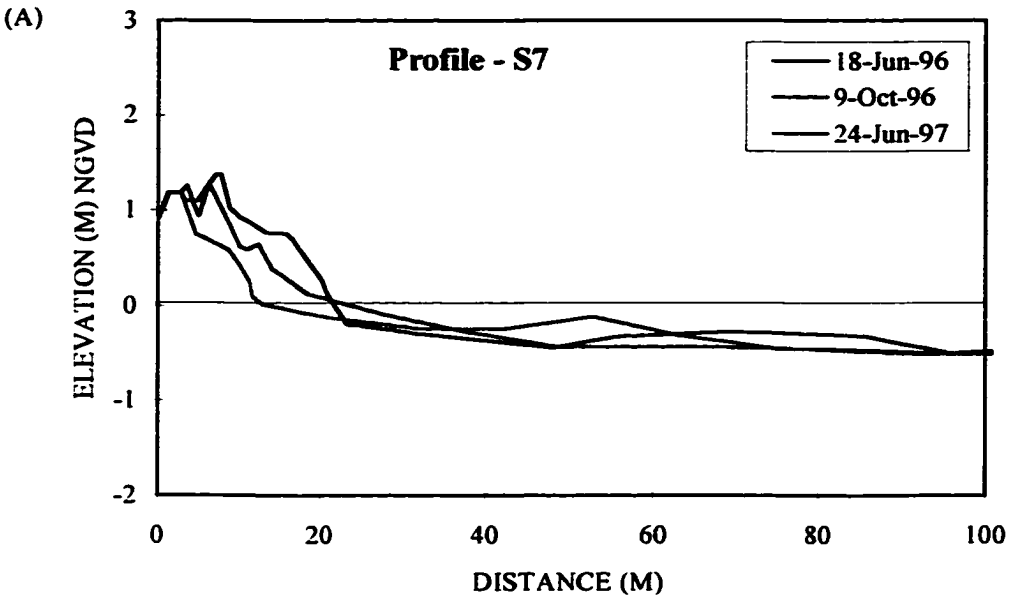

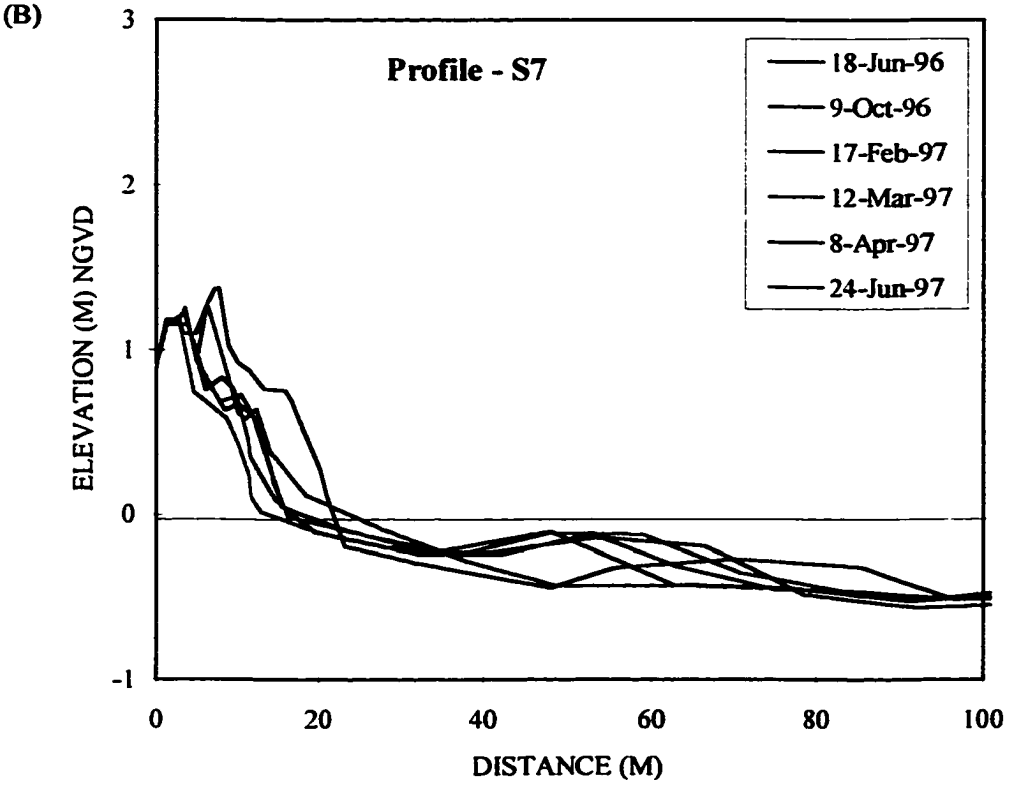

The upper plot (A) shows the pre- and post-Tropical Storm Josephine surveys, and the final survey. The lower plot (B) includes all surveys.

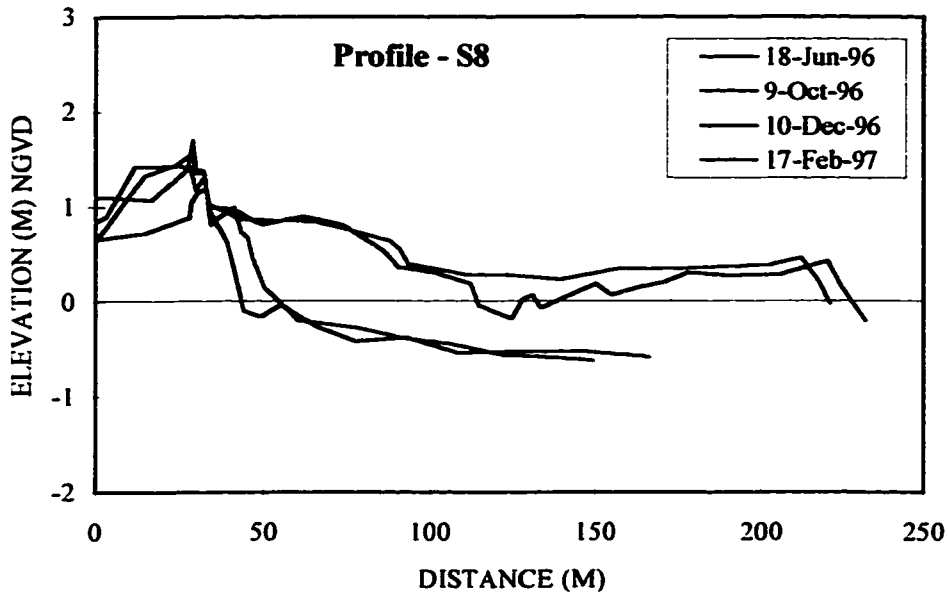

Tropical Storm Josephine overwashed the Gulf coast and deposited sediment along the backshore and foreshore at S8. Extratropical storms subsequently overwashed the Gulf coast and deposited additional material along the profile. Monitoring at this site was discontinued after the February survey was completed.

APPENDIX 2

Profiles of the beach and nearshore platform at the beach nourishment site adjacent to Fort Massachusetts (Figure 5.1). The plots show the results of the pre- and post-nourishment surveys, and the final survey.

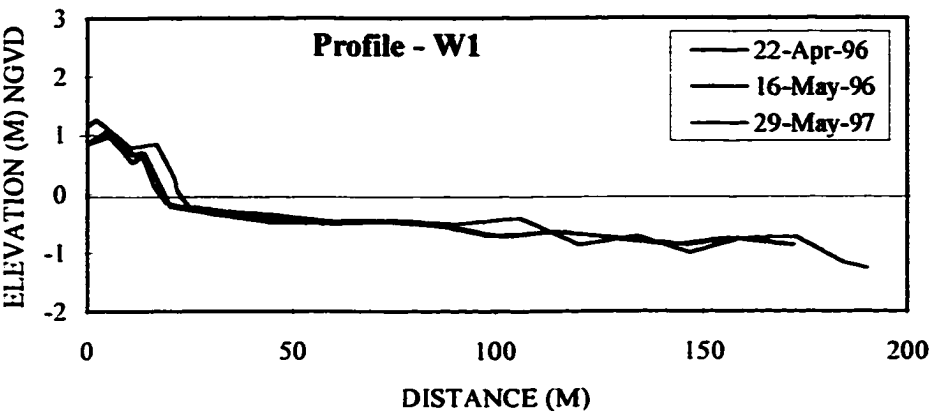

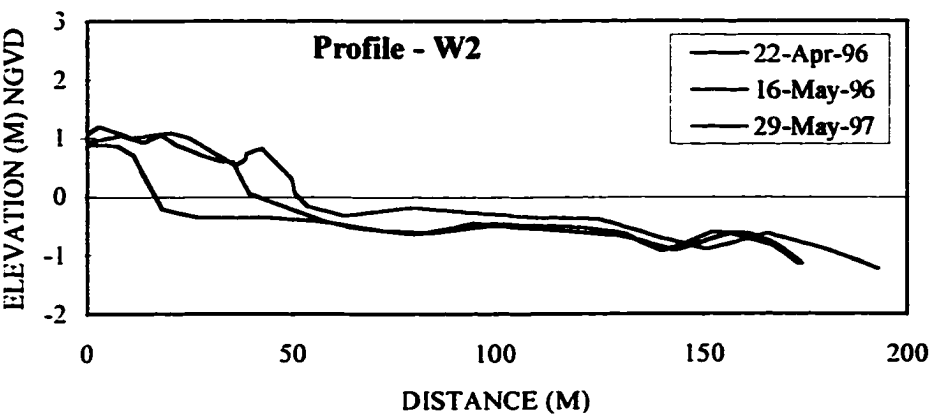

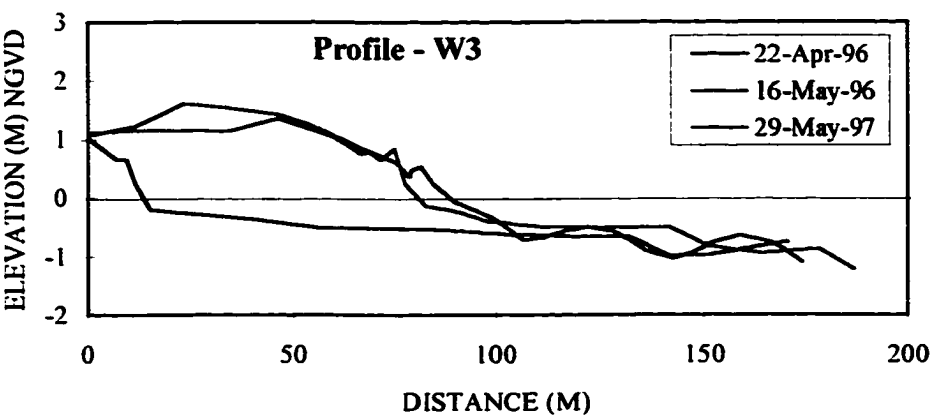

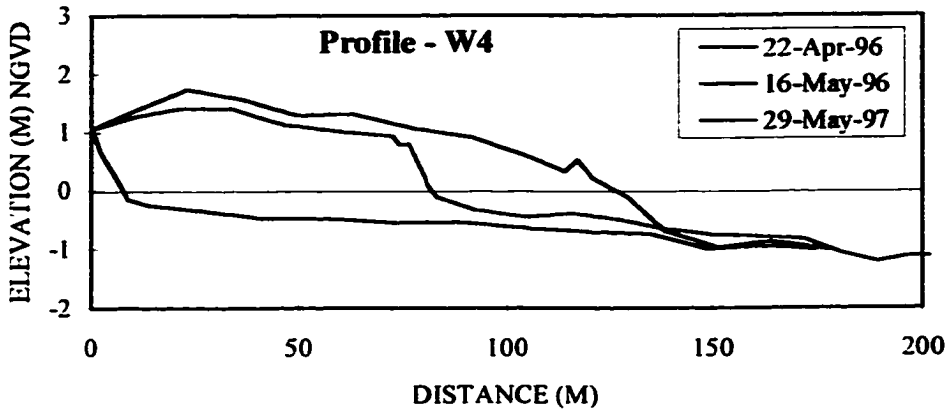

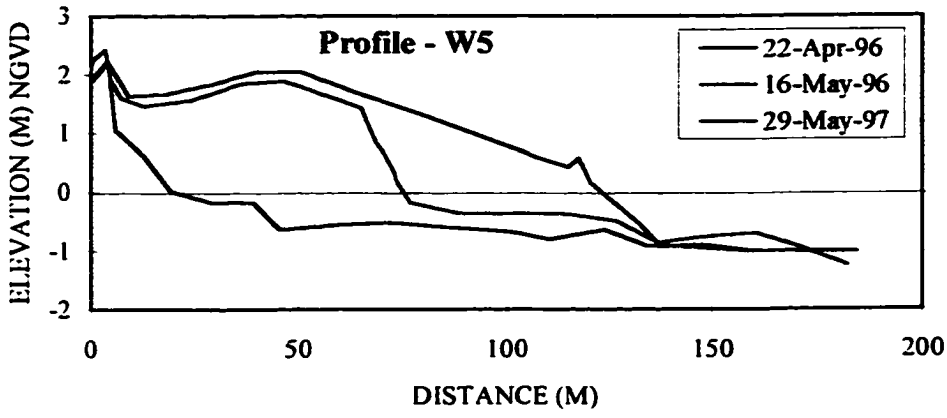

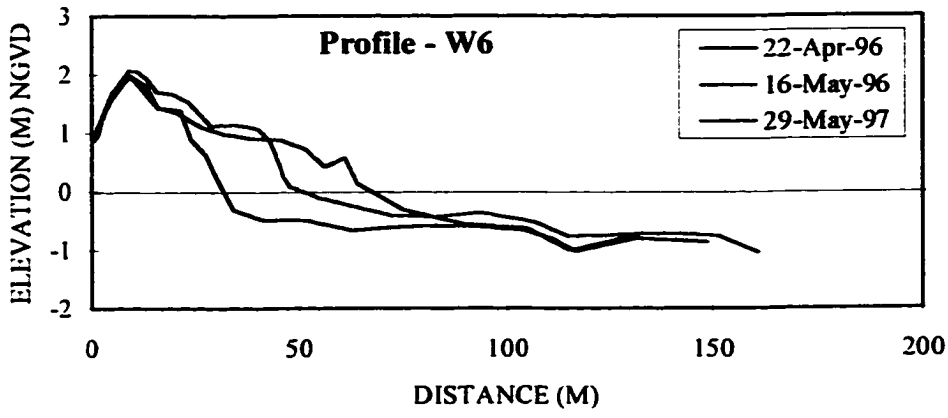

VITA

Phillip Lynn Chaney was born on March 9, 1958, in Shreveport, Louisiana. He spent his early years in Texarkana, Arkansas, before moving to the small town of Gillham, Arkansas, where he graduated from high school in May, 1976. Phillip studied agriculture at the University of Arkansas at Fayetteville and was awarded the degree of Bachelor of Science in December, 1980. He spent one year working in the oil exploration industry, where he became interested in cartography, then spent the next two years working in the commercial agriculture industry.

In August, 1984, Phillip returned to the University of Arkansas for one year to study the legal principles and techniques of land surveying. He spent the next four years working as an apprentice and was certified as a Professional Land Surveyor in July, 1989. He had returned to the University of Arkansas to study cartography and geography by that time and was awarded the degree of Master of Arts in August, 1990. Phillip spent the next year working as an instructor for the Department of Geography at the University of Arkansas, and as a GIS technician for the Soils Lab. He transferred to the Center for Advanced Spatial Technologies / National Center for Resource Innovations at the University of Arkansas where he spent the next two years working as a research assistant on GIS, GPS, and Remote Sensing projects.

In August, 1993, Phillip entered the graduate program in the Department of Geography and Anthropology at Louisiana State University where he became a candidate for the degree of Doctor of Philosophy. In September, 1998, he accepted a position as an instructor in the Department of Geography at Auburn University in Auburn, Alabama.

DOCTORAL EXAMINATION AND DISSERTATION REPORT

Candidate: Phillip L. Chaney

Major Field: Geography

Title of Dissertation: Extratropical Storms of the Gulf of Mexico and Their Effects Along the Northern Coast of a Barrier Island: West Ship Island, Mississippi

Approved:

Major Professor and Chairman

Dean of the Graduate School

EXAMINING COMMITTEE:

Date of Examination:

September 11, 1998

IMAGE EVALUATION TEST TARGET (QA-3)

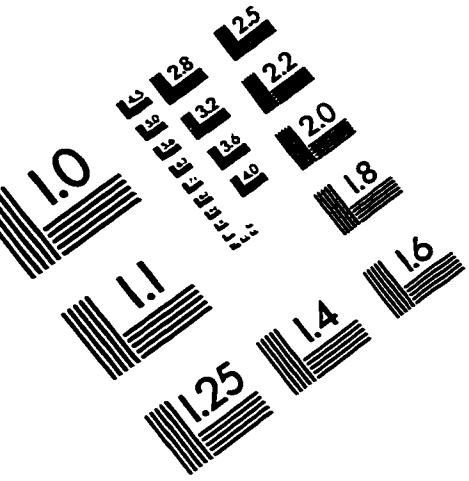

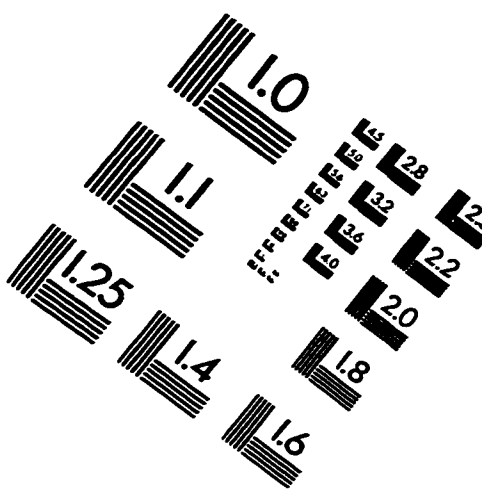

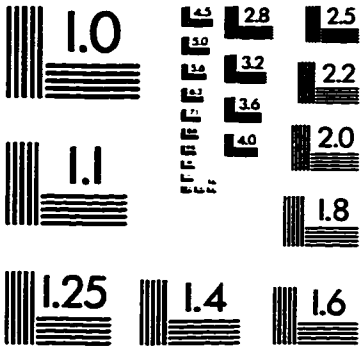

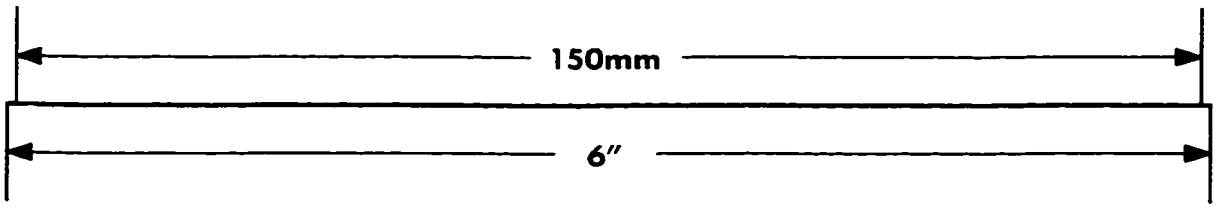

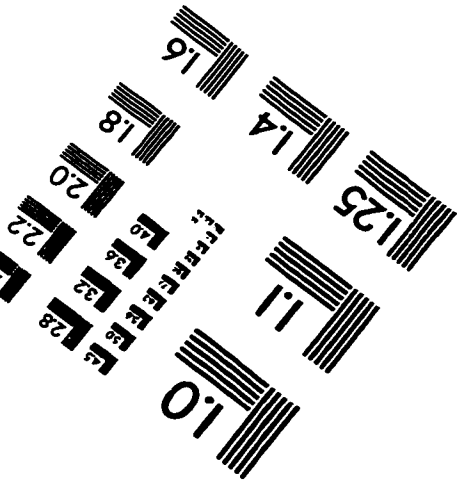

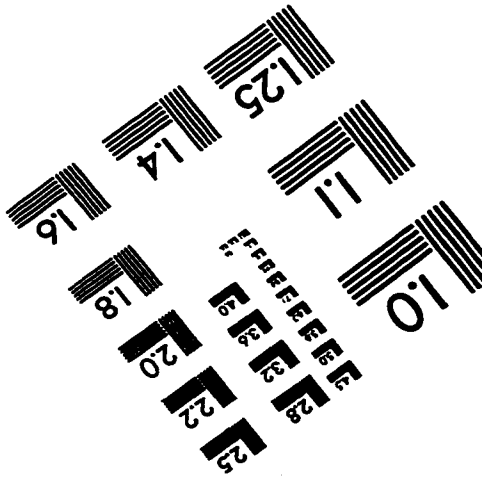

APPLIED IMAGE, Inc
1653 East Main Street
Rochester, NY 14609 USA
Phone: 716/482-0300
Fax: 716/288-5989